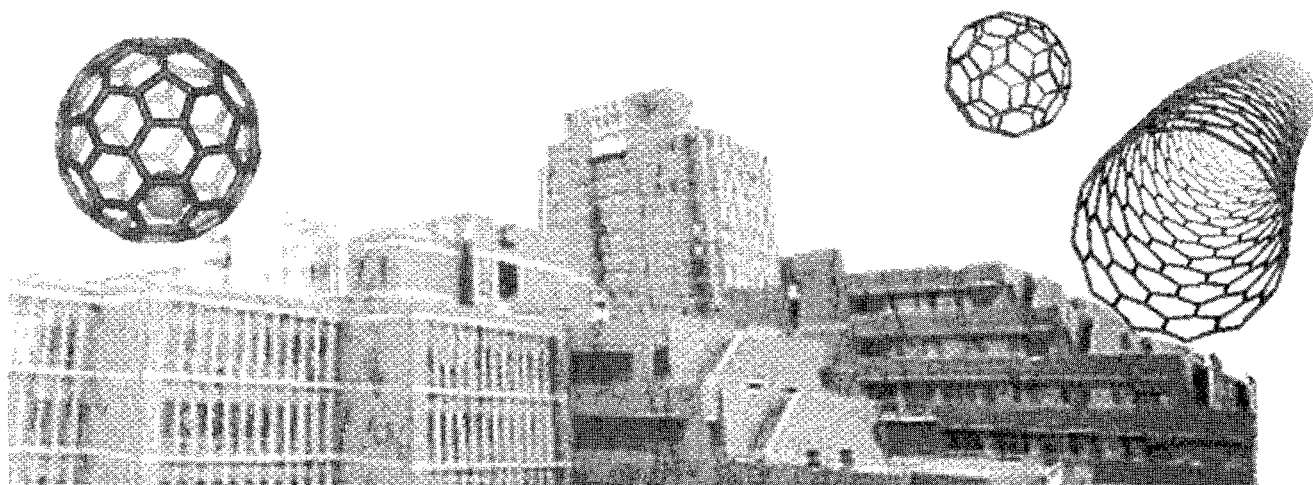


Abstracts
The 30th Commemorative Fullerene-Nanotubes
General Symposium

第 30 回記念フラーレン・ナノチューブ
総合シンポジウム

講演要旨集



January 7-9, 2006 Nagoya Aichi
平成 18 年 1 月 7 日—9 日 名城大学

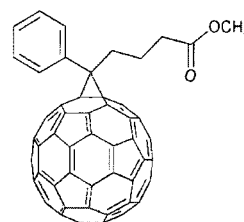
The Fullerenes and Nanotubes Research Society
フラーレン・ナノチューブ学会

NEW
[6,6]-Phenyl C₆₀ butyric acid methyl ester (PCBM)
65,916-9 100mg ¥95,000

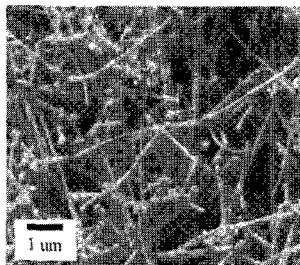
An n-channel organic semiconductor. For use as an n-type layer in organic photovoltaic devices. Soluble in CCl₄, 1,2-dichlorobenzene, CS₂, toluene, xylenes.

<Reference>

Frisbie, C.D.; et. al. *Chem. Mater.* **16**, 4436, (2004) Anthopoulos, T.D.; et. al., *Adv. Mater.* **16**, 2174, (2004)

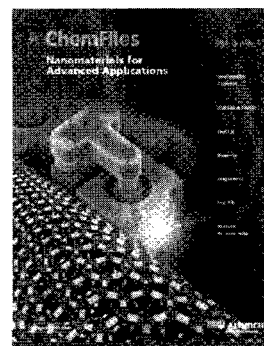

NEW
Carbon nanotubes, multi-walled, 90+%
65,925-8 2g ¥7,200; 10g ¥24,000

直径 110-170 nm
長さ 5-9 μm
不純物 Fe: <0.1%



ナノ材料の最新情報は
こちらからダウンロード
できます。

[www.sigma-aldrich.co.jp/
aldrich/nanopowder/](http://www.sigma-aldrich.co.jp/aldrich/nanopowder/)


Single-walled Nanotubes

Single-walled carbon nanotubes, octadecylamine functionalized ^{a)}		Single-walled carbon nanotubes, polyaminobenzenesulfonic acid functionalized ^{b)}	
65,248-2	10mg ¥40,000	63,923-0	50mg ¥41,300
SWNT 純度	80 - 90 %	SWNT 純度	70 - 85 % ^{c)}
直径	2 - 8 nm	ポリマー含有量	65 wt. %
長さ	500 - 1000 nm, bundles	ポリマー平均分子量	Mw 400-600
ODA 含有量	30 - 40 wt. %	直径	1.1 nm
金属含有量	4 %	長さ	500 - 1000 nm
溶解性	THF, 1,2-Dichlorobenzene, CS ₂ ≥ 1 mg/ml ベンゼン、トルエン、クロロホルムにも溶解	溶解性	H ₂ O = 5.0 mg/ml, DMF = 0.1 mg/ml, Ethanol = 0.05 mg/ml
a) Niyogi, S. et al. <i>Accts. Chem. Res.</i> 2002 , <i>35</i> , 1105.		b) Zhao, B. et al. <i>Adv. Funct. Mater.</i> 2004 , <i>14</i> , No. 1, 71-76. Zhao, B. et al. <i>J. Am. Chem. Soc.</i> 2005 , <i>127</i> , 8197.	
Single-walled carbon nanotubes, polyethyleneglycol functionalized		Single-walled carbon nanotubes	
65,247-4	10mg ¥40,000	65,251-2	250mg ¥46,600; 1g ¥151,200
SWNT 純度	80 - 90 %	SWNT 純度	90+ %
直径	4 - 5 nm	直径	0.8 - 1.6 nm
長さ	500 - 600 nm, bundles	長さ	< 0.5 μm
ポリマー含有量	30 wt. %	51,930-8	250mg ¥13,200; 1g ¥41,700
ポリマー平均分子量	Mw 840-10,000,000	SWNT 純度	50 - 70 %
金属含有量	6 %	直径	1.2 - 1.5 nm
溶解性	H ₂ O = 5.0 mg/ml	長さ	2 - 5 μm
Single-walled carbon nanotubes, carboxylic acid functionalized		63,679-7	250mg ¥28,600; 1g ¥89,000
65,249-0	250mg ¥44,400; 1g ¥144,000	SWNT 純度	50+ %
SWNT 純度	80 - 90 %	直径	1 - 2 nm
直径	4 - 5 nm	長さ	0.5 - 100 μm
長さ	500 - 1500 nm, bundles	58,970-5	1g ¥23,100; 5g ¥88,300
カルボン酸含有量	3-6 atomic %	SWNT 純度	12+ %
金属含有量	5-10 %	直径	0.9 - 1.2 nm
溶解性	DMF = 1.0 mg/ml, H ₂ O = 0.1 mg/ml	長さ	10 - 30 μm

新製品情報は <http://www.sigma-aldrich.co.jp/aldrich/MS/> から


SIGMA-ALDRICH

シグマ アルドリッチ ジャパン株式会社
〒140-0002 東京都品川区東品川2-2-24
天王洲セントラルタワー4F

カタログのご請求はe-mail、FAXまたは日本語サイトからどうぞ

■ 製品に関するお問い合わせは、弊社テクニカルサポートへ
TEL.03-5796-7330 FAX.03-5796-7335

■ 在庫照会・ご注文方法に関するお問い合わせは、弊社カスタマーサービスへ
TEL.03-5796-7320 FAX.03-5796-7325

Abstracts
The 30th Commemorative Fullerene-Nanotubes
General Symposium

第 30 回記念フラーレン・ナノチューブ
総合シンポジウム

講演要旨集

The Fullerenes and Nanotubes Research Society

The Chemical Society of Japan
Japan Society of Applied Physics

主催：フラーレン・ナノチューブ学会

共催：日本化学会

協賛：応用物理学会

Date: January 7th(Sat)~9th(Mon), 2006

Place: Meijo University

1-501 Shiogamaguchi, Tempaku-ku, Nagoya 468-8502

TEL: 052-832-1151

Presentation: Plenary Lecture (35 min presentation, 5min discussion)
Special Lecture (25 min presentation, 5min discussion)
General Lecture (10 min presentation, 5min discussion)
Poster Preview (1 min presentation, no discussion)

日時：平成 18 年 1 月 7 日（土）～9 日（月）

場所：名城大学

〒468-8502 愛知県名古屋市天白区塩釜口 1-501

TEL：052-832-1151

発表時間：基調講演	(発表 35 分・質疑応答 5 分)
特別講演	(発表 25 分・質疑応答 5 分)
一般講演	(発表 10 分・質疑応答 5 分)
ポスタープレビュー	(発表 1 分・質疑応答 なし)

展示団体御芳名(アイウエオ順、敬称略)

コスモ・バイオ(株)
 (株)島津製作所
 住友商事(株)
(株)ダイヤリサーチマーテック
 ナカライテスク(株)
 日本分光(株)
 フロンティアカーボン(株)
 (株)堀場製作所

広告掲載団体御芳名(アイウエオ順、敬称略)

オザワ科学(株)
 (株)化学同人
 コスモ・バイオ(株)
(株)サイエンスラボラトリーズ
 産業タイムズ社
 シグマ アルドリッチ ジャパン(株)
 (株)島津製作所
 住友商事(株)
(株)ダイヤリサーチマーテック
 (株)テクノ西村
 (株)東京インスツルメンツ
(株)東京プログレスシステム
 東レ(株)
 東洋炭素(株)
 ナカライテスク(株)
 日本電子(株)
 日本分析工業(株)
 (有)菱田商店
(株)日立ハイテクノロジーズ
 フロンティアカーボン(株)
 (株)堀場製作所
 (株)ラムダビジョン
 CAMPARI
 (有)新和
 まとい寿し
 めん処 うるぎ

Contents

Time Table	i
Chairperson	iii
Program	Japanese	iv
	English	xv
Abstracts	Plenary Lecture • Special lecture	1
	General lecture	7
	Poster preview	49
Author Index	191

目次

早見表	i
座長一覧	iii
プログラム	和文	iv
	英文	xv
講演予稿	基調講演・特別講演	1
	一般講演	7
	ポスター発表	49
発表索引	191

プログラム早見表

各項目敬称略

	1月7日(土)	1月8日(日)	1月9日(月)	
9:05	基調講演1 (大澤 映二) 9:05~9:50	特別講演3(Ales Mrzel) 9:00~9:30	特別講演5(畠 賢治) 9:00~9:30	9:00
9:50	一般講演3件 (ナノチューブの物性) 9:50~10:35	一般講演3件 (金属内包フラーレン) 9:30~10:15	一般講演3件 (ナノチューブ:生成と精製) 9:30~10:15	9:30
	休憩 10:35~10:50	休憩 10:15~10:30	休憩 10:15~10:30	
10:50	一般講演5件 (ナノチューブの物性) 10:50~12:05	一般講演3件 (金属内包フラーレン) 10:30~11:15	一般講演3件 (ナノチューブ:生成と精製2 件、ナノチューブ応用1件) 10:30~11:15	10:30
		一般講演3件 (フラーレンの化学) 11:15~12:00	一般講演3件 (ナノチューブ応用) 11:15~12:00	11:15
12:05	昼食 (12:05~13:20)	昼食 (12:00~13:20)		12:00
13:20	特別講演2(岡本 博) 13:20~13:50	授賞式 13:20~13:50	特別講演6(河合 孝純) 13:20~13:50	13:20
13:50	一般講演3件 (ナノチューブの物性) 13:50~14:35	特別講演4(橋本 久義) 13:50~14:20	一般講演3件 (ナノチューブ応用1件、ナノ チューブの物性2件) 13:50~14:35	13:50
	休憩 14:35~14:50	一般講演3件 (炭素ナノ粒子) 14:20~15:05	ポスタープレビュー 1分×44件 14:35~15:25	14:35
14:50	一般講演5件 (内包ナノチューブ3件、ナノ ホーン1件、その他1件) 14:50~16:05	休憩 15:05~15:20		
		一般講演2件(フラーレン固体) 15:20~15:50		15:25
16:05	ポスタープレビュー 1分×48件 16:05~16:55	ポスタープレビュー 1分×49件 15:50~16:40	ポスターセッション 15:25~16:55	
16:55	ポスターセッション 16:55~18:25	ポスターセッション 16:40~18:10		16:55
18:25				

1月7日(土)
チュートリアル 103講義室
15:00~16:30
講師 村山 英樹
(フロンティアカーボン(株)
副社長、開発センター長)

18:30~懇親会

基調講演 発表35分 質疑5分
特別講演 発表25分 質疑5分
一般講演 発表10分 質疑5分
ポスタープレビュー 発表1分 質疑なし

TIME TABLE

	Sat. Jan. 7	Sun. Jan. 8	Mon. Jan. 9
9:05	Plenary Lecture (Osawa) 9:05~9:50	Special Lecture (Ales Mrzel) 9:00~9:30	Special Lecture (Hata) 9:00~9:30
9:50	General Lecture[3] (Properties of Nanotubes) 9:50~10:35	General Lecture[3] (Metallofullerenes) 9:30~10:15	General Lecture[3] (Formation and Purification of Nanotubes) 9:30~10:15
	Break 10:35~10:50	Break 10:15~10:30	Break 10:15~10:30
10:50	General lecture[5] (Properties of Nanotubes) 10:50~12:05	General Lecture[3] (Metallofullerenes) 10:30~11:15	General Lecture[3] (Formation and Purification of Nanotubes, Application of Nanotubes) 10:30~11:15
		General Lecture[3] (Chemistry of Fullerenes) 11:15~12:00	General Lecture[3] (Application of Nanotubes) 11:15~12:00
12:05	Lunch (12:05~13:20)	Lunch (12:00~13:20)	
13:20	Special Lecture (Okamoto) 13:20~13:50	Awards Ceremony 13:20~13:50	Special Lecture (Kawai) 13:20~13:50
13:50	General Lecture[3] (Properties of Nanotubes) 13:50~14:35	Special Lecture (Hashimoto) 13: 50~14:20	General Lecture[3] (Application of Nanotubes, Properties of Nanotubes) 13:50~14:35
	Break 14:35~14:50	General Lecture[3] (Carbon Nanoparticles) 14:20~15:05	Poster Preview 1min x [44] 14:35~15:25
14:50	General Lecture[5] (Endohedral Nanotubes, Nanohorns, Miscellaneous) 14:50~16:05	Break 15:05~15:20	
		General Lecture[2] (Fullerene Solids) 15:20~15:50	Poster Session 15:25~16:55
16:05	Poster Preview 1min x [48] 16:05~16:55	Poster Preview 1min x [49] 15:50~16:40	
16:55	Poster Session 16:55~18:25	Poster Session 16:40~18:10	
18:25			

Sat. Jan. 7
Tutorial 103
15:00~16:30
Dr. Hideki Murayama

18:30~ Banquet
 Plenary Lecture 35min presentation, 5min discussion
 Special Lecture 25min presentation, 5min discussion
 General Lectures 10min presentation, 5min discussion
 Poster Preview 1min presentation, No discussion

座長一覧

1月7日(土)

(敬称略)

	時 間	座 長
基 調 講 演(大澤)	9:05 ~ 9:50	篠原 久典
一 般 講 演	9:50 ~ 10:35	大野 雄高
一 般 講 演	10:50 ~ 12:05	岡崎 俊也
特 別 講 演(岡本)	13:20 ~ 13:50	岩佐 義宏
一 般 講 演	13:50 ~ 14:35	丸山 茂夫
一 般 講 演	14:50 ~ 16:05	坂東 俊治
ポスタープレビュー	16:05 ~ 16:55	村上 陽一
ポスターセッション	16:55 ~ 18:25	竹延 大志

1月8日(日)

	時 間	座 長
特 別 講 演(Mrzel)	9:00 ~ 9:30	片浦 弘道
一 般 講 演	9:30 ~ 10:15	村田 靖次郎
一 般 講 演	10:30 ~ 11:15	兒玉 健
一 般 講 演	11:15 ~ 12:00	若原 孝次
特 別 講 演(橋本)	13:50 ~ 14:20	黒川 卓
一 般 講 演	14:20 ~ 15:05	小塩 明
一 般 講 演	15:20 ~ 15:50	岡田 晋
ポスタープレビュー	15:50 ~ 16:40	若林 知成
ポスターセッション	16:40 ~ 18:10	前田 優

1月9日(月)

	時 間	座 長
特 別 講 演(畠)	9:00 ~ 9:30	湯田坂 雅子
一 般 講 演	9:30 ~ 10:15	秋田 成司
一 般 講 演	10:30 ~ 11:15	吾郷 浩樹
一 般 講 演	11:15 ~ 12:00	鈴木 信三
特 別 講 演(河合)	13:20 ~ 13:50	斎藤 晋
一 般 講 演	13:50 ~ 14:35	菅井 俊樹
ポスタープレビュー	14:35 ~ 15:25	北浦 良
ポスターセッション	15:25 ~ 16:55	稲熊 正康

1月7日(土)

基調講演 発表35分・質疑応答5分
特別講演 発表25分・質疑応答5分
一般講演 発表10分・質疑応答5分
ポスタープレビュー 発表1分・質疑応答なし

開会の辞(9:00-9:05) 篠原久典

基調講演(9:05-9:50)

1S-1 ナノ炭素研究のあゆみ 大澤映二 1

一般講演(9:50-10:35)

ナノチューブの物性

1-1 様々な(n, m)ナノチューブの軸垂直励起による蛍光マッピング ○宮内雄平, 大場一輝, 丸山茂夫 7

1-2 単層カーボンナノチューブにおける発光と共鳴ラマン分光強度のファミリーパターン
○齋藤理一郎, J. Jiang, 佐藤健太郎, 小山祐司 8

1-3 局所応力場におけるカーボンナノチューブのナノラマン分光 ○矢野隆章, 井上康志, 河田聡 9

☆☆☆☆☆☆ 休憩 (10:35-10:50) ☆☆☆☆☆☆

一般講演(10:50-12:05)

ナノチューブの物性

1-4 単層カーボンナノチューブフォトルミネッセンスのカイラリティに依存した環境効果
○岩崎真也, 大野雄高, 村上陽一, 岸本茂, 丸山茂夫, 水谷孝 10

1-5 紫外光照射によって生ずる単層カーボンナノチューブのギャップ内発光中心
○ヤクボブスキー・コンスタンチン, 南 信次, 金 柄社, 宮下香苗, カザウィ・サイ, ナリニ・バラクリシュナン 11

1-6 Single walled carbon nanotube analysis: Rapid, robust acquisition and simulation of quantum and chiral maps to ease structural assignments. ○Adam M. Gilmore, Ray K. Kaminsky, James M. Mattheis 12

1-7 2層カーボンナノチューブの非線形光学応答と緩和ダイナミクス
○中村新男, 富川貴子, 今村禎允, 渡辺美樹, 濱中泰, 齋藤弥八, 吾郷浩樹 13

1-8 直流電場で誘起されたカーボンナノチューブ散逸構造への重力の影響 佐藤修一, ○佐野正人 14

☆☆☆☆☆☆ 昼食 (12:05-13:20) ☆☆☆☆☆☆

特別講演(13:20-13:50)

1S-2 単層カーボンナノチューブの超高速非線形光学応答 岡本博 2

一般講演(13:50-14:35)

ナノチューブの物性

1-9 SiC上に形成された高密度・高配向カーボンナノチューブの機械的特性
○楠美智子, 宇佐美肇彦, 伊岐見大輔, 三宅晃司 15

1-10 硬X線光電子分光法を用いたカーボンナノチューブとチタン電極界面の電子状態の研究
○近藤大雄, 二瓶瑞久, 川端章夫, 佐藤信太郎, 池永英司, 小島雅明, 金正鎮, 小林啓介, 小宮聡, 栗野祐二 16

1-11 カーボンナノチューブ片持ち梁の振動解析 ○秋田成司, 澤谷慎太郎, 中山喜萬 17

☆☆☆☆☆☆ 休憩 (14:35-14:50) ☆☆☆☆☆☆

一般講演(14:50-16:05)

内包ナノチューブ

1-12 第一原理計算によるPeapodのRBM ○岡田晋 18

1-13 鉄内包単層カーボンナノチューブの合成と電気特性計測
○李永峰, 島山力三, 金子俊郎, 泉田健, 岡田健, 加藤俊顕 19

1-14 単層カーボンナノチューブに内包された β カロテンの光学特性 ○柳和宏, 宮田耕充, 片浦弘道 20

ナノホーン

- 1-15 穴の開いたナノホーンの酢酸ガドリニウムによるキャップ効果 21
○弓削亮太, 宮脇仁, 湯田坂雅子, 久保佳実, 中村栄一, 磯部寛之, 依光英樹, 飯島澄男

その他：カーボンナノファイバー

- 1-16 円錐形ナノ空洞配列構造を有するカーボンナノファイバーの形成とその節での切断 22
○小塩明, 竹村雄太, 小海文夫

ポスタープレビュー(16:05-16:55)

ポスターセッション(16:55-18:25)

フラーレンの化学

- 1P-1 金ナノ粒子を介したフラーレン誘導体によるナノ薄膜の作製と特性 ○池田典昭, 朴鐘震, 森山広思 49
- 1P-2 水溶液中における電極上の膜中に取り込まれた開口C₆₀の電気化学 50
○小松真治, 渡辺健一, 石橋歩, 新留康郎, 村田理尚, 村田靖次郎, 小松紘一, 中嶋直敏
- 1P-3 新規C₆₀-TTP複合分子システムの合成と性質 ○池内貴宏, 宮本久一, 御崎洋二 51
- 1P-4 オリゴカルバズール部位を有する[60]フラーレン付加体の合成と性質 52
○今野高志, 中村洋介, 渡辺悟, 鈴木正人, 西村淳
- 1P-5 金微粒子を反応指示剤とするカーボンナノチューブの化学修飾の確認 53
○畔原宏明, 笠沼由香, 岡嶋孝治, 藤枝正, 安田俊夫, 廣岡誠之, 日高貴志夫, 林原光男, 徳本洋志
- 1P-6 酸素に結合したフラーレン誘導体の合成, 光物理的挙動および一重項酸素の発生成 54
○本間猛, 原拓生, 田島右副, 星野幹雄, 松本史朗, 武内一夫
- 1P-7 極性溶媒に高溶解性を示すフラーレン誘導体 ○川上公德, 遠田淳 55
- 1P-8 水素分子を内包した有機および有機金属フラーレン 56
○松尾豊, 磯部寛之, 田中隆嗣, 村田靖次郎, 村田理尚, 小松紘一, 中村栄一

金属内包フラーレン

- 1P-9 Gd@C₉₂のイオン化と化学修飾 ○河野孝佳, 松永洋一郎, 仲程司, 土屋敬広, 若原孝次, 前田優, 赤阪健, 大窪清吾, 加藤立久, 溝呂木直美, 小林郁, 永瀬茂 57
- 1P-10 La@C₇₄(C₆H₃Cl₂)-IIの単離および構造解析 ○菊池隆, 二川秀史, 若原孝次, 仲程司, 土屋敬広, 赤阪健, G. M. Aminur Rahman, 前田優, 与座健治, Ernst Horn, 溝呂木直美, 永瀬茂 58
- 1P-11 Gd₂@C₇₈の単離とキャラクタリゼーション 59
○竹松裕司, 河野孝佳, 仲程司, 土屋敬広, 若原孝次, 前田優, 赤阪健, 加藤立久
- 1P-12 Ce@C₈₂アニオンのランタノイド誘起NMRシフト解析 60
○山田道夫, 若原孝次, 廉永福, 土屋敬広, 赤阪健, マーカスヴェルヒリ, 溝呂木直美, 永瀬茂
- 1P-13 Luジメタロフラーレンの系統的研究: Lu₂C_{2n} (2n=74-86)の合成・単離・分子構造に関する研究 61
○梅本久, 井上崇, 富山徹夫, 北浦良, 菅井俊樹, 篠原久典

フラーレン固体

- 1P-14 トップダウン的手法によるフラーレンナノ粒子の生成 ○出口茂, 向井貞篤, 掘越弘毅 62
- 1P-15 三元系C₆₀化合物の構造と物性 ○何木隆史, 本橋寛, 緒方啓典 63
- 1P-16 ドデシル基を有するC₆₀誘導体塗布膜の有機TFT特性 64
○近松真之, 板倉篤志, 吉田郵司, 阿澄玲子, 菊地耕一, 八瀬清志
- 1P-17 高次フラーレンとその関連化合物の電子特性 65
○杉山博行, 長野高之, 今井久美子, 草井悠, 藤原明比古, 竹延大志, 岩佐義宏, 久保園芳博

炭素ナノ粒子

- 1P-18 放射性廃棄物に含まれる元素のカーボンナノカプセルへの内包に関する研究 ○山本和典 66
- 1P-19 中心に希土類金属炭化物を含有する多面体グラファイト粒子の生成 67
○小林慶太, 小塩明, 中川建雄, 小海文夫

ナノチューブ：生成と精製

1P-20	狭いカイラリティ分布のSWNTバルクACCVd合成 ○丸山茂夫, 宮内雄平, 嶋田行志, 村上陽一, 佐藤謙一, 尾関雄治, 吉川正人	68
1P-21	超音波霧化を用いた単層カーボンナノチューブ環状集合体の濃縮分離 ○小松直樹, 島脇孝典, 青沼秀児, 木村隆英	69
1P-22	ACCVd法による垂直配向SWNT膜の成長に関する最近の成果 ○エリック・エイナルソン, 門脇政幸, 村上陽一, 丸山茂夫	70
1P-23	過酸化水素による半導体カーボンナノチューブの選択的酸化 ○宮田耕充, 真庭豊, 片浦弘道	71
1P-24	RFプラズマCVDによるカーボンナノチューブの成長-触媒膜の前処理による成長温度の低温化 ○坂井孝充, 鈴木篤, 佐藤英樹, 畑浩一, 齋藤弥八	72
1P-25	アルコールCCVD法によるカーボンナノチューブの低温成長 ○日浅健, 中北剛史, 佐藤英樹, 畑浩一, 齋藤弥八	73
1P-26	垂直配向孤立単層カーボンナノチューブ形成におけるプラズマシース効果 ○加藤俊顕, 畠山力三, 田路和幸	74
1P-27	2層カーボンナノチューブの作製と精製 ○松本和代, 村上俊哉, 木曾田賢治, 一色俊之, 播磨弘	75
1P-28	単層カーボンナノチューブ作製における多孔質ガラスの内径効果 ○青木陽介, 鈴木信三, 片浦弘道, 長澤浩, 阿部久雄, 阿知波洋次	76
1P-29	H ₂ -Arガス中アーク放電におけるSWNTs成長でのCH ₄ , C ₂ H ₄ , C ₂ H ₂ 添加の影響 ○北村俊哉, 趙新洛, 井上栄, 安藤義則	77

内包ナノチューブ

1P-30	金属原子2個内包フラーレン・ピーポッドの選択的合成 ○石田将史, 西出大亮, 井上崇, 北浦良, 菅井俊樹, 篠原久典	78
1P-31	大きな直径の炭素ナノチューブにおけるC ₆₀ の内包と放出 ○范晶, 湯田坂雅子, 弓削亮太, 二葉ドン, 島賢治, 飯島澄男	79

ナノホーン

1P-32	酸化鉄ナノ粒子ラベルによる単層カーボンナノホーンの生体内磁気共鳴イメージング ○宮脇仁, 湯田坂雅子, 今井英人, 依光英樹, 磯部寛之, 中村栄一, 飯島澄男	80
1P-33	単層カーボンナノホーンの開口端構造が及ぼすシスプラチン放出への影響 ○安嶋久美子, 湯田坂雅子, アランメニエ, 宮脇仁, 飯島澄男	81

ナノチューブの物性

1P-34	分子動力学シミュレーションによる有限長SWNTのフォノン輸送 ○塩見淳一郎, 丸山茂夫	82
1P-35	GW近似のグラファイトのエネルギーバンドによるカタウラプロット ○大場一輝, 岡田晋, 三宅隆, 丸山茂夫	83
1P-36	AFMを用いたカーボンナノチューブ分散溶液の評価法 ○桑原彰太, 菅井俊樹, 篠原久典	84
1P-37	近接場ラマン分光で単層カーボンナノチューブを見る ○齊藤結花, 村上貴, 早澤紀彦, 片浦弘道, 河田聡	85
1P-38	DNAで包まれた単層カーボンナノチューブにおけるBreit-Wigner-Fano型ラマン線の特性 ○河本紘典, 内田貴司, 橋勝, 小島謙一	86
1P-39	ミセル内に可溶化された半導体単層カーボンナノチューブのビオローゲン添加によるバンドギャップ変化 ○松浦宏治, 齋藤毅, 岡崎俊也, 大嶋哲, 湯村守雄, 飯島澄男	87
1P-40	Si(111)間に挟まれた有限長CNTの電流・電圧特性の理論的研究 ○小林由和, 大森滋和, 笹野博之, 田中一義	88
1P-41	光照射によるカーボンナノチューブの損傷 ○鈴木哲, 前田文彦, 小林慶裕	89

ナノチューブの応用

1P-42	VUVドライブプロセスによるマルチウォールカーボンナノチューブの化学修飾 ○浅野高治, 近藤大雄, 川端章夫, 武井文雄, 二瓶瑞久, 栗野祐二	90
1P-43	カーボンナノチューブFETを用いた抗原センサーの作製 ○谷健太郎, 伊藤博史, 大野雄高, 岸本茂, 大河内美奈, 本多裕之, 水谷孝	91
1P-44	有機蛍光膜を用いた2極型電界放出ディスプレイのためのカーボンナノチューブ電子放出源の簡易作製 ○岩田展幸, 畑裕道, 吉國雅人, 山本寛	92

1月7日(土)

1P-45	垂直配向SWNT膜の簡便な配向維持剥離法および任意表面への再付着法の開発 ○村上陽一, 門脇政幸, エリックエイナルソン, 丸山茂夫	93
1P-46	垂直配向ナノチューブを用いたマイクロリアクター ○石神直樹, 吾郷浩樹, 本山幸弘, 高崎幹大, 品川直嗣, 高橋厚史, 辻正治	94
その他		
1P-47	カーボンナノウォールの成長と構造評価 ○吉村博史, 吉村昭彦, モリナ・モラレス・ペドロ, 中井宏, 小島謙一, 橘勝	95
1P-48	発煙硝酸中のニトロラジカルによるカーボンナノチューブの表面修飾 ○水野杏三, 関戸大, 大野正富	96

1月8日(日)

特別講演 発表25分・質疑応答5分
一般講演 発表10分・質疑応答5分
ポスタープレビュー 発表1分・質疑応答なし

特別講演(9:00-9:30)

- 2S-3 Subnanometer Diameter Nanowires and Nanotubes in the ternary molybdenum-chalcogen-halogen system 3
○Aleš Mrzel, Dragan Mihailović, Maja Remškar, Abdou Hassaien, Hiromichi Kataura

一般講演(9:30-10:15)

金属内包フラーレン

- 2-1 Sc_3C_{82} の構造決定 ○飯塚裕子, 若原孝次, 仲程司, 土屋敬広, 櫻庭明央, 前田優, 赤阪健, 与座健治, Ernst 23
Horn, 加藤立久, Michael T. H. Liu, 溝呂木直美, 小林郁, 永瀬茂
- 2-2 金属内包フラーレンと有機ドナーに基づく可逆なスピン移動システムの構築 ○佐藤久美子, 土屋敬 24
広, 若原孝次, 前田優, 仲程司, 赤阪健, 加藤立久, 大久保敬, 福住俊一, 溝呂木直美, 小林郁, 永瀬茂
- 2-3 ^{13}C NMRによるCeLa@ C_{80} アニオンの研究 25
○小牧友人, 兒玉健, 三宅洋子, 鈴木信三, 菊地耕一, 阿知波洋次

☆☆☆☆☆☆ 休憩 (10:15-10:30) ☆☆☆☆☆☆

一般講演(10:30-11:15)

金属内包フラーレン

- 2-4 軟X線磁気円二色性を用いたEr内包フラーレンの元素選択磁気測定 26
○沖本治哉, 中村哲也, 北浦良, 山田貴之, 北村豊, 松下智裕, 室隆柱之, 井上崇, 菅井俊樹, 七尾進, 篠原久典
- 2-5 $Ti_2C_2@C_{82}$ の紫外光電子分光 27
○加藤真之, 岩崎賢太郎, 日野照純, 吉村大介, 森部裕江, 沖本治哉, 伊藤靖浩, 菅井俊樹, 篠原久典
- 2-6 溶媒からの電子移動によるEr@ C_{82} の蛍光スイッチング ○大窪清吾, 岡崎俊也, 飯島澄男 28

一般講演(11:15-12:00)

フラーレンの化学

- 2-7 基底状態フラーレンへの脂肪族アミンからの一電子移動を利用したテトラアミノフラーレンエポキシドの 29
効率的合成 ○田中隆嗣, 中西和嘉, ロイック・ルミエグレ, 磯部寛之, 中村栄一
- 2-8 水素分子を内包したフラーレン C_{70} の合成 ○村田靖次郎, 前田修平, 村田理尚, 小松紘一 30
- 2-9 フラーレン誘導体添加によるアクリル系ポリマーの分解制御 31
○山舗智也, 田島右副, 櫻井敏彦, 島田良子, 大背戸浩樹

☆☆☆☆☆☆ 昼食 (12:00-13:20) ☆☆☆☆☆☆

授賞式(13:20-13:50)

特別講演(13:50-14:20)

- 2S-4 町工場こそ日本の宝。中国でできること、できないこと。 橋本久義 4

一般講演(14:20-15:05)

炭素ナノ粒子

- 2-10 X線回折法による爆発法ナノダイヤモンドの定量 小松直樹, ○門田直樹, 木村隆英, 大澤映二 32
- 2-11 溶液中のポリイン分子の分離および同定 ○若林知成, 土井達也, 梅田暎, 園田素啓, 戸部義人 33
- 2-12 ナノダイヤモンドのアニオン転移に対するマトリックス効果 ○小澤理樹, 稲熊正康, 高橋慎, 大澤映二 34

☆☆☆☆☆☆ 休憩 (15:05-15:20) ☆☆☆☆☆☆

1月8日(日)

一般講演(15:20-15:50)

フラーレン固体

- 2-13 トリフェニルメタン系色素によって安定化された孤立分子のC₆₀フラーライド塩の単結晶構造解析 35
○杉浦崇仁, 大澤映二, 森山広思
- 2-14 走査トンネル顕微鏡探針からの電子/正孔注入によるC₆₀分子のポリマー化 36
○野内亮, 増成宏介, 大田敏雄, 久保園芳博

ポスタープレビュー(15:50-16:40)

ポスターセッション(16:40-18:10)

フラーレンの化学

- 2P-1 C₆₀による含硫黄ヘテロ環状カルベンの捕捉 ○二川秀史, 仲程司, 土屋敬広, 若原孝次, G. M. Aminur 97
Rahman, 赤阪健, 前田優, Michael T. H. Liu, 目黒聡, 久新莊一郎, 松本英之, 溝呂木直美, 永瀬茂
- 2P-2 七重付加型フラーレン遷移金属錯体の合成と構造 ○藤田健志, 松尾豊, 中村栄一 98
- 2P-3 フラーレンC₆₀およびC₇₀とジアリールジアゾメタンの1,3-双極子反応における速度論 99
○北村啓, 清家望, 東帝治郎, 小久保研, 大島巧
- 2P-4 五重付加型[60]フラーレン-ルテニウム錯体とキラルジホスフィンによるジアステレオ選択的な金属錯体 100
合成 ○三谷友一, 松尾豊, 鐘羽武, 中村栄一
- 2P-5 C₆₀骨格を有するアミノ基修飾試薬のMALDI-TOF MS分析への応用 101
○津元裕樹, 高橋克昌, 幸田光復, 鈴木孝禎, 中川秀彦, 宮田直樹
- 2P-6 フラーレンのメカノケミカル水酸化反応のメカニズム ○久保貴裕, 松井栄太郎, 渡辺洋人, 仙名保 102
- 2P-7 n-hexane中のC₇₀の溶解度におよぼす温度、圧力効果 ○岡田真一, 澤村精治 103
- 2P-8 新規メタノ[60]フラーレンの合成と反応 ○多田智之, 石田康博, 西郷和彦 104

金属内包フラーレン

- 2P-9 SPring-8における金属内包フラーレンの粉末構造研究の最近の進展 105
○西堀英治, 寺内伊久哉, 石原将行, 高田昌樹, 坂田誠, 伊藤靖浩, 梅本久, 森部弘江, 井上崇, 篠原久典
- 2P-10 LaNd@C₇₂の合成とNd内包フラーレンの蛍光測定 106
○村田真美, 兒玉健, 三宅洋子, 鈴木信三, 菊地耕一, 阿知波洋次
- 2P-11 Reactivity of La₂@C₇₈ toward 2-Admantane-2,3-Diazirine: Structure Determination of Monoadduct La₂@C₇₈-(Ad) (I) 107
○Baopeng Cao, Tsukasa Nakahodo, Takatsugu Wakahara, Takahiro Tsuchiya, Kaoru Kobayashi, Shigeru Nagase, Takeshi Akasaka
- 2P-12 トルエン中におけるLa@C₈₂のラジカル反応 108
○高野勇太, 蓬田知行, 若原孝次, 土屋敬広, 仲程司, 前田優, 赤阪健, 加藤立久, 溝呂木直美, 永瀬茂
- 2P-13 高純度H₂@C₆₀の構造と物性 ○赤田美佐保, 谷垣勝己, 村田靖次郎, 小松絃一, 垣内徹, 澤博 109

フラーレン固体

- 2P-14 フラーレン・ナノウイスカーの構造(Ⅲ) ○土田諭, 本橋覚, 緒方啓典 110
- 2P-15 フレロイドナノウイスカーの合成と構造 ○本橋覚, 土田諭, 緒方啓典 111
- 2P-16 C₆₀単結晶における光キャリア生成とその輸送過程 ○田中領太, 秋元郁子, 神野賢一 112
- 2P-17 C₆₀ナノ・ウイスカー FETの作製と電気伝導特性 113
○小川健一, 池上亜紗土, 都司一, 加藤友裕, 青木伸之, 足立健治, 飯田貞博, 落合勇一

炭素ナノ粒子

- 2P-18 電気化学法によるカーボンナノホーンへの白金粒子担持とその磁性 114
○菅谷基広, 稲垣貴之, 湯田坂雅子, 坂東俊治, 飯島澄男
- 2P-19 ナノ炭素材料への高エネルギーイオン/原子衝突のシミュレーション:電子系の励起と構造変化 115
○宮本良之, Arkady Krashennnikov, David Tomanek

ナノチューブ:生成と精製

- 2P-20 スーパーグロース法を用いた二層カーボンナノチューブの比率制御 116
○山田健郎, 生井竜紀, 島賢治, 范晶, 湯田坂雅子, 二葉ドン, 水野耕平, 湯村守男, 飯島澄男

2P-21	一酸化炭素からの単層カーボンナノチューブ合成に与えるCo/Mo比の影響 ○西井俊明, 野田優, 杉目恒志, 榊山直人, 村上陽一, 丸山茂夫	117
2P-22	分散を用いた2層カーボンナノチューブの精製 ○吉田宏道, 菊池聡史, 菅井俊樹, 篠原久典	118
2P-23	異なる細孔径をもつメソポーラスシリカを用いたアルコールCCVD法による単層カーボンナノチューブの合成 ○泉裕也, 緒方啓典	119
2P-24	直径の小さい単層カーボンナノチューブの分散と分離 ○神田信, 前田優, 木村新一, 長谷川正, Yongfu Lian, 若原孝次, 赤阪健, Said Kazaoui, 南信次, 岡崎俊也, 清水哲夫, 徳本洋志, Jing Lu, 永瀬茂	120
2P-25	アルコールの触媒分解による単層ナノチューブの合成と特性 ○趙彦立, 世古和幸, 奥村健介, 齋藤弥八	121
2P-26	単原子層以下のNi担持による単層カーボンナノチューブの触媒成長 ○寛和憲, 野田優, 千足昇平, 丸山茂夫	122
2P-27	窒素雰囲気中におけるRh/Pd炭素混合ロッドを用いた単層カーボンナノチューブの作製 ○朝井信行, 鈴木信三, 片浦弘道, 阿知波洋次	123
2P-28	単層カーボンナノチューブ成長に用いる混合触媒の役割 ○村上俊也, 道上一也, 石垣悟, 松本和代, 木曾田賢治, 西尾弘司, 一色俊之, 播磨弘	124
2P-29	熱分解によるSiC(000-1)面上へのカーボンナノキャップ形成過程 ○丸山隆浩, 河村康之, H. Bang, 藤田奈緒美, 白岩倫行, 谷奥健次, 穂積葉子, 成塚重弥, 楠美智子	125

内包ナノチューブ

2P-30	単層カーボンナノチューブへのパラニトロアニリンの内包 ○村上貴, 齋藤結花, 片浦弘道, 塚越一仁, 柳和宏, 宮田耕充, 河田聡	126
2P-31	セシウムプラズマ照射法によるn型二層カーボンナノチューブの形成 ○李永峰, 泉田健, 島山力三, 金子俊郎, 岡田健, 加藤俊顕	127
2P-32	軟X線磁気円偏光2色性測定によるナノピーボットの磁化解析 ○北浦良, 沖本治哉, 中村哲也, 北村豊, 小川大輔, 篠原久典	128

ナノホーン

2P-33	カーボンナノホーンの高収率精製方法 ○田村豪主, 坂東俊治, 飯島澄男	129
2P-34	アークスートの分別とPt-Ru触媒の分散(メタノール活性) ○東敬亮, 丹羽宏彰, 篠原賢司, 滝川浩史, 榊原建樹, 徐国春, 伊藤茂生, 山浦辰雄, 三浦光治, 吉川和男	130

ナノチューブの物性

2P-35	カーボンナノチューブからの電界放出電流における安定性 ○小西康元, 田中博由, 潘路軍, 秋田成司, 中山喜萬	131
2P-36	望遠鏡構造の2層アームチューブの電気伝導度 ○田村了	132
2P-37	STMによる2層カーボンナノチューブの層間相互作用の直接観察 ○福井信志, 吉田宏道, 菅井俊樹, 平家誠嗣, 藤森正成, 諏訪雄二, 寺田康彦, 橋詰富博, 篠原久典	133
2P-38	ゼオライトCCVDにより合成した直径の細いDWNTからのフォトルミネッセンス観察 ○岸直希, 菊地聡史, 菅井俊樹, 篠原久典	134
2P-39	THz~可視領域に亘る偏光分光を用いたカーボンナノチューブの形状効果をもたらす光学特性の発見 ○秋間新真, J.L. Musfeldt, 松井広志, 豊田直樹, 下田英雄, O. Zhou, 白石誠司, 岩佐義宏	135
2P-40	Exciton-photon matrix elements in single-wall carbon nanotubes ○J. Jiang, 齋藤 理一郎, 小山 祐司, 佐藤 健太郎, J. S. Park	136
2P-41	水素原子を内包した有限長カーボンナノチューブにおける電子的、磁氣的性質 ○二川原賢啓, 大森滋和, 伊藤彰浩, 田中一義	137
2P-42	セラミクス内部に孤立した単層カーボンナノチューブの共鳴ラマン・蛍光スペクトル ○上野太郎, 大窪清吾, 宮原恒昱, 鈴木信三, 阿知波洋次, 塚越一仁, 岡崎俊也, 片浦弘道	138

ナノチューブの応用

2P-43	アミン分子修飾による大気中で安定なN型単層カーボンナノチューブ電界効果トランジスタの作製 ○松本哲憲, 鈴木哲, Goo-Hwan Jeong, 小林慶裕, 本間芳和	139
2P-44	カーボンナノチューブフィールドエミッタを用いたマイクロフォーカスX線源の開発 ○川北邦彦, 畑浩一, 佐藤英樹, 齋藤弥八	140
2P-45	バイオサーファクタントを用いたSWNTsの可溶化と特性評価 ○中嶋直敏, 石橋歩	141

1月8日(日)

2P-46	SWNTs溶液への近赤外レーザー照射	○成松香織, 篠原浩美, 新留康郎, 中嶋直敏	142
2P-47	マイクロチップ内部でのSWNTの誘電泳動	○品川直嗣, 吾郷浩樹, 石神直樹, 辻正治, 生田竜也, 高橋厚史	143
その他			
2P-48	金属触媒を用いない螺旋状炭素構造の形成	○小塩明, 田中輝之, 須内俊貴, 小海文夫	144
2P-49	フラーレン多価イオンクラスターの臨界サイズ	○中村正人, P.A. Hervieux	145

1月9日(月)

特別講演 発表25分・質疑応答5分
一般講演 発表10分・質疑応答5分
ポスタープレビュー 発表1分・質疑応答なし

特別講演(9:00-9:30)

- 3S-5 スーパーグロース:超効率高純度単層カーボンナノチューブの合成からスーパーキャパシターへの応用 5
島賢治

一般講演(9:30-10:15)

ナノチューブ:生成と精製

- 3-1 レーザー加熱ACVD法におけるSWNTs生成過程のその場ラマン・AFM観察 37
○千足昇平,村上陽一,宮内雄平,丸山茂夫
- 3-2 アルゴン及び窒素ガス雰囲気中における単層カーボンナノチューブの生成 38
○鈴木信三,朝井信行,片浦弘道,阿知波洋次
- 3-3 サファイア表面での水平配向SWNTの密度制御合成と偏光ラマン分光 39
○吾郷浩樹,上原直保,池田賢一,大堂良太,中村和浩,辻正治

☆☆☆☆☆☆ 休憩 (10:15-10:30) ☆☆☆☆☆☆

一般講演(10:30-11:15)

ナノチューブ:生成と精製

- 3-4 直流アーク放電法による二層ナノチューブの合成における典型金属元素添加の効果 ○稲倉秀樹 40
- 3-5 直噴熱分解合成法による単層カーボンナノチューブの選択的直径制御 41
○斎藤毅,大嶋哲,許維春,松浦宏治,岡崎俊也,湯村守雄,飯島澄男

ナノチューブの応用

- 3-6 スーパーグロース法を用いた形状制御可能なシングルウォールナノチューブ固体フレキシブル導電性 42
メソポーラス材料- ○二葉ドン,島賢治,平岡樹,山田健郎,水野耕平,早水裕平,生井竜紀,角館洋三,
棚池修,羽鳥浩章,三宅晃司,佐々木信也,湯村守男,飯島澄男

一般講演(11:15-12:00)

ナノチューブの応用

- 3-7 カーボンナノチューブのフッ素化、構造と性質 43
○東原秀和,有海英樹,野島由雄,沖野不二雄,金降岩,遠藤守信,川崎晋司,片浦弘道,湯田坂雅子,飯島澄男
- 3-8 カーボンナノチューブポリイミド複合材料を用いた非線形光導波路デバイス 44
○松崎瞬,板谷太郎,糸賀恵美子,井草正寛,片浦弘道,徳本圓,石田興太郎,榊原陽一
- 3-9 液相法によるカーボンナノチューブ透明フレキシブルトランジスタ 45
○高橋哲生,竹延大志,菅原孝宜,塚越一仁,青柳克信,岩佐義宏

☆☆☆☆☆☆ 昼食 (12:00-13:20) ☆☆☆☆☆☆

特別講演(13:20-13:50)

- 3S-6 ナノ炭素構造における様々な欠陥構造の生成と特性に関する分子動力学シミュレーション 河合孝純 6

一般講演(13:50-14:35)

ナノチューブの応用

- 3-10 ポリイミドを用いたカーボンナノチューブの孤立可溶化 ○重田眞宏,小松真治,中嶋直敏 46

ナノチューブの物性

- 3-11 メビウス形状ナノ炭素系における電子物性 ○針谷喜久雄 47
- 3-12 カーボンナノチューブにおけるバンドギャップと準粒子状態 三宅隆,赤井吉郎,○斎藤 晋 48

1月9日(月)

ポスタープレビュー(14:35-15:25)

ポスターセッション(15:25-16:55)

フラーレンの化学

- 3P-1 C_{60} と環状有機ケイ素化合物の光反応 146
○永塚淳子, 仲程司, 杉谷幸愛, 加田昌寛, 若原孝次, 前田優, 土屋敬広, 赤阪健, 佐々木佳子, 伊藤攻, 小林郁, 永瀬茂
- 3P-2 フラーレン多付加体の効率的な探索戦略:円錐積込法 ○樋田竜男, 内田勝美, 石井忠浩, 矢島博文 147
- 3P-3 フラーレン・キトサン複合体の合成とその抗酸化作用評価 ○根本勝理, 指輪仁之, 内田勝美, 矢島博文 148
- 3P-4 高水溶性フラーレノールのOnePot合成 ○立垣裕史, 川濱咲耶子, 松林賢司, 高田弘弥, 小久保研, 大島巧 149
- 3P-5 イリジウムを用いたC-H結合活性化による五重付加型フラーレンのアルキル化反応 150
○岩下暁彦, 松尾豊, 中村栄一
- 3P-6 神経成長因子によって誘導されるPC-12細胞の神経突起伸長に対する水溶性フラーレン誘導体の増強作用 151
○川原翔, 藤澤祐樹, 津元裕樹, 幸田光復, 鈴木孝禎, 中川秀彦, 宮田直樹
- 3P-7 フラーレンのメカノケミカル酸素酸化反応のメカニズム ○渡辺洋人, 松井栄太郎, 久保貴裕, 仙名保 152
- 3P-8 オープンケージ C_{60} 構造をもつ新規 C_{60} -フタロシアニン複合体の合成 ○橋本直明, 福田貴光, 小林長夫 153

金属内包フラーレン

- 3P-9 $Eu@C_{82}$ と $Gd@C_{82}$ の構造 ○溝呂木直美, 永瀬茂 154
- 3P-10 金属内包フラーレン成長機構 I I ○阿知波洋次 155
- 3P-11 $La@C_{82}(Ad)$ 単結晶のESRスペクトル 156
○奈良隆平, 前田優, 若原孝次, 土屋敬広, 竹内一宏, 福島誠, 赤阪健, 加藤立久
- 3P-12 $La_9@C_{80}$ カルベン誘導体の合成とキャラクターゼーション 157
○染谷知香, 山田道夫, 若原孝次, 土屋敬広, 前田優, 赤阪健, 溝呂木直美, 永瀬茂
- 3P-13 イオン移動能法によるスカンジウム内包フラーレンの研究 ○菅井俊樹, M.F.Jarrold, 篠原久典 158

フラーレン固体

- 3P-14 溶液プロセスで作製した C_{60} -Pdポリマー薄膜トランジスタの特性 159
○松岡亨卓, ケルマンカーン, 民谷栄一, 藤原明比古
- 3P-15 高機能フラーレン電界効果トランジスターデバイスの作製とパフォーマンス制御 160
○長野高之, 越智謙次, 草井悠, 大田敏雄, 今井久美子, 藤原明比古, 久保園芳博
- 3P-16 自己組織化単分子膜による有機FET電極表面修飾 廣芝伸哉, 石井久夫, 熊代良太郎, ○谷垣勝己 161
- 3P-17 溶液プロセスによるフラロドンドロン電界効果トランジスタの作製とその電子特性 162
○草井悠, 長野高之, 今井久美子, 久保園芳博, 酒向祐輝, 高口豊, 藤原明比古

炭素ナノ粒子

- 3P-18 ポリイン分子の共鳴ラマンスペクトル 土井達也, ○若林知成 163

ナノチューブ:生成と精製

- 3P-19 The ultrasonication power density effects on carbon nanotube dispersion in aqueous solutions 164
○カタリン ロメオ オルクレスク, 石井亨, 高橋照史, 内田勝美, 石井忠浩, 矢島博文
- 3P-20 単層カーボンナノチューブの高収率合成に向けたCVDプロセスのガス分析 165
○上原直保, 吾郷浩樹, 今村真悟, 辻正治
- 3P-21 アークプラズマジェット法で作製した単層カーボンナノチューブの精製 166
○鈴木智子, 州浜賢二, 趙新洛, 井上栄, 安藤義則
- 3P-22 Siナノ突起構造を形成した基板上へのカーボンナノチューブ成長 167
○松林摩衣, 佐藤英樹, 畑浩一, 三宅秀人, 平松和政, 大下昭憲, 齋藤弥八
- 3P-23 生体高分子溶液中における単層カーボンナノチューブの分散挙動と分光特性 168
○高橋照史, Catalin Romeo Luculescu, 内田勝美, 石井忠浩, 矢島博文
- 3P-24 金属層上に選択成長した垂直配向カーボンナノチューブ ○奥山博基, 岩田展幸, 山本寛 169
- 3P-25 Fe触媒を含む炭素電極を用いたカーボンナノワイヤーの作製 ○遠藤正明, 水谷昭彦, 趙新洛, 安藤義則 170

内包ナノチューブ

- 3P-26 電子線照射下におけるPeapod中のC₆₀の融合 ○越野雅至, 末永和智, 中村栄一 171

ナノホーン

- 3P-27 高純度カーボンナノホーン大量生成 ○蒔丈史, 糟屋大介, 吉武務, 久保佳実, 湯田坂雅子, 飯島澄男 172

ナノチューブの物性

- 3P-28 カーボンナノチューブの塑性変形メカニズム ○森英喜, 尾方成信, 秋田成司, 中山喜萬 173
- 3P-29 シリル基修飾したカーボンナノチューブのFET特性
○熊代良太郎, 大橋弘孝, 赤坂健, 前田優, 泉田健, 島山力三, 谷垣勝己 174
- 3P-30 孤立単層カーボンナノチューブにおける120テスラまでの強磁場磁気光学的研究
○横井裕之, 黒田規敬, 金柄祉, 宮下香苗, カザウイ・サイ, 南信次, 小嶋映二, 内田和人, 嶽山正二郎 175
- 3P-31 架橋単層カーボンナノチューブからのPL/ラマンスペクトルにおける環境効果
○小林慶裕, 高木大輔, 本間芳和 176
- 3P-32 単層カーボンナノチューブバンドルにおけるレーザー誘起欠陥のラマン分光による評価
○内田貴司, 橋勝, 小島謙一 177
- 3P-33 二層カーボンナノチューブの光物性
○上野太郎, 大窪清吾, 宮原恒昱, 鈴木信三, 阿知波洋次, 岡崎俊也, 塚越一仁, 片浦弘道 178
- 3P-34 ビーボッドのリチウムイオン貯蔵特性 ○川崎晋司, 岩井勇樹, 渡邊育美, 片浦弘道 179
- 3P-35 グラフェン固有欠陥の安定性 山下和晃, ○斎藤峯雄 180

ナノチューブの応用

- 3P-36 DNAと金属ナノ微粒子による架橋単層カーボンナノチューブの機能化
○Goo-Hwan Jeong, 松本哲憲, 鈴木哲, 小林康裕, 本間芳和 181
- 3P-37 DNA で包接された多層カーボンナノチューブの原子間力顕微鏡観察
○高橋宏寿, 沼尾茂悟, 坂東俊治, 飯島澄男 182
- 3P-38 ラジカル付加反応によるSWCNTおよびVGCFの誘導体化 ○郡司天博, 赤沢美菜子, 有光晃二, 阿部芳首 183
- 3P-39 長鎖ベンゼンジアゾニウム塩を用いた金属性SWNTsと半導体性SWNTsの分離
○豊田昇平, 友成安彦, 樋渡真敬, 村上裕人, 中嶋直敏 184
- 3P-40 カンファーで合成したカーボンナノチューブの優れた電界電子放出
○安田恭平, Mukul Kumar, 安藤義則, 平松美根男 185
- 3P-41 ペプチドポルフィリンで機能化した単層カーボンナノチューブから成る新規なナノハイブリッド光合成モデル
○斎藤健二, ソラジエ ナタリー, 福住俊一 186
- 3P-42 カップスタック型カーボンナノチューブの光誘起電子移動還元 ○大谷政孝, 斎藤健二, 福住俊一 187

その他

- 3P-43 FT-ICR質量分析装置によるコバルトクラスターとアルコール, エーテル, 炭化水素との化学反応
○吉松大介, 小泉耕平, 須山直紀, 丸山茂夫 188
- 3P-44 フラーレンの前臨床安全性薬理評価: 単回毒性と突然変異試験
○藤本由紀, 高田弘弥, 森友久, 松林賢司, 伊東忍, 三羽信比古, 澤口聡子 189

January 7th, Sat

Plenary Lecture : 35 min (Presentation) + 5 min (discussion)
Special lecture : 25 min (Presentation) + 5 min (discussion)
General lecture : 10 min (Presentation) + 5 min (discussion)
Poster preview : 1 min (Presentation), no discussion

Opening Ceremony (9 : 00-9 : 05) Hisanori Shinohara

Plenary Lecture (9 : 05-9 : 50)

1S-1 Recent Progress in Nano-Carbon Research Eiji Osawa 1

General lecture (9 : 50-10 : 35)

Properties of Nanotubes

- 1-1 Photoluminescence mapping of various (n, m) nanotubes by cross-polarized light 7
○Yuhei Miyauchi, Mototeru Oba, Shigeo Maruyama
- 1-2 Family pattern of photoluminescence and Raman intensity of single wall carbon nanotubes 8
○R. Saito, J. Jiang, K. Sato, Y. Oyama
- 1-3 Nanoscale uniaxial pressure effect of carbon nanotubes on the Raman spectra 9
○Taka-aki Yano, Yasushi Inouye, Satoshi Kawata

☆☆☆☆☆☆ Coffee Break (10 : 35-10 : 50) ☆☆☆☆☆☆

General lecture (10 : 50-12 : 05)

Properties of Nanotubes

- 1-4 Chirality-dependent environmental effect on photoluminescence of SWNTs 10
○Shinya Iwasaki, Yutaka Ohno, Yoichi Murakami, Shigeru Kishimoto, Shigeo Maruyama, Takashi Mizutani
- 1-5 Mid-gap luminescence centers in single-wall carbon nanotubes created by UV illumination 11
○Konstantin Iakoubovskii, Nobutsugu Minami, Yeji Kim, Kanae Miyashita, Said Kazaoui, Balakrishnan Nalini
- 1-6 Single walled carbon nanotube analysis : Rapid, robust acquisition and simulation of quantum and chiral maps to ease structural assignments. 12
○Adam M. Gilmore, Ray K. Kaminsky, James M. Mattheis
- 1-7 Third-order Nonlinear Optical Response and Relaxation Dynamics in Double-Walled Carbon Nanotubes 13
○Arao Nakamura, Takako Tomikawa, Sadanobu Imamura, Miki Watanabe, Yasushi Hamanaka, Yahachi Saito, Hiroki Ago
- 1-8 Effects of Gravity on SWCNT Dissipative Structures Induced by DC Electric Field 14
Syuichi Sato, ○Masahito Sano

☆☆☆☆☆☆ Lunch Time (12 : 05-13 : 20) ☆☆☆☆☆☆

Special lecture (13 : 20-13 : 50)

1S-2 Ultrafast optical nonlinearity in single-walled carbon nanotubes Hiroshi Okamoto 2

General lecture (13 : 50-14 : 35)

Properties of Nanotubes

- 1-9 Mechanical Characteristics of High-Density and Well-Aligned Carbon Nanotubes on SiC 15
○Michiko Kusunoki, Hatsuhiko Usami, Daisuke Igimi, Koji Miyake
- 1-10 Electronic structures of the interface between carbon nanotubes and titanium electrodes measured by hard x-ray photoemission spectroscopy 16
○Daiyu Kondo, Mizuhisa Nihei, Akio Kawabata, Shintaro Sato, Eiji Ikenaga, Masaaki Kobata, Jung-Jin Kim, Keisuke Kobayashi, Satoshi Komiya, Yuji Awano
- 1-11 Vibration analysis of carbon nanotube cantilevers 17
○Seiji Akita, Sintaro Sawaya, Yoshikazu Nakayama

☆☆☆☆☆☆ Coffee Break (14 : 35-14 : 50) ☆☆☆☆☆☆

General lecture (14 : 50-16 : 05)

Endohedral Nanotubes

- 1-12 First-principles calculations of the radial breathing mode of peapods 18
○Susumu Okada
- 1-13 Synthesis and electronic properties of Fe-filled single-walled carbon nanotubes 19
○Yongfeng Li, Rikizo Hatakeyama, Toshiro Kaneko, Takeshi Izumida, Takeru Okada, Toshiaki Kato

January 7th, Sat

- 1-14 Optical Properties of β -carotene inside Single-Walled Carbon Nanotubes 20
○Kazuhiro Yanagi, Yasumitsu Miyata, Hiromichi Kataura

Nanohorns

- 1-15 Cap effects of Gd acetate on nanohorn holes 21
○Ryota Yuge, Jin Miyawaki, Masako Yudasaka, Yoshimi Kubo, Eiichi Nakamura, Hiroyuki Isobe, Hideki Yorimitsu, Sumio Iijima

Miscellaneous : Carbon Nanofibers

- 1-16 Formation of Carbon Nanofibers Having an Array of Conical Nano Cavities and Snapping at Their Nodes 22
○Akira Koshio, Yuta Takemura, Fumio Kokai

Poster preview (16 : 05-16 : 55)

Poster session (16 : 55-18 : 25)

Chemistry of Fullerenes

- 1P-1 Fabrication and Properties of Self-assembled Monolayers modified with C_{60} -derivative Fixed on Gold Nanoparticles 49
○Noriaki Ikeda, Chyongjin Pac, Hiroshi Moriyama
- 1P-2 Electrochemistry of an Open-Cage C_{60} Embedded in a Film on an Electrode in an Aqueous Media 50
○Masaharu Komatsu, Kenichi Watanabe, Ayumi Ishibashi, Yasuro Niidome, Michihisa Murata, Yasujiro Murata, Koichi Komatsu, and Naotoshi Nakashima
- 1P-3 Synthesis and Properties of a New C_{60} -TTP Hybrid System ○Takahiro Ikeuchi, Hisakazu Miyamoto, Yohji Misaki 51
- 1P-4 Synthesis and Photophysical Properties of [60]Fullerene Adducts Carrying Oligocarbazole Moieties 52
○Takashi Konno, Yosuke Nakamura, Satoru Watanabe, Masato Suzuki, Jun Nishimura
- 1P-5 Confirmation of Chemical Modification of Carbon Nanotubes Using Gold Particles as Reaction Indicator 53
○Hiroaki Azebara, Yuka Kasanuma, Takaharu Okajima, Tadashi Fujieda, Toshio Yasuda, Motoyuki Hirooka, Kishio Hidaka, Mitsuo Hayashibara, Hiroshi Tokumoto
- 1P-6 Fullerene Derivatives Bound to Oxygen - Synthesis, Photophysical behavior, and Generation of Singlet Oxygen 54
○Takeshi Honma, Takumi Hara, Yusuke Tajima, Mikio Hoshino, Shiro Matsumoto, Kazuo Takeuchi
- 1P-7 Organofullerenes Highly Soluble in Polar Solvents ○Kiminori Kawakami, Jun Enda 55
- 1P-8 Organic and Organometallic Derivatives of Dihydrogen-encapsulated [60]Fullerene 56
○Yutaka Matsuo, Hiroyuki Isobe, Takatsugu Tanaka, Yasujiro Murata, Michihisa Murata, Koichi Komatsu, Eiichi Nakamura

Metallofullerenes

- 1P-9 Ionization and Chemical Functionalization of $Gd@C_{82}$ 57
○Takayoshi Kono, Yoichiro Matsunaga, Tsukasa Nakahodo, Takahiro Tsuchiya, Takatsugu Wakahara, Yutaka Maeda, Takeshi Akasaka, Shingo Okubo, Tatsuhisa Kato, Naomi Mizorogi, Kaoru Kobayashi, Shigeru Nagase
- 1P-10 Isolation and Characterization of $La@C_{74}(C_6H_5C_{12})-II$ 58
○Takashi Kikuchi, Hidefumi Nikawa, Takatsugu Wakahara, Tsukasa Nakahodo, Takahiro Tsuchiya, Takeshi Akasaka, G. M. Aminur Rahman, Yutaka Maeda, Kenji Yoza, Ernst Horn, Naomi Mizorogi, Shigeru Nagase
- 1P-11 Isolation and Characterization of $Gd_2@C_{78}$ 59
○Yuji Takematsu, Takayoshi Kono, Tsukasa Nakahodo, Takahiro Tsuchiya, Takatsugu Wakahara, Yutaka Maeda, Takeshi Akasaka, Tatsuhisa Kato, Shigeru Nagase
- 1P-12 Analysis of Lanthanide-Induced NMR Shifts of the $Ce@C_{82}$ Anion 60
○Michio Yamada, Takatsugu Wakahara, Yongfu Lian, Takahiro Tsuchiya, Takeshi Akasaka, Markus Waelchli, Naomi Mizorogi, Shigeru Nagase
- 1P-13 Systematic Study of Lutetium Endohedral Di-Metallofullerenes : Production, Isolation and Structural characterization of Lu_2C_{2n} ($2n=74-86$) 61
○Hisashi Umamoto, Takashi Inoue, Tetsuo Tomiyama, Ryo Kitaura, Toshiki Sugai, Hisasori Shinohara

Fullerene Solids

- 1P-14 Facile Generation of Fullerene Nanoparticles by Hand-Grinding ○Shigeru Deguchi, Sada-atsu Mukai, Koki Horikoshi 62
- 1P-15 The Structure and Physical Properties in Ternary C_{60} Compounds ○Takashi Naniki, Satoru Motohashi, Hironori Ogata 63
- 1P-16 Solution-Processed Organic Thin-Film Transistors Based on Dodecyl Substituted C_{60} Derivatives 64
○Masayuki Chikamatsu, Atsushi Itakura, Yuji Yoshida, Reiko Azumi, Koichi Kikuchi, Kiyoshi Yase

January 7th, Sat

- 1P-17 Electronic properties of higher fullerenes and their related compounds ○*Hiroyuki Sugiyama, Takayuki Nagano, Kumiko Imai, Haruka Kusai, Akihiko Fujiwara, Taishi Takenobu, Yoshihiro Iwasa, Yoshihiro Kubozono* 65

Carbon Nanoparticles

- 1P-18 Study on Encapsulation of Radioactive Waste Elements inside Carbon Nanocapsules ○*Kazunori Yamamoto* 66
- 1P-19 Preparation of polyhedral graphite particles including rare earth metal carbides in their centers ○*Keita Kobayashi, Akira Koshio, Tatsuo Nakagawa, Fumio Kokai* 67

Formation and Purification of Nanotubes

- 1P-20 Bulk ACCVD Generation of SWNTs with Narrow Chirality Distribution ○*Shigeo Maruyama, Yuhei Miyauchi, Takashi Shimada, Yoichi Murakami, Kenichi Sato, Yuji Ozeki, Masahito Yoshikawa* 68
- 1P-21 Isolation of Circular Aggregates of Single-Walled Carbon Nanotubes by Ultrasonic Atomization ○*Naoki Komatsu, Takanori Shimawaki, Shuji Aonuma, Takahide Kimura* 69
- 1P-22 Recent advances in growth of vertically aligned SWNT films by ACCVD ○*Erik Einarsson, Masayuki Kadowaki, Yoichi Murakami, Shigeo Maruyama* 70
- 1P-23 Selective Oxidation of Semiconducting Single-Wall Carbon Nanotubes by Hydrogen Peroxide ○*Yasumitsu Miyata, Yutaka Maniwa, Hiromichi Kataura* 71
- 1P-24 Growth of carbon nanotubes by RF-PECVD -Lowering of growth temperature by pretreatment of catalyst film- ○*Takamichi Sakai, Atsushi Suzuki, Hideki Sato, Koichi Hata, Yahachi Saito* 72
- 1P-25 Low-temperature growth of carbon nanotubes by alcohol CCVD ○*Ken Hiasa, Tsuyoshi Nakagita, Hideki Sato, Koichi Hata, Yahachi Saito* 73
- 1P-26 Plasma sheath effects on the growth of freestanding individual single-walled carbon nanotubes ○*Toshiaki Kato, Rikizo Hatakeyama, Kazuyuki Tohji* 74
- 1P-27 Synthesis and Purification of Double Walled Carbon Nanotubes ○*Kazuyo Matsumoto, Toshiya Murakami, Kenji Kisoda, Toshiyuki Isshiki, Hiroshi Harima* 75
- 1P-28 The Effect of intra-Pore Size of Porous Glass for the Preparation of Single-Wall Carbon nanotubes ○*Yosuke Aoki, Shinzo Suzuki, Hiromichi Kataura, Hiroshi Nagasawa, Hisao Abe, Yohji Achiba* 76
- 1P-29 Influence of CH₄, C₂H₄, or C₂H₂ gas addition on the growth of SWNTs in H₂-Ar arc discharge ○*T. Kitamura, X. Zhao, S. Inoue, Y. Ando* 77

Endohedral Nanotubes

- 1P-30 Selective Encapsulation of Dimetallofullerene into Single-Wall Carbon nanotubes ○*Masashi Ishida, Daisuke Nishide, Takashi Inoue, Ryo Kitaura, Toshiki Sugai, Hisanori Shinohara* 78
- 1P-31 Incorporation and release of C₆₀ in/from single-wall carbon nanotubes with large diameters ○*J. Fan, M. Yudasaka, R. Yuge, D. N. Futaba, K. Hata, S. Iijima* 79

Nanohorns

- 1P-32 In vivo magnetic resonance imaging of single-wall carbon nanohorns through labeling with magnetite nanoparticles ○*Jin Miyawaki, Masako Yudasaka, Hideto Imai, Hideki Yorimitsu, Hiroyuki Isobe, Eiichi Nakamura, Sumio Iijima* 80
- 1P-33 Structure of hole edges of single-wall carbon nanohorns and its influence on cisplatin release ○*Kumiko Ajima, Masako Yudasaka, Alan Maigne, Jin Miyawaki, Sumio Iijima* 81

Properties of Nanotubes

- 1P-34 Phonon transport in finite length SWNTs using molecular dynamics simulations ○*Junichiro Shiomi, Shigeo Maruyama* 82
- 1P-35 Kataura plot based on GWA graphene dispersion ○*Mototeru Oba, Susumu Okada, Takashi Miyake, Shigeo Maruyama* 83
- 1P-36 AFM Evaluation on Suspended Carbon Nanotubes ○*Shota Kuwahara, Toshiki Sugai, Hisanori Shinohara* 84
- 1P-37 Single-Walled Carbon Nanotubes Studied by Tip-enhanced Near-field Raman Spectroscopy ○*Yuika Saito, Takashi Murakami, Norihiko Hayazawa, Hiromichi Kataura, Satoshi Kawata* 85
- 1P-38 The feature of the Breit-Wigner-Fano Raman line in DNA-wrapped single-wall carbon nanotubes ○*Hironori Kawamoto, Takashi Uchida, Masaru Tachibana and Kenichi Kojima* 86
- 1P-39 Band-gap modulation of semiconductive single-walled carbon nanotube in micellar solution by addition of viologens ○*Koji Matsuura, Takeshi Saito, Toshiya Okazaki, Satoshi Ohshima, Motoo Yumura and Sumio Iijima* 87
- 1P-40 Theoretical Current-Voltage Characteristics of Finite-Length Carbon Nanotube Between Silicon(111) Electrodes ○*Yoshikazu Kobayashi, Shigekazu Ohmori, Hiroyuki Fueno, and Kazuyoshi Tanaka* 88
- 1P-41 Photon-Induced Damage Creation in Carbon Nanotubes ○*Satoru Suzuki, Fumihiko Maeda, Yoshihiro Kobayashi* 89

January 7th, Sat

Application of Nanotubes

- 1P-42** Chemical Modification of Multi-walled Carbon Nanotubes (MWNTs) by Vacuum Ultra-violet (VUV) Irradiation Dry Process ○*Koji Asano, Daiyu Kondo, Akio Kawabata, Fumio Takei, Mizuhisa Nihei, Yuji Awano* 90
- 1P-43** Fabrication of antigen sensor using carbon nanotube FETs 91
○*Kentaro Tani, Hiroshi Ito, Yutaka Ohno, Shigeru Kishimoto, Mina Okochi, Hiroyuki Honda, Takashi Mizutani*
- 1P-44** Easy Fabrication Process of Carbon Nanotube Emitters for Diode Type Field Emission Display with Organic Luminescence Thin Films ○*Nobuyuki Iwata, Yasunori Hata, Masato Yoshikuni, Hiroshi Yamamoto* 92
- 1P-45** Development of detachment method of vertically aligned SWNT films from substrates and their re-attachment to arbitrary surfaces ○*Yoichi Murakami, Masayuki Kadowaki, Erik Einarsson, Shigeo Maruyama* 93
- 1P-46** Microreactors Utilizing Vertically-Aligned Carbon Nanotubes 94
○*Naoki Ishigami, Hiroki Ago, Yukihiko Motoyama, Mikihiro Takasaki, Masashi Shinagawa, Koji Takahashi, Masaharu Tsuji*

Miscellaneous

- 1P-47** Growth and Characterization of Carbon Nanowalls 95
○*Hirofumi Yoshimura, Akihiko Yoshimura, Pedro Molina-Morales, Hiroshi Nakai, Kenichi Kojima, Masaru Tachibana*
- 1P-48** Surface Modification of Carbon Nanotube with NO₂ Radical in Fuming Nitric Acid 96
○*Kyozo Mizuno, Masaru Sekido, Masatomi Ohno*

January 8th, Sun

Special lecture : 25 min (Presentation) + 5 min (discussion)

General lecture : 10 min (Presentation) + 5 min (discussion)

Poster preview : 1 min (Presentation), no discussion

Special lecture (9 : 00-9 : 30)

- 2S-3 Subnanometer Diameter Nanowires and Nanotubes in the ternary molybdenum-chalcogen-halogen system 3
○Aleš Mrzel, Dragan Mihailović, Maja Remškar, Abdou Hassaien, Hiromichi Kataura

General lecture (9 : 30-10 : 15)

Metallofullerenes

- 2-1 Structural Determination of Sc₃C₈₂ ○Yuko Iiduka, Takatsugu Wakahara, Tsukasa Nakahodo, Takahiro Tsuchiya, Akihiro Sakuraba, Yutaka Maeda, Takeshi Akasaka, Kenji Yoza, Ernst Horn, Tatsuhisa Kato, Michael T. H. Liu, Naomi Mizorogi, Kaoru Kobayashi, Shigeru Nagase 23
- 2-2 Spin-Transfer System under Equilibrium Constructed from Endohedral Metallofullerenes and Organic Donors 24
○Kumiko Sato, Takahiro Tsuchiya, Takatsugu Wakahara, Yutaka Maeda, Tsukasa Nakahodo, Takeshi Akasaka, Tatsuhisa Kato, Kei Ohkubo, Shunichi Fukuzumi, Naomi Mizorogi, Kaoru Kobayashi, Shigeru Nagase
- 2-3 ¹³C NMR Study of CeLa@C₈₀ Anion 25
○Tomohito Komaki, Takeshi Kodama, Yoko Miyake, Shinzo Suzuki, Koichi Kikuchi, Yohji Achiba

☆☆☆☆☆☆ Coffee Break (10 : 15-10 : 30) ☆☆☆☆☆☆

General lecture (10 : 30-11 : 15)

Metallofullerenes

- 2-4 Element Specific Magnetization Measurements of Er Metallofullerenes by Soft X-ray Magnetic Circular Dichroism (SXMCD) 26
○Haruya Okimoto, Tetsuya Nakamura, Ryo Kitaura, Takayuki Yamada, Yutaka Kitamura, Tomohito Matsushita, Takayuki Muro, Takashi Inoue, Toshiki Sugai, Susumu Nanao, Hisanori Shinohara
- 2-5 The Ultraviolet Photoelectron spectra of Ti₂C₂@C₈₂ ○Masayuki Kato, Kentaro Iwasaki, Shojun Hino, Daisuke Yoshimura, Hiroe Moribe, Haruya Okimoto, Yasuhiro Ito, Toshiki Sugai, Hisanori Shinohara 27
- 2-6 Fluorescence switching in Er@C₈₂ by solvent-induced electron transfer ○Shingo Okubo, Toshiya Okazaki, Sumio Iijima 28

General lecture (11 : 15-12 : 00)

Chemistry of Fullerenes

- 2-7 Single Electron Transfer from Aliphatic Amines with [60]Fullerene at the Ground State and Facile Synthesis of Tetraaminofullerene Epoxide 29
○Takatsugu Tanaka, Waka Nakanishi, Loïc Lemiègre, Hiroyuki Isobe, Eiichi Nakamura
- 2-8 Synthesis of Fullerene C₇₀ Encapsulating Molecular Hydrogen 30
○Yasujiro Murata, Shuhei Maeda, Michihisa Murata, Koichi Komatsu
- 2-9 Control of Decomposition of Acrylic Polymers by dispersing Fullerene-derivatives 31
○Tomoya Yamashiki, Yusuke Tajima, Toshihiko Sakurai, Ryoko Shimada, Hiroki Osedo

☆☆☆☆☆☆ Lunch Time (12 : 00-13 : 20) ☆☆☆☆☆☆

Awards Ceremony (13 : 20-13 : 50)

Special lecture (13 : 50-14 : 20)

- 2S-4 Japan's Town Factories are World's Treasure -What they can and cannot make in China- Hisayosi Hashimoto 4

General lecture (14 : 20-15 : 05)

Carbon Nanoparticles

- 2-10 Quantitative analysis of detonation nanodiamonds with X-ray diffraction 32
Naoki Komatsu, ○Naoki Kadota, Takahide Kimura, Eiji Osawa
- 2-11 Separation and Characterization of Polyene Molecules in Solution 33
○Tomonari Wakabayashi, Tatsuya Doi, Rui Umeda, Motohiro Sonoda, Yoshito Tobe
- 2-12 Matrix Effects on the Transformation of Nanodiamonds to Nano-Onions 34
○Masaki Ozawa, Masayasu Inakuma, Makoto Takahashi, Eiji Osawa

January 8th, Sun

☆☆☆☆☆☆ Coffee Break (15 : 05-15 : 20) ☆☆☆☆☆☆

General lecture (15 : 20-15 : 50)

Fullerene Solids

- 2-13** Crystal Structures of Discrete C₆₀ Fullerenes Stabilized by Appropriate Triphenylmethane Cations 35
○Takahito Sugiura, Eiji Osawa, Hiroshi Moriyama
- 2-14** Polymerization of C₆₀ Molecules Induced by Hole / Electron Injection from a Scanning Tunneling Microscope Tip 36
○Ryo Nouchi, Kosuke Masunari, Toshio Ohta, Yoshihiro Kubozono

Poster preview (15 : 50-16 : 40)

Poster session (16 : 40-18 : 10)

Chemistry of Fullerenes

- 2P-1** Trapping of S-Heterocyclic Carbene with C₆₀ Probe Technique 97
○Hidefumi Nikawa, Tsukasa Nakahodo, Takahiro Tsuchiya, Takatsugu Wakahara, G. M. Aminur Rahman, Takeshi Akasaka, Yutaka Maeda, Michael T. H. Liu, Akira Meguro, Soichiro Kyushin, Hideyuki Matsumoto, Naomi Mizorogi, Shigeru Nagase
- 2P-2** Regioselective Synthesis and Structure of Hepta(organo)[60]fullerene-Transition Metal Complexes 98
○Takeshi Fujita, Yutaka Matsuo, Eiichi Nakamura
- 2P-3** Kinetics of 1,3-Dipolar Cycloaddition of Diaryldiazomethanes with Fullerenes C₆₀ and C₇₀ 99
○Hiroshi Kitamura, Nozomu Seike, Taijiro Higashi, Ken Kokubo, Takumi Oshima
- 2P-4** Diastereoselective Complexation of Chiral Diphosphine and Ruthenium-Pentaorgano[60]fullerene 100
○Yuichi Mitani, Yutaka Matsuo, Yu-Wu Zhong, Eiichi Nakamura
- 2P-5** Application of C₆₀-based amine-labeling reagents to MALDI-TOF MS analysis 101
○Hiroki Tsumoto, Katsumasa Takahashi, Kohfuku Kohda, Takayoshi Suzuki, Hidehiko Nakagawa, Naoki Miyata
- 2P-6** Mechanism of mechanochemical hydroxylation of fullerene 102
○Takahiro Kubo, Eitaro Matsui, Hiroto Watanabe, Mamoru Senna
- 2P-7** Effects of pressure and temperature on the solubility of C₇₀ in n-hexane ○Shinichi Okada, Seiji Sawamura 103
- 2P-8** Synthesis and Reactions of Novel Methano[60]fullerenes ○Tomoyuki Tada, Yasuhiro Ishida, Kazuhiko Saigo 104

Metallofullerenes

- 2P-9** Recent progress of powder diffraction study of endohedral metallofullerene at SPring-8 105
○Eiji Nishibori, Ikuya Terauchi, Masayuki Ishihara, Makoto Sakata, Masaki Takata, Yasuhiro Ito, Hisashi Umamoto, Hiroe Moribe, Takashi Inoue, Hisanori Shinohara
- 2P-10** Synthesis of LaNd@C₇₂ and Fluorescence Measurement of Nd-metallofullerenes 106
○Naomi Murata, Takeshi Kodama, Yoko Miyake, Shinzo Suzuki, Koichi Kikuchi, Yohji Achiba
- 2P-11** Reactivity of La₂@C₇₈ toward 2-Admantane-2,3-Diazirine : Structure Determination of Monoadduct La₂@C₇₈-(Ad)(I) 107
○Baopeng Cao, Tsukasa Nakahodo, Takatsugu Wakahara, Takahiro Tsuchiya, Kaoru Kobayashi, Shigeru Nagase, Takeshi Akasaka
- 2P-12** Radical Reaction of La@C₈₂ in Toluene 108
○Yuta Takano, Akinori Yomogita, Takatsugu Wakahara, Takahiro Tsuchiya, Tsukasa Nakahodo, Yutaka Maeda, Takeshi Akasaka, Tatsuhisa Kato, Naomi Mizorogi, Shigeru Nagase
- 2P-13** Structure and Properties of pure H₂@C₆₀ 109
○Misaho Akada, Katsumi Tanigaki, Yasujiro Murata, Koichi Komatsu, Toru Kakiuchi, Hiroshi Sawa

Fullerene Solids

- 2P-14** Structure of Fullerene Nanowhiskers (III) ○Satoru Tsuchida, Satoru Motohashi and Hironori Ogata 110
- 2P-15** Synthesis and structural investigation of fulleroid nanowhiskers ○Satoru Motohashi, Satoru Tsuchida, Hironori Ogata 111
- 2P-16** Photo-carrier generation and its transport process in pristine C₆₀ single crystals 112
○Ryota Tanaka, Ikuko Akimoto, Ken-ichi Kan'no
- 2P-17** Fabrication and Electrical Properties of FET devices Based on C₆₀ Nano-Whiskers 113
○Kenichi Ogawa, Asato Ikegami, Hajime Tsuji, Tomohiro Kato, Nobuyuki Aoki, Kenji Adachi, Sadahiro Iida, Yuichi Ochiai

January 8th, Sun

Carbon Nanoparticles

- 2P-18** Deposition of platinum nano particles on carbon nanohorn particles by electrochemistry and their magnetism 114
○*Motohiro Sugaya, Takayuki Inagaki, Masako Yudasaka, Shunji Bandow, Sumio Iijima*
- 2P-19** Simulation of high-energy ion/atom impact on nano-carbons : Electronic shake up and structural change 115
○*Yoshiyuki Miyamoto, Arkady Krasheninnikov, David Tomanek*

Formation and Purification of Nanotubes

- 2P-20** Tailored Synthesis of Double Walled Carbon Nanotubes by Super Growth 116
○*Takeo Yamada, Tatsunori Namai, Kenji Hata, Jing Fan, Masako Yudasaka, Don N. Futaba, Kohei Mizuno, Motoo Yumura, Sumio Iijima*
- 2P-21** Influence of Co/Mo Ratio on Synthesis of Single-Walled Carbon Nanotubes from Carbon Monoxide 117
○*Toshiaki Nishii, Suguru Noda, Hiroshi Sugime, Naoto Masuyama, Yoichi Murakami, Shigeo Maruyama*
- 2P-22** Purification of Double Wall Carbon Nanotubes by Dispersion 118
○*Hiromichi Yoshida, Satoshi Kikuchi, Toshiki Sugai, Hisanori Shinohara*
- 2P-23** Synthesis of single-wall carbon nanotubes by alcohol CCVD methods using mesoporous silica with different pore size 119
○*Yuya Izumi and Hironori Ogata*
- 2P-24** Dispersion and Separation of Small Diameter Single-Walled Carbon Nanotubes 120
○*Makoto Kanda, Yutaka Maeda, Shin-ichi Kimura, Tadashi Hasegawa, Yongfu Lian, Takatsugu Wakahara, Takeshi Akasaka, Said Kazaoui, Nobutsugu Minami, Toshiya Okazaki, Tetsuo Shimizu, Hiroshi Tokumoto, Jing Lu, Shigeru Nagase*
- 2P-25** Synthesis and characterization of single-walled carbon nanotubes by catalytic decomposition of alcohol 121
○*Yanli Zhao, Kazuyuki Seko, Kensuke Okumura and Yahachi Saito*
- 2P-26** Supported Ni catalysts of nominal submonolayers grew single-walled carbon nanotubes 122
○*Kazunori Kakehi, Suguru Noda, Shohei Chiashi and Shigeo Maruyama*
- 2P-27** Preparation of Single-Wall Carbon Nanotubes with Rh/Pd-Carbon Composite Rods in Nitrogen Atmosphere 123
○*Nobuyuki Asai, Shinzo Suzuki, Hiromichi Kataura, Yohji Achiba*
- 2P-28** Role of Bimetallic Catalysts for Growth of Single-Walled Carbon Nanotubes 124
○*Toshiya Murakami, Kazuya Mitikami, Satoru Ishigaki, Kazuyo Matsumoto, Kenji Kisoda, Koji Nishio, Toshiyuki Isshiki, Hiroshi Harima*
- 2P-29** Formation process of carbon nanocap from SiC(0001) surface through thermal decomposition 125
○*T.Maruyama, Y. Kawamura, H. Bang, N. Fujita, T. Shiraiwa, K. Tanioku, Y. Hozumi, S. Naritsuka, M. Kusunoki*

Endohedral Nanotubes

- 2P-30** Encapsulating p-nitroaniline into Single-Walled Carbon Nanotube 126
○*Takashi Murakami, Yuika Saito, Hiromichi Kataura, Kazuhito Tsukagoshi, Kazuhiro Yanagi, Yasumitsu Miyata, Satoshi Kawata*
- 2P-31** Formation of n-type double-walled carbon nanotubes by a Cs-plasma irradiation method 127
○*Yongfeng Li, Takeshi Izumida, Rikizo Hatakeyama, Toshiro Kaneko, Takeru Okada, Toshiaki Kato*
- 2P-32** Magnetic Analysis of Nano-peapods by Soft X-ray Magnetic Circular Dichroism (MCD) Spectroscopy 128
○*Ryo Kitaura, Haruya Okimoto, Tetsuya Nakamura, Yutaka Kitamura, Daisuke Ogawa and Hisanori Shinohara*

Nanohorns

- 2P-33** High Yield Purification of Carbon Nanohorn ○*Goshu Tamura, Shunji Bandow, Sumio Iijima* 129
- 2P-34** Fractionation of Arc-Soot and dispersion of Pt-Ru Catalysts. (Reactivity with Methanol) 130
○*Keisuke Higashi, Hiroaki Niwa, Kenji Shinohara, Hirofumi Takikawa, Guochun Xu, Shigeo Itoh, Tatsuo Yamaura, Kouji Miura, Kazuo Yoshikawa*

Properties of Nanotubes

- 2P-35** Stability of Field Emission Current from a Carbon Nanotube 131
○*Yasumoto Konishi, Hiroyoshi Tanaka, Lujun Pan, Seiji Akita, Yoshikazu Nakayama*
- 2P-36** Conductance of telescoped double-wall armchair nanotube ○*Ryo Tamura* 132
- 2P-37** Direct Observation of Inter-layer Interaction of Double-Walled Carbon Nanotubes by using UHV-STM 133
○*N. Fukui, H. Yoshida, T. Sugai, S. Heike, M. Fujimori, Y. Suwa, Y. Terada, T. Hashizume, H. Shinohara*
- 2P-38** Observation of Photoluminescence from Small-Diameter DWNTs Synthesized by the Zeolite-CCVD Method 134
○*Naoki Kishi, Satoshi Kikuchi, Toshiki Sugai, Hisanori Shinohara*

January 8th, Sun

- 2P-39** Morphology effect of optical properties in single walled carbon nanotubes detected by THz to Vis-polarized spectroscopy 135
○*N. Akima, J.L. Musfeldt, H. Matsui, N. Toyota, H. Shimoda, O. Zhou, M. Shiraiishi, Y. Iwasa*
- 2P-40** Exciton-photon matrix elements in single-wall carbon nanotubes ○*J. Jiang, R. Saito, Y. Oyama, K. Sato, J. S. Park* 136
- 2P-41** Electronic and Magnetic Properties of Finite-Length Carbon Nanotubes with Hydrogen Atoms Encapsulated 137
○*Masahiro Nigawara, Shigekazu Ohmori, Akihiro Ito, Kazuyoshi Tanaka*
- 2P-42** Resonance Raman and Photoluminescence Spectra of Suspended Single-Walled Carbon Nanotubes in Ceramics 138
○*Taro Ueno, Shingo Okubo, Tsuneaki Miyahara, Shinzo Suzuki, Yohji Achiba, Kazuhito Tsukagoshi, Toshiya Okazaki, Hiromichi Kataura*

Application of Nanotubes

- 2P-43** Air-Stable N-type Single-Walled Carbon Nanotube Field Effect Transistors Functionalized by Amine Molecules 139
○*Tetsunori Matsumoto, Satoru Suzuki, Goo-Hwan Jeong, Yoshihiro Kobayashi, Yoshikazu Homma*
- 2P-44** Development of Micro-focused X-ray Source by Using Carbon Nanotube Field Emitter 140
○*Kunihiko Kawakita, Koichi Hata, Hideki Sato, Yahachi Saito*
- 2P-45** Spectral Properties of Single-Walled Carbon Nanotubes Dissolved in Aqueous Solutions of Biosurfactants 141
○*Naotoshi Nakashima, Ayumi Ishibashi*
- 2P-46** NIR Laser Irradiation toward SWNTs in Solution 142
○*Kaori Narimatsu, Hiromi Shinohara, Yasuro Niidome, Naotoshi Nakashima*
- 2P-47** Dielectrophoresis of SWNTs in a Microchip 143
○*Masashi Shinagawa, Hiroki Ago, Naoki Ishigami, Masaharu Tsuji, Tatsuya Ikuta, Koji Takahashi*

Miscellaneous

- 2P-48** Metal-free Formation of Spiral Carbon Structures ○*Akira Koshio, Teruyuki Tanaka, Toshiki Sunouchi, Fumio Kokai* 144
- 2P-49** On Critical Sizes of Multiply-Charged Fullerene Clusters ○*Masato Nakamura, P. A. Hervieux* 145

January 9th, Mon

Special lecture : 25 min (Presentation) + 5 min (discussion)

General lecture : 10 min (Presentation) + 5 min (discussion)

Poster preview : 1 min (Presentation), no discussion

Special lecture (9 : 00-9 : 30)

3S-5 Super Growth : From Highly Efficient Impurity Free CNT Synthesis to Super-Capacitors and Much More *Kenji Hata* 5

General lecture (9 : 30-10 : 15)

Formation and Purification of Nanotubes

3-1 In-situ measurement of Raman scattering and AFM during laser-heated ACCVD growth process of SWNTs 37

○*Shohei Chiashi, Yoichi Murakami, Yuhei Miyauchi, Shigeo Maruyama*

3-2 Formation of Single-Wall Carbon Nanotubes in Argon and Nitrogen Gas Atmosphere 38

○*Shinzo Suzuki, Nobuyuki Asai, Hiromichi Kataura, Yohji Achiba*

3-3 Synthesis of Horizontally-Aligned SWNTs with Controllable Density on Sapphire Surface and their Polarized Raman 39

Spectroscopy ○*Hiroki Ago, Naoyasu Uehara, Ken-ichi Ikeda, Ryota Ohdo, Kazuhiro Nakamura, Masaharu Tsuji*

☆☆☆☆☆☆ Coffee Break (10 : 15-10 : 30) ☆☆☆☆☆☆

General lecture (10 : 30-11 : 15)

Formation and Purification of Nanotubes

3-4 Effects of typical metallic Elements added as Catalysts for production of DWCNTs by DC-Arc discharge method 40

○*Hideki Inakura*

3-5 Selective Diameter-Control of Single-Walled Carbon Nanotubes by the Enhanced Direct-Injection-Pyrolytic-Synthesis 41

(DIPS) Method ○*Takeshi Saito, Satoshi Ohshima, Wei-Chun Xu, Koji Matsuura, Toshiya Okazaki, Motoo Yumura and Sumio Iijima*

Application of Nanotubes

3-6 Super Growth : Shape Engineerable Single Walled Carbon Nanotube Solid as Flexible Conducting Mesoporous Material 42

○*Don N. Futaba, Kenji Hata, Tatsuki Hiraoka, Takeo Yamada, Kohei Mizuno, Yuhei Hayamizu, Tatsunori Namai, Yozo Kakudate, Osamu Tanaike, Hiroaki Hatori, Koji Miyake, Shinya Sasaki, Motoo Yumura, Sumio Iijima*

General lecture (11 : 15-12 : 00)

Application of Nanotubes

3-7 Fluorination of Carbon Nanotubes, Structures and Properties 43

○*Hidekazu Touhara, Hideki Arikai, Yoshio Nojima, Fujio Okino, Y. A. Kim, Morinobu Endo, Shinji Kawasaki, Hiromichi Kataura, Masako Yudasaka, Sumio Iijima*

3-8 Nonlinear Optical Waveguide Device Using Carbon Nanotube-Polyimide Composite Material 44

○*Shun Matsuzaki, Taro Itatani, Emiko Itoga, Masahiro Igusa, Hiromichi Kataura, Madoka Tokumoto, Kohtaro Ishida, Youichi Sakakibara*

3-9 Carbon nanotube transparent flexible transistors using solution process 45

○*Tetsuo Takahashi, Taishi Takenobu, Takayoshi Kanbara, Kazuhito Tsukagoshi, Yoshinobu Aoyagi, Yoshihiro Iwasa*

☆☆☆☆☆☆ Lunch Time (12 : 00-13 : 20) ☆☆☆☆☆☆

Special lecture (13 : 20-13 : 50)

3S-6 Molecular Dynamics Simulations for Formations and Properties of Various Defects on Carbon Nano-Structures 6

Takazumi Kawai

General lecture (13 : 50-14 : 35)

Application of Nanotubes

3-10 Individual solubilization of carbon nanotubes using polyimides 46

○*Masahiro Shigeta, Masaharu Komatsu, Naotoshi Nakashima*

Properties of Nanotubes

3-11 Electronic Properties in Möbius Nano-Carbon Materials ○*K. Harigaya* 47

3-12	Band Gap and Quasiparticle States in Carbon Nanotubes	Takashi MIYAKE, Yoshio AKAI, ○Susumu SAITO	48
------	---	--	----

Poster preview (14 : 35-15 : 25)

Poster session (15 : 25-16 : 55)

Chemistry of Fullerenes

3P-1	Photochemical reaction of C ₆₀ with cyclic organosilicon compounds	○Junko Nagatsuka, Tsukasa Nakahodo, Sachie Sugitani, Masahiro Kako, Takatsugu Wakahara, Yutaka Maeda, Takahiro Tsuchiya, Takeshi Akasaka, Yoshiko Sasaki, Osamu Ito, Kaoru Kobayashi, Shigeru Nagase	146
3P-2	A New Effective Search Algorithm for C ₆₀ R _n Structure : Cones Product Strategy	○Tatsuo Toida, Katsumi Uchida, Tadahiro Ishii, Hirofumi Yajima	147
3P-3	Syntheses of water-soluble fullerene-chitosan conjugates and their radical scavenging activities	○Katsumasa Nemoto, Hitoshi Sashiwa, Katsumi Uchida and Hirofumi Yajima	148
3P-4	One Pot Synthesis of Highly Water-Soluble Fullerenol	○Hiroshi Tategaki, Sayako Kawahama, Kenji Matsubayashi, Hiroya Takada, Ken Kokubo, Takumi Oshima	149
3P-5	Synthesis of Alkylated Pentamethyl[60]fullerene by Iridium Catalyzed C-H Bond Activation of Toluene	○Akihiko Iwashita, Yutaka Matsuo, Eiichi Nakamura	150
3P-6	Promoting effect of water-soluble fullerene derivatives on growth of neurites of PC-12 cells that were differentiated by nerve growth factor	○Syo Kawahara, Yuki Fujisawa, Hiroki Tsumoto, Kohfuku Kohda, Takayoshi Suzuki, Hidehiko Nakagaw, Naoki Miyata	151
3P-7	Mechanisms of mechanochemical oxidation of fullerene under oxygen atmosphere	○Hiroto Watanabe, Eitaro Matsui, Takahiro Kubo, Mamoru Senna	152
3P-8	Novel C ₆₀ -Phthalocyanine Conjugates Having Open-Cage C ₆₀ Skeleton	○Naoaki Hashimoto, Takamitsu Fukuda, Nagao Kobayashi	153

Metallofullerenes

3P-9	Endohedral Structures of Eu@C ₈₂ and Gd@C ₈₂	○Naomi Mizorogi, Shigeru Nagase	154
3P-10	A New Metallofullerene Growth Mechanism II	○Yohji Achiba	155
3P-11	ESR Spectrum of La@C ₈₂ (Ad) Single Crystal.	○Ryuhei Nara, Yutaka Maeda, Takatsugu Wakahara, Takahiro Tsuchiya, Kazuhiro Takeuchi, Makoto Fukushima, Takeshi Akasaka, Tatsuhisa Kato	156
3P-12	Synthesis and Characterization of Carbene Derivatives of La ₂ @C ₈₀	○Chika Someya, Michio Yamada, Takatsugu Wakahara, Takahiro Tsuchiya, Yutaka Maeda, Takeshi Akasaka, Naomi Mizorogi, Shigeru Nagase	157
3P-13	Ion Mobility Studies on Sc Metallofullerenes	○T. Sugai, M.F.Jarrold, H. Shinohara	158

Fullerene Solids

3P-14	Fabrication and characterization of solution-processed Pd-C ₆₀ polymer-based thin film transistors	○Yukitaka Matsuoka, Kagan Kerman, Eiichi Tamiya, Akihiko Fujiwara	159
3P-15	Fabrication of high performance fullerene field-effect transistor devices and their performance control	○Takayuki Nagano, Kenji Ochi, Haruka Kusai, Toshio Ohta, Kumiko Imai, Akihiko Fujiwara, Yoshihiro Kubozono	160
3P-16	Surface Modification using Self-assembled Monolayers on the Electrodes in Organic FETs	Nobuya Hiroshiba, Hisao Ishi, Ryotaro Kumashiro, ○Katsumi Tanigaki	161
3P-17	Fabrication of field-effect transistor devices with three types of fullerodendrons by solution process, and their electronic properties	○Haruka Kusai, Takayuki Nagano, Kumiko Imai, Yoshihiro Kubozono, Yuuki Sako, Yutaka Takaguchi, Akihiko Fujiwara	162

Carbon Nanoparticles

3P-18	Resonance Raman Spectra of Polyene Molecules	Tatsuya Doi, ○Tomonari Wakabayashi	163
-------	--	------------------------------------	-----

Formation and Purification of Nanotubes

3P-19	The ultrasonication power density effects on carbon nanotube dispersion in aqueous solutions	○Catalin Romeo Luculescu, Toru Ishii, Teruo Takahashi, Katsumi Uchida, Tadahiro Ishii, and Hirofumi Yajima	164
3P-20	Gas Analysis of CVD Processes for High-Yield Synthesis of Single-Walled Carbon Nanotubes	○Naoyasu Uehara, Hiroki Ago, Shingo Imamura, Masaharu Tsuji	165

January 9th, Mon

3P-21	Purification of single wall carbon nanotube made by arc plasma jet method ○Tomoko Suzuki, Kenji Suhama, Xinluo Zhao, Sakae Inoue, Yoshinori Ando	166
3P-22	Growth of carbon nanotubes on Si substrates with nanoprotusions ○Mai Matsubayashi, Hideki Sato, Koichi Hata, Hideto Miyake, Kazumasa Hiramatsu, Akinori Ohshita and Yahachi Saito	167
3P-23	Dispersion behavior and spectroscopic properties of SWNTs in various biopolymer solutions ○Teruo Takahashi, Catalin Romeo Luculescu, Katsumi Uchida, Tadahiyo Ishii, Hirofumi Yajima	168
3P-24	Selective Chemical Vapor Growth of Vertically Aligned Carbon Nanotubes on Patterned Metal Layers ○Hiroki Okuyama, Nobuyuki Iwata, Hiroshi Yamamoto	169
3P-25	Preparation of Carbon Nanowires by Using Carbon Electrode Containing Fe Catalyst ○M. Endo, A. Mizutani, X. Zhao, Y. Ando	170

Endohedral Nanotubes

3P-26	Coalescence of C ₆₀ in a peapod under electron irradiation ○Masanori Koshino, Kazutomo Suenaga, Eiichi Nakamura	171
--------------	---	-----

Nanohorns

3P-27	Large Scale Production of Carbon Nanohorns with High Purity ○Takeshi Azami, Daisuke Kasuya, Tsutomu Yoshitake, Yoshimi Kubo, Masako Yudasakaa, and Sumio Iijima	172
--------------	--	-----

Properties of Nanotubes

3P-28	Mechanism of Plastic deformation of Carbon Nanotubes ○Hideki Mori, Shigenobu Ogata, Seiji Akita, Yoshikazu Nakayama	173
3P-29	FET Properties of Surface Silylated Carbon Nanotubes ○Ryotaro Kumashiro, Hirotaka Ohashi, Takeshi Akasaka, Yutaka Maeda, Takeshi Izumida, Rikizo Hatakeyama, Katsumi Tanigaki	174
3P-30	High Field Magneto-optical Study of Unbundled Single-walled Carbon Nanotubes to 120 T ○Hiroyuki Yokoi, Noritaka Kuroda, Yeji Kim, Kanae Miyashita, Said Kazaoui, Nobutsugu Minami, Eiji Kojima, Kazuhito Uchida, Shojiro Takeyama	175
3P-31	Environmental effects of PL/Raman spectra from suspended SWNTs ○Yoshihiro Kobayashi, Daisuke Takagi, Yoshikazu Homma	176
3P-32	Raman study of laser-induced defects in single-wall carbon nanotube bundles ○Takashi Uchida, Masaru Tachibana, Kenichi Kojima	177
3P-33	Optical Properties of Double-Walled Carbon Nanotubes ○Taro Ueno, Shingo Okubo, Tsuneaki Miyahara, Shinzo Suzuki, Yohji Achiba, Toshiya Okazaki, Kazuhito Tsukagoshi, Hiromichi Kataura	178
3P-34	Lithium Ion Storage Property of Peapod ○Shinji Kawasaki, Yuki Iwai, Ikumi Watanabe, Hiromichi Kataura	179
3P-35	Energetics of Graphene intrinsic Defects Kazuaki Yamashita, ○Mineo Saito	180

Application of Nanotubes

3P-36	Suspended SWNTs Functionalization with DNA and Metal Nanoparticles ○G.-H. Jeong, T. Matsumoto, S. Suzuki, Y. Kobayashi, Y. Homma	181
3P-37	AFM imaging of wrapped multi wall carbon nanotube in DNA ○Hirotoshi Takahashi, Shigenori Numao, Shunji Bandow, Sumio Iijima	182
3P-38	Derivatization of SWCNT and VGCF by a radical addition reaction ○Takahiro Gunji, Minako Akazawa, Koji Arimitsu, Yoshimoto Abe	183
3P-39	Separation of Semiconducting and Metallic Single-Walled Carbon Nanotubes using a Long-Chain Benzenediazonium Compound ○Shouhei Toyoda, Yasuhiko Tomonari, Masataka Hiwatashi, Hiroto Murakami, Naotoshi Nakashima	184
3P-40	Excellent field emission from camphor-grown carbon nanotubes ○Kyohei Yasuda, Mukul Kumar, Yoshinori Ando, Mineo Hiramatsu	185
3P-41	Novel Photosynthetic Model Nanohybrids Composed of Single-Walled Carbon Nanotube Functionalized with Porphyrinic Peptides ○Kenji Saito, Nathalie Solladié, Shunichi Fukuzumi	186
3P-42	Photoinduced Electron Transfer Reduction of Cup-Stacked-Type Carbon Nanotube ○Masataka Ohtani, Kenji Saito, Shunichi Fukuzumi	187

January 9th, Mon

Miscellaneous

- 3P-43** FT-ICR Study of Reaction of Cobalt Clusters with Alcohol, Ether and Hydrocarbon 188
○*Daisuke Yoshimatsu, Kohei Koizumi, Naoki Suyama, Shigeo Maruyama*
- 3P-44** Preclinical Safety Evaluation of Fullerenes : Acute Oral Administration and Mutagenic Studies 189
○*Yuki Fujimoto, Hiroya Takada, Tomohisa Mori, Kenji Matsubayashi, Shinobu Ito, Nobuhiko Miwa, Toshiko Sawaguchi*

基調講演
Plenary Lecture

特別講演
Special Lecture

1S – 1 ~ 1S – 2

2S – 3 ~ 2S – 4

3S – 5 ~ 3S – 6

IS-1

RECENT PROGRESS IN NANO-CARBON RESEARCH

Eiji Ōsawa

*NanoCarbon Research Institute, 301 Toudai Kashiwa Venture Plaza, 5-4-19 Kashiwa-no-Ha,
Kashiwa 277-0882, Japan*

Fullerene/Nanotube Symposium Series began soon after the first isolation of C₆₀ by Krätschmer and Huffman, and grew larger in keeping pace with the development of nano-carbon research. We are now commemorating its 30th Symposium but it is surprising to realize that the actual time span since its start until the present time is only 13 years. We have been fortunate to witness, and even participate in the birth and growth of a new class of extremely interesting materials called nano-carbons that so far produced so many attractive structures and shapes one after the other.

Until now, new nano-carbons species have been obtained only by chance and properties have been unpredictable as well. Some day in the near future we would like to design produce tailor-made nano-carbons. In this lecture, I would like to review common properties, behaviors and principles underlying a large variety of the known forms in nano-carbons in order to help rational synthesis. Some of them are as follows:

Size – Those nano-carbon particles having single-digit nano-size in diameter are the most interesting, and still remain largely unexplored.

Agglutination during ‘bottom-up’ synthesis – The well-known tendency of nanoparticles to assemble spontaneously into micron-sized aggregates is actually of not much hazard in nano-carbons. Careful sonication generally suffices to destroy aggregates due to large surface area. Problem lies in much smaller but extremely tight *core* assemblies, often appear in 100-200 nm in diameter and supposed to have been formed during the synthesis from atomic carbons. Soot, carbon nanohorn and detonation nanodiamond are well-studied examples.

Phase transition between multi-shell fullerenes and nanodiamond occurs much faster than the graphite-diamond transition. It is likely that the phenomenon is general for nanoparticles, but the mechanism is probably related with the increased surface activity.

Re-organization of surface structure is often provoked but rarely accomplished, primarily because of the unavailability of single-digit nano-carbons in relation.

TEL:+81-4-7140-8671, FAX: +81-4-7140-8893, E-mail: OsawaEiji@aol.com

Ultrafast Optical Nonlinearity in Single-walled Carbon Nanotubes

Hiroshi Okamoto

Department of Advanced Materials Science, Univ. of Tokyo, Kashiwa, Chiba 277-8561, Japan

For the ultrafast optical-switching devices, nonlinear optical materials with large third-order nonlinear susceptibility $\chi^{(3)}$ and small relaxation time T_1 of photoexcited states are indispensable. One possible method is to utilize optical Stark effects of band-edge excitons in semiconductors. One-dimensional (1D) semiconductors are good targets, since excitonic effect is enhanced due to the singularity of 1D Coulomb potential. However, optical Stark effects have not been demonstrated in 1D systems, e.g., semiconductor quantum-wires nor conjugated polymers, as yet. In this study, we performed femtosecond pump-probe absorption spectroscopy on bundled single-walled carbon nanotubes (SWNTs) with the resonant excitation to the semiconducting SWNTs (SC-SWNTs). From the results, we have demonstrated that SC-SWNTs exhibit gigantic optical Stark effects at the excitonic absorption, which is responsible for large $\chi^{(3)}$ recently reported for resonant excitation conditions in degenerate configurations.

Figure 1 shows the spectra of the transient absorption changes ($\Delta\alpha$) of a SWNT film with a pump energy of $\hbar\omega_p=0.685$ eV, which is equal to the peak of the absorption (α) spectrum (the solid line). Just after the photoirradiation ($t_d=0.1$ ps), a large decrease in absorption is observed at around $\hbar\omega_p$. For the negative $\Delta\alpha$ peak at 0.685 eV, the response is extremely fast, occurring within the time resolution (~ 180 fs) [1]. The positive components at around 0.59 eV and 0.75 eV also include similar ultrafast components. Thus, the ultrafast component in the optical gap region shows a (+—) structure, which is characteristic of an optical Stark effect of a two-level system. For the off-resonant excitations, we have observed clear shifts of the absorption peak, which also support the presence of the optical Stark effects. Moreover, from the detailed analyses of the $\Delta\alpha$ spectra in the infrared region as well as in the near-infrared one, we have revealed that small T_1 (~ 1 ps) for SC-SWNTs is mediated by ultrafast exciton- and charge-transfer processes to metallic-SWNTs.

This work has been done in collaboration with A. Maeda, S. Matsumoto, and H. Kishida (Univ. of Tokyo), T. Takenobu and Y. Iwasa (Tohoku Univ.), H. Shimoda (Xintek Inc.), O. Zhou (Univ. of North Carolina), and M. Shiraishi (Osaka Univ.).

[1] A. Maeda et al., *Phys. Rev. Lett.*, **94**, 47404 (2005).

Corresponding Author: Hiroshi Okamoto

Tel: +81-4-7136-3771, FAX: +81-4-7136-3772, E-mail: okamotoh@k.u-tokyo.ac.jp

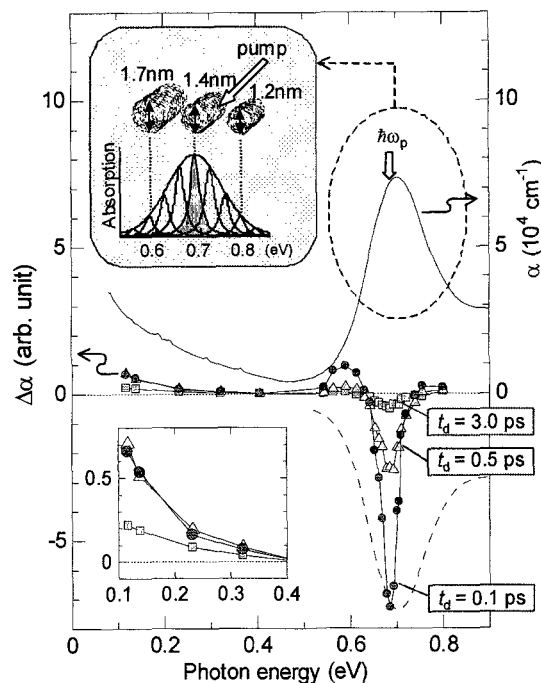


Fig. 1 Transient absorption ($\Delta\alpha$) spectra of a SWNT film with the pump energy of $\hbar\omega_p=0.685$ eV.

Subnanometer Diameter Nanowires and Nanotubes in the ternary molybdenum–chalcogen–halogen system

○Aleš Mrzel^{1,2}, Dragan Mihailović¹, Maja Remškar¹, Abdou Hassaien², Hiromichi Kataura²

¹ *Jozef Stefan Institute; Jamova 39, 1000 Ljubljana, Slovenia*

² *Nanotechnology Research Institute, National Institute of Advanced Industrial Science and Technology, Central 4, 1-1-1 Higashi, Tsukuba, Ibaraki 305-8562, Japan*

Compounds in the ternary molybdenum–chalcogen–halogen system appear to form a variety of different materials such as so-called Chevrel phases and some of ternary materials could be aligned in a class of quasi-one-dimensional materials. In 2001 a new nano-structured material was discovered with the proposed formula $\text{MoS}_{(2-x)}\text{I}_y$.¹ The material grown in the form of bundles composed of very fine nanotubes, approximately 1 nm in diameter. It exhibits excellent field emission properties, a large capacity for Li storage, great mechanical strength, a low shear modulus implying good tribological properties and an anomalously large paramagnetic susceptibility. Very recently the discovery of a new nanowire material with the formula $\text{Mo}_6\text{S}_3\text{I}_6$ was reported². The material can be synthesized in large quantities in a single step, yet is functionally and structurally similar to $\text{MoS}_2\text{I}_{1/3}$. It is composed of identical small-diameter nanowires, weakly bound in bundles, which can be handled in the similar way as carbon nanotubes, yet have the added advantage that they can be dispersed in different solvents including the water without using the surfactants. It is shown that the sulphur atoms in the nanowires of $\text{Mo}_6\text{S}_3\text{I}_6$ can be readily substituted with selenium atoms which are distributed in the resulting nanowires. In order to additionally functionalize some of the synthesized onedimensional structures a gold particles are reproducibly self assembled preferably onto the ends to the $\text{MoS}_{(2-x)}\text{I}_y$ nanotubes upon mixing of dispersion the nanotubes and 5 nm colloid gold dispersion.

References

1. Remškar M., *et al*, *Science*; 2001; 292; 479
2. D. Vrbanić, *et al*, *Nanotechnology* 2004; 15; 635

Corresponding author

Aleš Mrzel

email : ales.mrzel@ijs.si

2S-4

Japan's Town Factories are World's Treasure -What they can and cannot make in China-

Hisayoshi HASHIMOTO

*The National Graduate Institute for Policy Studies
7-22-1 Roppongi, Minato-ku, Tokyo 106-8677, Japan*

Surprise!

Corresponding Author Hisayoshi HASHIMOTO

E-mail : hasimoto@grips.ac.jp

Tel: +81-3-6439-6205

Fax: +81-3-6439-6010

URL: <http://www.ne.jp/asahi/hashimoto/seikendai/>

Super Growth: From Highly Efficient Impurity Free CNT Synthesis to Super-Capacitors and Much More

Kenji Hata

Research Center for Advanced Carbon Materials, National Institute of Advanced Industrial Science and Technology (AIST), Tsukuba, 305-8565, Japan

This presentation will provide an overview of our recent development of the “Super Growth” CVD. First, the synthesis of highly efficient impurity free SNWT forest will be described. Second, the growth dynamics will be explored with our recent advance in CNT synthesis, as well as characterizing the physical and chemical properties of SWNT forests. Third, various new forms of carbon nanotube material made by utilizing the super-growth technique will be demonstrated with emphasis on their applications such as super-capacitors. Lastly, challenges and future projects that are planned will be summarized.

References:

- [1] K. Hata, D. Futaba, K. Mizuno, T. Namai, M. Yumura, S. Iijima, *Science* 306 (2004) 1362
- [2] Don N. Futaba, Kenji Hata, Takeo Yamada, Kohei Mizuno, Motoo Yumura, and Sumio Iijima, *Physical Review Letters*, 95, 056104, (2005)

Corresponding Author Kenji Hata

E-mail kenji-hata@aist.go.jp

Tel&Fax 029-861-6763, FAX 029-861-4851

Molecular Dynamics Simulations for Formations and Properties of Various Defects on Carbon Nano-Structures

Takazumi Kawai

Fundamental and Environmental Research Laboratories, NEC Corporation

For the applications of carbon nanostructures to nano-scale devices, controlling the atomic scale defect structures is a big issue. For the first step to control defects, identification of the atomic structures on nano-carbons and their influence on the stability and electronic properties are very important. Here, various types of defect structures are investigated using tight-binding molecular dynamics simulations and DFT-LDA calculations.

Tight-binding molecular dynamics simulations of a C_2 molecule collision with nanotube surface shows that C_2 molecule is sometimes incorporated into nanotube sp^2 network and forms a new topological defect structure. A line defect consists of the new defects are known to represent ferromagnetic spin ordering[1]. In other runs of the same kind of simulations the C_2 molecule also irradiates several famous defect structures such as mono-vacancy, di-vacancy, and also Stone-Wales defect, although C_2 molecule often bounce back even with a high kinetic energy of ~ 20 eV.

We consider another interesting defect structure which is a junction of sp^2 network connected by sp^3 like four-fold carbon atoms. These junction structures are formed by the collision of a graphene sheet edge with a graphene sheet surface, and there are almost no reaction barriers for the formation[2]. The formation processes of the junction structures are also applied to nanotube T-junctions, where both the colliding graphene sheet and targeted graphene surface are curved.

Acknowledgement: I am grateful to all the collaborators, especially S.Okada, K.Nakada, and Y. Miyamoto. This work was in part performed under the management of Nano Carbon Technology project supported by NEDO.

[1] K. Nakada, K. Kuwabara, K. Daigoku, T. Kawai and, S. Okada, in preparation.

[2] T. Kawai, S. Okada, Y. Miyamoto, A. Oshiyama, Phys. Rev. B72, 035428 (2005).

Corresponding Author: Takazumi Kawai

E-mail: t-kawai@da.jp.nec.com, Tel: 029-850-1554, Fax 029-850-2647

一般講演
General Lecture

1-1 ~ 1-16

2-1 ~ 2-14

3-1 ~ 3-12

Photoluminescence mapping of various (n, m) nanotubes by cross-polarized light

○Yuhei Miyauchi, Mototeru Oba and Shigeo Maruyama

Department of Mechanical Engineering, The University of Tokyo, 7-3-1 Hongo, Bunkyo-ku, Tokyo 113-8656, Japan

Photoluminescence excitation (PLE) spectroscopy of single-walled carbon nanotubes (SWNTs) have been extensively studied for characterization of their unique electronic properties due to the one-dimensionality. Theoretical studies and recent experiments have demonstrated that these optical transitions in SWNTs are dominated by strongly correlated electron-hole states in the form of excitons. Major peaks in a PL map correspond to the excitation transition energy of the second subband (E_{22}) and the photon emission energy of the first subband (E_{11}) of a specific SWNT, and these peaks are assigned to particular (n, m) nanotube species [1]. On the other hand, we can also find lower-intensity features around main PL peaks in a PLE spectrum. Recently, we have clearly identified that some of these features are phonon sideband peaks by measuring isotopic shift in PLE measurement using SWNTs consisting of carbon-13 [2]. In addition to the direct experimental proof of the strong exciton-phonon interaction [3], we also found low-intensity ‘pure electronic’ features whose origin has never been elucidated [2]. To investigate the origin of these unassigned ‘pure electronic’ peaks, we have performed polarized-PLE spectroscopy on independently aligned SWNTs in a gelatin thin film, and some unassigned PL peaks of (7, 5) nanotubes were attributed to excitation by cross-polarized light to the nanotube axis [4].

In this report, we have studied polarized PLE spectra of various (n, m) nanotubes. Fig. 1 shows PL peaks attributed to excitation by cross-polarized light. Detailed experimental techniques for identification will be discussed. Obtained experimental Kataura plot for cross-polarized light will be compared with tight-binding calculation of SWNTs considering geometry optimization and curvature effect [5].

[1] S.M. Bachilo, M.S. Strano, C. Kittrell, R.H. Hauge, R.E. Smalley, R.B. Weisman, *Science* **298**, 2361 (2002).

[2] Y. Miyauchi and S. Maruyama, submitted to *Phys. Rev. Lett.*, cond-mat/0508232.

[3] V. Perebeinos, J. Tersoff, Ph. Avouris, *Phys. Rev. Lett.* **94**, 027402 (2005).

[4] Y. Miyauchi, and S. Maruyama, to be submitted.

[5] M. Oba, S. Okada, T. Miyake, S. Maruyama, the 30th Fullerene Nanotubes General Symposium, Nagoya (2006).

Corresponding Author: Shigeo Maruyama

TEL&FAX: +81-3-5800-6983

E-mail: maruyama@photon.t.u-tokyo.ac.jp

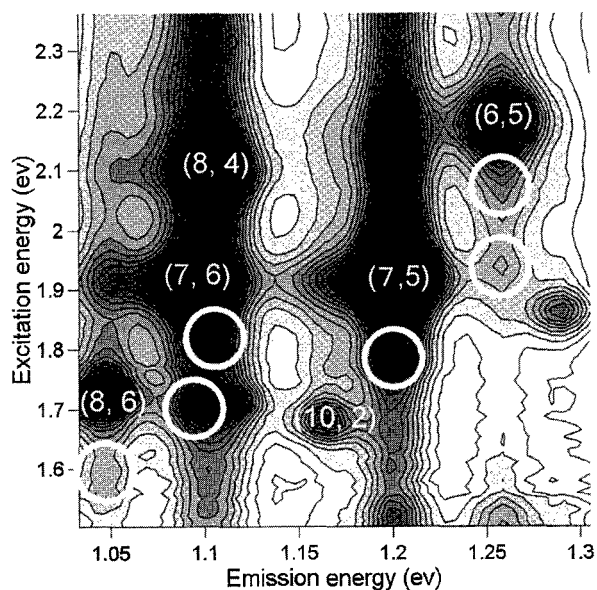


Fig. 1 Polarized PL map of dispersed SWNTs in surfactant solution. Peaks indicated by circles were attributed to excitation by cross-polarized light. Configuration of polarizations was for enhanced cross-polarized absorption.

Family Pattern of Photoluminescence and Raman Intensity of Single Wall Carbon Nanotubes

R. Saito[○], J. Jiang, K. Sato and Y. Oyama

Department of Physics, Tohoku Univ. and CREST JST, Sendai 980-8578

We present photoluminescence (PL) and resonance Raman intensity of a single wall carbon nanotube (SWNT) as a function of diameter and chiral angle. Since the electron-photon and electron-phonon matrix elements show highly anisotropic behavior in the k space, the obtained intensity strongly depends on chirality of SWNTs. The calculated intensity show a family pattern for (n, m) single wall carbon nanotubes in which $2n+m$ or $n-m = \text{constant}$ SWNTs show a systematic frequency and intensity changes. The calculated results are consistent with experimental results of relative intensity of G-band Raman intensity and radial breathing modes (RBM) intensity of single wall carbon nanotubes. Starting with our basic formulation within an extended tight binding calculation, we will overview our main progress obtained in this half year. We will compared with some experimental results of PL intensities to obtain the natural abundance of (n,m) nanotubes. This work is collaborated with MIT group of Prof. M. S. Dresselhaus, Tokyo Univ. group of Prof. S. Maruyama and AIST group of Dr. T. Okazaki.

References:

- (1) R. Saito et al., Phys. Rev. B, in press.
- (2) J. Jiang et al., Phys. Rev. B71, 205420 (2005), and *ibid.* in press.
- (3) Y. Oyama et al., Carbon in press.
- (4) K. Sato et al., in preparation.

Corresponding Author: Riichiro Saito

E-mail: rsaito@phys.tohoku.ac.jp

Tel&Fax 022-795-7754, 6447

Nanoscale uniaxial pressure effect of carbon nanotubes on the Raman spectra

*Taka-aki Yano ¹, Yasushi Inouye ¹⁻³ and Satoshi Kawata ¹⁻³

¹ Osaka University, Suita, Osaka 565-0871, Japan

² RIKEN, Wako, Saitama 351-0198, Japan

³ CREST, Japan Corporation of Science and Technology, Japan

When single wall carbon nanotubes (SWNTs) are pressed by external force, the structure and the electronic property of the SWNTs are changed. These changes can be spectroscopically analyzed by measuring a Raman spectrum under the pressure. In our study, we have measured

Raman scattering of the locally-pressurized SWNTs at nanometer scale by using a metal-coated atomic force microscope (AFM) tip that confines and enhances photons under the tip apex. Nano-Raman spectra of an isolated SWNT bundle were measured *in situ* while gradually applying uniaxial force up to 2.4 nN to it by a silver-coated AFM tip [2]. We found out pressure dependence of Raman frequencies of radial breathing mode (RBM) bands, the D-band and the G-band, which had not been observed yet in other micro-Raman experiments under hydrostatic pressure, as shown in fig. 1. Furthermore, pressure dependence of the Raman intensity, which was related to modification of the electronic band gap energies of SWNTs due to the radial deformation was investigated.

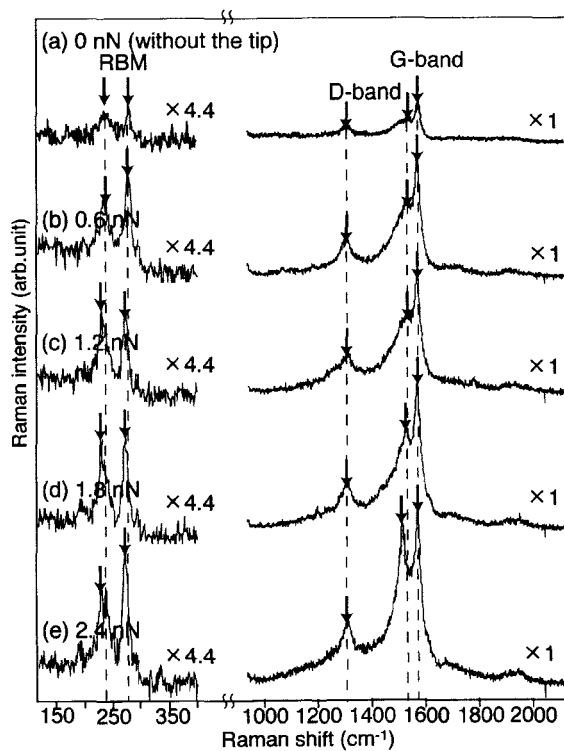


Fig. 1 Nano-Raman spectra measured by applying uniaxial force up to 2.4 nN.

References:

- [1] Y. Inouye and S. Kawata, *Opt. Lett.* **19**, 159 (1994).
- [2] T. Yano, Y. Inouye, and S. Kawata, submitted

Corresponding Author: Yasushi Inouye

E-mail: ya-inoue@ap.eng.osaka-u.ac.jp, Tel: +81-6-6879-4243, Fax: +81-6-6879-7330

Chirality-dependent environmental effect on photoluminescence of SWNTs

○ S. Iwasaki¹, Y. Ohno^{1,2}, Y. Murakami³, S. Kishimoto¹, S. Maruyama³, and T. Mizutani¹

¹ Dept. of Quantum Eng., Nagoya University, Furo-cho, Chikusa-ku, Nagoya 464-8603, Japan

² PRESTO/JST, 4-1-8 Honcho Kawaguchi, Saitama 332-0012, Japan

³ Dept. of Mechanical Eng., The University of Tokyo, 7-3-1 Hongo, Bunkyo-ku, Tokyo 113-8656, Japan

Optical transition energies in SWNTs are affected by environmental condition because the electric field regarding carrier-carrier interactions spreads outside the SWNTs. The SWNTs suspended in air are important samples as a reference to investigate the environmental effect [1]. We have investigated the PL and PLE map of SWNTs suspended in air for 20 chiralities, which is compared with the results reported for SDS-wrapped SWNTs [2].

An SEM image of our sample is shown in Fig. 1. The SWNTs suspended in air were grown on a grated quartz substrate by alcohol CVD. Figure 2 shows the energy shifts of E_{11} and E_{22} of air-suspended SWNTs from those of SDS-wrapped SWNTs as a function of chiral angle. Here, the open squares and closed circles represent type-I [(2n+m) mod 3 = 1] and type-II [(2n+m) mod 3 = 2] SWNTs, respectively. The E_{11} and E_{22} are mostly blueshifted by a few tens meV except for E_{22} of type-II SWNTs with small chiral angle (near Zigzag). The amounts of energy shifts, ΔE_{11} and ΔE_{22} , show different dependence on chiral angle between type-I and type-II. In the case of type-I SWNTs, ΔE_{11} is larger for larger chiral angle whereas ΔE_{22} is smaller for larger chiral angle. In contrast, type-II SWNTs shows opposite dependences. These results clearly show that the environmental effect on optical transition energies depends on the chirality (n , m).

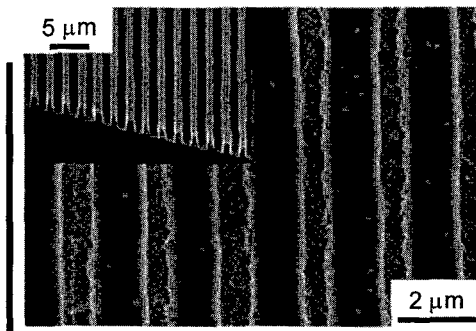


Fig. 1 SEM image of sample.

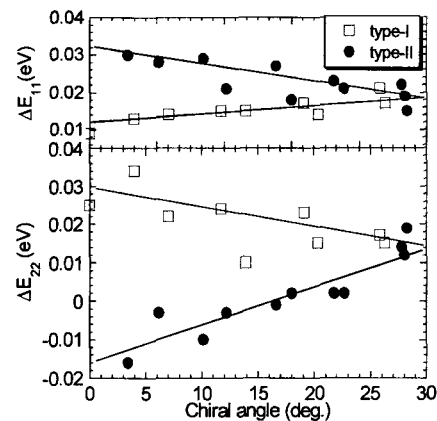


Fig. 2 Chiral angle dependence of ΔE_{11} , ΔE_{22} .

[1] J. Lefebvre *et al.*: Phys. Rev. Lett. **90** (2003) 217401

[2] R. B. Weisman *et al.*: Nano Lett. **3** (2003) 1235

Corresponding Author: Yutaka Ohno

E-mail: yohno@nuee.nagoya-u.ac.jp, TEL&FAX: 052-789-5387&052-789-5232

Mid-gap luminescence centers in single-wall carbon nanotubes created by UV illumination

Konstantin Iakoubovskii, Nobutsugu Minami, Yeji Kim, Kanae Miyashita, Said Kazaoui
Balakrishnan Nalini

Nanotechnology Research Institute, National Institute of Advanced Industrial Science and Technology (AIST), 1-1-1 Higashi, Tsukuba, Ibaraki 305-8565, Japan

We report the effect of UV illumination on optical properties of single-wall carbon nanotubes (SWNTs), isolated using various dispersants including carboxymethylcellulose (CMC), hydroxyethylcellulose (HEC), etc. Water solutions and cast films prepared using commercial SWNTs (HiPco, CoMoCAT and Carbolex) have been studied.

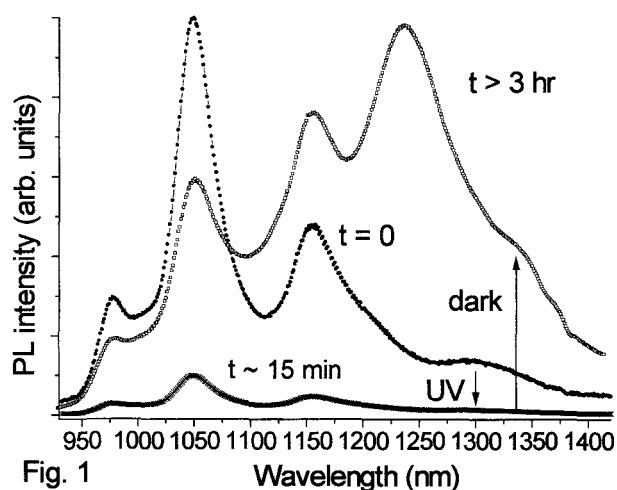


Fig. 1

Figure 1 outlines a summary of changes in PL spectra ($\lambda_{\text{ex}} = 662 \text{ nm}$) from CMC/CoMoCAT film: illumination by full spectrum of D₂ lamp ($I \sim 4 \text{ mW/cm}^2$) strongly reduces PL intensity in a timescale $t \sim 15 \text{ min}$. Illumination was carried out in vacuum to avoid sample oxidation. Interrupting illumination at this stage resulted in full recovery within 1 hr. However, longer illumination ($> 2 \text{ hr}$) produced significant spectral changes: weakening of the 980, 1050 and 1150 nm peaks and appearance of a strong signal at $\sim 1240 \text{ nm}$. Those changes could only be

observed at a few hrs after turning off D₂ lamp, but not during illumination; changed spectra were stable for at least 60 days and could not be reversed even by annealing.

The newly produced PL peaks have been studied in detail with PL, PL excitation (PLE), and optical absorption (OA), as a function of illumination wavelength and dispersant. We find that the presence of dispersant is essential for the UV-induced changes, and that the excitation spectrum of the changes matches the OA spectrum of the dispersant. The obtained results suggest the following scenario of those changes: during the first stage of UV illumination ($t \sim 15 \text{ min}$) charge transfer occurs between the dispersant and SWNT resulting in *reversible* quenching of OA and PL. However, prolonged illumination ($t > 2 \text{ hr}$) results in *irreversible*, probably photochemical, reactions between the dispersant and SWNT. As a result, defect states are created in the forbidden gap of SWNT. They could not be detected by OA, but produced new, rather efficient PL peaks. Polarization of those PL peaks could be induced by stretching polymer/SWNT films thus revealing the extended (1-D, rather than 0-D or "quantum dot like") character of the newly produced defect states. The position of those new peaks is dispersant dependent. The proposed model of 1-D defect states is further supported by the PLE results.

Corresponding Authors:

Konstantin Iakoubovskii TEL: +81-29-861-4433, FAX: +81-29-861-4433, E-mail: k.iakoubovskii@aist.go.jp
Nobutsugu Minami TEL: +81-29-861-9385, FAX: +81-29-861-6309, E-mail: n.minami@aist.go.jp

Single walled carbon nanotube analysis: Rapid, robust acquisition and simulation of quantum and chiral maps to ease structural assignments.

*Adam M. Gilmore, Ray K. Kaminsky, James M. Mattheis

*HORIBA JobinYvon Inc., Fluorescence Division, 3880 Park Ave., Edison, NJ
08822*

This paper describes improved methods for both data acquisition and analysis that are pertinent to interpreting the structural composition of single-walled carbon nanotube (SWNT) mixtures and suspensions. Rapid data acquisition is made possible with a specially configured spectrofluorometer which uses a liquid nitrogen cooled InGaAs array detector, imaging spectrograph, excitation reference photodiode and tunable xenon excitation source to collect seamless, instrument-corrected excitation-emission quantum maps. The preferred instrument configuration with the InGaAs array can generate a quantum map with both high S/N levels and spectral resolution in only seconds to minutes; previous single-channel InGaAs photodiode and photomultiplier detector measurements took hours to days. The standard spectral range for excitation and emission is from 250 nm to 1700 nm with an option to extend to 2200 nm. Robust analysis of the quantum maps is facilitated by a custom global analysis program (US Patent Pending) which incorporates a powerful 'double-convolution integral' DCI algorithm to simultaneously model the excitation and emission spectral bands for each SWNT species. The patented DCI algorithm reduces the number of free fitting parameters for the spectral simulation by up to a factor of 1000 compared to conventional 2 D spectral simulators. The global analysis yields quantitative information on the chirality and diameter parameters of SWNT species in a given mixture. Together the acquisition hardware and analysis software constitute significant developments with respect to enhanced sensitivity and statistical significance for quantifying the components of complex SWNT mixtures.

Corresponding Author: Adam M. Gilmore

Email: adam.gilmore@jobinyvon.com

Tel: 732-494-8660 x135

Fax: 732-549-5157

Third-order Nonlinear Optical Response and Relaxation Dynamics in Double-Walled Carbon Nanotubes

O.A. Nakamura¹, T. Tomikawa¹, S. Imamura¹, M. Watanabe¹, Y. Hamanaka², Y. Saito¹,
and H. Ago³

¹*Department of Applied Physics, Nagoya University, Nagoya 464-8603, Japan*

²*Nagoya Institute of Technology, Nagoya 466-8555, Japan*

³*Institute for Materials Chemistry and Engineering, Kyushu University,
Fukuoka 816-8580, Japan*

Single-walled carbon nanotubes (SWNTs) shows the large enhancement of the third-order nonlinear optical susceptibility $\chi^{(3)}$ due to the exciton effect and the van Hove singularity in optical transitions between valence and conduction bands[1,2]. In double-walled carbon nanotubes (DWNTs), interaction between inner and outer tubes modifies electronic and vibrational properties, and consequently nonlinear optical response and relaxation dynamics of excited states may be affected by the inter-wall interaction. In this presentation, we report on relaxation dynamics of photoexcited carriers and third-order nonlinear optical susceptibilities studied by femtosecond pump-probe spectroscopy.

Raw materials of DWNTs were produced by a chemical vapor deposition method using Fe nanoparticles with the diameter of 10 nm and MgO powder as catalysts. DWNTs were dispersed in water-surfactant to obtain individual nanotubes, each encased in a cylindrical micelle. The average diameters of inner and outer tubes are 1.4 and 2.2 nm, respectively. Pump-probe measurements have been carried out using a 150 fs-width pump pulse with the photon energy of 3.2 eV and a white continuum probe pulse.

Absorption spectra indicate sharp structures corresponding to different diameters and chirality. Relaxation times measured for the lowest band-to-band transitions of semiconducting inner tubes exhibit double-exponential decay behavior; the decay times of the fast and slow components are ~ 0.4 and 2.1-7.5 ps, respectively. In SWNTs the decay time in the range of 0.5-1.2 ps is strongly dependent on the photon energy, which is mainly due to the intraband relaxation of photoexcited carriers and defect trapping. Therefore, the energy-independent behavior of the fast component is in contrast to the result observed for SWNTs, indicating the existence of a carrier relaxation channel from inner to outer tubes. The slow component is ascribed to the non-radiative recombination of electrons and holes relaxed at the band bottom.

Third-order nonlinear optical susceptibilities $\chi^{(3)}$ in the non-degenerate configuration were also measured with the pump-probe method. The figure of merit $Im\chi^{(3)}/\alpha$ (α : absorption coefficient) is -2.4×10^{-14} esu cm around 1 eV, which is comparable to the value (-5.6×10^{-14} esu cm) for the E₁₁ transition in SWNTs.

[1] T. Tomikawa *et al.*, Abstract of 27th Fullerene Nanotubes Symposium, p.20, 2004.

[2] A. Maeda *et al.*, Phys. Rev. Lett. 94, (2005) 047404.

Corresponding Author: Arazo Nakamura.

TEL: +81-52-789-4450, FAX: +81-52-789-5316, E-mail: nakamura@nuap.nagoya-u.ac.jp

Effects of Gravity on SWCNT Dissipative Structures Induced by DC Electric Field

Syuichi Sato and ○Masahito Sano

*Department of Polymer Science and Engineering, Yamagata University
4-3-16 Jyonan, Yonezawa, Yamagata 992-8510 JAPAN*

Dissipative structures appear in non-equilibrium systems where either matter or energy is transferred between the systems and outsides. Examples include Benard convection and Belousov-Zhabotinsky reactions. Typically, these phenomena are modeled by non-linear equations with some kinds of feedback. As one process proceeds, another process that interacts non-linearly becomes active. These processes, then, limit or accelerate each other. Thus, identifying the relevant processes is quite important to understand dissipative phenomena.

Previously, we have reported that applying DC electric field to an aqueous dispersion of single-walled carbon nanotubes (SWCNTs) produces dissipative patterns on the anode surface. Experimentally, two flat parallel plates are laid horizontally and the top plate is made anodic. SWCNTs are treated in acids to afford negative charges. The patterns appear as a result of non-uniform SWCNT concentration distribution near the surface and disappear when the DC field is turned off. Initially uniformly distributed SWCNTs gather to form line segments which are connected to make polygonal cells. Afterward, SWCNTs start moving along the line toward the point where the cells meet and produce another types of well-defined patterns. We have found that there is a threshold voltage for the pattern formation and the size of the cells is exactly the same as the electrode separation. These properties resemble those of Benard convection. In the convection, both temperature gradient and gravity play the major role.

Stimulated by these similarities, we have investigated the effects of gravity. Two ITO plates were fixed in various orientations and the patterns were recorded. We have observed that the cell pattern appear irrespective of the plate orientation, implying that the gravitational effect is not relevant. On the other hand, the later pattern may be affected by the plate orientation.

Corresponding Author: Masahito Sano

E-mail: mass@yz.yamagata-u.ac.jp

Tel&Fax: +81-(0)238-26-3072

Mechanical Characteristics of High-Density and Well-Aligned Carbon Nanotubes on SiC

M. Kusunoki¹, H. Usami², D. Igimi¹ and K. Miyake³

¹Japan Fine Ceramics Center, Nagoya 456-8587, Japan

²Dept. of Materials Science & Engineering, Meijo Univ. Nagoya, 468-8502, Japan

³Advanced Industrial Science and Thechnology (AIST), Tsukuba, 305-8564, Japan

Carbon nanotubes (CNTs) have unique mechanical properties, such as high elastic modulus, high tensile and flexural strength. CNT filled polymer, ceramic and metal nano-composites have been synthesized for tribological applications. These composites showed that the friction resistance and wear rates were reduced through the addition of CNTs [1]. However, it is not easy to disperse CNTs uniformly in the composite. Furthermore, aligned CNTs up to several microns in thickness deposited on select substrates by chemical vapor deposition (CVD) are also expected to configure nanostructured surfaces in tribological applications. However, CNTs are subject to peeling off from the substrate surface.

We have reported well-aligned and high-density CNTs are synthesized by surface decomposition of SiC(0001). High resolution transmission electron microscopy revealed the CNTs connected directly to the SiC surface without any amorphous [2]. Then, it is expected that the CNTs adhere to the SiC substrate.

The present study described novel frictional response obtained by a flexibility of CNTs layer (Fig.1) and excellent erosion resistance against the collision of diamond abrasives (Fig.2) by high adhesion strength of CNTs layer. These results showed that the CNTs synthesized by the present method have the self-control ability of friction resistance and high erosive wear resistance.

[1] W. X. Chen et al., Tribol. Lett., 15, 275 (2003).

[2] M. Kusunoki et al., Chem. Phys. Lett., 366, 458 (2002).

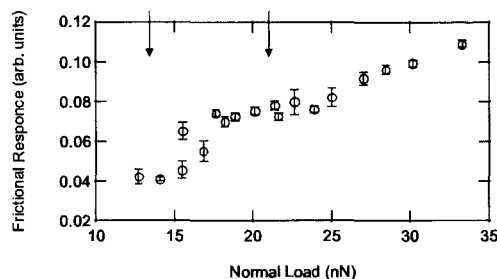


Fig. 1 Friction response measured by an AFM probe.

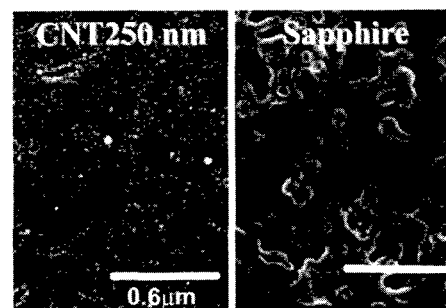


Fig. 2 SEM images of the CNT and Sapphire surfaces eroded with slurry including diamond abrasives (2 μ m in diameter accelerated with 0.4MPa air).

Electronic structures of the interface between carbon nanotubes and titanium electrodes measured by hard x-ray photoemission spectroscopy

○D. Kondo^{1,2}, M. Nihei^{1,2}, A. Kawabata^{1,2}, S. Sato^{1,2}, E. Ikenaga³, M. Kobata³, J.-J. Kim³, K. Kobayashi³, S. Komiya³, Y. Awano^{1,2}

¹Nanotechnology Research Center, Fujitsu Laboratories Ltd., ²Fujitsu Limited
10-1 Morinosato-Wakamiya, Atsugi 243-0197, Japan

³Japan Synchrotron Radiation Research Institute/SPring-8
1-1-1 Kouto Sayo-cho Sayo-gun, Hyogo 679-5198, Japan

Carbon nanotubes (CNTs) are a promising candidate for wiring materials in future LSI interconnects due to their unique electrical property. For such an application, it is important to achieve low-resistance ohmic contacts between CNTs and metal electrodes [1]. In this study, we have investigated the electronic structures at the interface using the hard x-ray photoemission spectroscopy (PES). The PES measurements were performed at the BL47XU in the SPring-8. CNTs were grown on a 30-nm nickel/50-nm titanium double layer deposited on a silicon substrate using chemical vapor deposition.

Figure 1 shows C 1s core-level spectra after the CNT growth. The spectra (a) and (b) were measured at different emission angles. It has been found that two features observed in the spectrum (a) are assigned to CNTs and titanium carbide (TiC). The observation of TiC means that good ohmic contacts were formed at the interface. However, no feature corresponding to TiC has been found in the spectrum (b). These results suggest that the oxidation of the titanium layer proceeded during the growth process, thus preventing TiC from being formed in the region near the surface.

Acknowledgement: The authors thank Dr. N. Yokoyama of Fujitsu Laboratories Ltd. for their support and useful suggestions. This work was supported by Advanced Nanocarbon Application Project, which consigned to Japan Fine Ceramics Center (JFCC New Energy and Industrial Technology Development Organization (NEDO) of Japan.

References: [1] M. Nihei *et al.*, IITC 2005.

Corresponding Author: Daiyu Kondo

E-mail: kondo.daiyu@jp.fujitsu.com

Tel&Fax: +81-46-250-8234&+81-46-250-8844

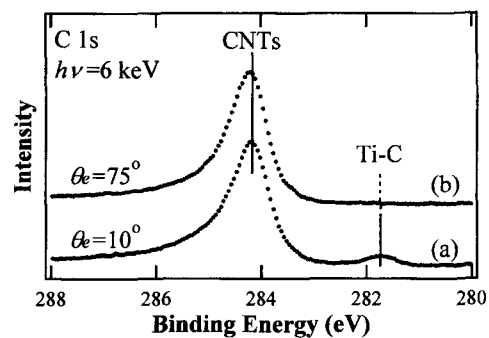


Figure 1 C 1s core-level spectra after the CNT growth.

Vibration analysis of carbon nanotube cantilevers

Seiji Akita¹, Shintaro Sawaya¹ and Yoshikazu Nakayama^{1,2}

¹*Department of Physics and Electronics, Osaka Prefecture University
1-1 Gakuen-cho, Sakai, Osaka 599-8531, Japan*

²*Handai Frontier Research Center, Graduate School of Engineering, Osaka University
Suita, Osaka 565-0871, Japan*

Cantilever miniaturization is crucial to realize highly sensitive mass detection based on the resonant frequency shift of the cantilever. Carbon nanotubes (CNTs) are appropriate for this applications because of their light weight, high aspect ratio, and extraordinary mechanical properties. In order to realize higher sensitivity, the detailed analysis of the vibration of the CNT cantilevers should be required. In this study, we have investigated the vibration of multiwall carbon nanotubes (MWCNT) using a nanomanipulation technique inside a scanning electron microscope (SEM)^{1,2} and molecular dynamics (MD) simulations.

Figure 1 shows an example of the resonant frequency curve for a MWCNT with the length of 6.7 μm and the diameter of 12 nm. The quality factor, Q , is ~ 1500 at the resonance of 730.26 kHz. The Q factors for several nanotubes examined were in the range of 300~2000. The intrinsic nanotubes should have higher Q factors because the nanotubes used in this experiment were covered slightly with contamination deposited during SEM observation.

We have performed the MD simulations for single-wall (SW) and double-wall (DW) CNTs with the same outer most layer of (15,15) and the length of 24.9 nm at constant temperatures of 1 and 300 K, where a MM3 potential set³ was used. The oscillation of the nanotubes for 1ns were calculated for the recovery process after the buckling of the nanotubes. The resonant frequencies are summarized in Table I. For both nanotubes, the resonant frequencies at 1 K are lower than that at 300 K. Furthermore, the temperature dependence of the resonant frequency of the SWCNT is larger than that of the DWCNT. This result implies the weak temperature dependence of the van-der-Waals interactions for the interlayer of the DWCNT. Whereas the spring constant for the DWCNT is larger than the SWCNT, the weight of the DWCNT is heavier than that of the SWCNT. As a result, the resonant frequency of the DWCNT becomes lower than that of the SWCNT. The significant energy dissipations for both CNTs at 1 and 300 K could not be observed for 1 ns. Further calculations are required accurate evaluations of the Q value.

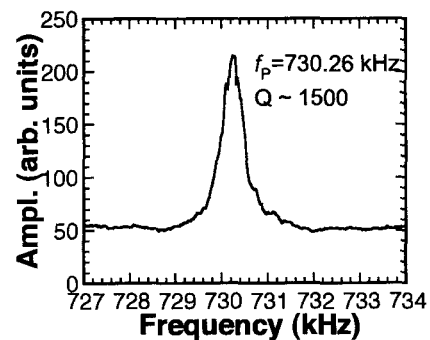


Fig.1 Resonant curve for the MWNT.

Table I. MD results of vibration analysis for the (15,15) SWCNT and the (10,10)-(15,15) DWCNT.

	1 K (GHz)	300 K (GHz)
SWCNT	8.5	12
DWCNT	7.1	11

References:

- 1) M. Nishio, S. Sawaya, S. Akita, and Y. Nakayama, *Appl. Phys. Lett.* **86**, 133111 (2005).
- 2) M. Nishio, S. Sawaya, S. Akita, and Y. Nakayama, *JVSTB* **23**, 1975(2005).
- 3) N. L. Allinger, F. Li and L. Yan: *J. Comput. Chem.* **11**, 848 (1990).

Corresponding Author: Seiji Akita,

TEL&FAX: +81-72-254-9265, **E-mail:** akita@pe.osakafu-u.ac.jp

First-principles calculations of the radial breathing mode of peapods

Susumu Okada

*Center for Computational Sciences, University of Tsukuba, Tennodai,
Tsukuba 305-8571*

Carbon nanotubes have been attracting a lot of attention in the both fields of pure and applied sciences due to their unique structural and electronic properties which are applicable for nano-scale devices. To utilize the nanotubes for the various purposes, it is important to characterize a diameter and a chiral angle of an individual single-walled carbon nanotube. Raman spectroscopic experiment is a promising tool for the identification and probing the geometric structure of nanotubes. In particular, the radial breathing mode (RBM) plays the crucial role to determine the diameter of the nanotubes. In addition to the structural identification, the RBM mode is also applicable for monitoring the modulation of surrounding condition of the nanotubes, such as intercalation and encapsulation of atoms and molecules. Indeed, Bandow et al showed that encapsulation of fullerenes into nanotubes induces small shift of the RBM frequency from the empty nanotube [1]. Further, they also reported that the shift strongly depends on the diameter of the nanotube.

In the present work, we reveal how the RBM frequency depends on the diameter of nanotubes for the fullerene encapsulation by using the first-principles total-energy calculations. We use peapods consisting of C_{60} and metallic (n, n) nanotubes ($n=9,10,11$, and 12). For the $(9,9)$ and $(10,10)$ nanotubes, we find that the RBM frequencies of the nanotubes shift upward by 86 cm^{-1} and 3 cm^{-1} for $C_{60}@ (9,9)$ and $C_{60}@ (10,10)$ peapods, respectively. In sharp contrast to the thin nanotubes, RBM frequencies of $(11,11)$ and $(12,12)$ nanotubes containing C_{60} shift downward by 2 cm^{-1} and 1 cm^{-1} from those of the empty $(11,11)$ and $(12,12)$ nanotubes, respectively. We find that the downward shift is induced by the small charge transfer from the π electron of the nanotube to the space between the nanotube and C_{60} .

References:

[1] S. Bandow, et al, Chem. Phys. Lett. **347**, 23 (2001).

Corresponding Author: Susumu Okada

E-mail: sokada@comas.frsc.tsukuba.ac.jp

Tel&Fax:029-853-5921/5924

Synthesis and electronic properties of Fe-filled single-walled carbon nanotubes

○Y. F. Li, R. Hatakeyama, T. Kaneko, T. Izumida, T. Okada, and T. Kato

Department of Electronic Engineering, Tohoku University, Sendai 980-8579, Japan

Single-walled carbon nanotubes (SWNTs) are known to be either metallic or semiconducting based on their chirality and diameter. A number of investigations on semiconducting SWNTs have led to the development of field-effect transistors (FETs). The pristine SWNTs are found to exhibit *p*-type behavior [1], which is mainly attributed to adsorption of oxygen on the SWNTs. *n*-type SWNTs FETs can be formed by doping impurities such as alkali-metals or other organic electron donors inside SWNTs [2, 3]. However, the current electronic devices based on SWNTs mainly utilize the charge of conductance electrons. Therefore it is quite natural to ask if both the charge and spin of electrons can be used in semiconducting SWNTs to further enhance the performance of devices. One of promising ways to realize the above purpose is to inject ferromagnetic elements such as Fe, Co or Ni into non-ferromagnetic SWNTs to make them magnetic.

In this study, we report on the synthesis of ferromagnetic semiconducting SWNTs by Fe filling. The synthesis of Fe-filled SWNTs is realized by using ferrocene as the starting material [4]. The structure and morphology of Fe-filled SWNTs is confirmed by several technologies which include HRTEM, EDX, and Raman Spectrum analyses. Electronic properties of SWNT-FET indicate that ferrocene-filled SWNTs exhibit an interesting ambipolar semiconducting behavior compared with typical pristine *p*-type SWNTs. In contrast, unipolar *n*-type characteristics for Fe-filled SWNTs are significantly found. Figure 1 depicts the current versus voltage ($I_{DS}-V_G$) characteristics of *n*-type Fe-filled SWNT-FET (right, open circle line) and pristine *p*-type SWNT-FET (left, circle line), which indicates ferromagnetic semiconducting SWNTs can be created by Fe filling.

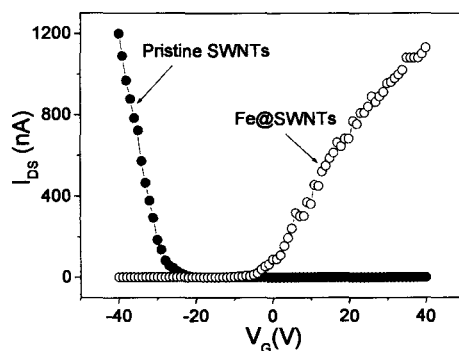


Fig. 1. $I_{DS}-V_G$ curves for *n*-type Fe-filled SWNTs (right) and *p*-type pristine SWNTs, respectively.

[1] R. Martel et al., Appl. Phys. Lett. **73**, 2447 (1998).

[2] T. Izumida et al., Jpn. J. Appl. Phys. **44**, 1606 (2005).

[3] T. Takenobu et al., Nature Materials **2**, 683 (2003).

[4] Y. F. Li et al., Abstract of 29th Fullerene General Symposium, 1P-33 (2005).

Corresponding Author: Yongfeng Li, **E-mail:** yfli@plasma.ecei.tohoku.ac.jp

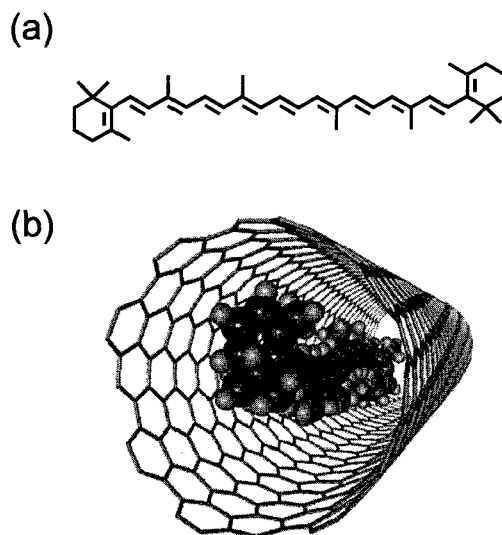
Tel & Fax: 81-22-795-7046/263-9225

Optical Properties of β -carotene inside Single-Walled Carbon Nanotubes

○Kazuhiro Yanagi, Yasumitsu Miyata, and Hiromichi Kataura

*Self-Assembled Nano-Electronics Group Nanotechnology Research Institute (NRI)
National Institute of Advanced Industrial Science and Technology (AIST)
1-1-1 Higashi, Tsukuba, Ibaraki 305-8562, Japan*

Abstract: Producing the next generation of technologies, such as all-optical switching devices, data processing using an optical-neural network, etc., requires the development of materials that have the following three features, (1) large third-order optical nonlinearity, (2) ultra-fast optical response, and (3) sufficient robustness for device application. π -conjugated polyene molecules have the potential to satisfy all three requirements since they satisfy the first and second ones. However, degradation of π -conjugate molecules is a bottleneck impeding their application to photonic devices. β -carotene is a model system for π -conjugated molecules. We found that β -carotene can be encapsulated inside single-walled carbon nanotubes (Car@SWCNTs). The conformation of the encapsulated β -carotene is discussed from its Raman spectra. The filling rate of β -carotene in Car@SWCNT is estimated from the absorbance of β -carotene in Car@SWCNT. We found that β -carotene in Car@SWCNT was quite stable under ambient conditions. The surrounding tube-wall protected β -carotene from reacting with radical species and suppressed its isomerization. Therefore, the encapsulation technique of β -carotene presented here can be a good breakthrough for application of π -conjugated molecules to photonic device materials.



(a) Chemical structure of β -carotene, and
(b) a schematic illustration of β -carotene
inside a (12,8) SWCNT.

Corresponding Author: Kazuhiro Yanagi

E-mail: k-yanagi@aist.go.jp

Tel. +81-29-861-3132, Fax. +81-29-861-2786

Cap effects of Gd acetate on nanohorn holes

OR. Yuge¹, J. Miyawaki², M. Yudasaka^{1,2}, Y. Kubo¹, E. Nakamura³, H. Isobe³, H. Yorimitsu³, and S. Iijima^{1, 2, 4}

¹*NEC, 34 Miyukigaoka, Tsukuba 305-8501, Japan*

²*SORST-JST, 34 Miyukigaoka, Tsukuba 305-8501, Japan*

³*The university of Tokyo, Hongo, Bunkyo-ku, Tokyo 113-0033, Japan*

⁴*Meijo University, 1-501 Shiogamaguchi, Tenpaku-ku, Nagoya, 468-8502, Japan*

Single-wall carbon nanohorns (SWNHs) have inherent hollow spaces, and the holes of the sheath walls can be opened easily by the heat treatment in oxygen (SWNHox). Various kinds of materials, such as C₆₀ [1] and Pt-compound [2], can be incorporated and released in/from the nanospace of SWNHox. Hashimoto et al [3] previously demonstrated using transmission electron microscopy that the Gd-acetate was deposited at the hole edges and inside SWNHox. It was also demonstrated that the Gd-acetate clusters had the cap effect, that is, they suppressed the C₆₀ incorporation into SWNHox. In this study, the cap effect of Gd acetates deposited at the hole edges and inside SWNHox was quantitatively evaluated through the analysis of the C₆₀ release from the inner space of SWNHox.

C₆₀ was incorporated inside SWNHox (C₆₀@SWNHox) by the nano-precipitation [1], and the holes of SWNHox were capped by Gd-acetate (Gd-C₆₀@SWNHox) [3]. By immersing C₆₀@SWNHox in toluene, about 90% of C₆₀ was released [1], while Gd-C₆₀@SWNHox, 60%. The SWNHox sheaths encapsulating the remaining-40% C₆₀ had the two types of Gd-acetate caps: one was the Gd-acetate cluster located inside the sheath, and the other one was that attached to the hole edge. The number ratio of SWNHox sheaths with the former and latter type caps was about 1:2. We removed the Gd-acetate caps by washing with water. After washing with water, most of the remaining-40% C₆₀ was released in toluene.

Acknowledgement:

This work was in part performed under the management of Nano Carbon Technology Project supported by NEDO. We also thank T. Azami and D. Kasuya for preparing SWNH samples.

Reference:

- [1] R. Yuge et al., *J. Phys. Chem.* **B109**, 17861 (2005).
- [2] K. Ajima, et al., *Mol. Pharm.*, in press.
- [3] A. Hashimoto, et al. *Proc. Natl. Acad. Sci.* **101**, 8527 (2004).

Corresponding Author: M. Yudasaka, R. Yuge.

TEL: +81-29-850-1190, FAX: +81-29-856-6137,

E-mail: yudasaka@frl.cl.nec.co.jp, ryuge@frl.cl.nec.co.jp

Formation of Carbon Nanofibers Having an Array of Conical Nano Cavities and Snapping at Their Nodes

○Akira Koshio, Yuta Takemura and Fumio Kokai

Department of Chemistry for Materials, Mie University, 1577 Kurimamachiya-cho, Tsu, Mie 514-8507, Japan

A catalytic chemical vapor deposition (CVD) method has been extensively investigated as a promising method for the growth of carbon nanofibers (CNFs) and carbon nanotubes. In fact, various structures of CNFs were formed by controlling growth conditions such as metal catalysts and reactant gases. Recently, we found that CNFs having an array of conical nano cavities were formed by an alcohol CVD method using indium tin oxide (ITO) / Fe as metal catalysts. The CNFs contain the conical nano cavities in a one-dimensional array at uniform intervals. In this study, we explored the most effective growth condition of the CNFs and studied on the possible formation mechanism of the one-dimensional array of conical nano cavities. Moreover, we report that the CNFs are easily snapped at their nodes corresponding to the bases of conical cavities.

A substrate for the CVD was prepared by spraying ethanol solution of InCl_3 , SnCl_2 and FeCl_3 on a Si plate maintained at $400\text{ }^\circ\text{C}$ followed by heating at $600\text{ }^\circ\text{C}$ for 30 min. in Ar atmosphere. The CVD growth of the CNFs was carried out at a vapor pressure of ethanol containing a small amount of CS_2 for 30 min.

Electron microscopic observation revealed that the inner structure consisted of an array of periodic conical cavities with lengths of 300-800 nm (Fig. 1(a)). Nodes of the CNFs, which correspond to the bases of conical cavities, are fragile due to the very thin structure. The CNFs can be easily cut in 1-10 pitch at the nodes like snapping branches by mechanical force such as ultrasonic irradiation (Fig. 1(b)). We suggest that the snapping technique using our CNFs may be suitable for controlling the length of CNFs.

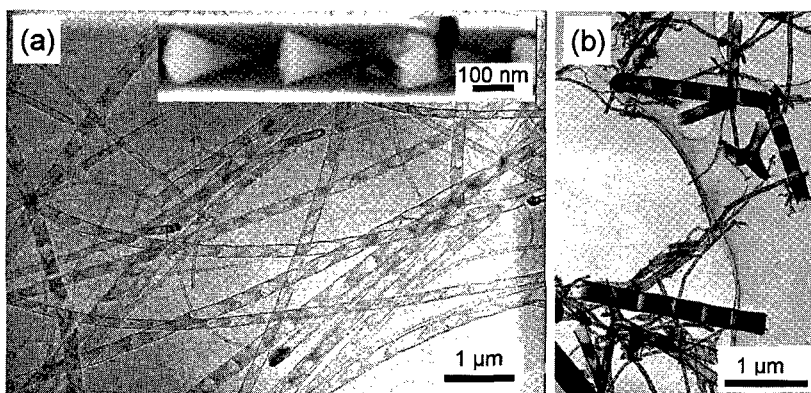


Fig. 1 (a) As-grown CNFs having an array of conical nano cavities. (b) Short CNFs snapped using ultrasonic irradiation.

Corresponding Author: Akira Koshio

E-mail: koshio@chem.mie-u.ac.jp **Tel&Fax:** +81-59-231-5370

Structural Determination of Sc₃C₈₂

○ Yuko Iiduka,¹ Takatsugu Wakahara,¹ Tsukasa Nakahodo,¹ Takahiro Tsuchiya,¹ Akihiro Sakuraba,² Yutaka Maeda,³ Takeshi Akasaka,*¹ Kenji Yoza,⁴ Ernst Horn,⁵ Tatsuhisa Kato,⁶ Michael T. H. Liu,⁷ Naomi Mizorogi,⁸ Kaoru Kobayashi,⁸ Shigeru Nagase*⁸

¹*Center for Tsukuba Advanced Research Alliance, University of Tsukuba,* ²*Graduate School of Science and Technology, Niigata University,* ³*Department of Chemistry, Tokyo Gakugei University,* ⁴*Bruker AXS K. K.,* ⁵*Department of Chemistry, Rikkyo University,* ⁶*Department of Chemistry, Josai University,* ⁷*Department of Chemistry, University of Prince Edward Island,* ⁸*Department of Theoretical Molecular Science, Institute for Molecular Science*

The structures and electronic properties of endohedral metallofullerenes have been extensively investigated both experimentally and theoretically.¹ It is widely accepted that the maximum-entropy-method (MEM)/Rietveld analysis of synchrotron X-ray powder diffraction data is powerful for structural determination of endohedral metallofullerenes. However, some of these structures such as Sc₃@C₈₂ do not correspond to energy minima or most stable structures. We report here structural determination of the Sc₃C₈₂ molecule by the ¹³C NMR spectroscopy and X-ray single-crystal structure analysis. It is remarkable that the endohedral structure of Sc₃C₈₂ is not Sc₃@C₈₂ but Sc₃C₂@C₈₀.²

(1) *Endofullerenes: A New Family of Carbon Clusters*; Akasaka, T., Nagase, S., Eds.; Kluwer: Dordrecht, 2002.

(2) Iiduka, Y. et al., *J. Am. Chem. Soc.* **2005**, *127*, 12500.

Corresponding author: Takeshi Akasaka

E-mail: akasaka@tara.tsukuba.ac.jp

Tel&Fax: +81-29-853-6409

Spin-Transfer System under Equilibrium Constructed from Endohedral Metallofullerenes and Organic Donors

○ Kumiko Sato¹, Takahiro Tsuchiya¹, Takatsugu Wakahara¹, Yutaka Maeda²,
Tsukasa Nakahodo¹, Takeshi Akasaka¹, Tatsuhisa Kato³, Kei Ohkubo⁴, Shunichi Fukuzumi⁴,
Naomi Mizorogi⁵, Kaoru Kobayashi⁵, Shigeru Nagase⁵

¹ Center for Tsukuba Advanced Research Alliance,
University of Tsukuba, Tsukuba, Ibaraki 305-8577, Japan

² Department of Chemistry, Tokyo Gakugei University, Koganei, Tokyo 184-8501, Japan

³ Department of Chemistry, Josai University, Sakado, Saitama 350-0295, Japan

⁴ Department of Material and Life Science, Graduate School of Engineering,
Osaka University, Suita, Osaka 565-0871, Japan

⁵ Institute for Molecular Science, Okazaki, Aichi 444-8585, Japan

Endohedral metallofullerenes have attracted special interests as new spherical molecules with unique electronic properties and reactivities, which are not seen in empty fullerenes [1]. Endohedral metallofullerenes are more easily reduced than empty fullerenes. The difference in redox potential is in fact one of the most important factor to control their reactivities [2].

Some charge transfer (CT) interaction between organic donor molecules and C₆₀ have been discussed so far [3] since the first report about the complex of C₆₀ with tetrakis(dimethylamino)ethylene by Allemand and co-workers [4].

Recently, we have studied the complexation behavior of endohedral metallofullerene La@C₈₂-A with azacrown ethers. La@C₈₂-A forms the complex with azacrown ethers via electron transfer process. However, the radical cation of the macrocycles was not so stable. In this context, we reported here the complexation behavior of La@C₈₂-A with organic donor molecules which form stable radical cations.

References

- [1] *Endofullerenes: A New Family of Carbon Clusters*; Akasaka, T.; Nagase, S., Eds.; Kluwer Academic Publishers: Dordrecht, 2002.
- [2] Akasaka, T.; Kato, T.; Kobayashi, K.; Nagase, S.; Yamamoto, K.; Funasaka, H.; Takahashi, T. *Nature* **1995**, *374*, 600.
- [3] (a) Saito, G.; Teramoto, T.; Otsuka, A.; Sugita, Y.; Ban, T.; Kusunoki, M.; Sakaguchi, K. *Synthetic Metals* **1994**, *64*, 359. (b) Konarev, D. V.; Neretin, I. S.; Saito, G.; Slovokhotov, Y. L.; Otsuka, A.; Lyubovskaya, R. N. *Dalton Trans.* **2003**, 3886.
- [4] Allemand, P. M.; Khemani, K. C.; Koch, A.; Wudl, F.; Holczer, K.; Dcnovan, S.; Grüner, G.; Thompson, J. D. *Science* **1991**, *253*, 301.

Corresponding Author: Takeshi Akasaka

Tel & Fax: +81-298-53-6409, E-mail: akasaka@tara.tsukuba.ac.jp

¹³C NMR Study of CeLa@C₈₀ Anion

○Tomohito Komaki, Takeshi Kodama, Yoko Miyake, Shinzo Suzuki,
Koichi Kikuchi, Yohji Achiba

Department of Chemistry, Tokyo Metropolitan University, Hachioji, 192-0397, Japan

Recently, Kato et al. revealed that an excess electron was located on a La dimer in La₂@C₈₀ anion by ESR spectroscopy [1]. Ce₂@C₈₀ has the same molecular structure as La₂@C₈₀, therefore an excess electron would be located on a Ce dimer in Ce₂@C₈₀ anion. Since Ce has one 4f electron, we have been interested in the magnetic interaction between an excess electron and two 4f electrons on a Ce dimer. Previously, we reported the ¹³C NMR spectra of Ce₂@C₈₀ anion [2], but we could not elucidate the magnetic interaction. In this work, to understand such an interaction, we produced CeLa@C₈₀ anion and measured its ¹³C NMR spectra because the magnetic interaction in CeLa@C₈₀ anion is simplified to an excess electron and only one 4f electron on a CeLa dimer.

Fig. 1(a) shows the ¹³C NMR spectra of MM'@C₈₀ (M, M' = La, Ce) mixture. The signals of CeLa@C₈₀ and Ce₂@C₈₀ approach those of La₂@C₈₀ at higher temperature. This feature is roughly explained by the decrease of magnetic moments based on Ce ions of CeLa@C₈₀ and Ce₂@C₈₀ when temperature rises. On the other hand, as shown in Fig. 1(b), the signals of CeLa@C₈₀ anion and Ce₂@C₈₀ anion are apart from the diamagnetic region at higher temperature, furthermore the shifts of the signals of CeLa@C₈₀ anion are larger than those of Ce₂@C₈₀ anion.

This study was partly supported by Industrial Technology Research Grant Program from New Energy and Industrial Technology Development Organization (NEDO) of Japan.

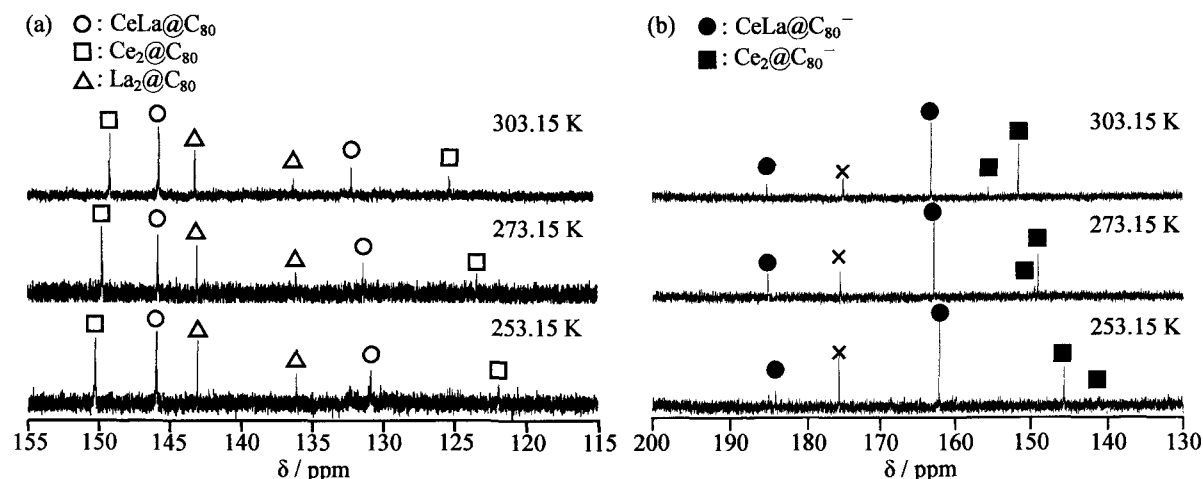


Fig. 1: ¹³C NMR spectra of MM'@C₈₀ (M, M' = La, Ce) mixture measured at 125 MHz in CS₂ (a), in triethylamine/acetone (b). The peak marked with x in Fig. 1(b) originates from impurity.

[1] T. Kato, et al., In *Fullerenes and Nanotubes: The Building Blocks of Next Generation Nanodevices*, Proceedings of the International Symposium on Fullerenes, Nanotubes, and Carbon Nanoclusters, The Electrochemical Society Inc, Pennington, 2003, p. 564.

[2] T. Ichikawa, et al., *The 28th Fullerene-Nanotubes General Symposium 26* (2005).

Corresponding Author: Takeshi Kodama

E-mail: kodama-takeshi@c.metro-u.ac.jp, Tel: +81-426-77-2530, Fax: +81-426-77-2525

Element Specific Magnetization Measurements of Er Metallofullerenes by Soft X-ray Magnetic Circular Dichroism (SXMCD)

○Haruya Okimoto¹, Tetsuya Nakamura², Ryo Kitaura¹, Takayuki Yamada³,
Yutaka Kitamura¹, Tomohito Matsushita², Takayuki Muro²,
Takashi Inoue⁴, Toshiki Sugai¹, Susumu Nanao³, and Hisanori Shinohara^{1,5}

¹Department of Chemistry and Institute for Advanced Research,
Nagoya University, Nagoya 464-8602, Japan

²Japan Synchrotron Radiation Research Institute, Hyogo 679-5198, Japan

³Institute of Industrial Science, University of Tokyo, Tokyo 153-8505, Japan

⁴Toyota Central R&D Laboratories, Inc., Nagakute, Aichi, 480-1192, Japan

⁵CREST, Japan Science and Technology Corporation, c/o Department of Chemistry,
Nagoya University, Nagoya 464-8602, Japan

Endohedral Metallofullerenes are expected to show novel magnetic properties due to encapsulated metal atoms. Magnetic properties of some mono-metallofullerenes, $M@C_{82}$ was studied by SQUID [1]. On the other hands, no magnetic property of di-metallofullerenes have been reported. Soft X-ray magnetic circular dichroism (SXMCD) is extremely sensitive method to obtain surface magnetization[2]. In this respect, SXMCD is very suitable for investigating the magnetic properties of small quantities of metallofullerenes embedded on a non-magnetic substrate. It is also a great advantage of SXMCD technique to obtain magnetization of metal ions in fullerenes separately from a diamagnetic fullerene cage according to an element specificity of SXMCD. Here, we report the magnetic property of mono- and di-erbium metallofullerenes, $Er@C_{82}$, $Er_2@C_{82}$, and $Er_2C_2@C_{82}$, as investigated by SXMCD.

SXMCD measurements have been performed on BL25SU in Spring-8. Er metallofullerenes were coated on a Au-Cu sample plate, and were baked at $\sim 400K$ in a load-lock chamber under the pressure of 1×10^{-5} Pa. The sample It was cooled down to 16K using a Liq.He continuous flow-type cryostat. Helical X-ray Absorption Spectroscopy and MCD spectra were measured by means of the total electron yield method.

Figure 1 shows temperature dependence of inverse of MCD intensity at a magnetic field up to 2 T. Inverse of MCD intensity corresponds approximately to $1/\chi$. We found that a magnetic moment of $Er_2@C_{82}$ increases 40% relative to that of $Er@C_{82}$, suggesting that the Er metallofullerenes may have ferromagnetic interaction below 20 K.

References:[1] H. Shinohara, *Rep. Prog. Phys.*, **63**, 843 (2000).

[2] T. Funk *et al.*, *Coord. Chem. Rev.*, **249**, 3 (2005).

Corresponding Author: Hisanori Shinohara

TEL: +81-52-789-2482, FAX: +81-52-789-1169, E-mail: noris@cc.nagoya-u.ac.jp

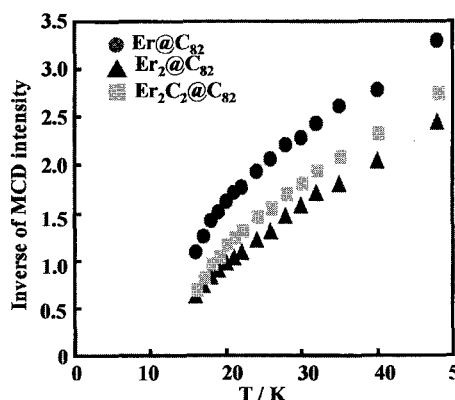


Fig 1. Temperature dependence of Inverse of MCD intensity

The Ultraviolet Photoelectron Spectra of $\text{Ti}_2\text{C}_2@C_{82}$

○ Masayuki Kato, Kentaro Iwasaki, Shojun Hino, Daisuke Yoshimura,
Hiroe Moribe, Haruya Okimoto, Yasuhiro Ito, Toshiki Sugai, Hisanori Shinohara

Chiba Univ., Institute of Molecular Science, Nagoya Univ.

The Ultraviolet Photoelectron Spectra (UPS) of $\text{Ti}_2\text{C}_2@C_{82}$ were measured in UVSOR BL8B2, Institute of Molecular Science.

The UPS of $\text{Ti}_2\text{C}_2@C_{82}$ are shown in Figure. The spectral onset position of these UPS is about 0.8 eV from the Fermi level. This value is analogous to those of other metallofullerenes in which even electrons are transferred to the cage (such as $\text{Tm}^{2+}@C_{82}^{2-}$, $\text{Y}_2^{6+}@C_{82}^{6-}$, etc.). There are distinct structures in the region shown in Figure. The spectral intensity of each structure changes upon the incident photon energy change. It is drastic in lower binding energy region of 1~4 eV (marked A to C).

The NMR analysis revealed that $\text{Ti}_2\text{C}_2@C_{82}$ has C_{3v} symmetry.⁽¹⁾ When metallofullerenes have the same cage structures with the same oxidation states of encapsulated atoms, their UPS usually resemble well. We have already reported the UPS of $\text{Y}_2\text{C}_2@C_{82}(\text{III})$ ⁽²⁾ which has the same C_{3v} symmetry. Present results on $\text{Ti}_2\text{C}_2@C_{82}$ are different from those of $\text{Y}_2\text{C}_2@C_{82}(\text{III})$ particularly in lower binding energy region. The UPS of $\text{Y}_2\text{C}_2@C_{82}(\text{III})$ are well reproduced by the MO calculation using $C_{3v}(8)$ geometry with C_{82}^{4-} electronic configuration. The difference among these two metallofullerenes implies that the interaction between encapsulated atoms Ti or Y and the cage is different; it could be large in $\text{Ti}_2\text{C}_2@C_{82}$.

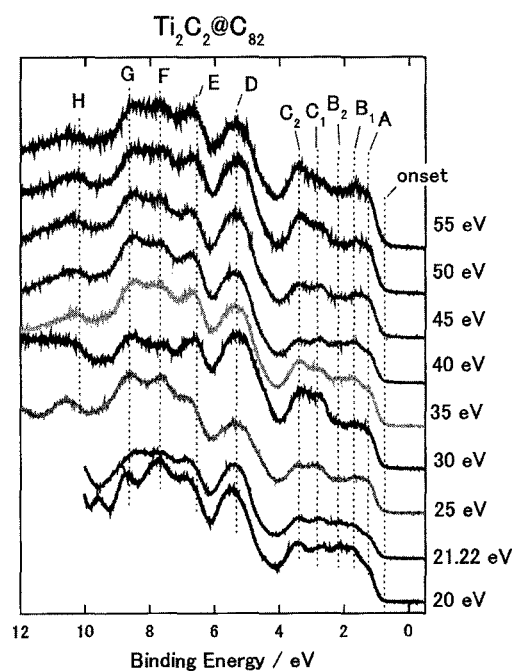
References:

- (1) H. Shinohara, Private communication.
- (2) S. Hino et al., *Phy. Rev. B*, in press.

Corresponding Author: Masayuki Kato

E-MAIL: m_kato@graduate.chiba-u.jp

TEL&FAX: 043-290-3481



Fluorescence switching in Er@C₈₂ by solvent-induced electron transfer

○Shingo Okubo, Toshiya Okazaki, Sumio Iijima

Research Center for Advanced Carbon Materials National Institute of Advanced Industrial Science and Technology (AIST), Tsukuba, 305-8565, JAPAN

Recent advances in molecular scale electronics have raised expectations that this technology may provide the building blocks for future generations of ultrasmall and ultradense electronic computer logic. In particular, fluorescent molecular photoswitches have attracted considerable attention because they can be used as erasable optical data-storage elements at a single molecular level. Here, we demonstrate “on/off” fluorescence switching of Er³⁺ ion in C_s-C₈₂ (Er@C₈₂-II) by reversibly controlling the electronic states of the C₈₂ fullerene cage.

Normally, fluorescence from Er@C₈₂ is significantly weak in the ordinal organic solvents such as chlorobenzene (“off” state) because the low-lying C₈₂ cage state effectively quenches the fluorescence (lower spectrum in Fig. 1). This is consistent with that fact that the onset of the absorption spectrum is beyond 2000 nm. However, if we change the solvents from chlorobenzene to pyridine, a strong enhancement of Er³⁺ emission at around 1.5 μm was observed (“on” state, upper spectrum in Fig. 1). It is well-known that C₈₂-based mono-metallofullerenes have anionic forms in pyridine [1,2]. The electron transfer from pyridine molecule to Er@C₈₂ severely diminishes the long wavelength absorption of the cage, and thus the Er³⁺ emission takes place.

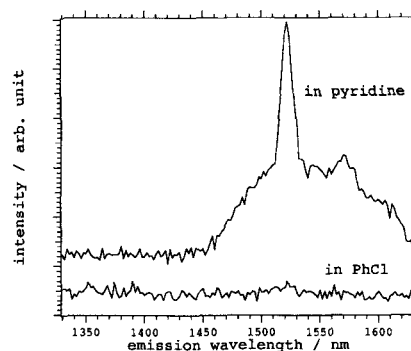


Fig. 1. Fluorescence spectra of Er@C₈₂-II

References

- [1] Okubo S., et al., *Abstract of 22nd Fullerene general symposium*, Okazaki, **2002**, p 33
 [2] Iiduka Y., et al., *J. Am. Chem. Soc.*, **2005**, *127*, 12500

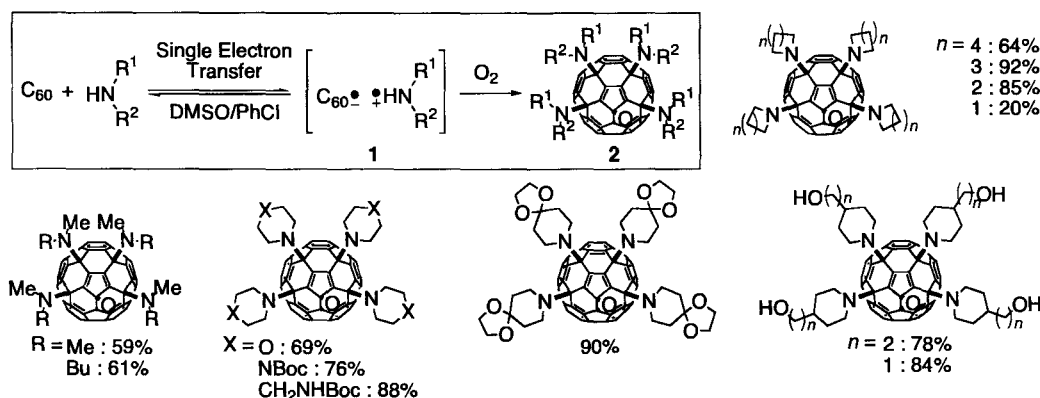
Corresponding: Toshiya Okazaki, e-mail: toshi.okazaki@aist.go.jp,
 tel: 029-861-4173, fax: 029-861-4851

Single Electron Transfer from Aliphatic Amines with [60]Fullerene at the Ground State and Facile Synthesis of Tetraaminofullerene Epoxide

○Takatsugu Tanaka, Waka Nakanishi, Loïc Lemiègre,
Hiroyuki Isobe, Eiichi Nakamura

Department of Chemistry, The University of Tokyo Hongo, Bunkyo-ku, Tokyo 113-0033, Japan

Amination of carbon clusters has been attracting the interest of chemists for a decade, for its own sake and for useful properties expected for the resulting amine-functionalized fullerene and carbon nanotube. Sometime ago, we investigated the synthesis of tetraaminofullerene epoxide **2** and reported that the photoirradiation in an aerated solution accelerates the reaction in moderate to high yield.^{1,2} We report herein the results of these studies that have largely resolved the synthetic and mechanistic questions.³ The key finding is that a mixture of C₆₀ and a secondary amine in a mixture of dimethylsulfoxide and chlorobenzene generates a long lived contact ion pair (**1**) as the result of amine-to-C₆₀ single electron transfer (SET). This reaction is applicable to cases where the previous photoreaction entirely failed, and the isolated yield is generally 60-90%. The new reaction does not require any light and adds to the repertoire of methods for large-scale preparation of functionalized fullerene derivative.



[1] Isobe, H.; Ohbayashi, A.; Sawamura, M.; Nakamura, E. *J. Am. Chem. Soc.* **2000**, *122*, 2669-2670. Isobe, H.; Tomita, N.; Nakamura, E. *Org. Lett.* **2000**, *2*, 3663-3665.

[2] Isobe, H.; Tanaka, T.; Nakanishi, W.; Lemiègre, L.; Nakamura, E. *J. Org. Chem.* **2005**, *70*, 4826-4832.

Corresponding Authors: Hiroyuki Isobe and Eiichi Nakamura

E-mail: hisobe@chem.s.u-tokyo.ac.jp and nakamura@chem.s.u-tokyo.ac.jp

Tel&Fax: 03-5800-6889

Synthesis of Fullerene C₇₀ Encapsulating Molecular Hydrogen

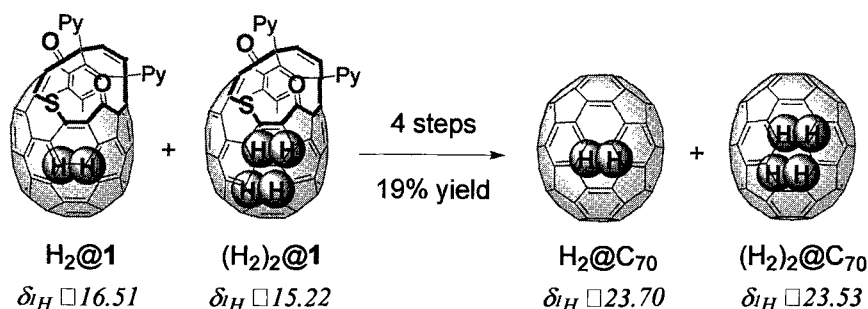
○ Yasujiro Murata,^{1,2} Shuhei Maeda,¹ Michihisa Murata,¹ and Koichi Komatsu¹

¹*Institute for Chemical Research, Kyoto University, Uji, Kyoto 611-0011, Japan*

²*PRESTO, Japan Science and Technology Agency (JST)*

The molecular surgical approach is a promising method to synthesize yet-unknown endohedral fullerenes and their derivatives, which includes creation of an orifice on the fullerene cage, insertion of a small guest through the orifice, and closure of the orifice with retention of the guest inside the fullerene. Actually, fullerene C₆₀ encapsulating a hydrogen molecule, H₂@C₆₀, was synthesized by this methodology.¹

Since the inner space of C₇₀ is larger than that of C₆₀, it might be possible that more than one small molecules be encapsulated. Recently open-cage C₇₀ derivative **1** was synthesized² by applying the procedure similar to that used for the synthesis of open-cage C₆₀.³ Molecular hydrogen was successfully inserted into **1** by treatment with high-pressure hydrogen gas (890 atm) at 200 °C. Not only H₂@**1** (97%) but also (H₂)₂@**1** (3%) were found to be formed under these conditions. Now the complete closure of orifice of H₂@**1** and (H₂)₂@**1** has been achieved without loss of encapsulated hydrogen molecule(s), thus having led to the formation of H₂@C₇₀ and (H₂)₂@C₇₀ for the first time. The ¹H NMR chemical shift of encapsulated hydrogen in each compound is shown below.



References:

1. Komatsu, K.; Murata, M.; Murata, Y. *Science* **2005**, *307*, 238-240.
2. Maeda, S.; Murata, M.; Murata, Y.; Komatsu, K. The 29th Fullerene-Nanotubes General Symposium 27 (2005).
3. Murata, Y.; Murata, M.; Komatsu, K. *Chem. Eur. J.* **2003**, *9*, 1600.

Corresponding Author: Koichi Komatsu

E-mail: komatsu@sci.kyoto-u.ac.jp

Tel: +81-774-38-3172 Fax: +81-774-38-3178

Control of Decomposition of Acrylic Polymers by dispersing Fullerene-derivatives

○Tomoya Yamashiki^{1,2}, Yusuke Tajima¹, Toshihiko Sakurai¹, Ryoko Shimada^{1,2},
and Hiroki Osedo²

¹ *Integrated Materials Research Laboratory, Riken, 2-1 Hirosawa, Wako-shi, Saitama 351-0198, Japan*

² *New Frontiers Research Laboratory, Toray Industries Inc., 1111 Tebiro, Kamakura-shi, Kanagawa 248-8555 Japan*

Photo-catalytic materials like TiO₂ have enormous applications from environmental field to energy field. These materials are usually dispersed as nm-sized particles into polymers in order to activate photo-catalytic process. But most of the matrix polymers are decomposed under strong oxidation by photo-catalytic process. In this work, we tested the possibility of suppressing polymer decomposition by the addition of fullerene into polymer. In our experiments, C₆₀ derivative¹⁾ is dispersed into conventional acrylic polymer and TiO₂ particles. These composites are spin-coated on substrates and irradiated to UV light. TGA analysis and IR spectroscopy are used for monitoring polymer decomposition process. As a result, it is proved that acrylic polymer decomposition by photo-catalytic process is suppressed by an addition of C₆₀ derivative (Fig.1). It is assumed that fullerene plays radical scavenger to prevent an enhancement of polymer decomposition.

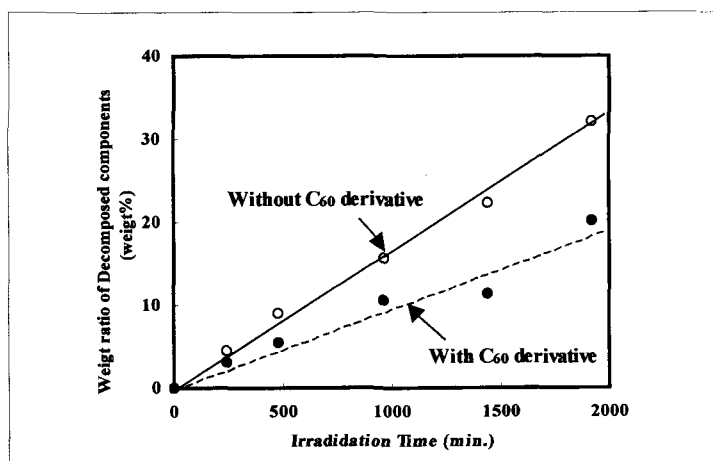


Fig.1 Weight loss of acryl-TiO₂ composites after UV-irradiation by TGA

1) Y. Tajima et al., Chem. Lett. 33(12), 2004, 1604-1605.

Corresponding Author Tomoya Yamashiki

E-mail: t.yamashiki@riken.jp

Tel: +81-48-467-9476, Fax: +81-48-467-8083

Quantitative analysis of detonation nanodiamonds with X-ray diffraction

Naoki Komatsu ^{a)}, Naoki Kadota ^{a)}, Takahide Kimura ^{a)}, Eiji Osawa ^{b)}

a) Department of Chemistry, Shiga University of Medical Science, Seta, Otsu, 520-2192

*b) NanoCarbon Research Institute Ltd., Rm 301, Toudai Kashiwa Venture Plaza, 5-4-19
Kashiwa-no-ha, Kashiwa, Chiba 277-0882*

Detonation nanodiamonds (*d*-NDs) are known to form tight aggregates and include substantial amount of other forms of carbons [1]. These properties are considered to hamper the characteristic application of *d*-NDs in spite of their availability and inexpensive price. Quite recently, however, Osawa and coworkers succeeded in disintegration of *d*-NDs to prepare stable colloid of primary particles of *d*-NDs [2]. They also reported quantitative analysis with X-ray diffraction (XRD) for the evaluation of the purity. Unfortunately, the reported purity of *d*-NDs, 77 %, is thought to be a little lower than the actual purity because much larger diamond (~1 μm) was used for the determination of the calibration line for *d*-NDs (~4 nm) [2]. Herein, we report more precise calibration line for *d*-NDs extrapolated by use of 30, 50 and 100 nm size of pure NDs.

Since pure NDs with 4 nm size are not available, particle size effect was estimated by using pure hydrogenated NDs with 30, 50 and 100 nm in average diameters (Tomei Diamond Co.) and zinc oxide (Aldrich, 99.9 % purity) as an internal standard. The area ratios of ND (111) and zinc oxide (101) on XRD were determined at three concentrations, 15 wt%, 20 wt%, 30 wt%, of zinc oxide for each size of NDs. As shown in Fig. 1, linear relations are obtained between the area ratios and the diameters, indicating that calibration line for any size of NDs can be extrapolated. A calibration line for 4 nm size NDs is shown in Fig. 2, from which the purity of *d*-NDs is determined to be 87 wt%.

Reference

- [1] V. Y. Dolmatov, *Russ. Chem. Rev.*, **70**, 607 (2001).
[2] A. Krüger, E. Osawa, *et al.*, *Carbon*, **43**, 1722 (2005).

Corresponding Author: Naoki Komatsu

E-mail: nkomatsu@belle.shiga-med.ac.jp

Tel: +81-77-548-2102, **Fax:** +81-77-548-2405

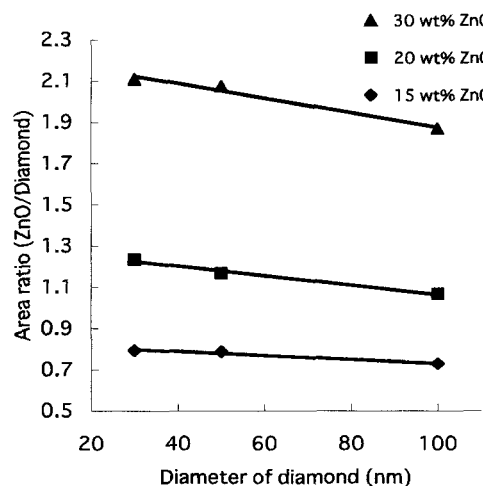


Fig. 1 Linear relations between particle size of NDs and area ratios on XRD.

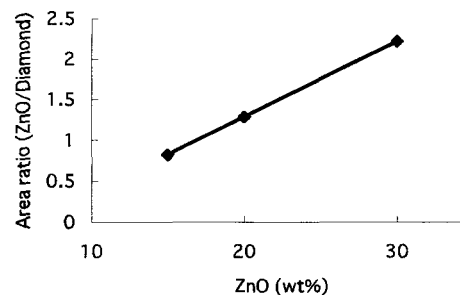


Fig. 2 Calibration line for 4 nm NDs.

Separation and Characterization of Polyynes in Solution

○T. Wakabayashi,¹ T. Doi,¹ R. Umeda,² M. Sonoda,² and Y. Tobe²

¹*Department of Chemistry, School of Science and Engineering, Kinki University,
Kowakae 3-4-1, Higashi-Osaka 577-8502, Japan*

²*Division of Frontier Materials Science, Graduate School of Engineering Science,
Osaka University, and CREST, Japan*

Abstract: Polyynes $\text{H}(\text{-C}\equiv\text{C-})_n\text{H}$ ($n \geq 2$) are of particular interest in connection with areas spanning from basic research such as in molecular spectroscopy to applications to combustion chemistry, planetary science, astrophysics, and non-linear optical properties in materials science [1,2]. We present here our recent progress on the production, separation, and characterization of the series of molecules in solution phase. In particular, the results from NMR characterization ensure the preparation in their macroscopic quantities. The resonance Raman spectroscopic study reveals molecular vibrations of the stretching modes and fragility against UV exposure. Also confirmed is the existence of another series of polyynic molecules as byproducts that form during the process in laser ablation of graphite particles suspended in the organic solvents. Based on the systematic behaviors of the retention times in the HPLC chromatogram and of the wavelength positions in the UV electronic absorption spectra, the products are classified and their formation mechanism is discussed.

References:

- [1] *Polyynes: Synthesis, Properties, and Applications*, ed. by F. Cataldo. Taylor & Francis CRC Press Inc. ISBN 157444512X (2005).
- [2] *Acetylene Chemistry: Chemistry, Biology, and Material Science*, ed. by F. Diederich et al. Wiley-VCH, ISBN 3-527-30781-8 (2005).

Correspondence to Dr. Tomonari Wakabayashi, wakaba@chem.kindai.ac.jp, Tel 06-6730-5880 (ex. 4101)

Matrix Effects on the Transformation of Nanodiamonds to Nano-Onions

○Masaki Ozawa, Masayasu Inakuma, Makoto Takahashi, and Eiji Ōsawa

*Nano-Carbon Research, Toudai Kashiwa Venture Plaza, 5-4-19, Kashiwa-no-ha, Kashiwa
277-0882 Chiba, Japan*

Between the two major forms of carbon, graphite and diamond, diamond stepped into nano-world earlier, in 1963. However, nanodiamond particles with average diameter of 4.3 nm synthesized by detonation of mixed explosives were acquired only as covalently bonded aggregates. This fatal defect as a nano-material has hindered the subsequent development, while the advent of fullerenes and nanotubes has pushed graphite up as one of the most essential pieces for nanotechnology. Development of beads-assisted wet disintegration methods broke this situation recently. The aggregates have been successfully broken up into primary nanodiamond particles, resulting in drastic change from slurry to transparent brown colloidal solution [1]. Hereby this 40-years-old material has become accessible to various approaches, such as chemical modifications and fabrication of composite materials

Nanodiamond dispersed sol-gel silica glass was synthesized by using tetramethyl orthosilicate and aqueous nanodiamond solution, and investigated by a high-resolution transmission electron microscope (HRTEM). Transparent brown glass was obtained at a low diamond concentration by following the standard procedure. As the diamond ratios increased, the composite turned darker and less transmissive. HRTEM observation demonstrated that wetting between diamond and silica is good enough to get nanodiamonds embedded in silica matrix.

Distinct stabilization of diamond particles due to silica matrix was found when the samples were annealed at 1050 °C in vacuo for densification of porous glasses. Most of the nanodiamonds, especially particles completely surrounded by silica, remain intact, although the same diamonds without silica start to convert into nano-onions at around 900 °C. Such stabilized particles show tolerance even to intense electron beam irradiation. Apparently nucleation of graphitic layer at diamond surface is the crucial point for the diamond-onion transformation. Careful microscopic observation indicates the transformation mechanism involving growth of spiroid [2] from surface to center of a nanodiamond particle.

References: [1] A. Krüger, F. Kataoka, M. Ozawa, T. Fujino, Y. Suzuki, A. E. Aleksenskii, A. Ya. Vul', E. Ōsawa, *Carbon* **43**, 1722 (2005). [2] M. Ozawa, H. Goto, M. Kusunoki, E. Ōsawa, *J. Phys. Chem. B* **106**, 7135 (2002).

Corresponding Author: Masaki Ozawa

E-mail: ozawa@nano-carbon.com, Tel: 04-7140-8671, Fax: 04-7140-8893

Crystal Structures of Discrete C₆₀ Fullerides Stabilized by Appropriate Triphenylmethane Cations

○Takahito Sugiura^{1,2}, Eiji Osawa², Hiroshi Moriyama¹

¹*Department of Chemistry, Toho University, Funabashi, Chiba 274-8510, Japan*

²*Nano-Carbon Research Institute Ltd., Kashiwa, Chiba 277-0882, Japan*

Quite limited number of X-ray diffraction data of C₆₀ anion radical salts have been reported,¹⁾ because of their intrinsic unstable nature of the radical anion. It has been hard to obtain fulleride crystals suitable for X-ray diffraction analysis; if crystals are formed, they are frequently small or twinned or have low resolution. The biggest obstacle for determining a structure is an intrinsic disorder of C₆₀ anion radical originated from the Jahn-Teller distortion. In this study, triphenylmethane dyes were used as counter cations to stabilize the C₆₀ anion radical and to reduce orientational disorder. We have tried to electrocrystallize C₆₀ anion salts, stabilized by appropriate triphenylmethane dye cations. Only [Brilliant green]⁺C₆₀⁻ salt has been so far characterized previously, we succeeded here to obtain crystal structures of another twotriphenylmethane-dyes (crystal violet and ethyl violet)-stabilized C₆₀ anion radical crystals. These salts are found to show rather stable semiconducting behavior.

Fulleride salts are synthesized and crystallized by electrocrystallization of C₆₀ and dye in chlorobenzene/ethanol in H-shaped glass cell equipped with platinum electrodes under a constant current (1-10 μA) for several weeks in an inert atmosphere. Spectroscopic data of UV-vis and IR for these salts and physical properties such as electric conductivity and magnetic susceptibility will be reported.

References:

(1)C. A. Reed and R. D. Bolskar, *Chem. Rev.*, **100**, 1075-1120 (2000).

Corresponding Author: Hiroshi Moriyama

E-mail: moriyama@chem.sci.toho-u.ac.jp

Tel: 047-472-1211, Fax:047-476-9449

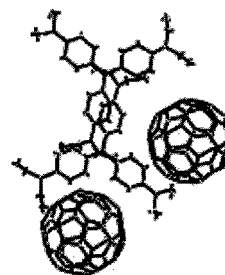


Fig 1 Crystal structure of [Ethyl Violet]⁺[C₆₀]⁻

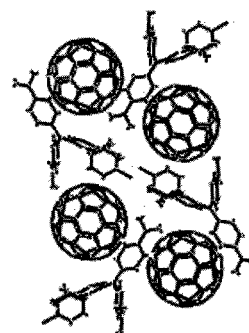


Fig 2 Crystal structure of [Crystal Violet]⁺[C₆₀]⁻

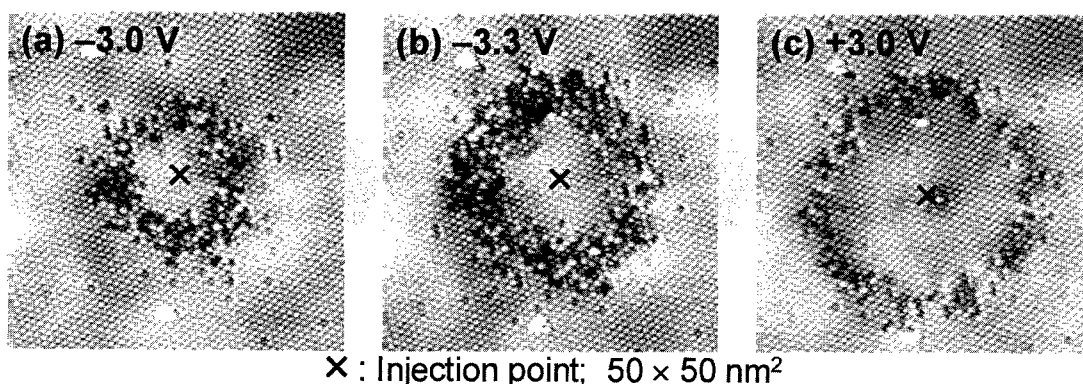
Polymerization of C₆₀ Molecules Induced by Hole / Electron Injection from a Scanning Tunneling Microscope Tip

○Ryo Nouchi, Kosuke Masunari, Toshio Ohta and Yoshihiro Kubozono

*Department of Chemistry, Okayama University, Okayama 700-8530, Japan,
and CREST, Japan Science and Technology Agency, Kawaguchi 322-0012, Japan*

The scanning tunneling microscope (STM) is a powerful tool for nanoscale modification of various surfaces. For the surface of closely packed C₆₀ layer, carrier (electron / hole) injection from an STM tip brings on the removal / movement [1] and polymerization [2] of C₆₀ molecules. The removal and movement of C₆₀ molecules are possible to be performed at single molecular scale. The polymerization is, however, hard to be achieved at single molecular precision because of the spatially spread of injected carriers. In this study, the spreading effect was investigated by the imaging of polymerized area before and after carrier injection.

The experimental procedure is as follows: The STM tip was placed on an injection point at a certain tip-sample distance (sample bias voltage: 2.0 V, tunneling current: 0.2 nA). Then, the voltage pulse was applied with the duration of 30 s. The figure shown below illustrates STM images taken sequentially after application of pulses with various voltages. First, -3.0 V pulse was applied (Fig. a). In this case, holes are injected as carriers since the applied sample bias voltage is negative. Second, -3.3 V pulse was applied at the same injection point (Fig. b). Finally, electrons were injected by the application of +3.0 V pulse (Fig. c). The fact that the diameter of the polymerized area increases by hole and electron injections, as is shown in Figs. b and c, indicates that the polymerization of C₆₀ monomers and the decomposition of polymers are induced by the injection of both carriers. In addition, it should be noted that the distribution of the polymerized molecules is ring-shaped. This fact suggests that the slowing down of carriers is necessary for the polymerization of C₆₀ molecules.



References:

- [1] K. Masunari *et al.*: The 29th Fullerene-Nanotubes General Symposium (2005) 1P-12.
[2] Y. Nakamura *et al.*: *Surf. Sci.* **528** (2003) 151.

Corresponding Author: Ryo Nouchi

E-mail: nouchi@cc.okayama-u.ac.jp

Tel: +81-86-251-7850, Fax: +81-86-251-7853

In-situ measurement of Raman scattering and AFM during laser-heated ACCVD growth process of SWNTs

○Shohei Chiashi, Yoichi Murakami, Yuhei Miyauchi and Shigeo Maruyama

*Department of Mechanical Engineering, The University of Tokyo
7-3-1 Hongo, Bunkyo-ku, Tokyo 113-8656, Japan*

We have built an atomic force microscope (AFM) with Raman scattering measurement capabilities and succeeded in synthesizing SWNTs on the AFM sample stage [1] using alcohol catalytic CVD method [2].

In this experimental apparatus, in-situ measurement of Raman scattering and AFM were performed while SWNTs were synthesized by using “laser-heated” cold-wall ACCVD method. Mo/Co metal particles, which were directly loaded on the silicon substrate [3], was used as the catalyst and CW-Ar-ion laser (488.0 nm, 50.0 mW) was used as the heating and Raman excitation. Fig. 1 shows the in-situ measurement of the intensity of the G-band

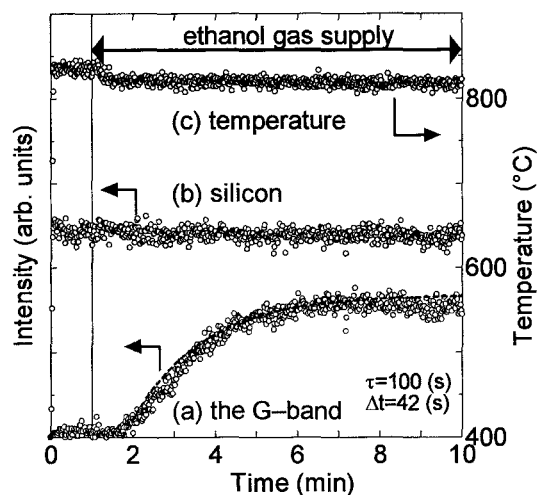


Fig. 1 . In-situ measurement of the Raman scattering intensity from (a) SWNTs and (b) the silicon substrate during the laser-heated CVD process. The sample temperature (c) was calculated from the temperature dependence of Raman shift from the silicon peak (520 cm^{-1} at 300 K).

(a) and Raman scattering peak from the silicon substrate (b) during the CVD process. The sample temperature (c) was calculated from the temperature dependence of Raman shift of the silicon peak [4]. About 40 s after the supply of the ethanol gas (0.1 Torr), the G-band appeared at 1570 cm^{-1} . The G-band intensity increased with time, but the intensity increase stopped about 4 min after the appearance of the G-band, which indicated the inactivation of the metal catalyst particles and the stop of the SWNTs growth. In the waiting time for the G-band appearance, SWNTs could not be found by in-situ AFM measurement.

[1] S. Chiashi, *et al.*, *Chem. Phys. Lett.*, **386** (2004) 89-94.

[2] S. Maruyama, *et al.*, *Chem. Phys. Lett.*, **360** (2002) 229-234.

[3] Y. Murakami, *et al.*, *Chem. Phys. Lett.*, **377** (2003) 49-54.

[4] M. Balkanski, *et al.*, *Phys. Rev. B*, **28**, **28** (1983) 1928-1934.

Corresponding Author: Shigeo Maruyama

E-mail: maruyama@photon.t.u-tokyo.ac.jp

Tel&Fax: +81-3-5800-6983

Formation of Single-Wall Carbon Nanotubes in Argon and Nitrogen Gas Atmosphere

○Shinzo Suzuki¹, Nobuyuki Asai¹, Hiromichi Kataura², and Yohji Achiba¹

¹*Department of Chemistry, Tokyo Metropolitan University, Tokyo 192-0397, Japan*

²*Nanotechnology Research Institute, National Institute of Advanced Industrial Science and Technology (AIST), Central 4, Higashi 1-1-1, Tsukuba, Ibaraki 305-8562, Japan*

The formation of single-wall carbon nanotubes (SWNTs) using laser vaporization technique in the different ambient gas atmosphere was investigated with the apparatus aimed for photoluminescence mapping, that was recently constructed in our laboratory (Lambda Vision Inc., PLE-250S).

Figure 1 shows a typical example of photoluminescence mapping of mono-dispersed semiconductive SWNTs, those prepared with Rh/Pd(1.2/1.2 atom%)-carbon composite rods in nitrogen and in Argon gas atmosphere, respectively. In comparison with the well-known result for Hipco nanotubes [1], the chirality distribution is found to be narrower for SWNTs prepared by laser vaporization technique.

It is interesting to see that, in the case of Argon, the peak corresponding to the chirality (7,6) is found to be the main feature. This chiral index is different from those reported recently as size-selected nanotubes ((6,5) by CoMoCAT [2], or (7,5) by DIPS [3]).

This study was partly supported by Industrial Technology Research Grant Program from New Energy and Industrial Technology Development Organization (NEDO) of JAPAN, and the Grants-in-Aid for Scientific Research (B) (No.16351104) from MEXT.

References: [1] Bachilo et al., *Science*, **298**, 2361(2002). [2] M. Zheng et al., *J. Am. Chem. Soc.*, **126**, 15490(2004). [3] T. Saito et al., *Abstract of General Symposium for Molecular Structure*, 2B17(2005).

Corresponding Author: Shinzo Suzuki

E-mail: suzuki-shinzo@c.metro-u.ac.jp **Tel:** +82-426-77-2533 **Fax:** +81-426-77-2525

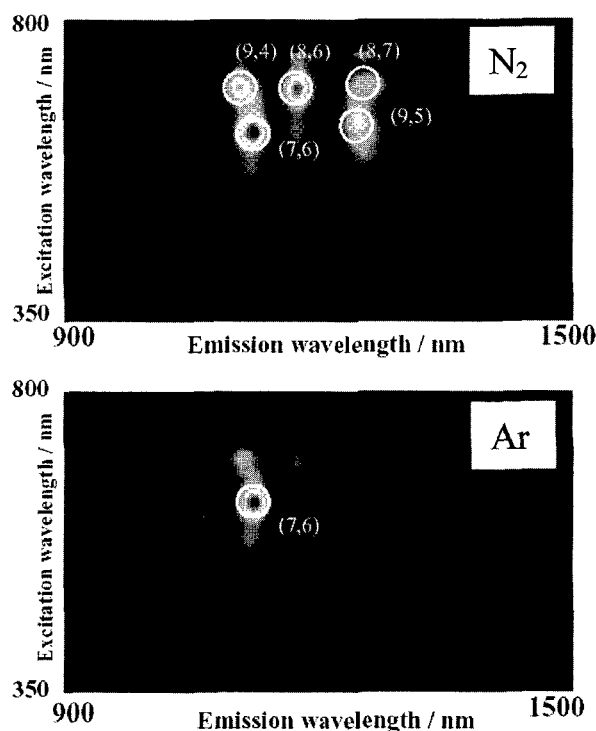


Figure 1.

Synthesis of Horizontally-Aligned SWNTs with Controllable Density on Sapphire Surface and their Polarized Raman Spectroscopy

○Hiroki Ago,^{*,1,2} Naoyasu Uehara,² Ken-ichi Ikeda,² Ryota Ohdo,²
Kazuhiro Nakamura,² Masaharu Tsuji^{1,2}

¹ *Institute for Materials Chemistry and Engineering, Kyushu University and CREST-JST, Fukuoka 816-8580, Japan*

² *Graduate School of Engineering Sciences, Kyushu University, Fukuoka 816-8580, Japan*

Recently, we have found that the horizontally-aligned single-walled carbon nanotubes (SWNTs) are formed on R- and A-faces of sapphire substrates (α -Al₂O₃), which is promising for nanoelectronics applications [1]. We used the colloidal particles of iron oxide with the mean diameter of 4 nm, but the SWNT yield was relatively low [1]. Here, we report on the facile synthesis of the aligned SWNTs on A-face sapphire with controllable nanotube density and the results of their polarized Raman spectra. The catalyst was prepared by simply dipping a substrate into the methanolic solution of Fe(NO₃)₃·9H₂O and MoO₂(acac)₂, where the addition of Mo improved the catalytic activity and reproducibility. The SWNT density was controlled by changing the metal concentration of the solution (Fig. 1), and the high nanotube density of $> 20 \mu\text{m}^{-2}$ was achieved. This high SWNT density allowed us to measure the polarized Raman spectra, as shown in Fig. 2. The spectra clearly indicate the formation of aligned and isolated SWNTs, not nanowires of metal or metal carbide.

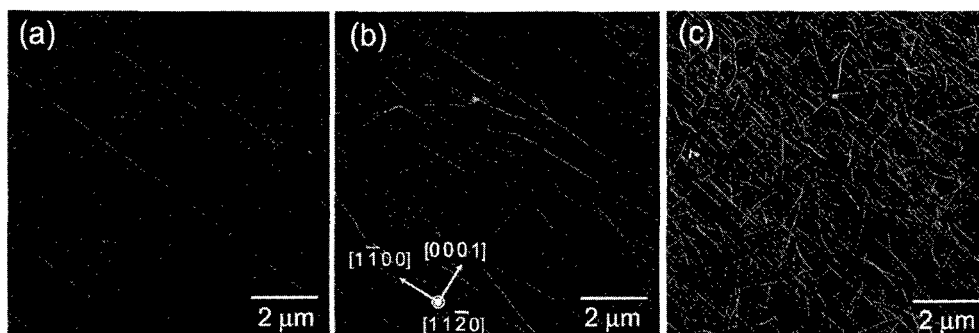


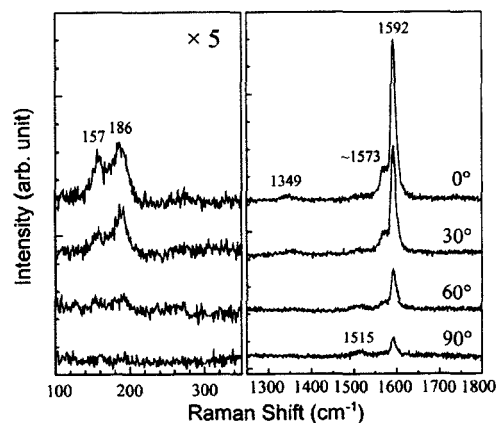
Figure 1 (top) AFM images of SWNTs synthesized on A-face sapphire substrates. The different metal concentrations were used; (a) 1×10^{-5} , (b) 1×10^{-4} , (c) 1×10^{-3} M.

Figure 2 (right) Polarized Raman spectra of SWNTs on the A-face sapphire measured for the high density SWNT array. The VV-configuration with 514.5 nm excitation was employed.

Acknowledgements The authors acknowledge support from CREST of Japan Science and Technology, Grant-in-aid for Scientific Research from MEXT (#16710087), and Nissan and Iketani Science Foundations.

References [1] H. Ago, K. Nakamura, K. Ikeda, N. Uehara, N. Ishigami, M. Tsuji, *Chem. Phys. Lett.*, **408**, 433 (2005).

Corresponding Author Hiroki Ago (TEL&FAX: +81-92-583-7817, E-mail: ago@cm.kyushu-u.ac.jp)



Effects of typical metallic Elements added as Catalysts for production of DWCNTs by DC-Arc discharge method

○Hideki Inakura

THE HONJO CHEMICAL CORPORATION

19-7, NIWAJIHONMACHI 4-CHOME NEYAGAWA-CITY OSAKA, JAPAN

Arc discharge method can produce several type carbon nanotubes such as Single-Wall nanotube and Multi-Wall nanotubes. Especially, under the condition that mixture of transition metallic elements (Co, Ni, Fe) and sulfur is added as catalysts and Hydrogen is added in atmosphere, Double Wall carbon nanotube grows selectively. Because of the necessity of catalysts, Single and Double wall nanotubes as produced include metal particles with graphite shell. This particles cause many problems such as difficulty of purification, damaged CNTs by heating process for instance FED manufacturing process, and so on.

In this study, we tried to synthesis DWCNTs from catalysts including typical metallic elements. We have used typical metallic elements (selected from Cu, Zn, Sn) and transition metallic elements (selected from Co, Ni, Fe) and Sulfur as catalysts. These elements and graphite powder were mixed and filled in graphite rods with hole. Using these rods as anode, DC-Arc discharge was generated in reaction chamber filled with hydrogen and argon mixture.

As a result, some kind of typical metallic elements with out Iron group elements were not effective to growth of CNTs. But mixing typical metallic elements with usual catalysts (Mixture of transition metallic elements and Sulfur) is not only critical to growth of DWCNTs, but also enhance that effect.

References: [1]J.L.Hutchison,et.al.,Carbon,761-770,39(2001)
[2]Y.Saito,et.al.,J.Phys.Chem.B,931-934,107(2003)

Corresponding Author: Hideki Inakura

E-mail: inakua@honjo-chem.co.jp

Tel&Fax: +81-72-827-3623 +81-27-827-1528

Selective Diameter-Control of Single-Walled Carbon Nanotubes by the Enhanced Direct-Injection-Pyrolytic-Synthesis (DIPS) Method

○¹ Takeshi Saito, ¹ Satoshi Ohshima, ^{1,2} Wei-Chun Xu, ^{1,3} Koji Matsuura, ^{1,4} Toshiya Okazaki,
¹ Motoo Yumura and ¹ Sumio Iijima

¹ *Research Center for Advanced Carbon Materials, National Institute of Advanced Industrial Science and Technology (AIST), Tsukuba 305-8565, Japan*

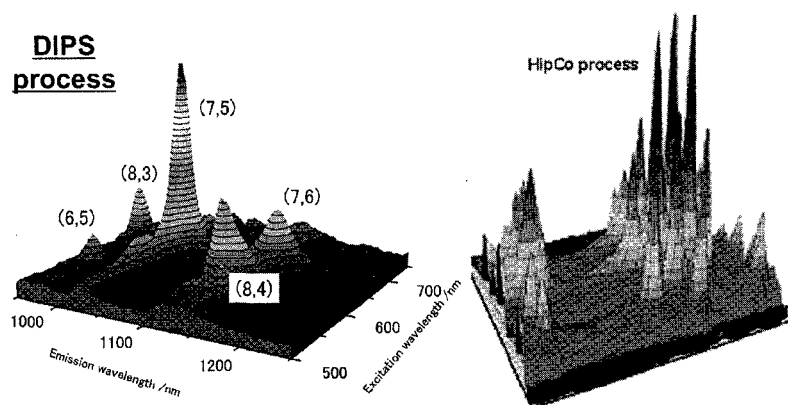
² *Institute of Research and Innovation (IRI), Kashiwa Laboratory, Kashiwa 277-0861, Japan*

³ *Japan Fine Ceramics Center, c/o Research Center for Advanced Carbon Materials, AIST, Tsukuba 305-8565, Japan*

⁴ *CREST, Japan Science Technology Corporation, c/o Research Center for Advanced Carbon Materials, AIST, Tsukuba 305-8565, Japan*

The controlled synthesis of single-walled carbon nanotubes (SWCNTs) in the structural characteristics, *i.e.*, diameter, length, number of defects and so forth, is an enabling step for realization of their many potential applications and fundamental studies requiring defined nanotube structures and properties. Above all, the controllability of the tube diameter would be the key to the chirality-controlled synthesis of SWCNTs. At the last symposium, we reported the selective diameter-control method in the SWCNTs synthesis, designated the Direct Injection Pyrolytic Synthesis (DIPS) method^{1,2}. Our results suggested that this method can tune the mean diameter of SWCNTs at any point within the range from ca. 0.8 nm to 2.0 nm selectively.

Here, we will report the details of the reaction conditions, such as reaction temperature and carbon sources at the meeting.



References: 1; Saito, T. *et al.*, *J. Phys. Chem. B*, **2005**, *109*, 10647-10652.

2; Saito, T. *et al.*, The 28th Fullerene-Nanotubes General Symposium, 1-9.

Corresponding Author: Takeshi Saito

E-mail: takeshi-saito@aist.go.jp Tel&Fax: +81-29-861-4863 (Fax: 3392)

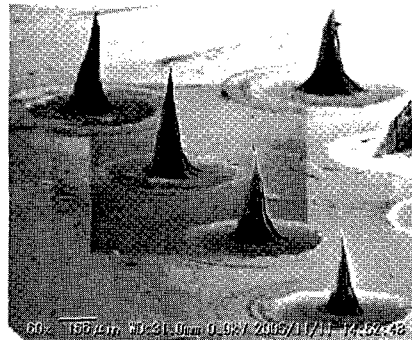
Super Growth: Shape Engineerable Single Walled Carbon Nanotube Solid as Flexible Conducting Mesoporous Material

- Don N. Futaba^{2,1}, Kenji Hata¹, Tatsuki Hiraoka¹, Takeo Yamada¹, Kohei Mizuno¹, Yuhei Hayamizu¹, Tatsunori Namai¹, Yozo Kakudate¹, Osamu Tanaike¹, Hiroaki Hatori¹, Koji Miyake¹, Shinya Sasaki¹, Motoo Yumura¹ and Sumio Iijima¹

¹ National Institute of Advanced Industrial Science and Technology (AIST), Tsukuba, 305-8565, Japan

² Japan Fine Ceramics Center, (AIST), Tsukuba, 305-8565, Japan

We present a new form of carbon nanotubes material where CNTs are aligned and packed densely in a bulk solid. This SWNT solid is fabricated from liquid-induced lateral collapse of the as-grown sparse SWNT forest synthesized by super-growth CVD [1]. The high-density packing follows from the alignment of the forest structure, and the resultant SWNT solid material displays a 20x increase in mass density (73% of the ideal) and a 70x increase in the Vickers hardness while retaining its alignment and high BET surface area. As such, SWNT solid is an ideal form of CNTs for material and energy storage. The high surface area and well-defined microscopic structure imply that SWNT solid can be regarded as mesoporous material which is conductive and flexible. In addition, we can engineer shapes during the solidification process suitable for various applications. These unique characters make SWNT solid as a valuable material for supercapacitor electrodes and flexible heaters. Furthermore, we show how partial shrinking of the as-grown material creates a “handle” for strong mechanical and/or electrical connection, such as commutator contacts for a DC motor. Through this method, the SWNT “brush” shows exceptional tribological character and wear rate and can be used as electrical contacts. The SWNT solid promises to open new frontiers in within the carbon nanotube field.



References:

- [1] K. Hata *et al*, Science, **306**, 1241 (2004).

Corresponding Author: Kenji Hata

E-mail: kenji-hata@aist.go.jp

Tel&Fax: (029) 861-5080 ext 46763

Fluorination of Carbon Nanotubes, Structures and Properties

○Hidekazu Touhara^A, Hideki Arikai^A, Yoshio Nojima^A, Fujio Okino^A, Y. A. Kim^B,
Morinobu Endo^B, Shinji Kawasaki^C, Hiromichi Kataura^D, Masako Yudasaka^E and
Sumio Iijima^{E,F}

^A Faculty of Textile Science and Technology, ^B Faculty of Engineering, Shinshu University, ^C Graduate School of Engineering, Nagoya Institute of Technology, ^D Nanotechnology Research Institute, National Institute of Advanced Industrial Science & Technology, ^E NEC Corporation, ^F Meijo University

Fluorination is one of the most effective chemical method to modify and control the structural and physical properties of carbon materials [1]. Fluorination is also effective for property control and functionalization of single-walled carbon nanotubes (SWNTs) [2]. In this paper, we report fluorination of various forms carbon nanotubes, and structures and properties of resulting compounds by the comparative methods. The nanotubes used were purified SWNTs (1.4-1.5 nm in diameter), double-walled carbon nanotubes (DWNTs, consisted of two pairs of DWNTs; inner tube:outer tube diameter (nm) = 0.7:1.3 and 0.9:1.58, respectively), cup-stacked carbon nanotubes (Cup-CNTs(GSI Creos Co.), 50-150 nm in diameter, 10-30 nm in wall thickness), and single-walled carbon nanohorns (NHs) and hole-opened carbon nanohorns (h-NHs).

The fluorination was carried out in the temperature range RT-773 K using 1 atm elemental fluorine. The limiting stoichiometry was $CF_{0.5}$ for SWNTs [2] and $CF_{0.3}$ for DWNTs indicating outer surface fluorination without disrupting the double-layered morphology [3]. RT fluorination was possible for Cup-CNTs with the stoichiometry $CF_{0.48}$ [4] and h-NHs with $CF_{0.84}$. Very interestingly, elemental fluorine was desorbed from the fluorinated h-NHs by heat treatment and/or evacuation indicating F_2 storage ability of the h-NHs. The discharge performance of Li cells with fluorinated carbon nanotubes (F-CNTs) cathodes will also be reported [5].

- 1) H. Touhara and F. Okino, *Carbon*, **38**, 242 (2000).
- 2) S. Kawasaki et al., *Phys. Chem. Chem. Phys.*, **6**, 1769 (2004) and references cited therein.
- 3) H. Muramatsu, et al., *Chem. Commun.*, **15**, 2002. (2005).
- 4) H. Touhara, *Mat. Res. Soc. Symp. Proc.* Vol. **85E**, HH12.3.1 (2005).
- 5) H. Touhara, *Fluorinated Materials for Energy Conversion*, Chap. 4, Elsevier (2005).

Corresponding Author: Hidekazu Touhara

E-mail: htohara@shinshu-u.ac.jp Tel/Fax: +81-268-21-5392/+81-268-21-5391

Nonlinear Optical Waveguide Device Using Carbon Nanotube-Polyimide Composite Material

○Shun Matsuzaki^{1,2}, Taro Itatani¹, Emiko Itoga¹, Masahiro Igusa¹, Hiromichi Kataura¹,
Madoka Tokumoto^{1,2}, Kohtaro Ishida², Youichi Sakakibara¹

¹National Institute of Advanced Industrial Science and Technology (AIST), Tsukuba 305-8565

²Graduate School of Science and Technology, Tokyo University of Science, Noda 278-8510

Optical waveguide using single-wall carbon nanotube (SWCNT) saturable absorber in a core is a very promising nonlinear optical device for optical telecommunication that enables strong confinement of light in the core with a long light-matter interaction length. The waveguide structure is also very important in that heat accumulation which inevitably follows the saturable absorption is expected to decrease by attaching efficient heat sink mechanisms.

Previously, we reported an optically uniform SWCNT-polyimide composite that may be usable as a core material.[1] With this material, in this study we have fabricated a buried waveguide structure. As shown in Fig. 1, a ridge core made of SWCNT-polyimide was formed on a SiO₂(15μm)/Si substrate by a reactive ion etching (RIE) method. This core was then buried with an epoxy resin with a refractive index almost equal to SiO₂. Figure 2 proves the formation of a buried waveguide.

Linear and nonlinear optical properties of the waveguide will be also reported.

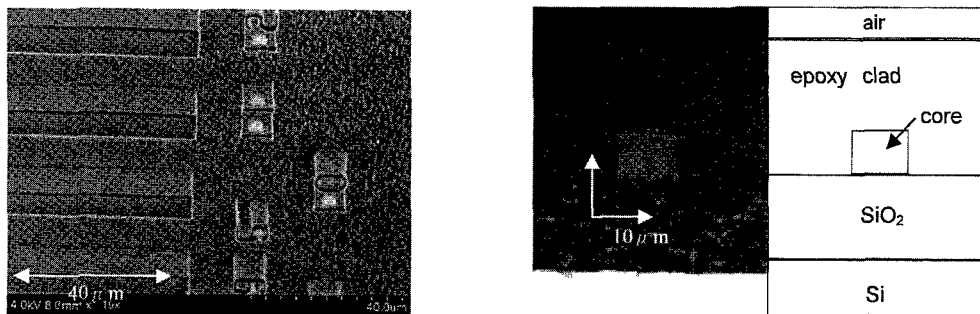


Fig. 1 SEM image of ridge core structures. Fig. 2 Optical microscope image of a cross section.

A part of this work was conducted in AIST Nano-Processing Facility, supported by "Nanotechnology Support Project" of the Ministry of Education, Culture, Sports, Science and Technology (MEXT), Japan.

[1] The 29th Fullerene-Nanotubes General Symposium, abstract p.55.

Corresponding Author: Youichi Sakakibara

TEL: +81-29-861-5456, FAX: +81-29-861-6301, E-mail: yo-sakakibara@aist.go.jp

Carbon nanotube transparent flexible transistors using solution process

○T. Takahashi¹, T. Takenobu^{1,2}, T. Kanbara^{1,3}, K. Tsukagoshi^{3,4}, Y. Aoyagi^{3,5}, Y. Iwasa^{1,2}

¹*Institute for Materials Research, Tohoku University, Katahira, Sendai 980-8577, Japan*

²*CREST, Japan Science and Technology Corporation, Kawaguchi 330-0012, Japan*

³*RIKEN, Hirosawa 2-1, Wako 351-0198, Japan*

⁴*PREST, Japan Science and Technology Corporation, Kawaguchi 330-0012, Japan*

⁵*Tokyo Institute of Technology, Yokohama 336-8502, Japan*

Now, flexible transistors based on a transparent semiconductor are an important focus of research, since the fusion of flexible electronics and transparent electronics is proposed for a number of novel applications. A promising application of transparent flexible thin film transistors (tf-TFTs) is their use as pixel switches in flexible active-matrix display. When we manufacture electronic devices of the display, we have to consider the process. We can simplify the fabrication sequence of large area displays by solution processes. Recently, tf-TFTs have been reported in single-walled carbon nanotubes (SWNTs) [1]. SWNT tf-TFTs showed high performance (hole mobility about 15, on to off ratio 10^5). In addition, the transistors were highly flexible and could be bent to a radius of 8mm without significant loss in performance. This indicate that SWNTs have high flexibility and good use suitability for flexible electronic devices. However, the transistors were fabricated by a complicated process of transferring SWNTs from high-temperature growth substrates to flexible ones.

Here, we demonstrate SWNT tf-TFTs based on solution process which is simpler to apply than one of the reported SWNT tf-TFT. Our tf-TFT exhibits hole mobility about $0.5 \text{ cm}^2/\text{Vs}$, on-to-off current ration of $\sim 10^4$, and the minimum radius of 7.5mm. This performance approaches the level needed as pixel switches. This work therefore represents a major step towards 'large area transparent plastic electronics'.

[1] Seung-Hyun Hur, O Ok Park, John. A. Rogers, Applied Physics Letters 86, 243502 (2005)

Corresponding Author : Tetsuo Takahashi

E-mail: tetsuo@imr.tohoku.ac.jp, Tel: +81-22-215-2032, FAX: +81-22-215-2031

Individual solubilization of carbon nanotubes using polyimides

Masahiro Shigeta[○], Masaharu Komatsu, Naotoshi Nakashima

*Department of Chemistry and Biochemistry
Graduate School of Engineering, Kyushu University
744 Motoooka, Fukuoka 819-0395, Japan*

Carbon nanotubes (CNTs) have a high potential for applications in energy, electronics, IT and materials. However, their insolubility in solvents has hindered chemical approaches using CNTs. Our interest is focused on the fundamental properties and applications of soluble carbon nanotubes in aqueous and organic systems¹⁾. Polymer wrapping is a powerful technique to construct CNTs-polymer composite materials. Polyimides are based on stiff aromatic backbones, and total aromatic polyimides are especially suitable polymers having unusual mechanical strength and high resistance to heat and chemical reactions. Combination of carbon nanotubes and polyimides is expected to play an important role in the development of novel nanocarbon composite polymers with high performance. We found that the polyimide results in individually dissolved SWNT solutions²⁾. Here, we describe the individually dissolution of SWNT and the formation of an organic gel of SWNTs/polyimide.

Polyimide was produced from 1, 4, 5, 8-naphthalenetetracarboxylic dianhydride and 4, 4'-diaminodiphenyl ether-2,2'-disulfonic acid, followed by neutralization with triethylamine. Typical procedures for the preparation of nanotube solubilization were as follows. A prescribed amount of SWNTs was added to a DMSO solution of the polyimide, and the mixture was sonicated for 1 h, followed by optional centrifugation at 10⁴g. Higher concentrations of SWNTs in polyimide solutions form a gel composed of individually dissolved SWNTs. The visible-near IR spectra of SWNTs/the polyimide showed characteristic features assignable to individually dissolved SWNTs. We also report fluorescence behaviors in the near-IR region, at the meeting.

References: 1) N. Nakashima, *International J. Nanoscience* 4 (2005) 119

2) M. Shigeta, M. Komatsu, N. Nakashima, *Chem. Phys. Lett.*, in press.

Corresponding Author E-mail: nakashima-tcm@mbox.nc.kyushu-u.ac.jp

Tel&Fax: +81-92-802-2840

Electronic Properties in Möbius Nano-Carbon Materials

Kikuo Harigaya

Nanotechnology Research Institute, AIST, Tsukuba 305-8568, Japan
Synthetic Nano-Function Materials Project, AIST, Tsukuba 305-8568, Japan

E-mail: k.harigaya@aist.go.jp

Recent theoretical developments on topological materials, Möbius nanographite and Möbius conjugated polymers, are reported. (I) In nanographite systems with the Möbius boundary condition, there appears a novel magnetic domain. However, this domain state competes against the helical magnetic states. Total energies of the latter states are always lower than that of the former state. Additionally, the domain wall appears in the charge density wave states. (II) Optical properties of Möbius conjugated polymers are studied. We discuss that oligomers with a few structural units are more effective than polymers, in order to measure effects of discrete wave numbers which are shift by the Möbius boundary from those of the periodic boundary. Certain components of the optical absorption for the electric field perpendicular to the polymer axis mix with the absorption spectra for the electric field parallel with the polymer axis. The polarization dependences of electric field of light can detect whether conjugated polymers have the Möbius boundary or not.

References

- [1] K. Wakabayashi and K. Harigaya: Magnetic structure of nano-graphite Moebius ribbon, J. Phys. Soc. Jpn. 72 (2003) 998-1001.
- [2] A. Yamashiro, Y. Shimoi, K. Harigaya, and K. Wakabayashi: Spin- and charge-polarized states in nanographene ribbons with zigzag edges, Phys. Rev. B 68 (2003) 193410.
- [3] K. Harigaya: Electronic properties of topological materials: Optical Excitations in Moebius conjugated polymers, J. Phys. Soc. Jpn. 74 (2005) 523-526.

Band Gap and Quasiparticle States in Carbon Nanotubes

Takashi Miyake, Yoshio Akai, and Susumu Saito○

Department of Physics, Tokyo Institute of Technology, Meguro-ku, Tokyo 152-8551, Japan

It is now well known that carbon nanotubes can show a variety of electronic properties depending on their network topology. One kind of achiral nanotubes, so-called armchair nanotubes, are metallic, while other nanotubes are semiconducting with moderate or narrow fundamental gap depending again on their network topology [1]. These rich electronic properties have attracted a great deal of interests in carbon nanotubes as next-generation electronics materials [2]. On the other hand, ironically due to this rich variety of network topology, a crystalline sample with uniform-topology nanotubes has not been produced yet, and the detailed geometries and the important electronic properties of nanotubes have not been measured experimentally with enough accuracy for a device use. Therefore, so far the predictive first-principles electronic-structure study has played an important role in this field. Their geometry deviations from graphite values such as bond lengths and angles are found to give sizable deviations in their electronic states using the density-functional theory [3]. Also we have studied the fundamental-gap values of semiconductor nanotubes using the state-of-the-art Green's function method called the *GW* approximation [4,5]. In this study [6] we report the systematic analysis of the so-called zigzag nanotubes including metallic nanotubes, moderate-gap semiconductor nanotubes, and the narrow-gap semiconductor nanotubes using the *GW* approximation, and discuss quasiparticle states and fundamental-gap values which should be measured not via photoabsorption/luminescence experiments but via photoemission and inverse photoemission experiments as well as STS experiments.

References:

1. N. Hamada, S. Sawada, and A. Oshiyama, *Phys. Rev. Lett.* **68**, 1579 (1992).
2. S. Saito, *Science* **278**, 77 (1997).
3. K. Kanamitsu and S. Saito, *J. Phys. Soc. Jpn.*, **71**, 483 (2002).
4. T. Miyake and S. Saito, *Phys. Rev. B* **68**, 155424 (2003).
5. T. Miyake and S. Saito, *Phys. Rev. B* **72**, 073404 (2005).
6. Y. Akai, T. Miyake, and S. Saito, to be published.

Corresponding Author Takashi Miyake, Susumu Saito**E-mail** miyake@stat.phys.titech.ac.jp, saito@stat.phys.titech.ac.jp**Fax** 03-5734-2739

ポスター発表
Poster Preview

1P-1 ~ 1P-48

2P-1 ~ 2P-49

3P-1 ~ 3P-44

Fabrication and Properties of Self-assembled Monolayers modified with C₆₀-Derivative Fixed on Gold Nanoparticles

○Noriaki Ikeda, Chyongjin Pac, Hiroshi Moriyama

Department of Chemistry, Faculty of Science, Toho University, Miyama, Funabashi, Chiba 274-8510, Japan

Electrode modifications have attracted much attention in the study of organic semiconductor devices in the recent years. From the viewpoint of optimization of the device efficiency, it has been recognized that organic/inorganic interface plays an important role. A variety of methods have been adopted to form fullerene molecular films, e.g., drop coating, Langmuir-Blodgett (LB) technique, self-assembled monolayers (SAMs). Among those, the formation, electrochemistry, photoelectrochemistry, and surface properties of fullerene SAMs have been much reported. Here, we synthesized C₆₀-derivatives¹⁾ whose SAMs were fabricated on solid substrate (Au electrode, ITO, quartz) (I). Moreover, multi-layer (II) was successfully prepared (Fig. 1). The modified films were characterized by UV-vis spectroscopy, cyclic voltammetry, X-ray photoelectron spectroscopy (XPS), and scanning electron microscope (SEM) (Fig. 2). The electrochemical and photoelectrical properties of those films were investigated. Details will be reported.

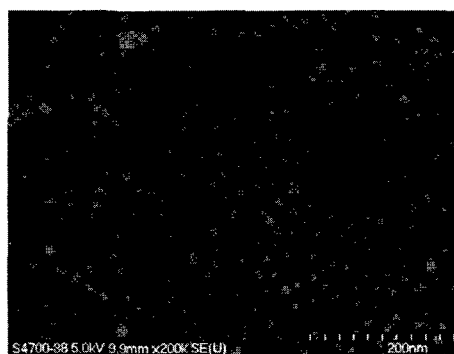
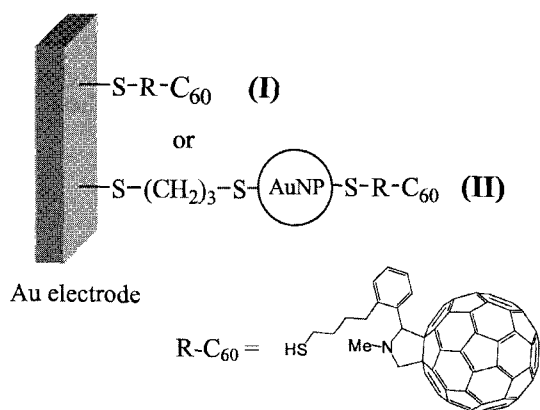


Fig. 2 SEM image of (II) on Au electrode.

Fig. 1 SAMs of C₆₀-derivatives (I) and multi-layer (II). AuNP indicates gold nanoparticle.

1) X. Shi, W. B. Caldwell, K. Chen, and C. A. Mirkin, *J. Am. Chem. Soc.*, **116**, 11598–11599 (1994).

Corresponding Author: Hiroshi Moriyama

E-mail: moriyama@chem.sci.toho-u.ac.jp

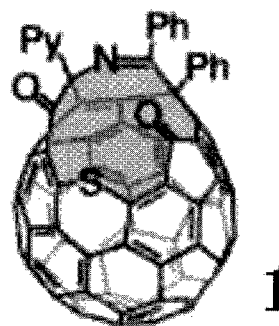
Tel: 047-472-1211, Fax: 047-476-9449

Electrochemistry of an Open-Cage C₆₀ Embedded in a Film on an Electrode in an Aqueous Media

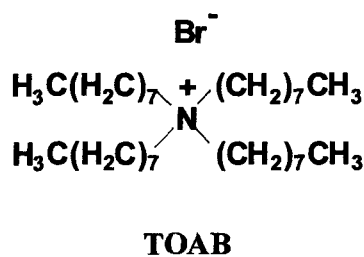
○Masaharu Komatsu¹, Kenichi Watanabe¹, Ayumi Ishibashi¹, Yasuro Niidome¹, Michihisa Murata², Yasujiro Murata², Koichi Komatsu², and Naotoshi Nakashima¹

¹Department of Applied Chemistry, School of Engineering, Kyushu University, 744 Motoooka, Nishi-ku, Fukuoka 819-0395, Japan, ²Institute of Chemical Research, Kyoto University, Gokasho, Uji, Kyoto 611-0011, Japan

Abstract: “Molecular surgery” of C₆₀ started since 2001.^{1,2} Rubin *et al.* developed a synthetic methods to open a cage on C₆₀¹, and Komatsu *et al.* described a “molecular suture” of open-caged C₆₀². The goal of this study is to understand an electron transfer between an electrode and the open-cage C₆₀ on electrodes. Here, the electron transfer between electrode and open-cage C₆₀, **1**³, embedded in the artificial lipid-like amphiphilic compound, tetra-*n*-octylammonium bromide (TOAB), film is described.



Four-consecutive one-electron reduction waves from C₆₀ moiety of **1** were observed in cyclic voltammogram for a **1**/TOAB film on a basal-plane pyrolytic graphite (BPG) electrode. On the contrary, no electrochemical communication was detected for a cast film of **1** solely on BPG. Stronger binding of electrogenerated **1**-anions with TOAB is considered to be important for the electrochemistry of **1** on the electrode.⁴



References: 1) Y. Rubin, *et al.*, *Angew. Chem., Int. Ed. Engl.*, **40**, 1543 (2001). 2) Y. Murata, M. Murata, *et al.*, *J. Am. Chem. Soc.*, **125**, 7152 (2003). 3) Y. Murata, *et al.*, *J. Eur. Chem.*, **9**, 1600 (2003). 4) N. Nakashima, “Fullerene Lipid Films”, in “Encyclopedia of Nanoscience and Nanotechnology, Vol. 3”, Ed. by Hari Singh Nalwa, American Scientific Publishers, 2004, pp. 545-565.

Corresponding Author: Naotoshi Nakashima

E-mail: nakashima-tcm@mbox.nc.kyushu-u.ac.jp

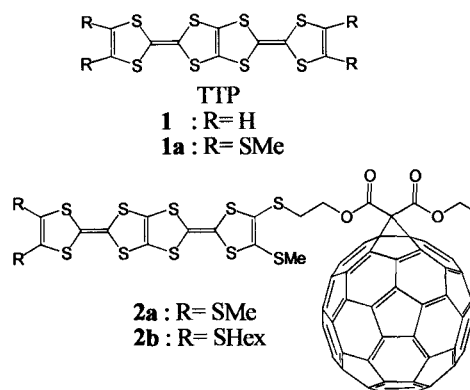
Tel&Fax: (+81)-92-802-2840

Synthesis and Properties of a New C₆₀-TTP Hybrid System

○Takahiro Ikeuchi, Hisakazu Miyamoto, Yohji Misaki

Department of Applied Chemistry, Faculty of Engineering, Ehime University

Recently C₆₀-tetrathiafulvalene (TTF) systems have attracted much attention as light-induced charge-separation systems for photovoltaic devices. We have found bis-fused TTF[2,5-bis(1,3-dithiol-2-ylidene) 1,3,4,6-tetrathiapentalene] (TTP, **1**) and its derivatives have produced many organic metals stable down to low temperatures. In this connection, hybrid systems composed of C₆₀ and TTP (**2**) are of interest as single component conductors as well as photoinduced electronic materials. We report herein synthesis and properties of a C₆₀-TTP hybrid system **2**.



The synthesis of **2a,b** has been achieved by Bingel-type cyclopropanation reaction between **3** and C₆₀ with CBr₄ and DBU in toluene. Cyclic voltammograms of **2a,b** consist of three pairs of oxidation waves corresponding to the TTP moiety, and four pairs of reduction ones due to C₆₀ moiety (Table 1). The reduction potentials of **2a** in o-dichlorobenzene (o-DCB) are comparable to those of C₆₀. On the other hand, the oxidation potentials of **2a,2b** in C₆H₅CN are lower than those of **1a** due to electron-withdrawing effect of C₆₀.

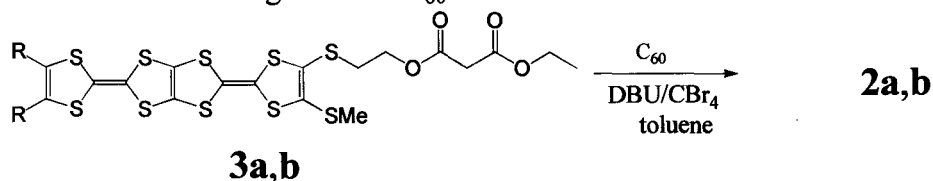


Table 1 Redox potentials of **2a,b** and their related compounds (V vs. Fc / Fc⁺, 0.05 M Bu₄NPF₆)

Compound	solvent	E_1^{ox}	E_2^{ox}	E_3^{ox}	E_4^{ox}	E_1^{red}	E_2^{red}	E_3^{red}	E_4^{red}
2a	o-DCB	0.02	0.26	0.46		-1.20	-1.56	-2.01	-2.54 ^a
2a	C ₆ H ₅ CN	0.10	0.31	0.59	0.73				
2b	C ₆ H ₅ CN	0.10	0.31	0.59	0.73				
C ₆₀	o-DCB					-1.18	-1.58	-2.03	-2.62 ^a
1a	C ₆ H ₅ CN	0.06	0.27	0.58	0.71				

^aIrreversible wave. Cathodic peak potentials.

References: Dirk M. Duldi, et al., J. Org. Chem., 68, 779 (2003)

Corresponding Author Takahiro Ikeuchi

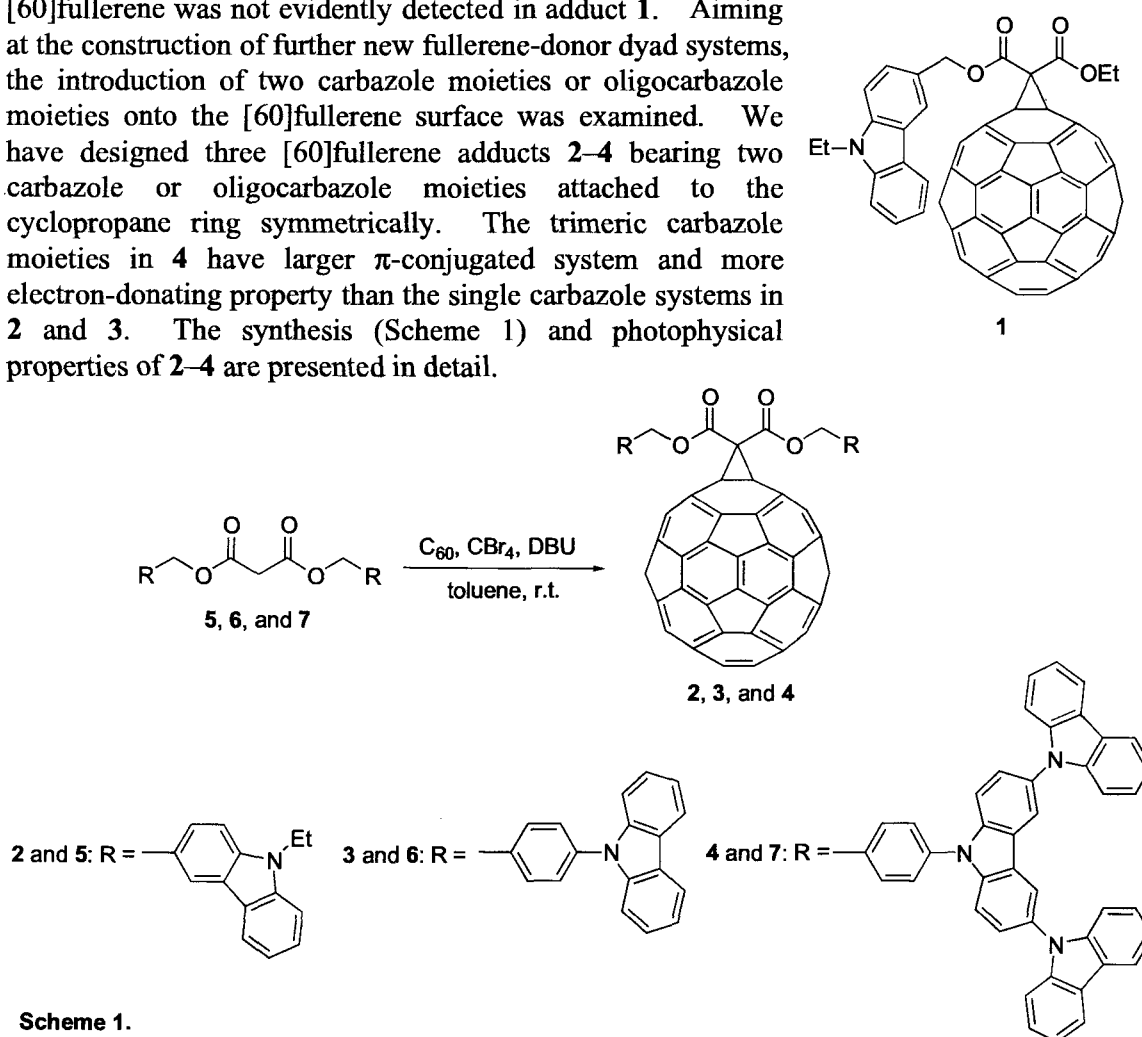
E-mail: kozo05jp@achem.en3.ehime-u.ac.jp

Synthesis and Photophysical Properties of [60]Fullerene Adducts Carrying Oligocarbazole Moieties

○Takashi Konno, Yosuke Nakamura, Satoru Watanabe, Masato Suzuki, and Jun Nishimura

Department of Nano-Material Systems, Graduate School of Engineering, Gunma University

[60]Fullerene–donor dyads linked by covalent bondings have attracted much interest from the aspects of charge-separated states arising from the intramolecular photoinduced electron transfer. Especially, porphyrins and related compounds have been extensively utilized among a variety of donor moieties. In contrast, there have been only a few examples of carbazole-linked fullerene adducts, although carbazole is a good electron donor known as a component of photoconductive poly(*N*-vinylcarbazole) (PVCz). Quite recently, we have successfully prepared [60]fullerene adduct **1** bearing a carbazole residue by using Bingel reaction. Unexpectedly, the photoinduced electron transfer via the excited states of [60]fullerene was not evidently detected in adduct **1**. Aiming at the construction of further new fullerene-donor dyad systems, the introduction of two carbazole moieties or oligocarbazole moieties onto the [60]fullerene surface was examined. We have designed three [60]fullerene adducts **2–4** bearing two carbazole or oligocarbazole moieties attached to the cyclopropane ring symmetrically. The trimeric carbazole moieties in **4** have larger π -conjugated system and more electron-donating property than the single carbazole systems in **2** and **3**. The synthesis (Scheme 1) and photophysical properties of **2–4** are presented in detail.



Scheme 1.

*Corresponding author: Yosuke Nakamura

E-mail: nakamura@chem.gunma-u.ac.jp Tel: +81-277-30-1312 Fax: +81-277-30-1314

Confirmation of Chemical Modification of Carbon Nanotubes Using Gold Particles as Reaction Indicator

° Hiroaki Azehara,¹ Yuka Kasanuma,¹ Takaharu Okajima,¹ Tadashi Fujieda,² Toshio Yasuda,² Motoyuki Hirooka,² Kishio Hidaka,² Mitsuo Hayashibara,² and Hiroshi Tokumoto¹

¹*Nanotechnology Research Center, Research Institute of Electronic Science, Hokkaido University, N21 W10, Kita-ku, Sapporo, Hokkaido 001-0021, Japan*

²*Materials Research Laboratory, Hitachi Ltd., 7-1-1 Omika-cho, Hitachi-shi, Ibaraki 319-1292, Japan.*

Chemical modification of carbon nanotubes (CNTs) is a key factor to increase their solubility, change their optical and electrical properties, and so on. At the same time, CNTs are believed to be ideal tips for scanning probe microscopes.¹ Especially, for chemical force microscopes² with molecular resolution, we must combine these two techniques and develop AFM with chemically modified CNT-tips. Prior to the usage, the CNT-tip ends should be confirmed that they are properly modified chemically. However, conventional spectroscopic methods can hardly confirm the chemical states of the CNT-end because the amount of their functional groups is too small to be detected.

In the present study, we try to label functional groups of CNTs with gold nano-particles. Since thiol atoms form covalent bonds with gold ones, we introduce thiol groups to CNTs at the final step of their modification and then exposed them to colloidal gold sol. The pale red gold sol decolorized immediately after it was contacted with the solution of CNTs, suggesting successful adsorption of gold particles to the CNT-ends. Further, the adsorption of gold particles to CNT-ends was more evidently confirmed by scanning transmission electron microscopy and atomic force microscopy. Based on these results, it is concluded that gold particles can be used as an indicator for thiol groups tethered to CNTs, and therefore as a confirmation means of the chemical modification of CNTs.

References

- (1) T. Uchihashi, N. Choi, M. Tanigawa, M. Ashino, Y. Sugawara, H. Nishijima, S. Akita, Y. Nakayama, H. Tokumoto, K. Yokoyama, S. Morita, M. Ishikawa, *Jpn. J. Appl. Phys.* 39, 8B, L887-L889 (2000).
- (2) S. S. Wong, E. Joselevich, A. T. Woolley, C.-L. Cheung, and C. M. Lieber, *Nature*, 394, 5255 (1998).

Corresponding Author: Hiroaki Azehara

E-mail: hazehara@es.hokudai.ac.jp

Tel: +81-11-706-9342; **Fax:** +81-11-706-9355

Fullerene Derivatives Bound to Oxygen - Synthesis, Photophysical behavior, and Generation of Singlet Oxygen

Takeshi Honma^{1,2}, Takumi Hara^{1,2}, Yusuke Tajima¹,
Mikio Hoshino¹, Shiro Matsumoto², Kazuo Takeuchi^{1,2}

¹Nanomaterial Processing Lab., RIKEN, Wako, 351-0198

²Department of Chemical Engineering, Saitama University, Saitama, 338-8570

Recently, we reported that the acetalization of fullerene epoxides with several carbonyl compounds readily takes place in the presence of Lewis acid to afford the corresponding 1,3-dioxolane derivatives of C₆₀. [1] Furthermore, we found that fullerene mono oxide, C₆₀O **1** gives 1,2-fullerene diol **3** with the use of Brønsted acids as catalysts. [2]

In this paper, we present photophysical properties of the triplet states of C₆₀ and several fullerene derivatives **1-3** (Fig.1) in toluene studied by laser flash photolysis. T-T absorption spectra of **1-3** are located at the wavelengths shorter than that of C₆₀. The triplet lifetimes were determined by monitoring the decay of the T-T absorption spectra. The triplet states of C₆₀ and **1-3** were effectively quenched by oxygen via energy transfer.

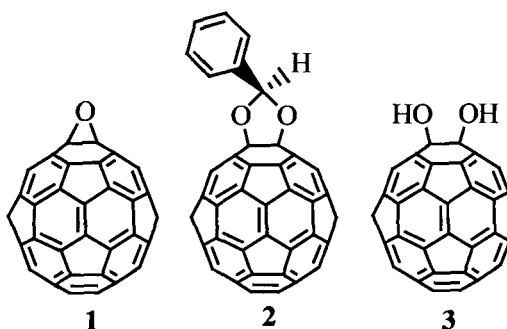


Fig.1 Fullerene derivatives

The formation of the singlet oxygen (¹O₂) was confirmed by observation of the emission spectrum of ¹O₂. In the formation of ¹O₂ observed for toluene solutions of C₆₀ and **1-3**, the difference in quantum yield is hardly discernible.

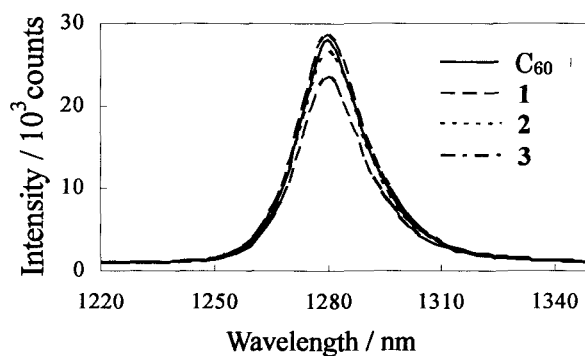


Fig.2 Emission spectrum from singlet oxygen generated by laser irradiation (532 nm) of C₆₀ and fullerene derivatives.

[1] Y. Shigemitsu, M. Kaneko, Y. Tajima, K. Takeuchi, *Chem.Lett.*, **2004**, 33 (12), 1604-1605.

[2] T. Honma, Y. Tajima, D. Yamazaki, T. Sasaki, K. Takeuchi, K. Tanaka, The 29th Fullerene-Nanotubes General Symposium, 66 (2005).

Corresponding Author: Yusuke Tajima

E-mail: tajima@riken.jp, Tel&Fax: +81-48-467-9309, FAX: +81-48-462-4702

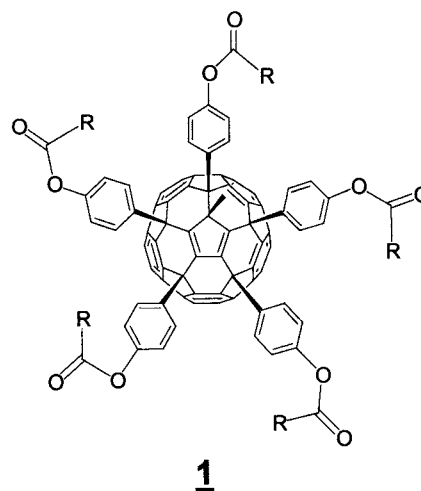
Organofullerenes Highly Soluble in Polar Solvents

○Kiminori Kawakami and Jun Enda

Mitsubishi Chemical Group Science and Technology Research Center, Inc
 1000, Kamoshida-cho Aoba-ku, Yokohama 227-8502, Japan

We previously reported the synthesis of air-stable organofullerenes by mono-methylation of pentaorgano-mono-hydro[60]fullerene that Nakamura et al. had developed.^{1,2} These fullerene derivatives exhibit not only unique properties but also sufficient stability as commercial products. However, they are insoluble in esters such as PGMEA (propylene glycol monomethyl ether acetate), a polar solvent generally used in industrial processes. In this study we prepared $C_{60}(4-C_6H_4OCOR)_5Me$ (**1**) with various R group and evaluated the solubility of the products in polar solvents.

Compounds **1a-1g** were prepared in quantitative yield by esterification of $C_{60}(4-C_6H_4OH)_5Me$ under basic condition with a small excess of acid chlorides (RCOCl). Among them, derivatives with linear R group (i.e. **1a-1c**) exhibited low solubility in PGMEA (< 5mg/mL). On the other hand, derivatives with branched R group such as **1d-1e** exhibited higher solubility in PGMEA (> 50mg/mL). Further, derivatives which possess bulky rotatable part on the ester moiety (**1f-1g**) exhibited excellent solubility. In this context, $C_{60}(4-C_6H_4OCH_2COO-t-C_4H_9)_5Me$ also exhibited remarkable solubility in PGMEA (> 100mg/mL). Further, we will discuss thermal and optical properties as well as air-stability of these derivatives.



1a: R = CH₃, **1b:** R = C₂H₅, **1c:** R = n-C₃H₇
1d: R = i-C₃H₇, **1e:** R = t-C₄H₉,
1f: R = CH₂-i-C₃H₇, **1g:** R = CH₂-t-C₄H₉

In this presentation, we will also introduce other fullerene derivatives available by Mitsubishi Chemical group.

References:

- [1]K. Kawakami and J. Enda, *The 29th Fullerene Nanotubes General Symposium 1P-1 (2005)*
 [2]M. Sawamura, H. Iikura, and E. Nakamura, *J. Am. Chem. Soc.*, **1996**, *118*, 12850,

Corresponding author: Kiminori Kawakami

E-mail: 5503334@cc.m-kagaku.co.jp

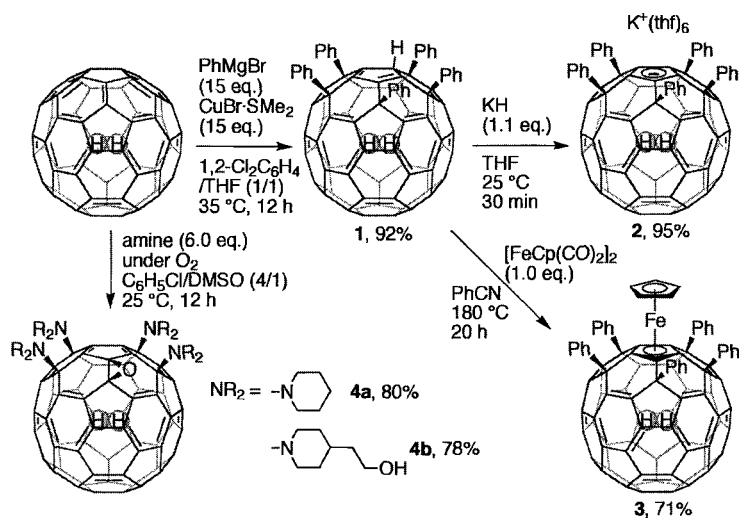
TEL/Fax: +81-45-963-4484/+81-45-963-443

Organic and Organometallic Derivatives of Dihydrogen-encapsulated [60]Fullerene

○ Yutaka Matsuo, Hiroyuki Isobe, Takatsugu Tanaka, Yasujiro Murata,
Michihisa Murata, Koichi Komatsu, and Eiichi Nakamura

Nakamura Functional Carbon Cluster Project, ERATO, Japan Science and Technology Agency, and Department of Chemistry, The University of Tokyo, and Institute for Chemical Research, Kyoto University

Abstract: Regioselective multi-addition reaction of organocopper and amine compounds onto dihydrogen encapsulated [60]fullerene, $H_2@C_{60}$, produced a variety of organic and organometallic derivatives of $H_2@C_{60}$. The X-ray crystallographic analysis of dihydrogen encapsulated bulky ferrocene, $Fe(H_2@C_{60}Ph_5)C_5H_5$, showed the presence of the dihydrogen molecule located almost in the center but slightly away from the ferrocene moiety. The 1H NMR chemical shift values for the encapsulated molecular hydrogen indicated that these values are susceptible to the magnetic environment of inside as well as outside of the fullerene cage.



References: Matsuo, Y.; Isobe, H.; Tanaka, T.; Murata, Y.; Murata, M.; Komatsu, K.; Nakamura, E. *J. Am. Chem. Soc.*, in press.

Corresponding Author: Yutaka Matsuo

E-mail: matsuo@chem.s.u-tokyo.ac.jp

Tel&Fax: +81-3-5841-1476

Ionization and Chemical Functionalization of Gd@C₈₂

○Takayoshi Kono¹, Yoichiro Matsunaga¹, Tsukasa Nakahodo¹, Takahiro Tsuchiya¹,
Takatsugu Wakahara¹, Yutaka Maeda², Takeshi Akasaka^{1,*}, Shingo Okubo³, Tatsuhisa
Kato⁴, Naomi Mizorogi³, Kaoru Kobayashi³, Shigeru Nagase³

¹Center for Tsukuba Advanced Research Alliance, University of Tsukuba,
Tsukuba, Ibaraki 305-8577, Japan

²Department of chemistry, Tokyo Gakugei University, Koganei, Tokyo 184-8501, Japan

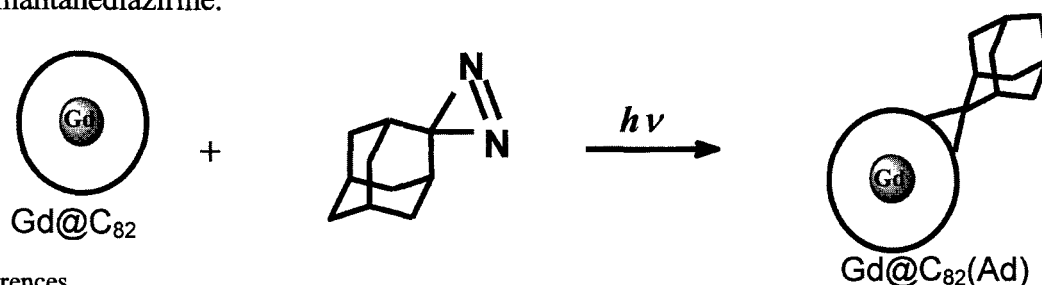
³Institute for Molecular Science, Okazaki, Aichi 444-8585, Japan

⁴Department of Chemistry, Josai University, Sakado, Saitama 350-0295, Japan

Chemistry of endohedral metallofullerenes is one of the most exciting topics in the fullerene science. They could give rise to new species or materials with novel properties which are unexpected for hollow fullerenes¹⁾. Among these, Gd@C₈₂ is of particular interest because of the relationship which has potential for some new materials such as MRI contrasting agents²⁻⁴⁾. The derivatization of Gd@C₈₂ is a key step for developing its application in the field of medicinal use.

Recently, we have verified the carbon cage symmetries of several endohedral metallofullerenes by the NMR measurement. Meanwhile, we have found that the addition of adamantylidene carbene to La@C₈₂ selectively proceeds to afford the mono-adduct⁵⁾. The selectivity of the reaction is very important for further applications.

In this context, we report here the chemical characterization of Gd@C₈₂ by means of ¹³CNMR measurement of its anion and the regioselective reaction of Gd@C₈₂ with adamantanediazirine.



References

- 1) *Endofullerenes: A New Family of Carbon Clusters*; Akasaka, T. and S. Nagase, Eds., Dordrecht, 2002.
- 2) Kato, H. et al. *Chem. Phys. Lett.* **2000**, 324, 255.
- 3) Zhang, Y. et al. *Chem. Lett.* **2005**, 34, 1264
- 4) Chen, C. et al. *Nano Lett.* **2005**, 5, 2050
- 5) Maeda, Y. et al. *J. Am. Chem. Soc.* **2004**, 126, 6858.

Corresponding author: Takeshi Akasaka

Tel & Fax: +81-29-853-6409, E-mail: akasaka@tara.tsukuba.ac.jp

Isolation and Characterization of La@C₇₄(C₆H₃Cl₂)-II

○Takashi Kikuchi,¹ Hidefumi Nikawa,¹ Takatsugu Wakahara,¹ Tsukasa Nakahodo,¹
Takahiro Tsuchiya,¹ Takeshi Akasaka,¹ G. M. Aminur Rahman,¹ Yutaka Maeda,²
Kenji Yoza,³ Ernst Horn,⁴ Naomi Mizorogi,⁵ and Shigeru Nagase⁵

¹Center for Tsukuba Advanced Research Alliance, University of Tsukuba, Tsukuba
Ibaraki 305-8577, Japan

²Department of Chemistry, Tokyo Gakugei University, Koganei, Tokyo 184-8501, Japan

³Bruker AXS K. K., Yokohama, Kanagawa 221-0022, Japan

⁴Department of Chemistry, Rikkyo University, Tokyo 171-8501, Japan

⁵Department of Theoretical Molecular Science, Institute for Molecular Science, Okazaki,
Aichi 444-8585, Japan

In 1991, Smalley and co-workers reported that La@C₆₀, La@C₇₄, and La@C₈₂ were produced in the soot, but only La@C₈₂ was extracted with toluene¹. Since then, the chemistry of soluble metallofullerenes has been started by centering on that of La@C₈₂, and up to now many soluble endohedral metallofullerenes have been separated and characterized. However, insoluble metallofullerenes such as La@C₆₀ and La@C₇₄ have not yet been isolated although they are regularly observed in the raw soot by mass spectrometry.

Recently, we have reported the first isolation of La@C₇₄ as a metallofullerene derivative². Three isomers, La@C₇₄(C₆H₃Cl₂) Ia-Ic, were isolated and their ¹H and ¹³C NMR spectra indicate that they have the same cage structure in which the addition position of the dichlorophenyl group affords different structures. Finally, the X-ray crystallographic analysis of isomer Ia unambiguously verified the structure of the novel endohedral metallofullerene derivative with the C₇₄(D_{3h}) cage.

We herein report the isolation of new isomers, La@C₇₄(C₆H₃Cl₂) IIa-IIc, and their structural determination by mass and spectroscopic measurements.

1) Y. Chai, T. Guo, C. Jin, R. E. Haufler, L. P. Felipe, F. Chibante, J. Fure, L. Wang, M. J. Alford, R. E. Smalley, *J. Phys. Chem.* **1991**, *95*, 7564-7568.

2) H. Nikawa, T. Kikuchi, T. Wakahara, T. Nakahodo, T. Tsuchiya, G. M. A. Rahman, T. Akasaka, Y. Maeda, K. Yoza, E. Horn, N. Mizorogi, S. Nagase, *J. Am. Chem. Soc.* **2005**, *127*, 9684-9685.

Corresponding Author: Takeshi Akasaka

Tel&Fax +81-29-853-6409, E-mail: akasaka@tara.tsukuba.ac.jp

Isolation and Characterization of $Gd_2@C_{78}$

○ Yuji Takematsu¹, Takayoshi Kono¹, Tsukasa Nakahodo¹, Takahiro Tsuchiya¹,
Takatsugu Wakahara¹, Yutaka Maeda², Takeshi Akasaka^{1,*}, Tatsuhisa Kato³, Shigeru Nagase⁴

¹*Center for Tsukuba Advanced Research Alliance, University of Tsukuba,
Tsukuba, Ibaraki 305-8577, Japan*

²*Department of chemistry, Tokyo Gakugei University, Koganei, Tokyo 184-8501, Japan*

³*Department of chemistry, Josai University, Sakado, Saitama 350-0295, Japan*

⁴*Institut for Molecular Science, Okazaki, Aichi 444-8585, Japan*

Endohedral metallofullerenes encapsulate one or more metal atoms inside a hollow fullerene cage. These fullerenes have attracted special attention because they engender new spherical molecules with unique electronic properties and structures that are unexpected for empty fullerenes.¹⁾

Among these, the gadolinium metallofullerenes have attracted special interest because of the promising applications to magnetic resonance imaging (MRI).²⁻⁷⁾ The gadolinium metallofullerene isolated and structurally characterized so far is $Gd@C_{82}$. On the other hand, we have recently reported isolation, characterization, and theoretical study of $La_2@C_{78}$.⁸⁾ We here in report the isolation and characterization of $Gd_2@C_{78}$ by means of mass, absorption and EPR spectroscopic measurements.

References)

- 1) *Endofullerenes: A New Family of Carbon Clusters*; Akasaka, T. et al. Dordrecht, 2002.
- 2) Mikawa, M. et al. *Bioconjugate Chem.* 2001,12,510
- 3) Kato, H. et al. *J. Am. Chem. Soc.* 2003, 125, 4391
- 4) Bolskar, R. D. et al. *J. Am. Chem. Soc.* 2003,128, 5471
- 5) Toth, E. et al. *J. Am. Chem. Soc.* 2004, 127, 799
- 6) Sitharaman, B. *Nano Lett.* 2004, 12, 2373.
- 7) Sabrina, L. et al. *J. Am. Chem. Soc.* 2005, 127, 9368
- 8) Cao, B. et al. *J. Am. Chem. Soc.* 2004, 126, 9164.

Corresponding author; Takeshi Akasaka, Te l& Fax: +81-29-853-6409, E-mail: akasaka@tara.tsukuba.ac.jp

Analysis of Lanthanide-Induced NMR Shifts of the Ce@C₈₂ Anion

○Michio Yamada,¹ Takatsugu Wakahara,¹ Yongfu Lian,¹ Takahiro Tsuchiya,¹ Takeshi Akasaka,¹ Markus Waelchli,² Naomi Mizorogi,³ and Shigeru Nagase³

¹Center for Tsukuba Advanced Research Alliance, University of Tsukuba, Tsukuba, Ibaraki 305-8577, Japan, ²Bruker Biospin K. K., Tsukuba, Ibaraki 305-0051, Japan, ³Department of Theoretical Molecular Science, Institute for Molecular Science, Okazaki, Aichi 444-8585, Japan

Abstract: Endohedral metallofullerenes have attracted wide interest because of their possible applications in the fields of nanomaterial and biomedical science. Much attention has been paid to encapsulation of lanthanide atoms having *f* electrons, as seen for Tm@C₈₂,¹ Ce@C₈₂,² Pr@C₈₂,³ Gd@C₈₂,⁴ and Eu@C₈₂.⁵ For their electronic and magnetic properties, cage structures and metal positions play an important role. Recently, we have succeeded in determining the cage frameworks of La@C₈₂,⁶ Ce@C₈₂,⁷ and Pr@C₈₂⁸ by measuring the ¹³C NMR spectra of their anions. From the MEM/Rietveld analysis of synchrotron powder diffraction data of Sc@C₈₂,⁹ Y@C₈₂,¹⁰ and La@C₈₂,¹¹ Takata and co-workers have determined that the metal atom is located at an off-centered position on the C₂ axis adjacent to a hexagonal ring of the C₈₂ cage. These agree with theoretical prediction.¹² From the MEM/Rietveld analysis, however, it is recently reported that Eu@C₈₂⁵ and Gd@C₈₂¹³ have an anomalous structure, in which the metal atom having *f* electrons is located on the C₂ axis but is adjacent to the C-C double bond on the opposite side of the C_{2v}-C₈₂ cage. We here report the position of the Ce atom in Ce@C₈₂ by means of paramagnetic NMR spectral analysis of its anion and density functional calculations.

References: (1) Kodama, T. et al., *J. Am. Chem. Soc.* **2002**, *124*, 1452. (2) Ding, J. et al., *J. Phys. Chem.* **1996**, *100*, 11120. (3) Ding, J. et al., *J. Am. Chem. Soc.* **1996**, *118*, 11254. (4) Funasaka, H. et al., *Chem. Phys. Lett.* **1995**, *232*, 273. (5) Sun, B.-Y. et al., *Angew. Chem. Int. Ed.* **2005**, *44*, 4568. (6) Akasaka, T. et al., *J. Am. Chem. Soc.* **2000**, *122*, 9316. (7) Akasaka, T. et al., *J. Am. Chem. Soc.* **2004**, *126*, 4883. (8) Akasaka, T. et al., *Chem. Phys. Lett.* **2002**, *360*, 235. (9) Takata, M. et al., *Chem. Phys. Lett.* **1998**, *298*, 79. (10) Takata, M. et al., *Nature* **1995**, *377*, 46. (11) Nishibori, E. et al., *Chem. Phys. Lett.* **2000**, *330*, 497. (12) Kobayashi, K. et al., *Chem. Phys. Lett.* **1998**, *282*, 325. (13) Nishibori, E. et al., *Phys. Rev. B* **2004**, *69*, 113412.

Corresponding Author: Takeshi Akasaka, E-mail: akasaka@tara.tsukuba.ac.jp, Tel&Fax: +81-298-53-6409

Systematic Study of Lutetium Endohedral Di-Metallofullerenes Production, Isolation and Structural characterization of Lu₂C_{2n} (2n=74-86)

○Hisashi Umemoto¹, Takashi Inoue², Tetsuo Tomiyama¹, Ryo Kitaura¹,
Toshiki Sugai¹ and Hisanori Shinohara^{1,3,4}

¹Department of Chemistry, Nagoya University, Nagoya 464-8602, Japan

²Toyota Central R&D Laboratories, Inc., Nagakute, Aichi, 480-1192, Japan

³Institute for Advanced Research, Nagoya University, Nagoya 464-8602, Japan

⁴CREST, Japan Science and Technology Corporation, c/o Department of Chemistry,
Nagoya University, Nagoya 464-8602, Japan

For di-metallofullerenes¹ with various metal atoms, the metallofullerenes based on C₈₀/C₈₂ cages usually have much higher abundance than others, so that the most studies so far have concentrated on the C₈₀/C₈₂ based di-metallofullerenes. However, di-metallofullerenes based on other cage sizes may exhibit some unique and novel electronic properties.

Here, we report the first systematic study of the production, isolation and structural characterization of a series of Lu di-metallofullerenes Lu₂C_{2n} (2n=74-86). Lu₂C_{2n} (2n=74-86) are isolated by multi-stage HPLC method and characterized by LD-TOF-MS, UV-Vis-NIR absorption and ¹³C NMR. Table 1 summarizes the symmetries obtained by ¹³C NMR for a series of Lu di-metallofullerenes which are produced and isolated in this study. The current study provides an important basis for a further investigation of metallofullerenes in a broad size ranges.

Cage size	Isolated Lu ₂ C _{2n}	Symmetry
C ₇₂	Lu ₂ C ₂ @C ₇₂	C _s
C ₇₄	Lu ₂ C ₂ @C ₇₄	C ₂
C ₇₆	Lu ₂ @C ₇₆	T _d
C ₇₈	Lu ₂ @C ₇₈	C _{2v}
C ₈₀	Lu ₂ @C ₈₀	C _{2v}
	Lu ₂ C ₂ @C ₈₀	C _{2v}
C ₈₂	Lu ₂ @C ₈₂	C _s , C _{2v} , C _{3v}
	Lu ₂ C ₂ @C ₈₂	C _s , C _{2v} , C _{3v}
C ₈₄	Lu ₂ @C ₈₄	D _{2d} , C ₁
	Lu ₂ C ₂ @C ₈₄	D _{2d}
C ₈₆	Lu ₂ @C ₈₆	C _{2v}

Table 1. A series of Lu di-metallofullerenes which are produced and isolated.

References:

[1] H. Shinohara, *Rep. Prog. Phys.*, **63**, 843 (2000).

Corresponding Author: Hisanori Shinohara

TEL: +81-52-789-2482, FAX: +81-52-789-1169, E-mail: noris@cc.nagoya-u.a.jp

Facile Generation of Fullerene Nanoparticles by Hand-Grinding

○Shigeru Deguchi, Sada-atsu Mukai, and Koki Horikoshi

Extremobiosphere Research Center, Japan Agency for Marine-Earth Science and Technology (JAMSTEC), 2-15 Natsushima-cho, Yokosuka 237-0061, Japan.

Fullerenes are hydrophobic carbon allotropes, and are not at all soluble in water. However, nanoparticles of them remain dispersed in water even without the aid of a dispersing agent such as a surfactant.¹ On one hand, the dispersion may help to develop new biotechnological applications of fullerenes without performing chemical modification to endow water solubility. On the other hand, concern has been raised for the potential environmental impact of the dispersion. Indeed, the first report on the cytotoxicity of the C₆₀ nanoparticles has not only attracted considerable scientific interest but also drawn keen public attention.²

The obvious approach to prepare small particles is a top-down approach, in which bulk solid is reduced to small particles by mechanical forces. However, this approach usually gives the particles on the order of microns in size. Thus, the nanoparticles, including those of C₆₀, are generally produced by bottom-up approaches, in which molecules are allowed to assemble into nanoparticles in solutions or gas through chemical reactions.

We found that in the case of fullerene C₆₀, nanoparticles including those as small as 20 nm are produced readily by hand-grinding bulk solid in an agate mortar. To our knowledge, preparation of nanoparticles by such a facile procedure is unprecedented, and is related closely to solid properties of C₆₀. The hand-ground nanoparticles of C₆₀ dispersed in water, just like those prepared by the conventional solution processes. ¹³C-NMR measurements revealed that all 60 carbons of the C₆₀ molecules in the nanoparticles are equivalent, indicating no significant chemical reaction took place during hand-grinding. Structure, size, and properties of the hand-ground C₆₀ nanoparticles will be presented.

1) S. Deguchi, R. G. Alargova, K. Tsujii, *Langmuir*, **2001**, 17, 6013-6017. 2) E. Oberdörster, *Environ. Health Perspect.*, **2004**, 112, 1058-1062.

Corresponding Author: Shigeru Deguchi

shigeru.deguchi@jamstec.go.jp

tel: +81-46-867-9679 / fax: +81-46-867-9715

The Structure and Physical Properties in Ternary C₆₀ Compounds

○Takashi Naniki , Satoru Motohashi , Hironori Ogata

Dept. of Materials Chemistry, Hosei University

3-7-2 Kajino cho, Koganei, Tokyo, 184-8584. Japan

Since the discovery of superconductivity in Na_xX_yC₆₀ (X=N: *T_c*=12K, X=H: *T_c*=15K), there has been many interests in the structure and the electronic states of the Na-X-C₆₀ ternary systems. It has been suggested that nitrogen or hydrogen in the systems contribute not only to a spacer which suppress the structural instability but also to the electronic states near the Fermi level.

In the present work, Cs(NaH)_xC₆₀ compounds (x=1~10) were synthesized, and their structures and electronic properties were investigated by powder X-ray diffraction, magnetic susceptibility and solid state NMR measurements.

Stoichiometric amounts of Cs, C₆₀, and NaH were mixed and ground in a glove box and transferred into an ESR quartz tube in a glove box. These raw materials in the sealed tubes were reacted in a furnace at 390°C for 74hours.

Figure 1 shows the powder x-ray diffraction profile of CsNaHC₆₀ compound at room temperature. The diffraction profile can be indexed with a orthorhombic lattice(space group: *Immm*) of lattice constants of *a*=9.069 Å, *b*=10.192 Å and *c*=14.128 Å. Detail results on the correlation between structures and electronic properties of these materials will be discussed in the presentation.

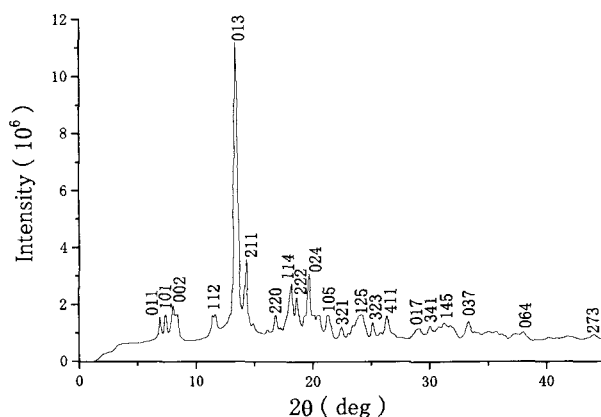


Fig1. Powder x-ray diffraction profile of CsNaHC₆₀ compound at r.t.

[1] K.Imaeda et al, Solid State Communication, Vol99, No7, 479-482(1996)

Corresponding Author: Hironori Ogata, E-mail: hogata@k.hosei.ac.jp

Tel&Fax: 042-387-6229

Solution-Processed Organic Thin-Film Transistors Based on Dodecyl Substituted C₆₀ Derivatives

○M. Chikamatsu¹, A. Itakura¹, Y. Yoshida¹, R. Azumi¹, K. Kikuchi² and K. Yase¹

¹Photonics Research Institute, National Institute of Advanced Industrial Science and Technology (AIST), Central 5, 1-1-1 Higashi, Tsukuba, Ibaraki 305-8565, Japan
²Department of Chemistry, Tokyo Metropolitan University, Hachioji 192-0397, Japan

We have reported solution-processed n-type organic thin-film transistors (OTFTs) based on long-chain alkyl-substituted C₆₀, C₆₀-fused *N*-methylpyrrolidine-*meta*-C_n phenyl (C₆₀MC_n (n= 8,12,16)), exhibit high electron mobility [1-2]. In this study, for evaluating the effect of alkyl-chain orientation, we fabricate and characterize OTFTs based on various dodecyl substituted C₆₀ derivatives (table 1).

Films of C₆₀ derivatives were fabricated on highly doped silicon wafers covered with SiO₂ by spin coating from chloroform solution under ambient condition. Source and drain gold electrodes were deposited on the films. The TFT characteristics were measured in a vacuum at room temperature.

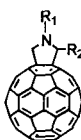


Table 1. Dodecyl substituted C₆₀ derivatives.

Compounds	R ₁	R ₂
C60OC12	Me	<i>ortho</i> -C ₁₂ H ₂₅ Ph
C60MC12	Me	<i>meta</i> -C ₁₂ H ₂₅ Ph
C60PC12	Me	<i>para</i> -C ₁₂ H ₂₅ Ph
C60C12	Me	C ₁₂ H ₂₅
C60NC12	C ₁₂ H ₂₅	H

Figure 1 shows out-of-plane XRD patterns of C60C12 and C60MC12 films. Film crystallinity is different in the two films. The spacings of the (001) plane in the C60C12 and C60MC12 films are calculated to 2.48 nm and 2.32 nm, respectively. Field-effect electron mobilities of C60C12- and C60MC12-TFT exhibit 0.002 cm²/Vs and 0.09 cm²/Vs, respectively. These results indicated that alkyl-chain orientation of C₆₀ derivatives strongly affects the film crystallinity and TFT performance.

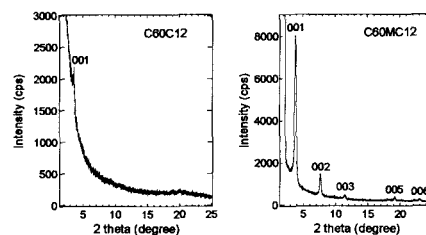


Fig. 1. Out-of-plane XRD patterns of C60C12 and C60MC12 films.

[1] M. Chikamatsu et al., Appl. Phys. Lett. **87**, 203504 (2005).

[2] M. Chikamatsu et al., The 29th Fullerene-Nanotubes General Symposium, 2-14 (2005).

Corresponding Author: Masayuki Chikamatsu

TEL: +81-29-861-6252, FAX: +81-29-861-6303, E-mail: m-chikamatsu@aist.go.jp

Electronic properties of higher fullerenes and their related compounds

○Hiroyuki Sugiyama^{1,2}, Takayuki Nagano^{1,2}, Kumiko Imai², Haruka Kusai¹,
Akihiko Fujiwara^{2,3}, Taishi Takenobu^{2,4}, Yoshihiro Iwasa^{2,4} and Yoshihiro Kubozono^{1,2}

¹Department of Chemistry, Okayama University, Okayama 700-8530, Japan

²CREST, Japan Science and Technology Corporation, Kawaguchi, 322-0012, Japan

³Japan Advanced Institute for Science and Technology, Ishikawa 923-1292, Japan

⁴Institute of Material Research, Tohoku University, Sendai 980-8577, Japan

Fullerenes are π -electron enriched materials which can produce novel physical properties such as metallic behavior and superconductivity. In metal intercalated C_{60} , the electron transfer from metal atoms to C_{60} molecules plays an important role to the metallic behavior and superconductivity. In endohedral metallofullerenes, the electron transfer occurs from the encapsulated metal atoms to the fullerene cage, leading to the semiconductors with very small band gaps. Therefore, it is meaningful to investigate the electronic structures of various types of fullerenes. In this study, we have fabricated field-effect transistor (FET) devices with thin films of higher fullerenes, C_{76} and C_{78} , and studied their FET properties in order to clarify the electronic properties of higher fullerenes; two isomers, I and II, are independently studied for C_{78} . The structures and electronic properties of metal intercalated higher fullerenes, Rb_xC_{76} and Rb_xC_{78} , have also been studied.

The drain current I_D versus drain-source voltage V_{DS} plots of FET device with thin films of C_{76} is shown in Figure 1. The field-effect mobility, μ , was estimated to be $3.5 \times 10^{-5} \text{ cm}^2 \text{ V}^{-1} \text{ s}^{-1}$ from the plots (Figure 1), and the μ of C_{78} (I) FET was estimated to be $4.2 \times 10^{-4} \text{ cm}^2 \text{ V}^{-1} \text{ s}^{-1}$. These values are lower than that of the C_{60} FET device, $0.6 \text{ cm}^2 \text{ V}^{-1} \text{ s}^{-1}$ [1]. The difference in the μ value between C_{60} and higher fullerenes is due to the crystallinity of the thin films. Therefore, the ordered structures are indispensable for high-performance FET devices. The optical absorption spectra of the thin films of C_{76} and C_{78} have also been measured in order to estimate the band gaps. Furthermore, the structures of Rb_xC_{76} and Rb_xC_{78} have also been studied by the X-ray powder diffraction with synchrotron radiation. The electronic properties will also be reported on the basis of temperature dependent ESR spectra of Rb_xC_{76} and Rb_xC_{78} .

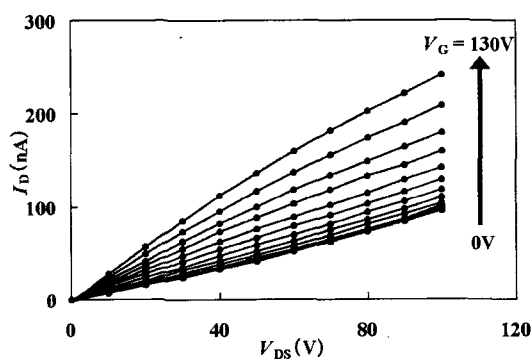


Fig.1. $I_D - V_{DS}$ plots of C_{76} FET

References

[1] S. Kobayashi et al., *Appl. Phys. Lett.* **2003**, *82*, 4581.

Corresponding Author : Hiroyuki Sugiyama

E-mail : sugihiro@cc.okayama-u.ac.jp , **Tel** : +81-86-251-7850 , **Fax** : +81-86-251-7853

Study on Encapsulation of Radioactive Waste Elements inside Carbon Nanocapsules

○Kazunori Yamamoto

*Nanomaterials Group, Quantum Beam Science Directorate, Nuclear Science Research
Institute,
Japan Atomic Energy Agency, Tokai-mura, Naka-gun, Ibaraki 319-1195, Japan*

Abstract:

Although nuclear energy is the only non-greenhouse gas-emitting energy sources that can effectively replace fossil fuels and satisfy global demand at present [1], there is still opposition to the peaceful use of nuclear power. The main objection against nuclear power is the risk of spread of “radioactivity” (radionuclides) to the environment where it may cause health effects in human.

Carbon nanocapsules are known to engage many kinds of elements in their inner cavity. The elements that were reported to be encapsulated in carbon nanocapsules are: lanthanides such as La, Ce, Pr, Nd, Gd, Tb, Dy, Ho, Er, Tm and Lu, actinides such as Th and U, alkaline earth such as Ca and Sr, transition elements such as Sc, Ti, V, Cr, Mn, Fe, Co, Ni, Cu, Y, Zr, Nb, Mo, Ru, Rh, Pd, Hf, Ta, W, Re, Os, Ir, Pt and Au, and some other elements such as B, Si, S, Ge, Se, Sb [2]. The elements that can be engaged in carbon nanocapsules will increase in number, because there are more than 10 elements that have not been tested, such as Tc, Pm, Ac, Pa, Np, Pu, Am, and Cm, each of which is expected to be engaged in carbon nanocapsules.

It should be emphasized that most of the elements in a typical nuclear spent fuel also appear in the elemental table where the elements can be engaged in nanocapsules. Considering chemical stability of carbon and also mechanical stability of graphene wall in nanocapsules, the capsule will act as a perfect barrier to radionuclide release.

References:

1. P. Moore, “Statement to the Congressional Subcommittee on Energy & Resources”, April 28 (2005).
2. Y. Saito and S. Bandow, *Fundamentals of Carbon Nanotubes* (in Japanese), Korona-sha (1998).
3. K. Yamamoto, T. Wakahara and T. Akasaka, *Prog. Nucl. Energy*, **47**, 616-623(2005).

Corresponding Author: Kazunori Yamamoto

E-mail: yamamoto.kazunori@jaea.go.jp

Tel&Fax: +81-29-282-6474&+81-29-284-3813.

Preparation of polyhedral graphite particles including rare earth metal carbides in their centers

○Keita Kobayashi, Akira Koshio, Tatsuo Nakagawa and Fumio Kokai

Department of Chemistry for Materials, Mie University, 1577 Kurimamachiya, Tsu, Mie 514-5807, Japan

Polyhedral graphite (PG) particles are turbostratic graphite balls of sub-micron sizes. Kokai and co-workers reported that the PG particles were produced using pulsed CO₂ laser irradiation onto pure graphite target [1, 2]. The preparation of PG particles needs high pressure of Ar atmosphere (> 0.8 MPa). Recently, we produced single-wall carbon nanohorns aggregated around metal or metal carbide (M-SWNH) particles by continuous wave Nd:YAG laser irradiation onto graphite target containing iron-group metals and Ti in Ar gas atmosphere [3]. In this study, we performed laser vaporization of graphite containing rare earth oxide (M₂O₃) (M = Y, Gd and La) in Ar gas atmosphere (0.1 – 0.9 MPa).

Single-wall carbon nanotubes (SWNTs) and carbon nanocapsules including MC₂ (MC₂-CNCs) were obtained at an Ar gas pressures of 0.1 MPa. PG particles including MC₂ in their centers (MC₂-PG particles) (Figs. 1 and 2) were obtained at more than 0.3 MPa. With further increasing Ar gas pressure, the yield of MC₂-PG particles increased and facets of MC₂-PG particles were clearly developed. Unlike the formation of M-SWNH particles by using iron-group metals and Ti, the product did not contain M-SWNH particles. We will discuss the formation of these various products.

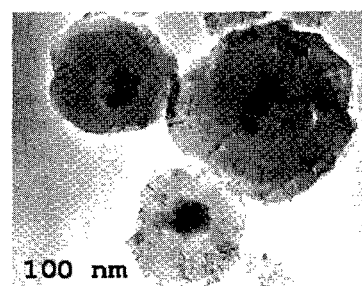


Fig. 1. Transmission electron microscope image of YC₂-PG particles

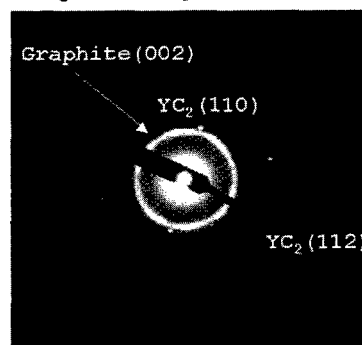


Fig. 2. Electron diffraction patterns of an YC₂-PG particle

References

- [1] F. Kokai et al., *Appl. Phys. A*, **77**, 69 (2003).
- [2] F. Kokai et al., *Carbon*, **42**, 2515 (2004)
- [3] K. Kobayashi et al, *Abstract of The 29th Fullerene-Nanotubes General Symposium*, **8** (2005).

Corresponding Author: Fumio Kokai

TEL: +59-231-9424, FAX: +59-231-9424, E-mail: kokai@chem.mie-u.ac.jp

Bulk ACCVD Generation of SWNTs with Narrow Chirality Distribution

○Shigeo Maruyama¹⁾, Yuhei Miyauchi¹⁾, Takashi Shimada¹⁾, Yoichi Murakami¹⁾,
Kenichi Sato²⁾, Yuji Ozeki³⁾ and Masahito Yoshikawa²⁾

1) Department of Mechanical Engineering, The University of Tokyo
7-3-1 Hongo, Bunkyo-ku, Tokyo 113-8656, Japan

2) Specialty Chemicals Research Lab., Chemical Research Labs., Toray Industries, Inc.
9-1, Oe-cho, Minato-ku, Nagoya 455-8502, Japan

3) R&D Planning Dept., Technology Center, Toray Industries, Inc.
1-1, Sonoyama 1-chome, Otsu, Shiga 520-8558, Japan

By scaling up the alcohol CCVD (ACCVD) generation technique [1,2] of single-walled carbon nanotubes (SWNTs), bulk amount of sample is being prepared. By dissolving zeolite used as catalysts support, purified SWNTs as shown in Fig. 1 are produced.

In order to determine the chirality distribution of SWNTs, dispersed and centrifuged SWNTs in NaDDBS/D₂O was examined by the fluorescence spectroscopy with scanning excitation energy [3] as in Fig. 2. 'As-grown' sample (20 mg) was sonicated for 30 min in 10g of D₂O with 0.5 wt % NaDDBS. After centrifuged at 436,000g × 1 hour, supernatants was used for the measurements. Narrow chirality distribution with bright (7,5) nanotube was obtained. This chirality distribution is equivalent to the case with CVD temperature at about 700 °C in the standard ACCVD method [4]. This sample with bright emission and with relatively narrow chirality distribution is useful for spectroscopic studies.

References:

- [1] S. Maruyama et al., Chem. Phys. Lett., 360 (2002) 229.
- [2] Y. Murakami et al., Chem. Phys. Lett., 374 (2003) 53.
- [3] S.M. Bachilo et al., Science 298 (2002) 2361.
- [4] Y. Miyauchi et al., Chem. Phys. Lett., 387 (2004) 198.

Corresponding Author: Shigeo Maruyama
E-mail: maruyama@photon.t.u-tokyo.ac.jp
Tel & Fax: +81-3-5800-6983



Fig. 1 Ten grams of purified SWNTs.

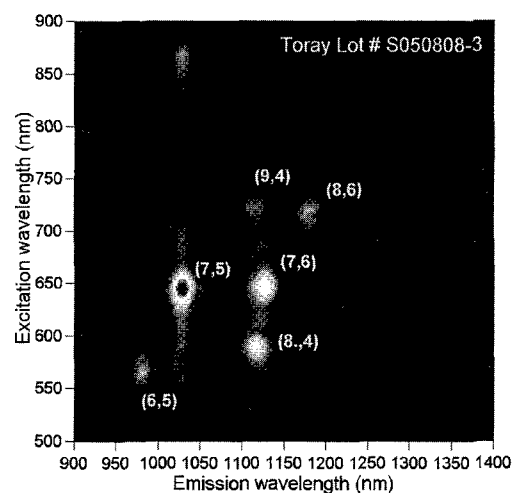


Fig. 2 Chirality distribution of SWNTs measured by fluorescence spectroscopy.

Isolation of Circular Aggregates of Single-Walled Carbon Nanotubes by Ultrasonic Atomization

Naoki Komatsu^{a)}, Takanori Shimawaki^{a,b)}, Shuji Aonuma^{b)}, Takahide Kimura^{a)}

a) Department of Chemistry, Shiga University of Medical Science, Seta, Otsu, 520-2192

b) Osaka Electro-Communication University, Neyagawa, Osaka 572-8530

Although rings of carbon nanotubes (CNTs) are predicted to have interesting magnetic properties, facile preparation or isolation methods of the rings with high purity are not yet reported. We describe here a convenient method for the isolation of circular single-walled carbon nanotubes (*c*-SWCNTs) using ultrasonic atomization [1].

A suspension of SWCNTs was bath-sonicated at 20 °C and the resulted mist above the surface was exposed to the flow of gas (Fig. 1). The SWCNTs blown into the receiver (1) were found to consist of *c*-SWCNTs exclusively by TEM analyses (Fig. 2a), while the ones from other parts of the glassware and residue (2 – 5) included only a little or no circles. They have round or oval shape with 0.5 – 3.3 μm in diameters (Fig. 2b), and some of them may be interlocked (Fig. 2c). When much shorter SWCNTs were used, Christmas wreath-shaped aggregates of SWCNTs were observed (Fig. 2d).

From the viewpoint of the isolation mechanism, the relatively small droplets including circular SWCNTs are thought to be carried to a receiver, while larger droplets including textures of string-shaped SWCNTs were not blown by the gas.

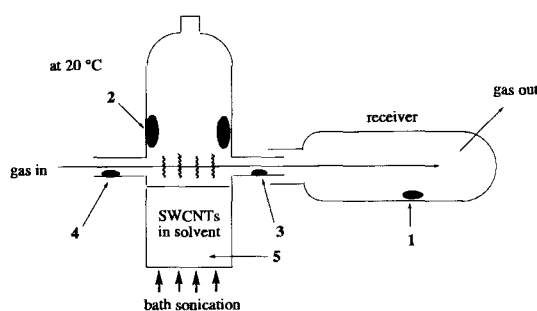


Fig. 1 Apparatus for ultrasonic isolation of circular SWCNTs

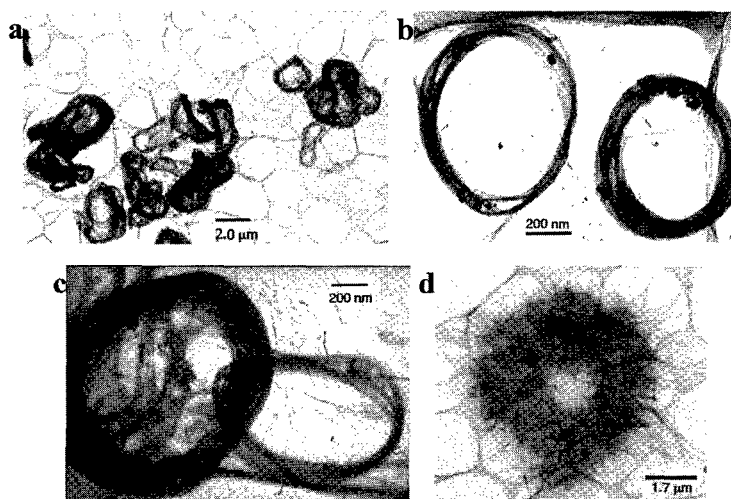


Fig. 2 TEM images of 1

[1] N. Komatsu, T. Shimawaki, S. Aonuma, T. Kimura, submitted for publication.

Corresponding Author: Naoki Komatsu

TEL: +81-77-548-2102, FAX: +81-77-548-2405, E-mail: nkomatsu@belle.shiga-med.ac.jp

Recent advances in growth of vertically aligned SWNT films by ACCVD

○Erik Einarsson, Masayuki Kadowaki, Yoichi Murakami, and Shigeo Maruyama

Department of Mechanical Engineering, The University of Tokyo, Tokyo 113-8656, Japan

In a previous study, we showed that the thickness of vertically aligned (VA) SWNT films produced by the alcohol catalytic CVD method [1] can be determined during growth by *in situ* optical absorbance measurements [2]. This was achieved by exploiting the relationship between the optical absorbance of a VA-SWNT film and its thickness [2]. An analytical description of the growth was developed based on these measurements [3], which shows the catalyst activity decreases exponentially with increasing CVD reaction time. Thus, the final film thickness is largely determined by the initial catalyst activity; however, the factors affecting the catalyst activity are not yet well understood.

In the current study, we observed that the initial catalyst activity is sensitive to the ambient chamber pressure at which VA-SWNT growth occurs. This is shown in Figure 1 for three separate cases. In the 600 Pa case a film with a thickness of 6 μm was grown, as shown in Figure 2a, whereas the 800 Pa case (Fig 2b) produced a film 21 μm thick. The enhanced growth may be attributed to an increase in the ethanol dissociation rate, or the pressure change may have altered the flow dynamics inside the reaction chamber. Further studies are underway to clarify the underlying mechanism.

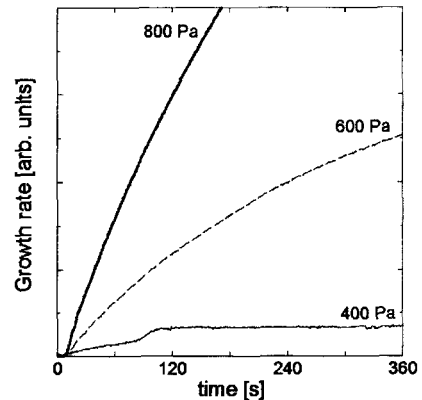


Fig. 1: Pressure dependence of the initial growth rate of VA-SWNT films

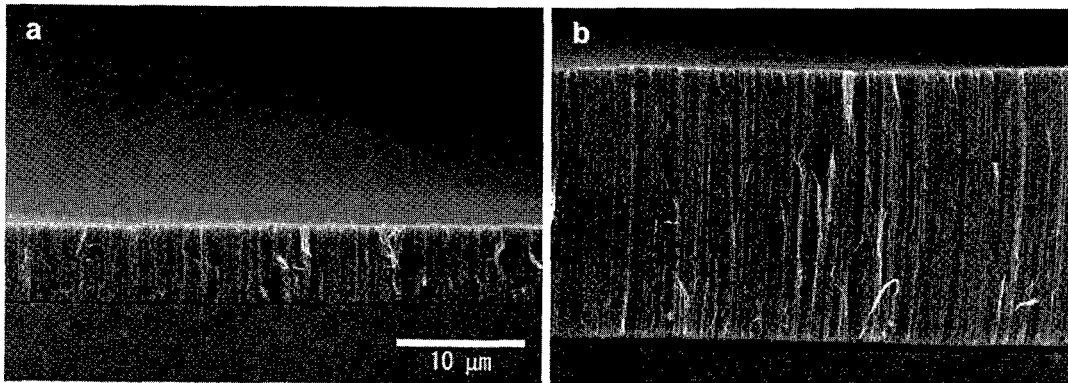


Fig. 2: (a) VA-SWNTs grown at an ambient ethanol pressure of 600 Pa. The film is approximately 6 μm thick. (b) Growth at an ethanol pressure of 800 Pa resulted in VA-SWNT films with thicknesses greater than of 20 μm . The scale bar applies to both images.

[1] Y. Murakami, S. Chiashi, Y. Miyauchi, M. Hu, M. Ogura, T. Okubo, and S. Maruyama, *Chem. Phys. Lett.* **385** (2004) 298.

[2] S. Maruyama, E. Einarsson, Y. Murakami, and T. Edamura, *Chem. Phys. Lett.* **403** (2005) 320.

[3] E. Einarsson, Y. Murakami, and S. Maruyama, in preparation.

Corresponding Author: S. Maruyama

TEL/FAX: +81-3-5800-6983, email: maruyama@photon.t.u-tokyo.ac.jp

Selective Oxidation of Semiconducting Single-Wall Carbon Nanotubes by Hydrogen Peroxide

○ Yasumitsu Miyata^{1,2}, Yutaka Maniwa^{1,3}, Hiromichi Kataura²

¹*Department of Physics, Tokyo Metropolitan University, 1-1 Minami-Osawa, Hachioji, Tokyo 192-0397, Japan*

²*Nanotechnology Research Institute (NRI), National Institute of Advanced Industrial Science and Technology (AIST), 1-1-1 Higashi, Tsukuba 305-8562, Japan*

³*CREST, Japan Science and Technology Corporation (JST), Japan*

Single-wall carbon nanotubes (SWCNTs) occur as both metal and semiconductor types. However as yet, none of the synthetic methods used to prepare SWCNTs are in fact selective towards the production of either pure metallic or pure semiconducting SWCNTs. This is a major drawback with regards to applications, where SWCNT purity is essential. For example, metallic SWCNTs are highly desired as nanometer-size conductors, while semiconducting SWCNTs are required as field effect transistors and saturable absorbers. As such, the selective purification of metallic and semiconducting SWCNTs represents a very important target.

Here, we report an optical study of SWCNTs oxidized in H₂O₂. Commercially available HiPco was purified and used as the starting material to obtain SWCNT samples, which were then oxidized in heated H₂O₂. From an analysis of the integrated intensity of the absorption bands of metallic and semiconducting SWCNTs, it was estimated that the concentration of metallic SWCNTs in the final product was higher than 80 %. The enrichment of metallic SWCNTs was not observed during oxidation in air. Absorption spectroscopy confirmed that SWCNTs were weakly doped with H₂O₂. It was suggested that the faster oxidation of semiconducting SWCNTs was due to its higher reactivity resulting from hole-doping by H₂O₂.

Corresponding Author: Hiromichi Kataura

E-mail: h-kataura@aist.go.jp

TEL: 029-861-2551, Fax: 029-861-2786

Growth of carbon nanotubes by RF-PECVD - Lowering of growth temperature by pretreatment of catalyst film -

○Takamichi Sakai¹, Atsushi Suzuki¹, Hideki Sato¹, Koichi Hata¹, Yahachi Saito²

¹*Department of Electrical and Electronic Engineering, Mie University
1577 Kurima-machiya-cho, Tsu 514-8507, Japan*

²*Graduate school of engineering, Nagoya University
Furo-cho, Chikusa-ku, Nagoya 464-8603, Japan*

A radio frequency plasma enhanced chemical vapor deposition (RF-PECVD) method is one of the most suitable growth method of CNTs for fabrication process of field emission displays (FEDs) because of possibilities for low temperature and large area CNTs growth. We have examined CNTs growth characteristics by the RF-PECVD method with an intent of controlling the growth of the CNTs for the FEDs application. In this paper, we show effects of granulation of the catalyst to temperature for CNTs growth.

CNTs were grown in an RF-PECVD apparatus with conventional planar type capacitively-coupled plasma source. A discharge frequency was 13.56MHz. Silicon (100) single crystal (10x10 mm²) on which catalyst iron (Fe) was deposited by vacuum evaporation was used as a substrate for CNTs growth. The thickness of catalyst iron was 3 nm. The process of CNTs growth consisted of two steps. First, the substrate was annealed as a pretreatment in a vacuum of about 4.0x10⁻³ Pa. The pretreatment temperature was 650°C. Second, plasma was generated in an atmosphere of CH₄ and H₂ and CNTs were grown on the substrate. Gases flow rates were 80 sccm for CH₄ and 20 sccm for H₂. Pressure during the CNTs growth was 67Pa. The growth temperature was varied from 650°C to 500°C. The CNTs grown on the substrates were observed by a scanning electron microscope (SEM) and a transmission electron microscope (TEM).

Fig.1 (a) is an SEM image of the surface on the substrate pretreated at 650°C. Formation of nanoparticles was confirmed. Fig.1 (b) and (c) are SEM images of CNTs grown at 550°C and 500°C after the pretreatment at 650°C, respectively. Both of the CNTs were multiwalled CNTs that had about 9 nm in average diameter. Thickness of CNTs layer grown at 550°C and 500°C were 4 μm and 400 nm, respectively. These results show that enough granulation of the catalyst is indispensable for the lowering of growth temperature of CNTs.

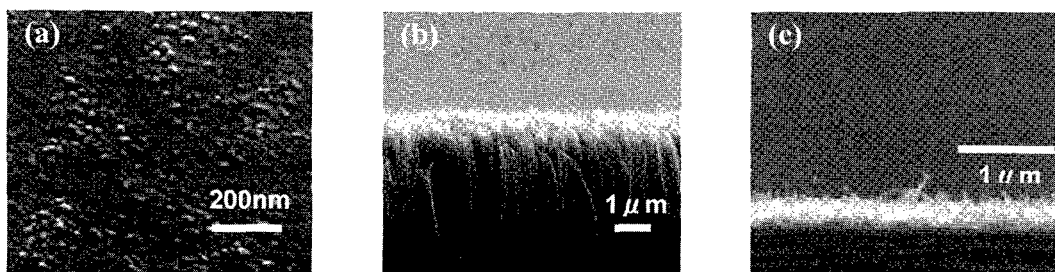


Fig.1 SEM images of (a) the surface on the substrate pretreated at 650°C, and the CNTs grown at (b) 550°C and (c) 500°C after the pretreatment at 650°C.

Corresponding Author: Takamichi Sakai

E-mail: t.sakai@elec.mie-u.ac.jp

Tel/Fax: +81-59-231-9404

Low-temperature growth of carbon nanotubes by alcohol CCVD

○Ken Hiasa¹, Tsuyoshi Nakagita¹, Hideki Sato¹, Koichi Hata¹, Yahachi Saito²

¹*Department of Electrical and Electronic Engineering, Mie University,
1577 Kurima-machiya-cho, Tsu 514-8507, Japan*

²*Department of Quantum Engineering, Nagoya University,
Furo-cho, Nagoya 464-8603, Japan*

Development of technique to synthesize carbon nanotubes (CNTs) directly onto substrate at low cost and at low temperature ($< 600^{\circ}\text{C}$) contributes to applications of CNTs to electronic device such as field emission displays (FEDs). We have found that it is possible to synthesize CNTs by alcohol catalyst chemical vapor deposition (ACCVD), which has recently attracted much attention as a simple growth method of CNTs, at lower temperature than that of conventional CCVD methods. In this study, we have examined dependence of CNTs growth on growth temperature under an intention to lower the growth temperature by alcohol CCVD.

An ACCVD system used in this study consisted of a gas introduction system, a mechanical vacuum pump and a quartz tube reactor heated by an electric furnace. Ethanol (purity: 99.5%) was used as carbon feedstock. A Co-Al bilayer film deposited by vacuum evaporation was employed as a catalyst film. Co was deposited onto Al film that was previously deposited onto a *p*-type silicon (100) wafer ($10 \times 10 \text{mm}^2$) as a buffer layer. Thickness of Co and Al film were 2nm and 20nm, respectively. Growths of CNTs were carried out under a pressure of 40Torr in an ethanol atmosphere. The growth time was 10 min.

Fig.1 shows cross sectional scanning electron microscope (SEM) images of CNTs synthesized at 450°C and 550°C . Thickness of CNTs layer for 450°C and 550°C are 170nm and 400nm, respectively. Observation of CNTs synthesized at 450°C by transmission electron microscope (TEM) showed that it was multi-walled carbon nanotube. These results show that it is possible to grow CNTs at temperature as low as 450°C by the alcohol CCVD.

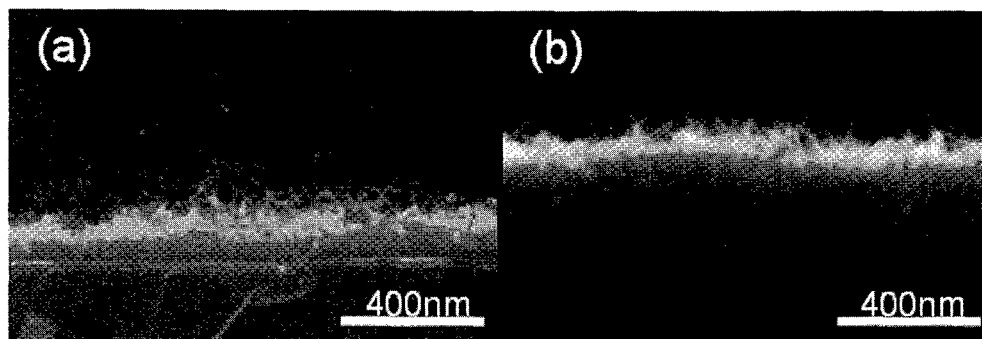


Fig.1 Cross sectional SEM images of CNTs layer grown at (a) 450 and (b) 550°C .

Corresponding Author: Ken Hiasa
E-mail : hiasa@elec.mie-u.ac.jp
Tel&Fax : +81-59-231-9404

Plasma sheath effects on the growth of freestanding individual single-walled carbon nanotubes

○ T. Kato¹, R. Hatakeyama¹, and K. Tohji²

¹Department of Electronic Engineering, Tohoku University, Sendai 980-8579, Japan

²Graduate School of Environmental Studies, Tohoku University, Sendai 980-8579, Japan

Recently, freestanding individual single-walled carbon nanotubes (SWNTs) were successfully produced on a silicon-based flat substrate, owing to a diffusion plasma-enhanced chemical vapor deposition (PECVD) method by our group [1]. This ultimate technique, three-dimensional alignment control of individual SWNTs, can provide huge opportunities to develop a new-type architecture for SWNT devices. In order to fully use potential abilities of this unique-shape SWNTs, however, a more precise control is inevitable on the part of tube structures such as tube-alignment, -electric property, -diameter, -length, and so on. For the purpose of overcoming the above-mentioned critical issue, roles of plasma sheath have quantitatively been discussed with detailed plasma measurements and simple calculations.

Figures 1(a) and (b) describe typical scanning electron microscope (SEM) and transmission electron microscope (TEM) images of the freestanding individual SWNTs produced with the diffusion PECVD method, respectively. Most all of tip parts of freestanding SWNTs vibrate intensely (Fig. 1(a)). The main diameter of SWNTs produced is around 3 nm, which is slightly larger than that of general SWNTs. According to simple calculations and Langmuir probe measurements, it is found that an electric field strength on the tip part of individual SWNT is above 1.2 V/ μm , which is strongly enhanced compared with a macro scale electric field (0.01V/ μm) owing to the unique shape of freestanding SWNTs (Fig. 1(c)). A comparison between thermal energy, which disturb tube alignment, and rotation energy caused by the plasma sheath electric field (Fig. 1(d)) provides a strong evidence that the plasma sheath electric field affects the freestanding alignment of individual SWNTs directly.

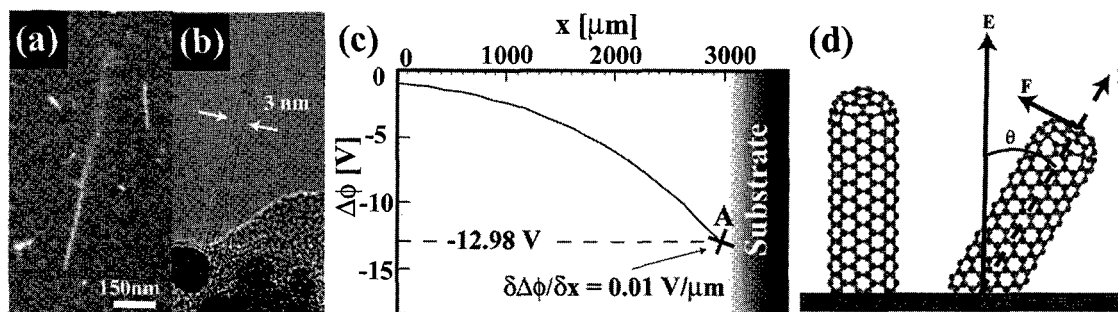


Fig.1 (a)SEM and (b)TEM images of freestanding SWNTs. (c) A potential profile in the plasma sheath calculated with Poisson's equation. (d) Schematic images of the individual SWNTs alignment. (E, P, and F describe a vector of electric field, a dipole, and a force, respectively. θ denote an angle between the tube and field.)

Reference: [1] T. Kato, et al., Abstracts of the 29th Fullerene-Nanotubes General Symposium, p. 10, 2005.
Corresponding: T. Kato, kato@plasma.ecei.tohoku.ac.jp, TEL: +81-22-795-7046, FAX: +81-22-263-9225

Synthesis and Purification of Double Walled Carbon Nanotubes

○ Kazuyo Matsumoto¹, Toshiya Murakami¹, Kenji Kisoda², Toshiyuki Isshiki¹,
and Hiroshi Harima¹

¹*Dept. Electronics and Information Science, Kyoto Institute of Technology, Kyoto 606-8585,
Japan*

²*Wakayama University, Wakayama 640-8510, Japan*

Chirality and wall numbers are both key factors determining physical properties of carbon nanotubes (CNTs). Double-walled carbon nanotubes (DWNTs) have advantages over single-walled nanotubes (SWNTs) in the mechanical toughness and chemical stability. Thin DWNTs show strong one-dimensional character like SWNTs. Motivated by such high potentials for future applications, we are aiming at establishing an efficient and selective growth method for thin DWNTs.

Here we report an experimental result focusing on post-purification processes for CNT products grown by chemical vapor deposition (CVD). Hexane was used for the carbon source with a combined catalyst of cobalt acetate, ammonium iron acetate and ammonium molybdate tetrahydrate supported in MgO power. The products were purified by oxidation in air and washing in acids, and characterized by Raman scattering and transmission electron microscopy (TEM). When the purification processes were optimized, two clear peaks were observed in Raman spectra (Fig.1) at around 160 and 300 cm^{-1} for the radial breathing mode. As depicted in a typical TEM image (Fig.2), the purified samples were dominated by DWNTs with outer- and inner-tube diameters of 1.3-1.6 and 0.7-1.0 nm, respectively, and the tube diameters had relatively narrow distributions.

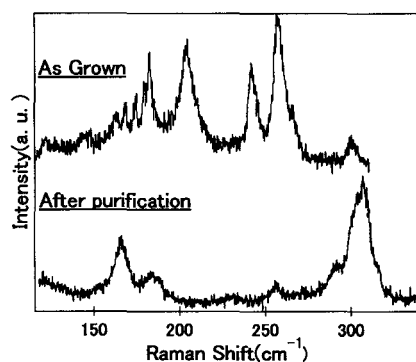


Fig.1 RBM spectra excited at 488.0nm

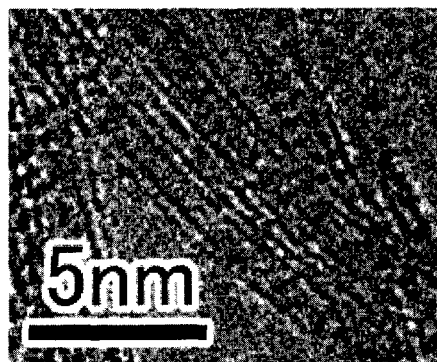


Fig.2 TEM image of DWNTs

Corresponding Author: Kazuyo Matsumoto

E-mail: dj010729@djedu.kit.ac.jp

The Effect of Intra-Pore Size of Porous Glass for the Preparation of Single-Wall Carbon Nanotubes

○Yosuke Aoki¹, Shinzo Suzuki¹, Hiromichi Kataura², Hiroshi Nagasawa³,
Hisao Abe⁴, and Yohji Achiba¹

¹*Department of Chemistry, Tokyo Metropolitan, Tokyo 192-0397, Japan*

²*Nanotechnology Research Institute, National Institute of Advanced Industrial Science and Technology (AIST), Central 4, Higashi 1-1-1, Tsukuba, Ibaraki 305-8562, Japan*

³*Life Science System Division, EBARA Corporation, 4-2-1 Honfujisawa, Fujisawa-shi, Kanagawa 251-8502, Japan*

⁴*Research and Development Section, Ceramics Research Center of Nagasaki, 605-2 Hiekoba-go, Hasami-cho, Higashisonogi-gun, Nagasaki 859-3726, Japan*

Last year, it was confirmed that single-wall carbon nanotubes (SWNTs) have been successfully prepared by applying alcohol-CCVD technique [1] utilizing porous glass (PG) as metal-supported material [2]. Since PG having several different inner-pore sizes can be easily obtained, by controlling the ambient temperature in the PG preparation process, it is interesting to see whether the formation process of SWNTs is influenced by the inner-pore size of PG having similar grain size.

In the previous investigation, it was recognized that SWNTs could be prepared by utilizing PG having ≤ 30 nm inner-pore size [3]. In this presentation, it is demonstrated that SWNTs can also be prepared by using PG having much larger inner-pore size (up to ~ 200 nm). Also, it was found that, as larger the inner-pore size of PG becomes, the reaction temperature giving the best yield of SWNTs shifts to the lower. Raman spectra of SWNTs obtained with ACCVD technique at the same ambient temperature by using PGs having larger inner-pore size indicate broader diameter distributions for them. The experimental findings of absorption and fluorescence spectroscopy for these SWNTs are presented and used for further discussion.

This study was partly supported by Industrial Technology Research Grant Program from New Energy and Industrial Technology Development Organization (NEDO) of JAPAN, and the Grants-in-Aid for Scientific Research (B) (No.16351104) from MEXT.

References:

- [1] S. Maruyama et al., *Chem. Phys. Lett.*, **360**, 229(2002). [2] Y. Aoki et al., *Chem. Lett.*, **562**, 34(2005).
[3] Y. Aoki, S. Suzuki, H. Kataura, Y. Achiba, H. Nagasawa and H. Abe, *Proceeding of the 3rd Annual Meeting of Society of Nano science and Technology*, PS4-53(2005).

Corresponding Author: Shinzo Suzuki

E-mail: suzuki-shinzo@c.metro-u.ac.jp, **Tel:** +82-426-77-2533, **Fax:** +81-426-77-2525

Influence of CH₄, C₂H₄, or C₂H₂ gas addition on the growth of SWNTs in H₂-Ar arc discharge

○T. Kitamura, X. Zhao, S. Inoue, and Y. Ando

21st COE Program “Nano Factory”, Department of Materials Science & Engineering,
Meijo University, Tenpaku-ku, Nagoya 468-8502, Japan

High-yield and high-crystallinity single-wall carbon nanotubes (SWNTs) have been mass-produced by a dc arc discharge evaporation of carbon anode containing 1at% Fe catalyst in H₂-Ar mixture gas¹⁾. H₂ gas selectively etches the amorphous carbon in the growth process of SWNTs by forming gaseous hydrocarbon. However, the yield of SWNT production, the ratio of the obtained SWNT mass to the evaporated anode mass, is only ~ 4%. In the present study, CH₄, C₂H₄, or C₂H₂ gas have been added into H₂-Ar mixture gas to improve the yield of SWNT production.

Figure 1 shows the Raman spectra of SWNTs prepared in H₂-Ar-1%CH₄ mixture gas, and a strong RBM peak at 189 cm⁻¹ and a weak RBM peak at 269 cm⁻¹ can be seen in the inset. The RBM peak at 269 cm⁻¹ comes from the SWNTs with 0.9 nm in diameter, and become stronger with the increase of partial pressure of CH₄ gas. Figure 2 shows the G/D ratio obtained from Raman spectra of SWNTs prepared in H₂-Ar-CH₄, H₂-Ar-C₂H₄, and H₂-Ar-C₂H₂ mixture gas. The addition of 1%CH₄ results in the highest G/D ratio, and it has been found that the yield of SWNT production increase 1% also. As increasing the partial pressure of CH₄ gas, a lot of carbon smoke takes place in the growth process of SWNTs, resulting in the quick decrease of G/D ratio. In the case of C₂H₄ or C₂H₂ gas, the G/D ratios with addition are always lower than that without addition of these gases. This may be due to their low bonding energy and low decomposition temperature.

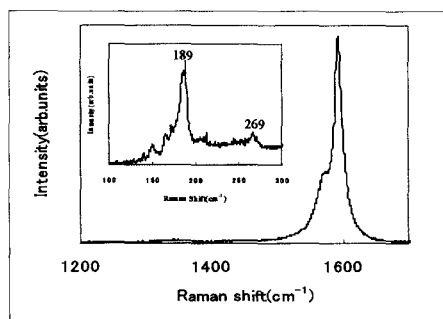


Fig. 1 Raman spectra of SWNTs

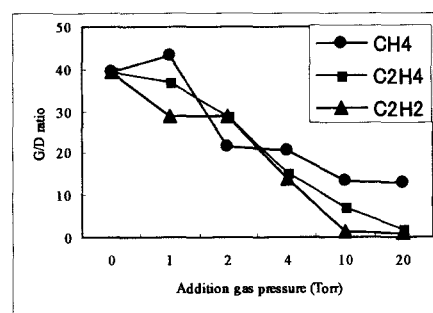


Fig. 2 G/D ratio from Raman spectra

Reference

1) X. Zhao *et al.*, *Chem. Phys. Lett.*, **373** (2003) 266.

Corresponding Author: T. Kitamura (E-mail: toshi119@rg8.so-net.ne.jp)

Selective Encapsulation of Dimetallofullerene into Single-Wall Carbon nanotubes

OM. Ishida¹, D. Nishide¹, T. Inoue¹, R. Kitaura^{1,2}, T. Sugai^{1,2}, H. Shinohara^{1,2}¹Department of Chemistry, Nagoya University, Nagoya 464-8602, Japan²Institute for Advanced Research, Nagoya University, Nagoya 464-8602, Japan

It is well known theoretically [1] and experimentally [2] that the dispersion and small electrostatic interactions occurs between single-wall carbon nanotubes (SWNTs) and fullerenes inside peapods. Furthermore, the electronic charge upon fullerene cages will affect the encapsulation yield of peapods. To obtain information on the encapsulation mechanism, we have prepared the peapods using the mixture of two metallofullerenes and tried to estimate the encapsulation yield of each metallofullerenes.

A schematic view of peapods synthesis is shown in Figure 1. Using this doping method, one can simultaneously estimate the sublimation quantity and encapsulation yield of each metallofullerenes. The metallofullerenes, Dy₂C₂@C₈₂ and Gd@C₈₂, were used for peapods synthesis, in which their electronic charges of each fullerene cages are known to be C₈₂⁶⁻ and C₈₂³⁻, respectively. Peapods were prepared by the vacuum sublimation method [3]. An ampoule was evacuated to 1.0×10^{-5} Torr and then vacuum sealed. The sealed ampoule was heated at 773 K for 2 days in a furnace. The ampoule was cooled down to room temperature. An energy dispersive x-ray (EDS) spectrometer was used for characterizing the encapsulated metal atoms.

Figure 2 shows EDS spectra of peapods and sublimed fullerenes. In the capillary, each metallofullerenes exists almost at the same ratio. On the other hand, the EDS spectrum of peapods indicates that Dy₂C₂@C₈₂ has encapsulated into SWNTs more efficiently than Gd@C₈₂. This strongly suggests that encapsulation yield of mixed-peapods strongly depends on the charge state of metallofullerenes.

References:

- [1] S. Okada et al., Phys. Rev. Lett. **86**, 3835 (2001)
 [2] D. J. Hornbaker et al., Science **295**, 828 (2002)
 [3] H. Hirahara et al. Phys. Rev. Lett. **85**, 5384 (2001)

Corresponding Author: Hisanori Shinohara
 E-mail: noris@cc.nagoya-u.ac.jp
 Tel: +81-52-789-2482 Fax: +81-052-789-1169

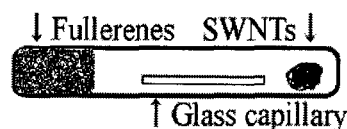


Figure 1. Schematic view of mixed-peapods synthesis.

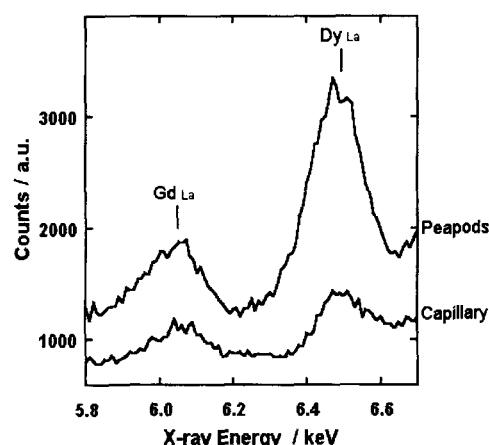


Figure 2. The EDS spectra of peapods and fullerenes inside capillary.

Incorporation and release of C₆₀ in/from single-wall carbon nanotubes with large diameters

○ J. Fan¹, M. Yudasaka^{1,2}, R. Yuge², D.N. Futaba³, K. Hata³, S. Iijima^{1,4}

¹*SORST, Japan Science and Technology Agency, c/o NEC, 34 Miyukigaoka, Tsukuba, Ibaraki 305-8501, Japan*

²*NEC Corporation, 34 Miyukigaoka, Tsukuba, Ibaraki 305-8501, Japan*

³*Research Center for Advanced Carbon Materials, National Institute of Advanced Industrial Science and Technology (AIST), 1-1-1 Higashi, Tsukuba, Ibaraki 305-8501, Japan*

⁴*Meijo University, 1-501 Shiogamaguchi, Tenpaku-ku, Nagoya, Aichi 468-8502, Japan*

Aiming to use single-wall carbon nanotubes (SWNTs) as carriers of biological materials, the biological materials are attached to the outside walls of SWNTs through physical interactions or chemical reactions. By incorporating the biological materials inside the SWNTs, the functions of SWNTs as the carriers will be broadened. Various biological materials have large sizes, therefore the SWNTs with large diameters are useful as the carriers. Since not much is known about the incorporation and release of materials in/from large-diameter SWNTs, we studied it with C₆₀ and the results are introduced in this report.

The super-growth SWNTs were synthesized by water-assisted CVD [1]. The holes were opened by heating up to 550°C with a rising rate of 1°C/min in dry air [2]. The methods of incorporation and release of C₆₀ in/from SWNTs were the same with those reported previously [3]. As a result, we found that the number of C₆₀-encapsulating SWNTs was large when the tube diameter was 5 nm or less. Sometimes the C₆₀ molecules aligned on a line along the edges inside thick nanotubes, which would mean that the thick tubes were sometimes flattened. The released quantity of C₆₀ was about 60% in toluene-ethanol (4:1 in weight). SWNTs with diameters in a range of 3 to 5 nm released more C₆₀ than other diameter distributions. We infer that the stability of C₆₀ inside thick tubes is less than in the thin tubes because the stability of C₆₀ inside thick tubes would be gained through small contact areas of C₆₀-C₆₀ and/or C₆₀-wall by taking multi-helical arrangements [4] and others.

[1] K. Hata et al, *Science* 2004, 306, 1362.

[2] J. Fan et al, *J. Phys. Chem. B* to be published.

[3] R. Yuge et al, *J. Phys. Chem. B* 2005, 109, 17861.

[4] K. S. Troche et al, *Nano Lett.* 2005, 5, 349.

Corresponding author: Masako Yudasaka

E-mail: yudasaka@frl.ci.nec.co.jp

Tel: +81-29-856-1940, Fax: +81-29-850-1366.

***In vivo* magnetic resonance imaging of single-wall carbon nanohorns through labeling with magnetite nanoparticles**

○Jin Miyawaki,¹ Masako Yudasaka,^{1,2} Hideto Imai,² Hideki Yorimitsu,³
Hiroyuki Isobe,³ Eiichi Nakamura³ and Sumio Iijima^{1,2}

¹*JST/SORST, c/o NEC, 34 Miyukigaoka, Tsukuba, Ibaraki 305-8501, Japan*

²*NEC, 34 Miyukigaoka, Tsukuba, Ibaraki 305-8501, Japan*

³*The University of Tokyo, Hongo, Bunkyo, Tokyo 113-0033, Japan*

Aggregate size (ca. 100 nm) of single-wall carbon nanohorns (SWNHs) [1] corresponds to a condition for passive targeting toward cancer tumors by the enhanced permeability and retention (EPR) effect [2]. Moreover, *in vitro* studies have demonstrated low/non-cytotoxicity of SWNHs and their capabilities for drug incorporation and release [3, 4]. Therefore, SWNHs are one of candidates for drug carriers in cancer therapy. Further development on biomedical applications of SWNHs and assessment of their toxicological hazards in living body, however, require non-anatomical *in vivo* observation of their motions and accumulative behaviors. Here, we show our success of *in vivo* magnetic resonance imaging (MRI) of SWNHs through attaching superparamagnetic magnetite, a MRI contrast agent.

Attachment of nanoparticles (6 nm in diameter) of superparamagnetic magnetite to SWNHs was achieved through a deposition of iron acetate clusters on hole-opened SWNHs (oxNHs) in ethanol at room temperature, followed by heat-treatment at 400°C in Ar. *In vivo* MRI visualized that when magnetically labeled oxNHs were administered into mouse via tail vein, they accumulated in the spleen and kidneys. Histopathological examinations supported the MRI results. The simple magnetite-attaching method would be applicable to any kind of carbon nanotubes, thus should facilitate the toxicity assessment of nanotubes and their applications in bioscience and biotechnology.

Acknowledgement: We thank Dr. T. Azami and Dr. D. Kasuya for preparing NHs, and Varian Technologies Japan Ltd. and BioView Co. for the NMR measurements and MRI observations.

References: [1] S. Iijima, et al., *Chem. Phys. Lett.*, **309**, 165 (1999). [2] H. Maeda, et al., *Bioconjugate Chem.*, **3**, 351 (1992). [3] T. Murakami, et al., *Mol. Pharm.*, **1**, 399 (2004). [4] K. Ajima, et al., *Mol. Pharm.*, in press.

Corresponding authors: Jin Miyawaki and Masako Yudasaka **E-mail:** jin_m@frl.cl.nec.co.jp (Miyawaki), yudasaka@frl.cl.nec.co.jp (Yudasaka) **Tel:** +81-29-856-1940 **Fax:** +81-29-850-1366

Structure of hole edges of single-wall carbon nanohorns and its influence on cisplatin release

○ Kumiko Ajima¹, Masako Yudasaka^{1,2} Alan Maigné¹, Jin Miyawaki¹ & Sumio Iijima^{1,2,3}

¹ SORST-JST, c/o NEC 34 Miyukigaoka, Tsukuba, Ibaraki 305-850, Japan

² NEC, 34 Miyukigaoka, Tsukuba, Ibaraki 305-850, Japan

³ Meijo University, 1-501 Shiogamaguchi, Tenpaku-ku, Nagoya 468-8502, Japan

We have been studying applications of single-wall carbon nanohorns (SWNHs) to drug delivery systems, and previously showed that the incorporation of drugs and release are possible [1, 2]. Effects of the released drugs were also confirmed in vitro assays [1, 2]. Recently, we found that the release sometimes became extremely slow, or even stopped on the way. We clarified its reasons which are introduced in this report.

We incorporated cisplatin (CDDP) inside SWNHs in dimethyl formamide and studied the CDDP release from SWNHs in PBS [2]. The CDDP@NHh could release 70% of CDDP in PBS, while CDDP@NHox released only about 15% [3]. Here, NHh denotes SWNH having holes with hydrogen-terminated edges [4], and NHox denotes that having holes with oxygen-containing functional groups (NHox). To find reasons why the release was stopped at 15% for CDDP@NHox, we carried out the studies shown below.

CDDP@NHh and CDDP@NHox had similar structures, and both contained same amount (18 weight %) of CDDP. CDDP structure was kept in both CDDP@NHh and CDDP@NHox. Therefore we thought the stopping of the CDDP release from NHox was caused certain actions of PBS on CDDP@NHox. To clarify the certain actions, we treated NHh and NHox with PBS (PBS-NHh, PBS-NHox). Their TGA showed that the combustion temperature of PBS-NHox decreased by about 160°C, but not that of PBS-NHh. According to our previous report, this combustion-temperature decrease is due to the chemical structure changes of the functional groups at the holes edges of NHox [4]. We believe that the chemical structure changes of the hole edges of NHox brought by PBS was the major reason for the CDDP-release from NHox stopping at 15%, which will be discussed in detail in the talks.

Acknowledgement: We thank Dr. T. Azami and Dr. D. Kasuya for preparing single-wall carbon nanohorns.

References : 1) T. Murakami, et al. *Mol. Pharmaceutics*, **1**, 399 (2004). 2) K. Ajima, et al. *Mol. Pharmaceutics*, in press (2005). 3) K. Ajima, et al. *The 29th Fullerene-Nanotubes General Symposium*, 2P-44 (2005). 4) J. Miyawaki, et al. *J. Phys. Chem. B* **108**, 10732 (2004).

Corresponding author: Kumiko Ajima, Masako Yudasaka

E-mail: kumikoajima@frl.cl.nec.co.jp, yudasaka@frl.cl.nec.co.jp

Tel: +81-(0)29-856-1940, **Fax:** +81-(0)29-850-1366.

Phonon transport in finite length SWNTs using molecular dynamics simulations

○Junichiro Shiomi and Shigeo Maruyama

*Department of Mechanical Engineering, The University of Tokyo
7-3-1 Hongo, Bunkyo-ku, Tokyo 113-8656, Japan*

Single-walled carbon nanotubes (SWNTs) are expected to possess high thermal conductivity due to their quasi-one-dimensional structure and strong carbon bonds [1]. While experimental attempts to characterize heat conduction of SWNT encounter technical difficulties, the classical molecular dynamics (MD) simulations hold advantage as the heat conduction is phonon-dominated. MD simulations give us access to detail properties such as length dependence of thermal conductivity. Furthermore, by analyzing temporal evolution of spatio-temporal spectra by performing the wavelet transform or the short time Fourier transform, one can probe dynamics of individual phonon modes and their contribution to the overall heat conduction.

Our early MD studies showed the power-law length dependence of SWNT thermal conductivity up to sub-micrometers length [2]. This has been discussed in relation with the one-dimensional heat conduction where theoretical models exhibit divergence of the thermal conductivity with respect to the tube length [3]. Here, we report our recent results of the simulation covering larger range of nanotube length and with longer sampling time. Results indicate that thermal conductivity is likely to converge where the length dependence falls off from the power law at the nanotube length of the order of a micrometer. The results, together with the observation of detailed phonon dynamics, will be compared with available studies of phonon transport equations. The detail pictures of the phonon transport can be probed by exciting heat pulse or wave packet and tracing their propagation. For finite length SWNTs, phonon dependent contributions to the heat conduction are investigated in terms of transport properties of phonon modes in the key branches.

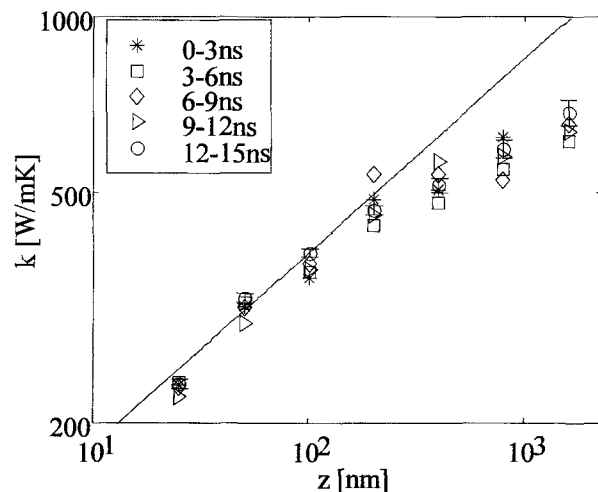


Fig. 1 The length dependence of thermal conductivity of finite length (5,5)-SWNTs. Different marks denotes the sampling intervals. The solid line indicates the power-law relation, $k \propto L^{1/3}$.

[1]. S. Berber, *et.al.*, *Phys. Rev. Lett.* **84**, (2000) 4613.

[2]. S. Maruyama, *et.al.*, *Micro. Therm. Eng.* **7**, (2003) 41

[3]. R. Livi and S. Lepri, *Nature* **421**, (2003) 327

Corresponding Author: Shigeo Maruyama

E-mail: maruyama@photon.t.u-tokyo.ac.jp,

Tel/Fax: +81-3-5800-6983

Kataura plot based on GWA graphene dispersion

○Mototeru Oba¹⁾, Susumu Okada²⁾, Takashi Miyake³⁾, and Shigeo Maruyama¹⁾

1) Department of Mechanical Engineering, The University of Tokyo
7-3-1 Hongo, Bunkyo-ku, Tokyo 113-8656, Japan

2) Institute of Physics and Center for Computational Sciences, University of Tsukuba
1-1-1 Tennodai, Tsukuba 305-8751, Japan

3) Department of Physics, Tokyo Institute of Technology
2-12-1 Oh-okayama, Meguro-ku, Tokyo 152-8551, Japan

Peaks of joint density of states (JDOS) of single-walled carbon nanotubes (SWNTs) plotted against diameter is called Kataura plot [1] and conveniently used for interpretation of resonant Raman scatterings, optical absorption and fluorescence spectroscopy.

There are two ways to calculate the plot: one is to calculate SWNT energy band directly; another is to use zone-folding approximation to the calculated energy band of a graphene sheet. Since the former is too heavy to calculate with *ab-initio* calculation such as local density approximation (LDA) and GW approximation (GWA), a comprehensive technique to compensate the curvature effect on zone-folding method (Fig. 1) is desired.

Here, Kataura plot calculated from geometry optimized nanotube structure was compared with the simple zone-folding approximation within Hamada-TB [2] level as in Fig. 2. After the full understanding of geometry effect and deviation of compensation function, this compensation function was applied to the dispersion relation of graphene calculated with GWA.

[1] H.Kataura et al., Synth. Met. 103 (1999) 2555.

[2] N.Hamada et al., Phys. Rev. Lett. 68 (1992) 1579.

Corresponding Author: Shigeo Maruyama

E-mail: maruyama@photon.t.u-tokyo.ac.jp,

Tel/Fax: +81-3-5800-6983

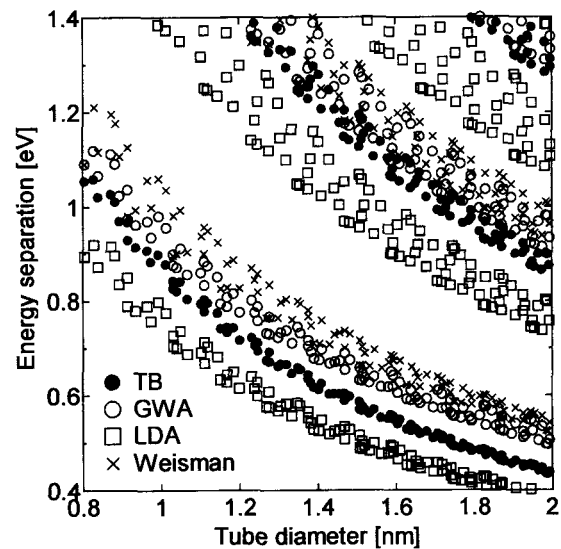


Fig. 1 Kataura plot from zone-folding of graphene with GWA, LDA, TB models.

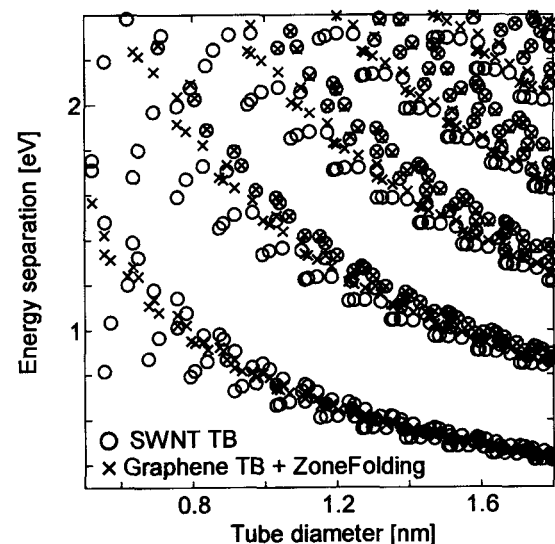


Fig. 2 Curvature effect in Kataura plot examined by Hamada-TB level.

AFM Evaluation on Suspended Carbon Nanotubes

○Shota Kuwahara¹, Toshiki Sugai¹ and Hisanori Shinohara^{1,2,3}

¹Department of Chemistry, Nagoya University, Nagoya 464-8602, Japan

²Institute for Advanced Research, Nagoya University, Nagoya 464-8602, Japan

³CREST, Japan Science and Technology Agency, c/o Department of Chemistry, Nagoya University, Nagoya 464-8602, Japan

Optical characterization with absorption and emission of suspended carbon nanotubes has shown remarkable progress on evaluating structural and electronic properties of nanotubes. These optical properties have been believed to come from individually isolated nanotubes without any experimental evidence. To study and evaluate properties of the suspended nanotubes, such as numbers of nanotubes in each bundle and bundle concentration, we have developed a new spray technique coupled with AFM observations. With this technique, the number density of nanotube bundles is evaluated through sonication and centrifugal sedimentation processes coupled with optical characterization.

SWNTs of purified HiPco were dispersed in aqueous sodium dodecyl sulfate (SDS) surfactant [1 wt %] with bath sonicator (sample 1). The resulting suspension was then treated in a probe-tip ultrasonicator (SONIFIER 250) for 30 min (sample 2). After sonication, the sample was centrifuged (HITACHI CS100GXL) at 197,000g for 1 hour (sample 3) [1]. These samples were observed by AFM (Veeco Digital Instruments NanoscopeIV), absorption spectroscopy (JASCO V-570) and spectrofluorometer (SHIMADZU). AFM samples were prepared by the spray technique with the suspension.

The AFM images show nanotube bundles together with uniform thin layers of SDS with the height of 2-3 nm. The ratio between observed amounts of SDS and that of nanotubes show the number density of nanotube bundles in the suspension using the concentration of SDS. Figure 1 shows that the number density increases as the sonication power is increasing from sample No. 1 to No. 2 suggesting debundling thick bundles into individual nanotubes. The results also show that ultracentrifugal sedimentation from No. 2 to No. 3 changes the density to half of its original. With co-observed height and length distribution and optical observation, further analyses on absorption and emission cross section of the suspension and their dependence on the bundle size are in progress.

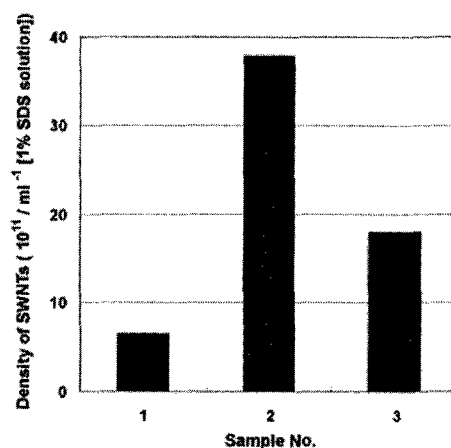


Figure 1: Changes of Density of carbon nanotubes in SDS solutions about each sample.

References:

[1] M. J. O'Connell, et al.: *Science* 297 593 (2002).

Corresponding Author: Hisanori Shinohara

E-mail: noris@cc.nagoya-u.ac.jp

TEL: +81-52-789-2482, FAX: +81-52-789-1169

Single-Walled Carbon Nanotubes Studied by Tip-enhanced Near-field Raman Spectroscopy

○ Yuika Saito¹, Takashi Murakami^{1,2}, Norihiko Hayazawa¹, Hiromichi Kataura³
and Satoshi Kawata^{1,4}

¹*RIKEN (Institute of Physical and Chemical research), Wako, Saitama 351-0198, Japan*

²*Department of Physics, Gakushuin University, Mejiro, Toshima-ku, Tokyo 171-8588, Japan*

³*National Institute of Advanced Science and Technology (AIST), Nanotechnology Research Institute, Tsukuba, 305-8562, Japan*

⁴*Department of Applied Physics, Osaka University, Suita, Osaka 565-0871, Japan*

Raman scattering from molecules adsorbed on metallic nanostructures is strongly enhanced due to excitation of localized surface plasmon polaritons. This phenomenon is known as surface enhanced Raman scattering (SERS). Even a single metallic nanostructure, e.g. metallic needle tip, can induce SERS at its apex, which is called tip-enhanced near-field Raman scattering (TERS). TERS provides detailed chemical information in nanometer scale and is a suitable tool for characterization of carbon nanotubes.

We investigate the polarization property in tip-enhanced Raman spectroscopy by employing a radial plate consisting of four divided half-wave plates each with a different orientation of the slow axis. The radial plate provides both longitudinal (parallel to the tip axis) and lateral (perpendicular to the tip axis) polarization of the electric field on the sample plane by selecting the proper polarization of the incident field. Single-walled carbon nanotubes are investigated with this polarization control. The radial breathing mode (RBM) and the G-band, which belong to different vibrational symmetries, show opposite polarization dependences. We will also report the investigation of the polarization selectivity of the tip-enhanced efficiency within the G-band.

Until now, almost all TERS spectroscopy has been operated in transmission mode because of experimental confinement. However, the transmission configuration cannot afford opaque or thick samples whereas reflection mode can. We have successfully measured TERS in reflection-mode. In this system, both illumination of incident laser and collection of Raman signals are performed from upward through long working distance objective lens that can be applied for any substrates. We will also demonstrate TERS results on silicon substrates.

Corresponding Author: Yuika Saito

E-mail: yuika@riken.jp

Tel: 048-467-9339, Fax: 048-462-4653

The feature of the Breit-Wigner-Fano Raman line in DNA-wrapped single-wall carbon nanotubes

○Hironori Kawamoto, Takashi Uchida, Masaru Tachibana and Kenichi Kojima

Graduate School of Integrated Science, Yokohama City University, 22-2 Seto, Kanazawa-ku, Yokohama 236-0027 Japan

Breit-Wigner-Fano (BWF) Raman line in DNA-wrapped single-wall carbon nanotubes (SWNTs) was investigated. For as-produced HiPco SWNT bundles, the asymmetric profile of BWF line is clearly observed with an excitation energy of 2.33 eV (Fig.1a). The asymmetric feature almost disappears in isolated HiPco SWNTs by DNA wrapping in aqueous solution (Fig.1b). The change provides evidence that the asymmetric feature of BWF line is attributed to the bundling effect of SWNTs. In addition, the asymmetric feature of BWF line strongly appears when the DNA-wrapped SWNTs are exposed to air. This means that the rebundling in the DNA-wrapped SWNTs can occur due to drying. According to the change of BWF line, the debundling and rebundling of DNA-wrapped SWNTs can occur due to hydrating and drying, respectively. Such reversible feature of DNA-wrapped SWNTs suggests that they are promising materials for biosensors and drug delivery devices.

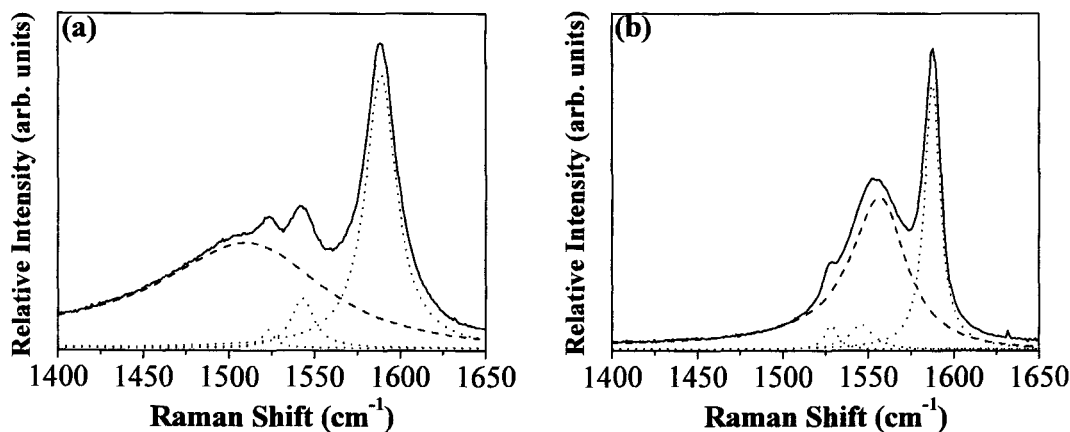


Fig. 1 TM bands in typical Raman spectra for (a) as-produced HiPco SWNT bundles, and (b) DNA-wrapped HiPco SWNTs in aqueous solution, taken with an excitation energy of 2.33 eV (532 nm) at 296 K. The TM band was fitted with three Lorentzian (dotted) lines and one BWF (dashed) line.

Corresponding Author: Masaru Tachibana

E-mail: tachiban@yokohama-cu.ac.jp

Tel: +81-45-787-2307, Fax: +81-45-787-2307

Band-gap modulation of semiconductive single-walled carbon nanotube in micellar solution by addition of viologens

○Koji Matsuura,^{1,2} Takeshi Saito¹, Toshiya Okazaki^{1,3}, Satoshi Ohshima¹,
Motoo Yumura¹ and Sumio Iijima¹

¹ *Research Center for Advanced Carbon Materials, National Institute of Advanced Industrial Science and Technology, Tsukuba, 305-8565*

² *Japan Fine Ceramics Center*

³ *CREST, Japan Science Technology Corporation*

Semiconductive single-walled carbon nanotube (sSWCNT) can be a macromolecular probe for environment of coating materials by detecting its band-gap modulation (BGM). By insertion of charged and non-charged organic molecules to w/w 1% sodium dodecyl sulfonate (SDS) micelle, the BGM were investigated by absorption and photoluminescence (PL) spectroscopies. Uniform red-shifts were observed in the absorption spectra of (d) phenyl viologen (PV^{2+}) and (e) methyl viologen (MV^{2+}) (Figure 1), while the significant shifts were not induced by addition of non-charged (b) 4,4'-dimethylbiphenyl and (c) 6,6'-bi-3-picoline. We consider that the larger red-shift in MV^{2+} addition than PV^{2+} is due to the amounts of the viologens inserted to the hydrophobic domain of SDS micelle. In PL mappings after addition of the viologens, E_{11} emissions of both type I and II¹ sSWCNTs were uniformly red-shifted. These phenomena would be explained to hole-doping effect by insertion of the cationic viologens to SDS micelles, not by matrix-imposed stress-induction. The detail PL results and electronic structures of sSWCNTs will be discussed at the meeting.

¹Type I and II are defined by $\text{mod}(2n+m, 3) = 1$ and 2, respectively.

Corresponding Author Koji Matsuura

E-mail koji-matsuura@aist.go.jp

Tel: +81-29-861-4654;

Fax: +81-29-861-4851

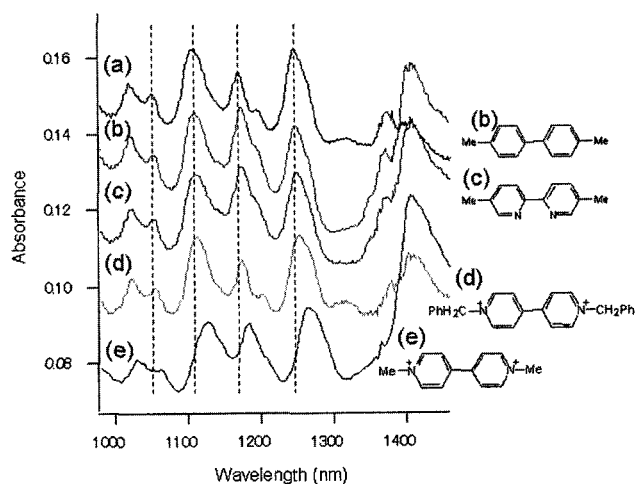


Figure 1. Absorption spectrum of sSWCNTs in (a) w/w 1% SDS micellar dispersion. Spectra (b) ~ (e) are after addition of the organic molecules shown in this figure. The peaks are attributed to semiconductive E_{11} transitions.

Theoretical Current-Voltage Characteristics of Finite-Length Carbon Nanotube between Silicon(111) Electrodes

○Yoshikazu Kobayashi¹⁾, Shigekazu Ohmori²⁾,
Hiroyuki Fueno^{1,3)}, and Kazuyoshi Tanaka^{1,3)}

¹⁾*Department of Molecular Engineering, Graduate School of Engineering, Kyoto University,
Kyoto, 615-8510, Japan*

²⁾*Venture Business Laboratory, Kyoto University, Kyoto, 606-8501, Japan*

³⁾*CREST, Japan Science and Technology Agency (JST), Japan*

Since the discovery of electronic transport property of carbon nanotube (CNT), a large number of studies have been carried out toward its application to many fields. In particular, CNTs have been attracting much attention for making molecular devices, since CNTs are expected to give a high-speed transistor due to ballistic conduction. Recently, it has been suggested that individual metallic single-walled CNT (SWCNT) with tunneling barriers resulting from division into short nanotube sections can be used for the single-electron transistor (SET) [1] and that SWCNT functionalized with hydrogen on the side wall can be expected as a quantum dot [2].

On this background, here we investigated current-voltage (I - V) characteristics of (a) CNT (6,6) wire and (b) CNT (6,6) wire functionalized with hydrogen sandwiched between silicon electrodes with Si(111) surface. The transmission spectrum was computed using TranSIESTA-C program package [4]. In TranSIESTA-C, the charge density distribution is calculated with density functional theory (DFT). Effect of the finite bias is taken into account using non-equilibrium Green's function (NEGF) method [3]. I - V characteristics was obtained from the transmission spectrum using the Landauer-Büttiker formula [3].

In the presentation, we will report quantum phenomena such as Coulomb blockade in the system (b). Moreover, we will compare I - V characteristics of the system (a) with that of the system (b).

References:

[1] H. W. Ch. Postma et al., *Science*, **293**, 76 (2001).

[2] K. Sueishi et al., *Abst. 28th Fullerene-Nanotube General Symposium*, **28**, 131 (2004).

[3] S. Datta, *Electronic Transport in Mesoscopic Systems* (Cambridge University Press, New York, 1996).

[4] M. Brandbyge et al., *Phys. Rev. B* **65** 165401 (2002).

Corresponding Author: Yoshikazu Kobayashi

Email: yoshikazu@bunnshikout17.mbox.media.kyoto-u.ac.jp

Tel: +81-75-383-2551 &FAX: +81-75-383-2556

Photon-Induced Damage Creation in Carbon Nanotubes

○ Satoru Suzuki, Fumihiko Maeda, Yoshihiro Kobayashi

*NTT Basic Research Laboratories, NTT Corporation, Atsugi, Kanagawa 243-0198
CREST, JST*

Our previous studies have shown that low-acceleration-voltage electron irradiation inevitably damages single-walled carbon nanotubes (SWNTs) [1]. This phenomenon can also be utilized for spatially selective removal of SWNTs [2], conversion of electric property of a SWNT-FET from metallic to semiconducting [3], and making a SWNT insulating [4]. Here, we show that SWNTs are also damaged by low-energy photon irradiation in an ultra-high vacuum.

SWNTs grown by the ethanol-CVD method were exposed to white light in an ultra-high vacuum at beamline ABL-3B in the synchrotron radiation facility of the NTT Atsugi R&D Center. The photon energies were dispersed in a wide energy range of the vacuum-ultra-violet region, but they were mostly below 1 keV. The irradiation dose was estimated to be of the order of 10^{20} /cm².

The light irradiation drastically decreased G-band intensity in the Raman spectrum of the SWNTs, as shown in Fig. 1. This result is very similar to those obtained when SWNTs are irradiated by low-acceleration-voltage electrons, and indicate that the SWNTs are heavily damaged. It also strongly suggests that the low-energy photon and electron irradiation damage occurs without assistance of gases in the circumference.

References:

- [1] S. Suzuki et al., *Jpn. J. Appl. Phys.* 43 (2004) L1118.
- [2] S. Suzuki et al., *Jpn. J. Appl. Phys.* 44 (2005) L113.
- [3] A. Vijayaraghavan et al., *Nano Lett.* 5 (2005) 1575.
- [4] S. Suzuki et al., *Jpn. J. Appl. Phys.* 44 (2005) in press.

Corresponding Author: Satoru Suzuki

E-mail: ssuzuki@will.brl.ntt.co.jp

Tel: +81-46-240-3632

Fax: +81-46-240-4711

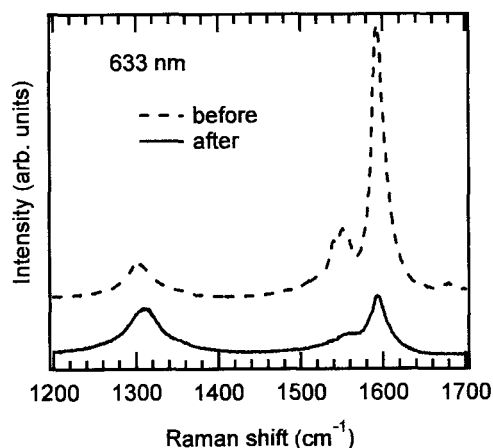


Fig. 1. Raman spectra of the SWNTs before and after the synchrotron radiation light irradiation.

Chemical Modification of Multi-walled Carbon Nanotubes (MWNTs) by Vacuum Ultra-violet (VUV) Irradiation Dry Process

○Koji Asano^{1,2}, Daiyu Kondo³, Akio Kawabata³, Fumio Takei⁴,
Mizuhisa Nihei³ and Yuji Awano^{1,2}

¹Fujitsu Limited, Atsugi, 243-0197 Japan, ²CREST/JST,

³Nanotechnology Research Center, Fujitsu Laboratories Ltd, Atsugi, 243-0197 Japan

⁴Fujitsu Laboratories Ltd, Atsugi, 243-0197 Japan

Controlled chemical modification of the sidewalls of CNTs is one of the most fundamental technologies for device applications, such as transistors, sensors, and so forth [1,2]. There are few reports on the dry process for chemical modification, although a dry process has many advantages compared to a wet process because of its controllability of aggregation. Mawhinney [3] and Cai [4] reported that the oxidation of single-walled carbon nanotubes (SWNTs) in an ozone or UV/O₃ reaction produced a series of oxygenated groups. However, they did not estimate the amount of functional groups quantitatively.

We have developed a fast dry oxidation process for CVD grown multi-walled carbon nanotubes (MWNTs) using VUV (Vacuum Ultra Violet light ($\lambda = 172\text{nm}$)) irradiation. We introduced carboxyl groups as many as 3% of the carbon atoms within one minute at room temperature as shown in Fig.1. The MWNTs with the carboxyl groups were analyzed by attenuated total reflection (ATR) FT-IR, transmission electron microscopy, and x-ray photoemission spectroscopy. The attachment of the carboxyl groups was further confirmed by reacting ferritin molecules with the MWNTs.

We believe that active oxidizing species such as singlet oxygen are related to the high-speed mechanism in the reaction system. **References:**

- [1] K. Matsumoto et. al., JJAP, (2003), 42,2415
- [2] M. Nihei et. al, Proc. of IEEE/IITC, 234 (2005)
- [3] D.B. Mawhinney et. al, CPL, (2000), 324, 213
- [4] L.Cai et al, Chem. Mater., (2002), 14, 4235

Corresponding Author: Yuji Awano

E-mail: y.awano@jp.fujitsu.com

Tel&Fax: +81-46-250-8234 (Fax: 8844)

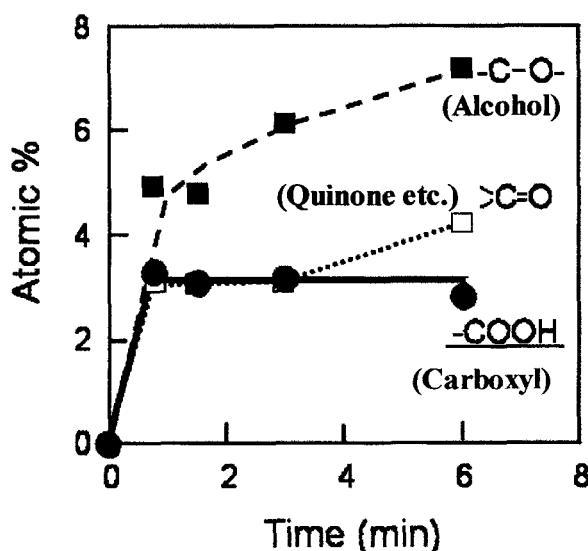


Fig.1 Reaction time dependence of 'Dry Oxidation'

Fabrication of antigen sensor using carbon nanotube FETs

○K. Tani¹, H. Ito², Y. Ohno¹, S. Kishimoto¹, M. Okochi², H. Honda², and T. Mizutani¹

¹Dept. of Quantum Eng., Nagoya University, Furo-cho, Chikusa-ku, Nagoya 464-8603, Japan

²Dept. of Chemical Eng. and Biotech., Nagoya Univ., Furo-cho, Chikusa-ku, Nagoya
464-8603, Japan

Carbon nanotube (CNT) FETs have attracted much attention for a variety of applications. Recently, the CNT biosensors have been reported [1,2]. However, the sensors have the problem of exposing the electrodes directly to the solution. In this study, we have fabricated the CNT-FETs, in which the contact electrodes are covered with insulator, and studied the effects of the antibody-antigen reaction on the drain current.

Figure 1 shows an SEM image and a schematic cross section of the CNT sensor we fabricated. The open window on the CNT is used for the detection of antibody-antigen reaction. By this structure, it is possible to avoid the problem of exposing electrodes directly to phosphate buffered saline (PBS) solution. Figure 2 shows the time dependence of the drain current of the CNT-FET. The current oscillation was caused by the periodic adding of the water. This is probably due to the change in the pH of the solution. The base line of the oscillation decreased when the PBS with antigen (10 mg/ml) was added in the solution. This probably reflects the antibody-antigen reaction suggesting the possibility of the CNT-FETs as the antigen sensors.

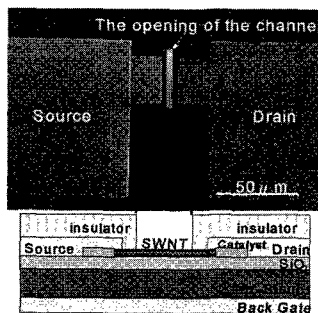


Fig. 1. SEM image and schematic cross section of the fabricated CNT sensor.

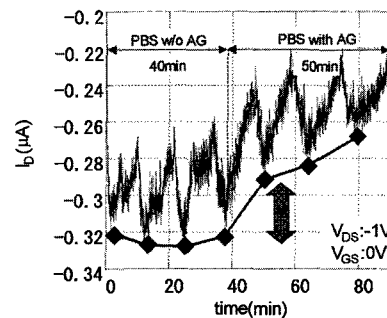


Fig. 2. Time dependence of the drain current.

[1] R. J. Chen, H. C. Choi, S. Bangsaruntip, E. Yenilmez, X. Tang, Q. Wang, Y. Chang, and H. Dai, J. AM. CHEM. SOC. **126**, 1563 (2004).

[2] A. Kojima, C. K. Hyon, T. Kamimura, M. Maeda, and K. Matsumoto, Jpn. Appl. Phys. **44**, 1596 (2005).

Corresponding Author: Kentaro Tani

E-mail: h046415m@mbox.nagoya-u.ac.jp, Tel&Fax: +81-52-789-5388&+81-52-789-5455

Easy Fabrication Process of Carbon Nanotube Emitters for Diode Type Field Emission Display with Organic Luminescence Thin Films

○Nobuyuki Iwata, Yasunori Hata, Masato Yoshikuni and Hiroshi Yamamoto

Department of Electronics & Computer Science, CST Nihon University

We propose a novel low voltage acceleration field emission display (LV-FED) by using organic luminescence films and carbon nanotube (CNT) emitters as a cold cathode. The proposed LV-FED has a diode-type structure and is assembled by placing the CNT emitters close to the luminescence layers with the μm order of distance. The applied voltage between the anode (luminescence layers) and the cathode (CNT emitters) works also as electric field which transports injected electrons in the luminescence film to the recombination interface with holes.

In this study we fabricated CNT emitters by the following easy processes; screen-printing (SP), spreading by spray (SS) and spin-coating (SC) methods. The fabrication processes, conditions and emission current obtained are listed in Table I. In the case of SS and SC, decanted suspension of CNT's was used after sonicating the solution of CNT. The reason why somewhat low current density is probably due to the long cathode-anode distance, about $200\mu\text{m}$. The SEM image showed that individual CNT's with about 100nm - 500nm were dispersed with the density of $1.2 \times 10^7 \text{ cm}^{-2}$. We will discuss observed luminescence concerned with the emitters fabricated.

Table I : Fabrication processes of CNT emitters, condition and emission current

	SP	SS	SC
Solution	α -terpineol(2.99g)+ ethylcellulose(0.16g)	Tetrahydrofuran (THF)	Dimethylformamide (DMF)
CNT powder (wt%)	0.66	0.05	0.02
Dissolution	magnetic stirring at 70°C for 30min	sonication for 12h	sonication for 12h
Deposition	squeeze	0.1MPa, 1sec*50, 300°C	2200rpm, 60sec
Annealing	Dry 150°C, Bake 400°C	Bake 400°C	Dry 150°C, Bake 400°C
Current Density at 350V ($\mu\text{A}/\text{cm}^2$)	9 (after irradiation of excimer laser)	17	85

Development of detachment method of vertically aligned SWNT films from substrates and their re-attachment to arbitrary surfaces

○Yoichi Murakami, Masayuki Kadowaki, Erik Einarsson, Shigeo Maruyama

*Dept. of Mechanical Engineering, The University of Tokyo
7-3-1 Hongo, Bunkyo-ku, Tokyo, 113-8656 Japan*

Abstract:

A hot-water assisted detachment method for the peeling-off of our vertically aligned single-walled carbon nanotube (VA-SWNT) films [1] from substrates has been developed. In particular, we found that the VA-SWNT films grown on quartz substrates (Fig. 1a) is efficiently peeled off by submersing the substrate into heated distilled water (schematic in Fig. 1). The detached film floats on the water surface (Fig. 1b). The key point is to use *warm water* above 60 °C, because the water in R.T. is almost ineffective for the detachment, as has been confirmed with excellent reproducibility [2].

Furthermore, the detached film is readily re-attached to arbitrary surfaces such as Si substrates (Fig. 1c) and transparent plastic films (Fig. 1d). SEM observation confirms that the morphology before detachment (Fig. 2a) is perfectly preserved even after the re-attachment to other substrate (Fig. 2b). Detailed procedure, possible applications, and mechanism of the hot-water assisted process, will be presented in the symposium.

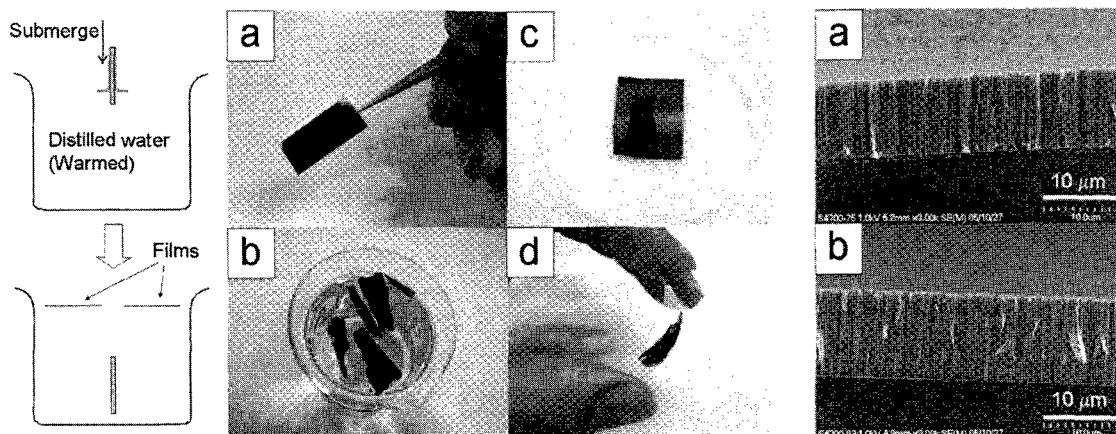


Fig. 1. Photos of the VA-SWNT films (a) before and (b) after detachment, and after re-attachment to (c) Si substrate and (d) transparent film. All the films in (b-d) are the same as that in (a). The left figure shows schematic of the process.

Fig. 2. SEM image of the film (a) before detachment and (b) after re-attachment on Si.

[1] Y. Murakami et al., Chem. Phys. Lett. **385** (2004) 298. [2] Y. Murakami et al., to be submitted.

Corresponding Author: Shigeo Maruyama,

E-mail: maruyama@photon.t.u-tokyo.ac.jp Tel&Fax: +81-3-5800-6983

Microreactors Utilizing Vertically-Aligned Carbon Nanotubes

○ Naoki Ishigami,^a Hiroki Ago,^{*,a,b} Yukihiro Motoyama,^{a,b} Mikihiro Takasaki,^a
Masashi Shinagawa,^a Koji Takahashi,^c and Masaharu Tsuji^{a,b}

^aGraduate School of Engineering Sciences, Kyushu University, Kasuga, Fukuoka 816-8560, Japan

^bInstitute for Materials Chemistry and Engineering (IMCE), Kyushu University and CREST-JST

^cGraduate School of Engineering, Kyushu University

Carbon nanotubes are one of promising materials as catalyst support, because of their high surface area, feasibility to chemical modifications, and mechanical/chemical stability [1]. However, these are severe limitations in the use for catalyst support due to the high cost of nanotubes and their poor solubility. Recently, microfluidic devices have been attracted a great interest as efficient and continuous reactors [2]. Generally, catalysts are immobilized on the walls of microchannels by chemical modification or vacuum deposition so that a catalytic reaction occurs only at surface of the channel.

We have applied carbon nanotubes to the catalyst support by growing them inside a microchip. The nanotube-incorporated microchip has many advantages; (i) nanotubes are fixed inside the channel so that dispersion of nanotubes in solvent is unnecessary, (ii) large contact area is expected because the nanotubes cover the whole channel, (iii) collection of nanotubes after a chemical reaction, such as filtration, is not required, and (iv) an electrochemical reaction or sensing can be performed due to their high electrical conductivity. We grew vertically-aligned multi-walled carbon nanotubes inside a channel (Fig. 1) and chemically modified them with Pt nanoparticles. Hydrosilylation of olefin, which proceeds in the presence of Pt catalyst, was performed as a model reaction of catalysis, as shown in Fig. 2. The silane conversion reached 70 % after 1 hour of the experiment. We believe that our idea of incorporating nanotubes into microfluidic devices may find promising applications, because a small amount of nanotubes work uniquely and efficiently.

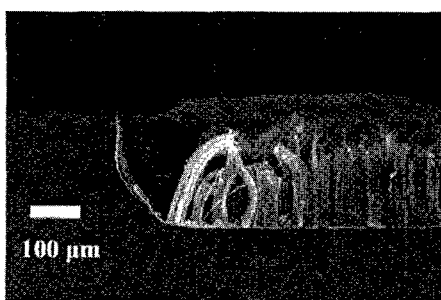


Figure 1. SEM image of vertically-aligned carbon nanotubes grown inside the microchannel.

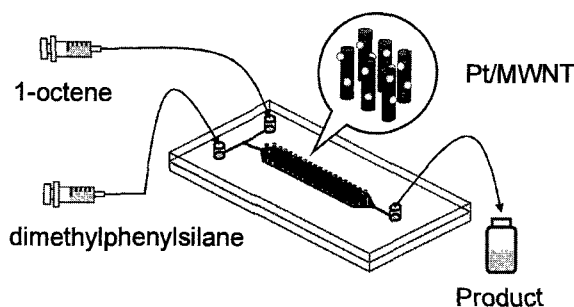


Figure 2. Illustration of the hydrosilylation reaction in the Pt/MWNT-immobilized microreactor. The size of the reaction zone is $2.5 \times 20 \times 0.2 \text{ mm}^3$.

Acknowledgements: The authors acknowledge support from CREST-JST, Grant-in-aid for Scientific Research from MEXT (#16710087), and Nissan Science Foundation. HA thanks Prof. K. Tanaka for helpful suggestions.

References: [1] P. Serp, M. Corrias, P. Kalck, *Appl. Catal. A*, **253**, 337 (2003).

[2] W. Ehrfeld, V. Hessel, H. Lowe eds., *Microreactors*, Wiley-VCH (2000).

Corresponding Author: Hiroki Ago (Tel&Fax: +81-92-583-7817, E-mail: ago@cm.kyushu-u.ac.jp)

Growth and Characterization of Carbon Nanowalls

○ Hirofumi Yoshimura¹, Akihiko Yoshimura², Pedro Molina-Morales³, Hiroshi Nakai³,
Kenichi Kojima¹, Masaru Tachibana¹

¹International Graduate School of Arts and Sciences, Yokohama City University

²Graduate school of Integrated Science, Yokohama City University

³Ishikawajima-Harima Heavy Industries Co., Ltd.

Carbon nanowalls are one of carbon material with two-dimensional structure. They attracted attention due to their unique shape, which may enable their usage of gas storage devices, membranes for electrochemical energy storage, and field emitters. The structural characterization is indispensable for their practical applications [1, 2, 3].

The carbon nanowalls used in this work were produced on quartz and Si substrates coated Ni, Ni/ITO, Ni/Cr or without any catalysts using a gas mixture of CH₄, H₂ and Ar by dc PECVD method. Their lateral sizes were controlled from 0.3 μm to 1.5 μm, by growth conditions. SEM was used to observe morphologies of carbon nanowalls and Raman spectroscopy and XRD were used to evaluate their structure.

Fig.1 shows the SEM images of carbon nanowalls prepared by dc PECVD method under different growth times. It shows small flakes grow to large sheets gradually and wavy sheets form the network structure. From their Raman spectra and XRD data, we will discuss growth mechanism and structure of the carbon nanowalls in this report.

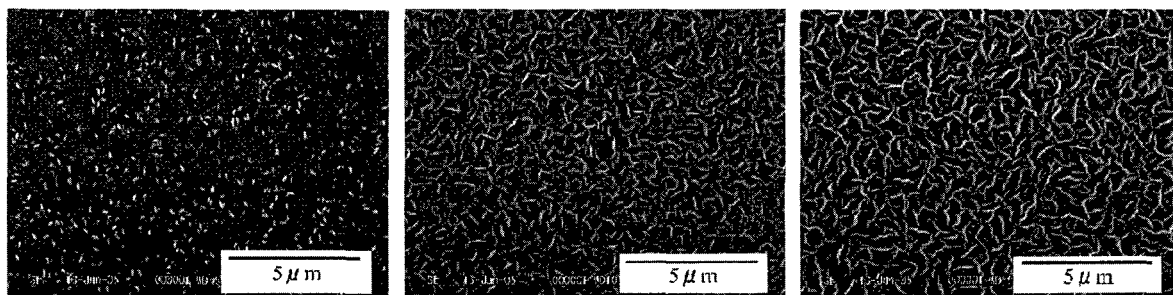


Fig.1 SEM images of carbon nanowalls prepared under different growth times (from left, 5min, 10min and 20min, respectively).

[1]Yihong Wu, Peiwen Qiao, Towchong Chong, Zexiang Shen, *Adv. Mater.*, **14**, 64 (2002)

[2]M. Hiramatsu, K. Shiji, H. Amano, M. Hori, *Appl. Phys. Lett.*, **84**, 4708 (2004)

[3]S. Kurita, A. Yoshimura, H. Kawamoto, T. Uchida, K. Kojima, M. Tachibana, P. Molina-Morales, H. Nakai, J. *Appl. Phys.*, **97**, 104320 (2005)

Corresponding Author: Masaru Tachibana

TEL: +81-45-787-2307, Fax: +81-45-787-2307, E-mail:tachiban@yokohama-cu.ac.jp

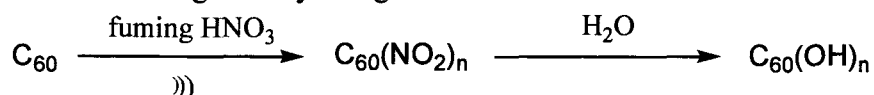
Surface Modification of Carbon Nanotube with NO₂ Radical in Fuming Nitric Acid

○Kyozo Mizuno, Masaru Sekido, Masatomi Ohno

*Department of Advanced Science and Technology, Toyota Technological Institute,
2-12-1 Hisakata, Tempaku, Nagoya 468-8511, Japan*

While surface modification by organic reactions has been thoroughly studied in fullerene chemistry, such for carbon nanotube is now rising and variety of reactions on the sidewall have been demonstrated recently. In this report we wish to demonstrate the methods to prepare water-soluble SWNT using simple NO₂ radical reaction as a key step.

The aimed radical is available directly from NO₂ gas dissolved in aq. HNO₃ (fuming nitric acid). Related works are preceded for the addition reaction of SWNT with NO₂ gas in organic solvent by Moriyama* and the oxidation reaction of SWNT with HNO₃-H₂SO₄ by the pioneer Smalley. For comparison, heterogeneous conditions using fuming HNO₃ was carried out first with [60]fullerene, and sonication of suspended black powder C₆₀ in this solvent was found to cause dissolution gradually and give fullerenol as a brown solution.



With this result in hand, SWNT was sonicated in 2ml fuming HNO₃ at 60°C for 10h by Branson ultra sonic cleaner (42kHz). After dilution, the products were separated by filtration with Millipore membranes filter (10μm), and washed with water. The residue was put into 10ml water and further sonicated at 60 °C for 10h, followed by filtration with the same filter. We obtained black dispersed solution, which kept stable dispersion for over one month.

The AFM images of SWNT [a) before and b) after treatment in Fig. 1] showed that SWNT was cut after the treatment. The Raman spectrum also showed stronger D-band (ca. 1300cm⁻¹), which is consistent with sidewall modification. We believe that the second sonication with NH₃ or H₂S and application to DWNT may be interesting in our present method.

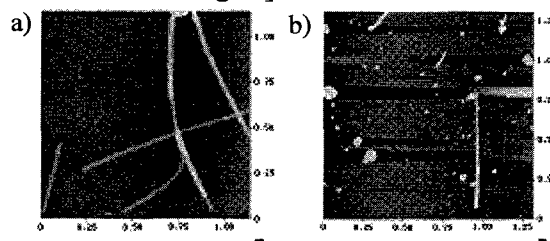


Fig. 1 AFM images of SWNT a) before, b) after

References : H. Moriyama, Abstracts of The 25th Fullerene-Nanotubes Memorial Symposium, 1P-55 (2003)

Corresponding Author : Kyozo Mizuno

E-mail : sd00152@toyota-ti.ac.jp

Tel&Fax : (TEL) (+81) 52-809-1841, (FAX) 052-809-1721

Trapping of S-Heterocyclic Carbene with C₆₀ Probe Technique

○Hidefumi Nikawa¹, Tsukasa Nakahodo¹, Takahiro Tsuchiya¹, Takatsugu Wakahara¹,
G. M. Aminur Rahman¹, Takeshi Akasaka¹, Yutaka Maeda², Michael T. H. Liu³,
Akira Meguro⁴, Soichiro Kyushin⁴, Hideyuki Matsumoto⁴,
Naomi Mizorogi⁵ and Shigeru Nagase⁵

¹Center for Tsukuba Advanced Research Alliance, University of Tsukuba,
Tsukuba, Ibaraki 305-8577, Japan

²Department of Chemistry, Tokyo Gakugei University, Koganei, Tokyo 184-8501, Japan

³Department of Chemistry, University of Prince Edward Island, Charlottetown,
Prince Edward Island, C1A4P3 Canada

⁴Department of Applied Chemistry, Faculty of Engineering, Gunma University, Kiryu,
Gunma 376-8515, Japan

⁵Department of Theoretical Molecular Science, Institute for Molecular Science,
Okazaki, Aichi 444-8585, Japan

Recently, Wiberg and co-workers reported the preparation of TTF analogue with a disilane backbone, obtained from the reaction of the isolable disilene with carbon disulfide[1]. They suggested that S-heterocyclic carbene intermediate plays the important role in the process of the generation of TTF analogue. Meanwhile, heterocyclic carbenes have attracted special attention as a spin source, ligand, catalyst and so forth, due to their unique coordination properties. Recently, we have reported the generation of a tetracyclosilene by the photolysis of the *anti*-dodecaisopropylcyclo[4.2.0.0^{2,5}]octasilane[2]. Herein we report the generation of S-heterocyclic carbene with a cyclotetrasilane backbone by [2+3] cycloaddition of tetracyclosilene with carbon disulfide[3]. The carbene has been confirmed by trapping it with C₆₀ as a chemical probe[4]. The structural determination of the obtained C₆₀ derivative has been performed by spectroscopic and X-ray crystallographic analysis.

Scheme.

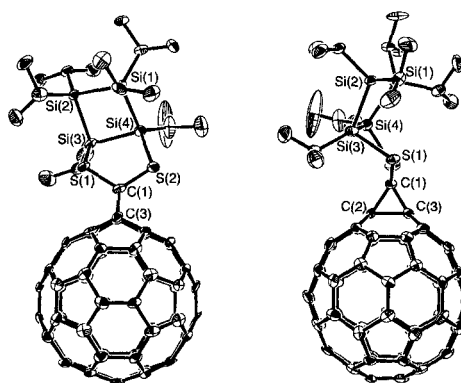
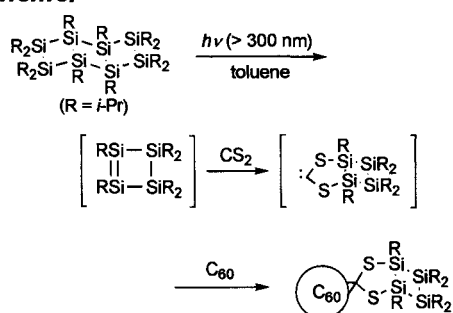


Figure. Crystal structure of C₆₀(C₁₉H₄₂S₂Si₄).

[1] N. Wiberg *et al.* *Chem. Eur. J.* **8**, 2730 (2002). [2] S. Kyushin *et al.* *Chem. Lett.* 494 (2000).

[3] H. Nikawa *et al.* *Angew. Chem. Int. Ed.* in press. [4] a) T. Akasaka *et al.* *J. Am. Chem. Soc.*, **122**, 7134 (2000). b) T. Wakahara *et al.* *J. Am. Chem. Soc.* **124**, 9465 (2002). c) M. T. H. Liu *et al.* *J. Org. Chem.* **68**, 7471 (2003). d) M. O. Ishitsuka *et al.* *Tetrahedron Lett.* **45**, 6321 (2004).

Corresponding Author: Takeshi Akasaka

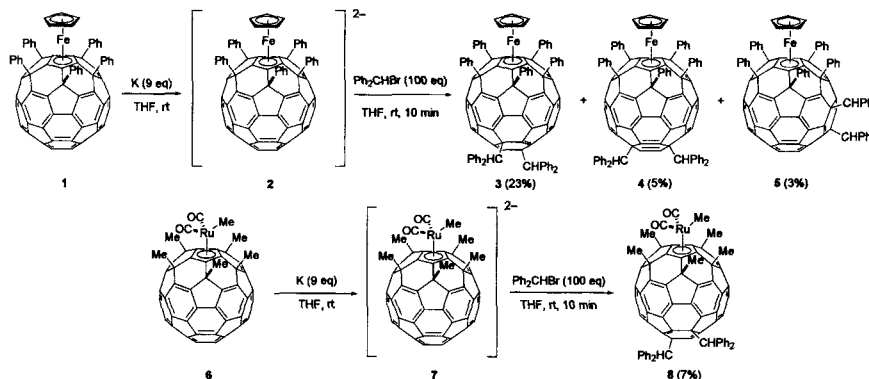
TEL: +81-29-853-6409, FAX: +81-29-853-6409, E-mail: akasaka@tara.tsukuba.ac.jp

Regioselective Synthesis and Structure of Hepta(organo)[60]fullerene-Transition Metal Complexes

○Takeshi Fujita¹, Yutaka Matsuo², and Eiichi Nakamura^{1,2}

¹*Department of Chemistry, The University of Tokyo and* ²*Nakamura Functional Carbon Cluster Project, ERATO, JST, Hongo, Bunkyo-ku, Tokyo 113-0033, Japan*

Regioselective functionalization of fullerenes is one of the challenges in fullerene chemistry due to their complicated reactivity. However, we achieved this goal by reduction of penta(organo)[60]fullerene-transition metal complexes with potassium. Herein we report the regioselective synthesis of three kinds of hepta(organo)[60]fullerene-iron complexes by the reduction of buckyferrocene **1** followed by trapping with alkyl bromide. And also we applied this reaction to the synthesis of hepta(organo)[60]fullerene-ruthenium complexes having carbonyl ligands.



Buckyferrocene **1** was first reduced with nine equivalent of potassium in THF to give a dianion **2**, and then treated with excess amount of α -bromodiphenylmethane to afford three isomers of heptaadducts **3**, **4**, and **5**. The structures of these compounds were determined by X-ray analysis. The three isomers of UV-vis-NIR spectra were quite different from each other due to having different π -conjugated systems. On the other hand, a fullerene-ruthenium complex **6**, which has two carbonyl ligands, was reduced without any decomposition and followed by the addition of the same halide to give a corresponding heptaadduct **8**. We also report the spectroscopic properties of the dianions, the intermediates of these reactions.

Corresponding Author: Eiichi Nakamura

E-mail: nakamura@chem.s.u-tokyo.ac.jp

Tel&Fax: +81-(0)3-5800-6889

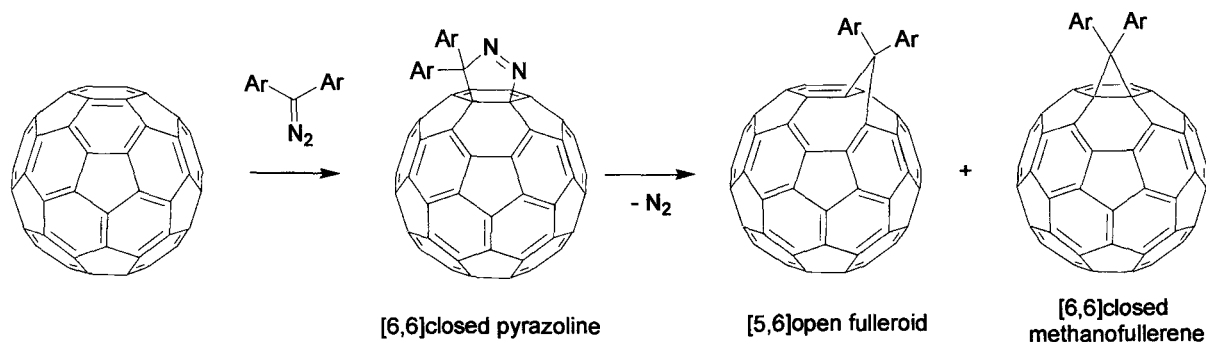
Kinetics of 1,3-Dipolar Cycloaddition of Diaryldiazomethanes with Fullerenes C₆₀ and C₇₀

○H. Kitamura, N. Seike, T. Higashi, K. Kokubo, and T. Oshima

*Department of Applied Chemistry, Graduate School of Engineering, Osaka University,
Suita, Osaka 565-0871, Japan*

Due to the highly conjugated low-lying LUMO orbital, C₆₀ is demonstrated to easily undergo electrocyclic reactions such as 1,3-dipolar cycloaddition and Diels-Alder reaction. Diazoalkanes are well known to react with C₆₀ to give two monoadducts, [6,5] open fulleroids and [6,6] closed methanofullerenes, via nitrogen-release from the primary adducts [6,6] pyrazolines.

However, to our best knowledge, little is known about the kinetic features of these reactions. We, therefore, investigated the kinetics of 1,3-dipolar cycloaddition of a series of *meta*- and *para*-substituted diphenyldiazomethanes (DDMs) with fullerenes C₆₀ and C₇₀ at 30°C in toluene. The second-order rate constants for the primary addition of unsubstituted DDM to C₆₀ and C₇₀ were 0.113 and 0.078 s⁻¹ M⁻¹, respectively. It was found that C₆₀ reacted ca 1.5 times faster than C₇₀ with DDMs and the rates increased with the increase of electron-donating ability of the substituents. The Yukawa-Tsuno equation gave the excellent correlations; $\log k^X/k^0 = -1.61(\sigma + 0.216\Delta\sigma_R^+) + 0.02$ (n = 12, R² = 0.98) for C₆₀, and $\log k^X/k^0 = -1.66(\sigma + 0.167\Delta\sigma_R^+) + 0.00$ (n = 12, R² = 0.98) for C₇₀, respectively. Plots of $\log k(C_{60})$ against $\log k(C_{70})$, $\log k(DDQ)$, and $\log k(TCNE)$ provided the linear correlations with the slopes of 0.99, 1.57, and 2.57, respectively, reflecting the redox potentials as well as the LUMO coefficients of the acceptors.



Corresponding Author: Takumi Oshima

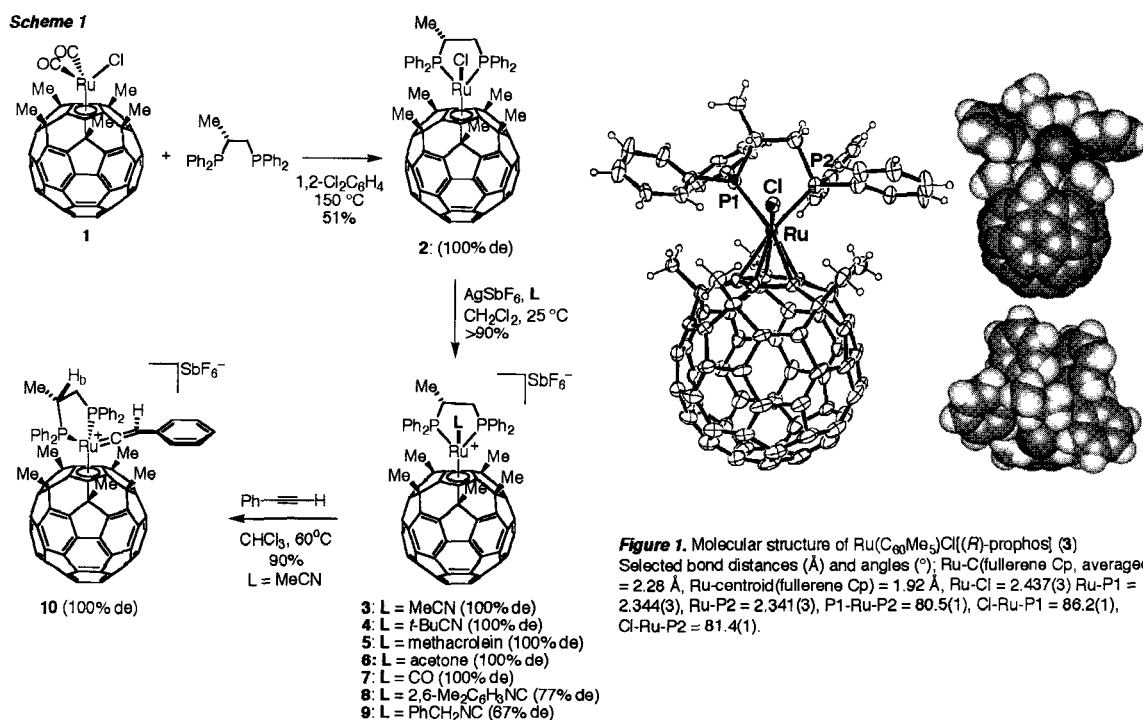
TEL: +81-6879-4591, FAX: +81-6-6879-4593, E-mail: oshima@chem.eng.osaka-u.ac.jp

Diastereoselective Complexation of Chiral Diphosphine and Ruthenium-Pentaorgano[60]fullerene

○ Yuichi Mitani,¹ Yutaka Matsuo,² Yu-Wu Zhong² and Eiichi Nakamura^{1,2}

¹Department of Chemistry, The University of Tokyo and ²Nakamura Functional Carbon Cluster Project, ERATO, JST, Hongo, Bunkyo-ku, Tokyo 113-0033, Japan

Control of stereochemistry at the metal center of half-sandwich transition metal complexes plays an important role in both catalytic and stoichiometric enantioselective transformation reactions. Herein we report the diastereoselective complexation of $\text{Ru}(\text{C}_{60}\text{Me}_5)\text{Cl}(\text{CO})_2$ (**1**) with (*R*)-prophos ligand [(*R*)-1,2-bis(diphenylphosphino)propane], giving an enantiomerically pure and configurationally stable chiral-at-metal complex, $\text{Ru}(\text{C}_{60}\text{Me}_5)\text{Cl}((R)\text{-prophos})$ (**2**). This complex was diastereoselectively converted into cationic complexes, $[\text{Ru}(\text{C}_{60}\text{Me}_5)((R)\text{-prophos})\text{L}][\text{SbF}_6^-]$ ($\text{L} = \text{MeCN}$ (**3**), *t*-BuCN (**4**), methacrolein (**5**), acetone (**6**), CO (**7**), 2,6-Me₂C₆H₃NC (**8**), BnNC (**9**)) and vinylidene complex (**10**) was also obtained diastereoselectively by treatment of **3** with phenylacetylene.



Corresponding Author: Eiichi Nakamura

TEL/FAX: +81-(0)3-5800-6889, E-mail: nakamura@chem.s.u-tokyo.ac.jp

Application of C₆₀-based amine-labeling reagents to MALDI-TOF MS analysis

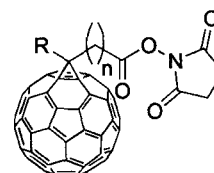
○Hiroki Tsumoto^{1,2}, Katsumasa Takahashi¹, Kohfuku Kohda², Takayoshi Suzuki¹,
Hidehiko Nakagawa¹ and Naoki Miyata¹

¹Graduate School of Pharmaceutical Sciences, Nagoya City University,
Tanabe-dori, Mizuho-ku, Nagoya 467-8603, Japan

²Faculty of Pharmaceutical Sciences, Musashino University,
Shin-machi, Nishitokyo, Tokyo 202-8585, Japan

Peptide mass fingerprinting (PMF) is a mass spectrometric technique for identification of proteins. The masses of tryptic peptides from digested protein are matched to the theoretical peptides in database. To identify the parent protein with greater accuracy and confidence, the number of identified tryptic peptides is important. Matrix-assisted laser desorption/ionization time-of-flight (MALDI-TOF) mass spectrometry is generally used in the PMF method. However, it is somewhat difficult to analyze small molecules ($m/z < 500$ Da) by MALDI-TOF mass spectrometry. This is in part due to the poor ionization efficiency for the lack of high-proton-affinity functional groups and to the presence of matrix-related ion peaks in the low-mass range.

Our strategy is to use a physico-chemical property of C₆₀ for the analysis of small molecules by MALDI. In the 28th symposium, we reported the synthesis of amine-labeling reagents containing C₆₀ moiety (Figure 1). C₆₀-derivatization of tryptic peptides results in a theoretical monoisotopic mass-increase of 878.07 (1), 883.10 (2), 955.98 (3) and 756.00 (4), respectively. There are three advantages in the C₆₀-derivatization method. The first is the increased sensitivity caused by C₆₀ moiety. The second is the mass shift toward higher mass range from the matrix range. The third is the relative quantification of tryptic peptides by using the isotope-coded light (1) and heavy (2) reagents. The improved ionization efficiency of the C₆₀-labeled peptide and the increased mass of the C₆₀-labeled analytes including amino acids and peptides were demonstrated using negative ion mode.



- 1: R = C₆H₅, n = 3
- 2: R = C₆D₅, n = 3
- 3: R = C₆H₄Br, n = 3
- 4: R = H, n = 0

Figure 1.

To demonstrate the identification of a protein with increased sensitivity and sequence coverage, the tryptic peptides from cytochrome c were treated with reagent 1. The new peaks a ~ e were obtained in the m/z 1000 ~ 2000 range and the sequence of the peaks was identified from the increase of the mass (Figure 2). In this symposium, we report the potential use of the C₆₀-derivatization method for the identification and quantification of proteins.

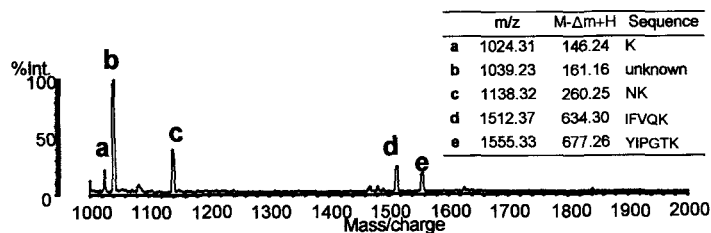


Figure 2.

Corresponding Author: Naoki Miyata

Tel & Fax: +81-52-836-3407, E-mail: miyata-n@phar.nagoya-cu.ac.jp.

Mechanism of mechanochemical hydroxylation of fullerene

○T. Kubo, E. Matsui, H. Watanabe and M. Senna

*Faculty of Science and Technology, Keio University,
3-14-1 Hiyoshi Kohoku-ku, Yokohama 223-8522, Japan*

Out of many possibilities to make fullerene (C_{60}) water-soluble, a mechanochemical route by milling C_{60} with alkali metal hydroxide seems attractive, due to its simplicity and ecological benignity. The reaction is known to be sensitive to the atmosphere and amount of additives. Zhang et al. prepared fullerene hydroxide (fullerenol or $C_{60}(OH)_n$) by milling in air and adding a large amount of alkali metal hydroxide [1]. Komatsu et al. on the other hand, reported dimerization of fullerene by milling C_{60} in an inert gas atmosphere and adding alkali metal hydroxide in a catalytic quantity [2]. However, most of the reaction mechanisms are still open.

We here examine the reaction mechanism of fullerenol formation via a mechanochemical route, by comparing with known mechanisms of the similar reactions via a photochemical route [3], by zooming up the formation and properties of intermediate active species.

Fullerene and one of the hydroxides of Li, Na, K were mixed at the molar ratio, 1:250 with a vibro-mill (Fritsch Vibratory Micro-Mill, Pulverisette 0) for 5h, dispersed in water and filtrated. The filtrate was mixed with methanol and the precipitate was collected by centrifugation. A black powdery substance was characterized by FT-IR and UV-vis spectra.

In most of the cases, we obtained $C_{60}(OH)_n$ with n-value between 8 and 15. Unlike the cases with sodium or potassium hydroxide, C-H bond formation was observed in addition to the parallel formation of fullerenol, when we used $LiOH \cdot H_2O$. From ESR spectra, we confirmed the participation of the cation radical of C_{60} by using potassium methoxide as a nucleophilic reagent. ESR g-value was changed from 2.0029 to 2.0044. Infrared spectra showed addition of methoxy group.

We therefore think the mechanism of cation radical generation to be similar to the case of photochemical pathways and this radical is a key active species for the present mechanochemical hydroxylation. We also speculate the increase in the electron density around oxygen to ease bond formation to the positively charged part of the cation radical of C_{60} .

References: [1] Pu Zhang, Hualong Pan, Doufang Liu, Zhi-Xin Guo, Fushi Zhang, Daoben Zhu, *Synth. Commun.* **2003**, *33*, 2469-2474

[2] K. Komatsu, *Top Curr. Chem.* **2005**, *254*, 185-206

[3] A. I. Shames, E. A. Karz, S. D. Goren, D. Faiman, S. Shtutina, *Mate. Sci. Eng.* **1997**, *B45*, 134-139

Corresponding Author: M. Senna

E-mail senna@aplc.keio.ac.jp

Tel&Fax Tel.: +81-045-566-1569; fax: +81-045-564-0950

Effects of pressure and temperature on the solubility of C₇₀ in *n*-hexane

○Shinichi Okada, Seiji Sawamura

Department of Applied Chemistry, Faculty of Science and Engineering,
Ritsumeikan University, Kusatsu, 525-8577, Japan.

We have reported that the solubility of C₆₀ in *n*-hexane increases with increasing pressure up to 400 MPa at 298.2 K in the preceding paper [1]. In the present study, we measured the solubility of C₇₀ in *n*-hexane at temperatures in the range of 288.2 – 318.2 K and pressures up to 435 MPa.

A clamp-type optical cell designed by us [2] (the light-path length is 1.0 mm) was used for solubility measurement. A small amount of C₇₀ and *n*-hexane were put in the cell and then the cell was pressed. The cell was shaken on a thermoregulated seesaw for a few weeks, during which the visible absorption spectra of the solution in the cell were repeatedly measured until the absorbance became constant. Calibration method for changes of the light-path length and molar absorption coefficient caused by changes in pressure and temperature was previously reported [3].

Solubility of C₇₀ in *n*-hexane was shown in Fig. 1. It increased with increasing pressure having a breaking point around 100 MPa at all temperatures. The volume change, ΔV , accompanying the dissolution of C₇₀ in *n*-hexane, was estimated to be $-55.3 \pm 5.3 \text{ cm}^3 \text{ mol}^{-1}$ at 0.10 MPa and $-10.4 \pm 1.1 \text{ cm}^3 \text{ mol}^{-1}$ at 400 MPa using a thermodynamic equation of $[\partial \ln X / p]_T = -\Delta V/RT$. The difference between these values is too large to be ascribed to the volume reduction of a solid phase of C₇₀ by pressure. Interestingly the solubility- pressure curve of C₆₀ in *n*-hexane at 298.2 K (Fig. 1) has a similar breaking point around 50 MPa, which is assigned to a phase transition between solid phase such as C₆₀ (fcc form) and a solvate [1]. For C₇₀, similar phase transition in the solid phase may be caused by pressure though there have not been any other suggestive reports.

References:[1]S. Sawamura, *et al.*, *Chem. Phys. Lett.*, **299**, 177 (1999). [2] S. Sawamura, *et al.*, *J. Solution Chem.*, **16**, 649 (1987). [3] S. Sawamura, *et al.*, *J. Phys. Chem.*, **B105**, 2429 (2001).

Corresponding Author: Seiji Sawamura

E-mail: sawamura@se.ritsumei.ac.jp

Tel: +81-77-566-1111, Fax: +81-77-561-2629

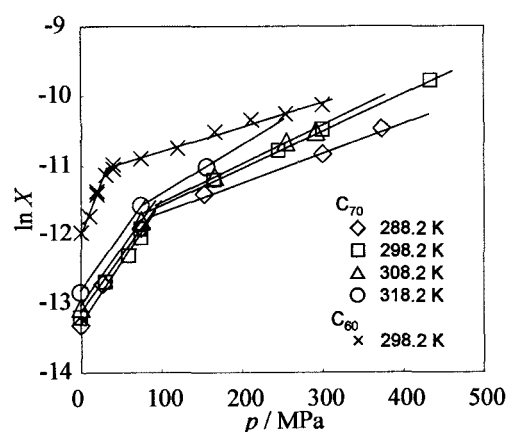


Fig. 1. Logarithm of the solubility (molar fraction) of C₆₀ and C₇₀ in *n*-hexane.

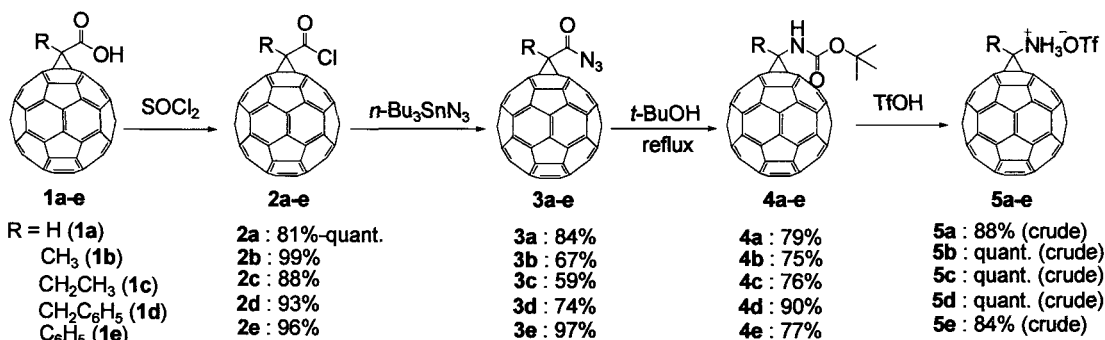
Synthesis and Reactions of Novel Methano[60]fullerenes

○Tomoyuki Tada, Yasuhiro Ishida, and Kazuhiko Saigo

*Department of Chemistry and Biotechnology, The University of Tokyo,
Tokyo 113-8656, Japan*

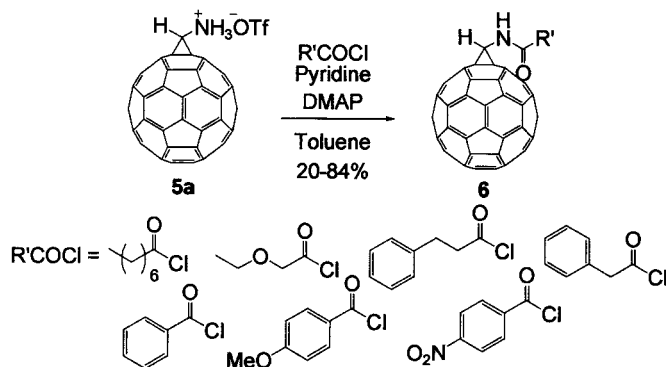
Recently, we have reported on the synthesis of [60]fullerenoacetyl chloride **2a** and found that **2a** was a versatile precursor for the preparation of various [60]fullerenoacetic acid esters and amides [1]. Moreover we have firstly succeeded in the synthesis of aminomethano[60]fullerenes **5a-e** upon applying the Curtius rearrangement of acyl azides **3a-e** [2].

Scheme 1 : Synthesis of Aminomethano[60]fullerenes 5a-e

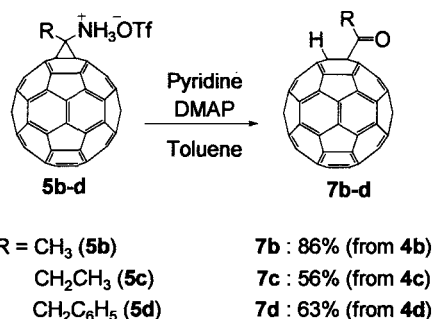


In order to evaluate the utility of **5a-e** as a precursor of various methano[60]fullerene derivatives, the condensation reaction with acyl chloride was investigated. As expected, the free amine, generated *in situ* by treatment of **5a** with a base, reacted with various acyl chlorides to afford the corresponding amides **6** in moderate to good yields (Scheme 2). Moreover, we found that **5b-d**, which possess an alkyl group such as methyl, ethyl, benzyl at the methano-bridge carbon, were converted to dihydro[60]fullerene derivatives **7b-d** under basic conditions (Scheme 3).

Scheme 2 : Formation of the amides 6 from 5a



Scheme 3 : Reaction of 5b-d with a base



References: [1] H. Ito, T. Tada, M. Sudo, Y. Ishida, T. Hino and K. Saigo, *Organic Letters*, **15**, 2643, (2003).

[2] T. Tada, Y. Ishida and K. Saigo, *Organic Letters*, to be published.

Corresponding Author : Kazuhiko Saigo

Tel : +81-3-5841-7266, **Fax :** +81-3-5802-3348, **E-mail :** saigo@chiral.t.u-tokyo.ac.jp

Recent progress of powder diffraction study of endohedral metallofullerene at SPring-8

○Eiji Nishibori, Ikuya Terauchi, Masayuki Ishihara, Makoto Sakata, Masaki Takata, Yasuhiro Ito, Hisashi Umemoto, Hiroe Moribe, Takashi Inoue, Hisanori Shinohara

*Department of Applied Physics, Nagoya University, Nagoya 464-8603,^A Japan., Japan
Synchrotron Radiation Research Institute, 1-1-1 Kouto Sayo-cho Sayo-gun Hyogo
679-5198 Japan Japan. Toyota Central R&D Labs., Inc., 41-1, Aza Yokomichi, Oaza
Nagakute, Nagakute-cho, Aichi-gun, Aichi-ken, 480-1192, Japan., Department of
Chemistry, Nagoya University, Nagoya 464-8602, Japan.*

Abstract: Endohedral metallofullerenes have attracted wide interests due to their characteristic structural and electronic properties. We have been developing the both experimental and analytical technique for synchrotron radiation powder diffraction study of endohedral metallofullerene at SPring-8. Over 37 kinds of powder data of mono-, di- and tri-metal metallofullerenes have been measured at SPring-8. The lattice constants of these materials have been determined by LeBail method. The volume of unit cell has been calculated from the lattice constants. It is found that the volume of crystal is closely relating to the number of carbon atoms in fullerene cage. The fact suggests that metal-carbide encapsulation has easily been detected only from cell volume. Furthermore, the possible isomers can be selected by the value of lattice constants. We also found that our previous structural studies^{1,2} of Sc₃C₈₂ and Sc₂C₈₄ had fallen into a local minimum, because Sc₃C₈₂ and Sc₂C₈₄ are metal-carbide endohedral metallofullerene, (Sc₃C₂)@C₈₀ and (Sc₂C₂)@C₈₂ from the volumes.

The powder structural studies of (Sc₃C₂)@C₈₀ and (Sc₂C₂)@C₈₂ using recent SPring-8 powder data have been performed by the MEM/Rietveld method. The precise structures including C₂ encapsulations and multiple disorders of metal atoms of them have been determined in this study.

References:

1. Takata, M., et al., *Phys. Rev. Lett.*, **1999**, 83, 2214-2217
2. Takata, M, et al., *Phys. Rev. Lett.*,

Corresponding Author: Eiji Nishibori

E-mail : eiji@mcr.nuap.nagoya-u.ac.jp

Tel&Fax: +81-52-789-3702/+81-52-789-3724

Synthesis of LaNd@C₇₂ and Fluorescence Measurement of Nd-metallofullerenes

○Naomi Murata, Takeshi Kodama, Yoko Miyake, Shinzo Suzuki,
Koichi Kikuchi, Yohji Achiba

Department of Chemistry, Tokyo Metropolitan University, Hachioji, 192-0397, Japan

Up to now, fluorescence from encapsulated Er³⁺ has been observed for Er₂@C₈₂ [1,2], Er_xSc_{3-x}N@C₈₀ (x=1-3) [3], and recently (Er₂C₂)@C₈₂ [4]. In contrast, no other metallofullerenes show fluorescence from encaged metals. In the previous symposium, we reported the synthesis and the UV-Vis-NIR absorption spectra of Nd₂@C₇₂ and Nd₂C₈₀ [5]. In the present work, we newly synthesized LaNd@C₇₂ and tried to measure fluorescence of Nd₂@C₇₂, Nd₂C₈₀, and the mixture of MM'@C₇₂ (M,M'=La,Nd).

Soot containing La, Nd-metallofullerenes was produced by direct-current (60A) arc discharge of La/Nd/C composite rods (La:Nd:C=1.5:1.5:97) under a 500 torr He atmosphere. Both empty fullerenes and metallofullerenes were extracted from the raw soot by refluxing with 1,2,4-trichlorobenzene for 8h. The mixture of MM'@C₇₂ were separated by multi-step high-performance liquid chromatography. As shown in Fig. 1, the mass spectrum of the mixture was well reproduced by calculation when the mixing ratio of La₂@C₇₂, LaNd@C₇₂, and Nd₂@C₇₂ is 1:3:1.5.

Nd₂@C₇₂, Nd₂C₈₀ and the mixture of MM'@C₇₂ were dissolved in a mixture of cis and trans decalins (decahydro-naphtalene) and measured fluorescence with the excitation wavelength of 633 nm. At room temperature, no fluorescence was observed for all the samples. At 77 K, only the mixture of MM'@C₇₂ showed the quite weak emission around 1100 nm. These results imply only LaNd@C₇₂ show the fluorescence. To confirm it, we plan to measure fluorescence by another excitation wavelength.

This study was partly supported by Industrial Technology Research Grant Program from New Energy and Industrial Technology Development Organization (NEDO) of Japan.

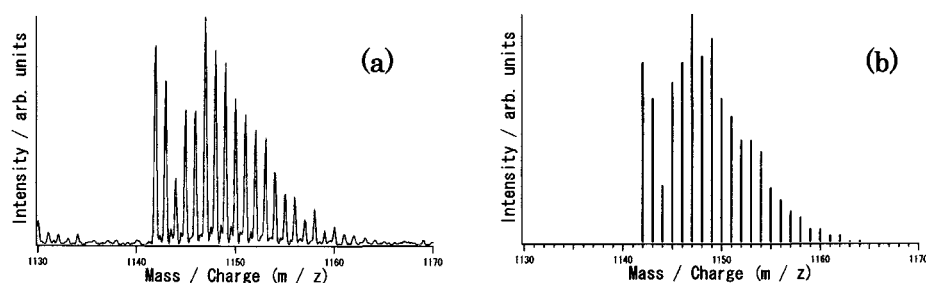


Fig. 1 Positive-ion mass spectrum of the MM'@C₇₂ sample after HPLC separation: (a) observed and (b) calculated isotropic distributions for MM'@C₇₂.

- [1] X. Ding *et al.*, *Chem. Phys. Lett.*, **269**,72(1997).
- [2] R. M. Macfarlane *et al.*, *Phys. Rev. Lett.*, **79**, 1397(1997).
- [3] R. M. Macfarlane *et al.*, *Phys. Rev. Lett.*, **343**, 229(2001).
- [4] Y. Ito *et al.*, *The 29th Fullerene-Nanotubes General Symposium*, 98(2005).
- [5] N. Murata *et al.*, *The 29th Fullerene-Nanotubes General Symposium*, 168(2005).

Corresponding Author: Takeshi Kodama

E-mail: kodama-takeshi@c.metro-u.ac.jp, Tel: +81-426-77-2530, Fax: +81-426-77-2525

Reactivity of $\text{La}_2@C_{78}$ toward 2-admantane-2,3-diazirine: structure determination of monoadduct $\text{La}_2@C_{78}(\text{Ad})$ (I)

O Baopeng Cao,¹ Tsukasa Nakahodo,¹ Takatsugu Wakahara,¹ Takahiro Tsuchiya,¹ Kaoru Kobayashi,² Shigeru Nagase,² and Takeshi Akasaka^{1*}

¹*Center for Tsukuba Advanced Research Alliance, University of Tsukuba, Tsukuba 305-8577, Japan*

²*Department of theoretical Molecular Science, Institute for Molecular Science, Okazaki 444-8585, Japan*

It is well known that the reactivities and electronic properties of an empty fullerene could be modified upon incorporation of a metallic guest species, which awards plentiful, various materials with novel properties and potential application perspectives associated with the incarcerated metal.¹ Based on these modified reactivities, functionalization of metallofullerenes could further afford some new derivatives that bear special functional groups and present intriguing properties. A communication between the dynamic motion of the two cerium atoms within $\text{Ce}_2@C_{80}$ and exohedral groups, for example, is fulfilled either by disilylation of this molecule with 1,1,2,2-tetrakis-(2,4,6-trimethylphenyl)-1,2-disilirane or through [2+3] cyclo-addition of an N-trityloxazolidinone to it.² So far, however, investigations on reactivities of metallofullerenes are focused on the most abundant species, $\text{La}@C_{82}$, $\text{La}_2@C_{80}$, and $\text{M}_3\text{N}@C_{80}$; rare attention has been given to those with smaller cages because of their scarcity. Recently, benefiting from a newly developed separation method, we have isolated a new metallofullerene, $\text{La}_2@C_{78}$, with enough quantity for spectroscopic characterization.³ UV-vis-NIR absorption and CV measurement on $\text{La}_2@C_{78}$ have revealed that its electronic structure as well as chemical reactivity toward di-silirane are quite varied from those of C_{78} . The specifics that $\text{La}_2@C_{78}$ presents are not limited on these – it is found that $\text{La}_2@C_{78}$ is distinct from $\text{Sc}_3\text{N}@C_{78}$ in electronic structure though ¹³C NMR and theoretical approaches toward the structure determination of $\text{La}_2@C_{78}$ and $\text{Sc}_3\text{N}@C_{78}$ have disclosed that the two metallofullerenes not only possess exactly the same C_{78} -cage but also bear an identical intramolecular electron transfer. All these novelties that $\text{La}_2@C_{78}$ exhibits drive us toward an in-depth structural elucidation on the location of the two encapsulated La-atoms. Functionalization of metallofullerene with a diazirine has been demonstrated to be an efficient way for growth of a single crystal toward a final solution of the metallofullerene's structure.⁴ Here we report the thermal and photochemical reactivities of $\text{La}_2@C_{78}$ toward 2-admantane-2,3-diazirine. We found that the thermal and photochemical reactivities of $\text{La}_2@C_{78}$ with this diazirine are quite different – the thermal reaction yields many monoadduct-isomers without regioselectivity whereas the photochemical one is regioselective and generates only two monoadducts with a molar ratio of ~ 5:1. The major isomer obtained photochemically has been isolated and characterized by mass, absorption, and NMR spectroscopic analyses.

1. *Endofullerenes: A New Family of Carbon Clusters*; Akasaka, T. & Nagase, S. Eds., Kluwer Academic: Dordrecht, 2002.
 2. M. Yamada, T. Nakahodo, T. Akasaka et al. *J. Am. Chem. Soc. ASAP* (2005).
 3. B. Cao, T. Wakahara, T. T. Akasaka, et al. *J. Am. Chem. Soc.* **126**, 9164-9165(2004).
 4. Y. Iiduka, T. Wakahara, T. Akasaka, et al. *J. Am. Chem. Soc.* **127**, 12500-12501(2005)
- Correspondence should addressed to: Prof. Takeshi Akasaka; E-mail: akasaka@tara.tsukuba.ac.jp; Tel & Fax: 81-29-853-6409.

Radical Reaction of La@C₈₂ in Toluene

○ Yuta Takano¹, Akinori Yomogita¹, Takatsugu Wakahara¹, Takahiro Tsuchiya¹, Tsukasa Nakahodo¹, Yutaka Maeda², Takeshi Akasaka¹, Tatsuhisa Kato³, Naomi Mizorogi⁴, and Shigeru Nagase⁴,

¹Center for Tsukuba Advanced Research Alliance, University of Tsukuba, Tsukuba 305-8577, Japan, ²Department of Chemistry, Tokyo Gakugei University, Koganei 184-8501, Japan, ³Department of Chemistry, Josai University, Sakado, Saitama 350-0295, Japan, ⁴Department of Theoretical Molecular Science, Institute for Molecular Science, Okazaki, Aichi 444-8585, Japan

Endohedral metallofullerenes have attracted considerable interest for their potential applications as nano-scale electronic devices on the basis of their spherical structure with unique properties.¹ La@C₈₂ has been recognized as a prototype of endohedral metallofullerenes. An important aspect of the chemistry of La@C₈₂ is its reactivity towards free radicals on a fullerene cage. P. J. Krusic et al. have first reported the radical reaction of C₆₀.² In comparison of reactivity of C₆₀, La@C₈₂ shows higher reactivity owing to narrower HOMO-LUMO gap than that of C₆₀.

We report here the reaction of La@C₈₂ with benzyl radical to afford the corresponding stable adducts (La@C₈₂-CH₂C₆H₅). Three isomers of La@C₈₂-CH₂C₆H₅ were isolated from the reaction mixture by HPLC. All of them are EPR inactive indicating their closed-shell electronic structures. The ¹H and ¹³C NMR spectra show the peaks corresponded to the introduced benzyl group. Cyclic and differential pulse voltammograms reveal their characteristic redox potentials.

References

1. For a recent review, see: *Endofullerenes: A New Family of Carbon Clusters*; Akasaka, T.; Nagase, S., Eds; Kluwer Academic Publishers: Dordrecht, The Netherlands, 2002.
2. P. J. Krusic, E. Wasserman, P. N. Keizer, J. R. Morton and K. F. Preston, *Science*, 1991, 254, 1183.

Corresponding Author: Takeshi Akasaka

E-mail: akasaka@tara.tsukuba.ac.jp

TEL&Fax: +81-298-53-6409

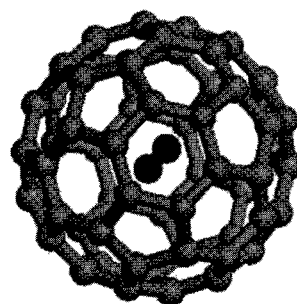
2P-13

Structure and Properties of pure $H_2@C_{60}$

○ Misaho Akada¹, Katsumi Tanigaki^{1,2}, Yasujiro Murata³, Koichi Komatsu³,
Toru Kakiuchi⁴, Hiroshi Sawa⁴

¹Graduate School of Science, Tohoku University, Sendai, 980-8578, Japan: ²CREST, Japan Science and Technology Agency, Kawaguchi, Japan: ³Institute for Chemical Research, Kyoto University, Uji, Kyoto 611-0011, Japan: ⁴Institute of Materials Structure Science, High Energy Accelerator Research Organization, Tsukuba, 305-0801, Japan

A molecular surgery technique in fullerenes has successfully produced a sufficient amount of a new hydrogen-molecule endohedral C_{60} molecule [1] for studying solid state properties. One of the important applications could be for survey of the mechanism of superconductivity in C_{60} fullerides. In the course of the studied in 1990's after the discovery of superconductivity in alkali C_{60} fullerides, the superconductivity mechanism of these family has been understood in the framework of phonon-mediated BCS formalism and the superconducting critical temperature T_c has been predominantly controlled by the density of state $N(E_F)$ at the Fermi level. However, the phonons importantly involved to make paired electrons are not confidentially discussed and the answer to the question as to what kind of phonons, intra-phonons (molecular vibrations) or inter-phonons (lattice phonons), make the greater coupling with conduction electrons still remains to be answered. One of the good ideas will be to change the intra- and the inter- phonons to a large extent without disturbing the electronic states to a large extent. We have demonstrated that a new $H_2@C_{60}$ gives rise to a pronounced influence on phonons in its solid states as well as T_c of its superconducting $K_3H_2@C_{60}$ compound compared to that in C_{60} [2]. This was in a similar tendency to that reported for $Ar@C_{60}$ [3]. In this meeting, we present the experiments of structure and properties performed using newly prepared high purity $H_2@C_{60}$.



[1] Koichi Komatsu, Michihisa Murata and Yasujiro Murata: *Science*, **307** (2005) 238-240

[2] Misaho Akada et. al., The 29th Fullerene-Nanotubes General Symposium, 2-11 (2005)

[3] S. Ito, H. Takagi et al., The 27th Fullerene·Nanotubes General Symposium, 3-9 (2004)

Corresponding Author: Misaho Akada, **E-mail:** akada@sspns.phys.tohoku.ac.jp

Tel&Fax: +81-22-795-6468/+81-22-795-6470

Structure of Fullerene Nanowhiskers (III)

○ Satoru Tsuchida, Satoru Motohashi and Hironori Ogata
 Dept. of Materials Chemistry, Hosei University
 3-7-2 Kajino cho, Koganei, Tokyo, 184-8584, Japan

The crystal structure and the nature of the molecular motion in C_{70} nanowhisker (C_{70} -NW) were investigated by powder x-ray diffraction (XRD), solid-state ^{13}C cross-polarization magic angle spinning (CP/MAS) NMR and wide-line ^{13}C - or ^1H -NMR techniques. The temperature dependence of spin-lattice relaxation time (T_1) are shown in Fig. 1. The activation energy (E_a) of C_{70} molecules is evaluated to be 13.7 kJ/mol, which is slightly smaller than that of C_{70} solid ($E_a=22\text{kJ/mol}$). This fact suggests that C_{70} molecules in C_{70} -NW are more loosely packed than those in C_{70} solid. No clear evidence of first-order phase transition is observed from 297 K to 170 K. Figure 2 shows wide-line ^1H -NMR spectra of C_{70} -NWs as a function of temperature. Two peaks observed at 8 and 2 ppm at 283 K are attributed to the methane and methyl group on the isopropyl alcohol, respectively. This fact shows that isopropyl alcohol molecules are included in C_{70} -NW crystal. Detailed results on the XRD measurements and ^{13}C - and ^1H -NMR will be presented in the conference.

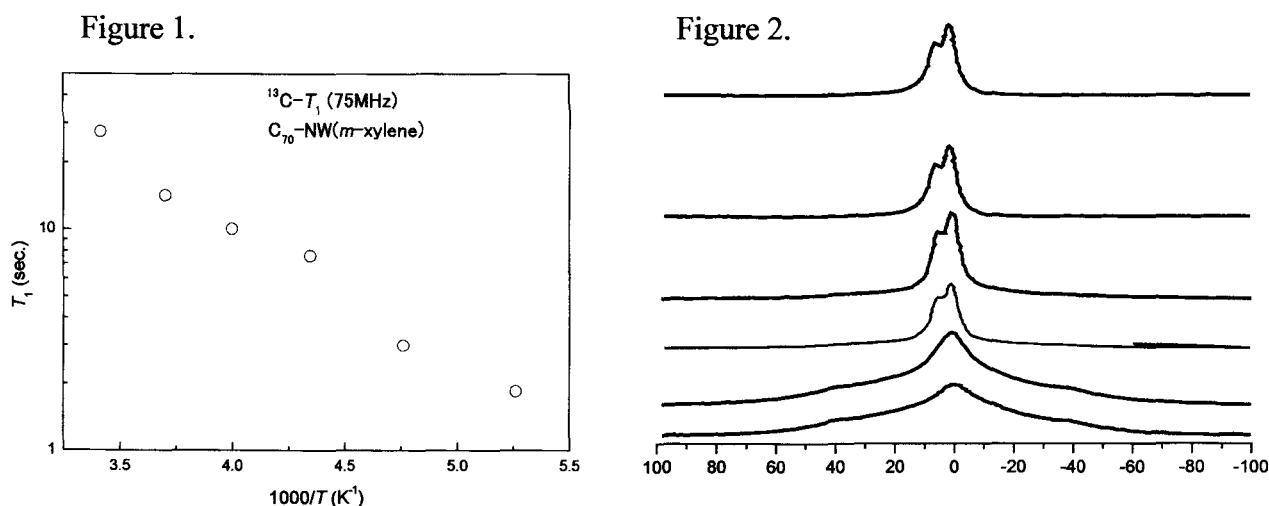


Fig 1.(a) Temperature dependence of ^{13}C - T_1 of C_{70} -NWs..

Figure 2. Temperature dependence of wide-line ^1H -NMR spectrum for C_{70} -NW

Corresponding Author: Hironori Ogata, E-mail: hogata@k.hosei.ac.jp

Tel&Fax: 042-387-6229

Synthesis and structural investigation of fulleroid nanowhiskers

○Satoru MOTOHASHI, Satoru TSUCHIDA, and Hironori OGATA

*Department of Material Chemistry, Hosei University
Kajino-cho3-7-2, Koganei, Tokyo 184-8584, Japan*

Since the discovery of C_{60} nanowhisker [1], several kinds of nanowhiskers such as C_{70} , $C_{60}[C(COOC_2H_5)_2]$ et al. were fabricated by liquid-liquid interfacial precipitation (LLIP) method [2,3]. In this study, we present the results of the synthesis and structural investigation of several kinds of fulleroid nanowhiskers.

For synthesis of the fulleroid nanowhiskers, the saturated toluene solution of 4,4'-dimethoxydiphenylfulleroid($C_{61}(C_6H_4OCH_3)_2$) purified by HPLC was prepared and poured into a glass bottle. Then isopropyl alcohol was added into the bottle to form a liquid-liquid interface. The bottle was capped and kept in the refrigerator for 2 weeks at 5°C , under illumination of a fluorescent lamp. The particles precipitated from the liquid-liquid interface were obtained. Fig.1 shows an optical microscope image of obtained sample. Needle-like crystals (nanowhiskers) were observed.

To determine the crystal structure of the sample, powder x-ray diffraction measurement were carried out using the synchrotron radiation source at BL-1B of the KEK. Fig.2 shows the x-ray diffraction patterns of $C_{61}(C_6H_4OCH_3)_2$ nanowhisker at room temperature. The profile of $C_{61}(C_6H_4OCH_3)_2$ nanowhisker can be assigned to monoclinic structure with $a=14.16\text{ \AA}$, $b=10.21\text{ \AA}$, $c=14.00\text{ \AA}$, $\beta=104.69^\circ$.

Detailed results of the structure of $C_{61}(C_6H_4OCH_3)_2$ nanowhisker and the other fulleroid nanowhiskers will be discussed at the meeting.

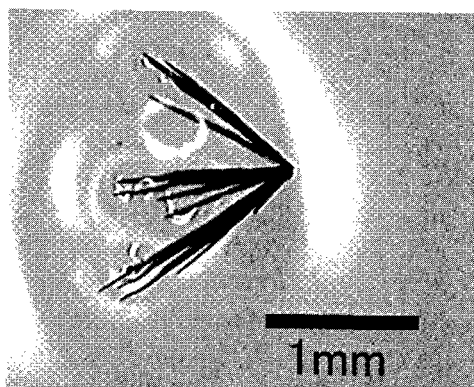


Fig.1 Optical microscope image of $C_{61}(C_6H_4OCH_3)_2$ nanowhisker

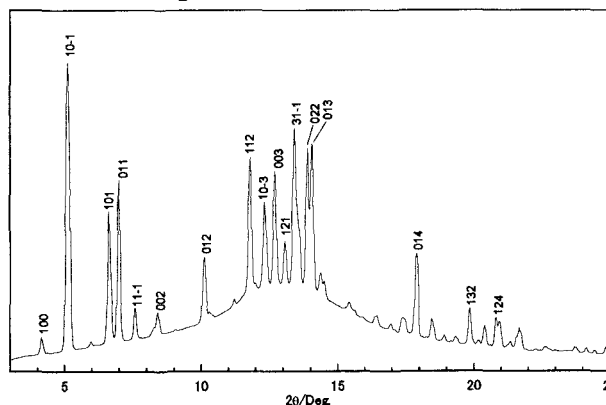


Fig.2 X-ray diffraction profile for $C_{61}(C_6H_4OCH_3)_2$ nanowhisker ($\lambda=1.0\text{ \AA}$)

Reference

- [1]K.Miyazawa et al., *J.Mater.Res.*, **17**, 83 (2002)
- [2]K.Miyazawa et al., *J.Am.Ceram.Soc.*, **85**, 1297 (2002)
- [3]K.Miyazawa et al., *J.Mater.Res.*, **18**, 2730 (2003)

Corresponding Author: Hironori OGATA

TEL&FAX: +81-042-387-6229 E-Mail: hogata@k.hosei.ac.jp

Photo-carrier generation and its transport process in pristine C₆₀ single crystals

○Ryota Tanaka, Ikuko Akimoto and Ken-ichi Kan'no

Graduate School of Systems Engineering, Wakayama University

Aiming to understanding the whole relaxation processes following optical excitation in C₆₀ crystals, we have investigated the carrier generation mechanism in connection with the photoluminescence process. From past studies, it has become clear that the carrier generation originates from thermal dissociation of Frenkel exciton^[1], and luminescence from localized exciton is enhanced by capturing the Frenkel exciton to the localized state^[2]. In the present report, to confirm anti-correlation between the carrier generation and the luminescence process^[3], we measured photocurrent and photoluminescence in one and the same crystal. The photocurrent was measured by Time-of-Flight method, and the photoluminescence through ITO electrodes and mica thin films was observed by a microspectroscopy method.

In figure 1, temperature dependence of photocurrent and photoluminescence intensities are shown by Arrhenius plot. In the range higher than 100K where the photocurrent becomes observable, the luminescence originates from radiative decay of localized exciton. The thermally activated behavior of the photocurrent exhibits anti-correlation to quenching of the photoluminescence. This relation is interpreted by that enhancement of carrier generation directly leads reduction of luminescence intensity. They can fit with the same activation energy of 99meV by assuming thermal activated population transfers from the Frenkel exciton (solid lines in Fig.1). The estimated activation energy suggests that the localized state, which exist below 120meV from the Frenkel exciton state, doesn't contribute to the carrier generation.

On the other hand, obtained time response of photocurrent is of “dispersive-type”, and almost decays as $t^{-\alpha}$ ($\alpha \sim 1$). Such response in TOF method has been attributed to anomalous dispersion of drift carriers. Carrier transport in C₆₀ crystals seems to obey a hopping process, and the obtained response suggests the existence of continuous distribution of hopping sites in barrier height and distance.

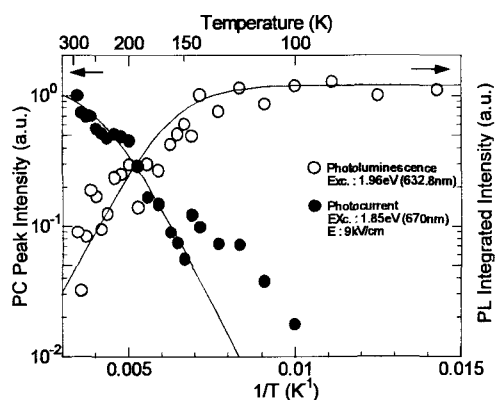


Fig.1 : Temperature dependence of photocurrent (●) and photoluminescence(○)

[1]K.Kan'no , R.Tanaka , T.Koyanagi and I.Akimoto
AIP Conf. Proceedings 786 (2005) 46

[2]I.Akimoto , K.Kan'no
J.Phys.Soc.Jpn.71 (2002) 630

[3]R.Tanaka , I.Akimoto , K.Kan'no
Abstract of the 28th Fullerene-Nanotubes General Symposium 2P-40 (2005)

Corresponding Author; Ryota Tanaka

TEL; 073-457-8295, E-mail; s053027@center.wakayama-u.ac.jp

Fabrication and Electrical Properties of FET devices

Based on C₆₀ Nano-Whiskers

○ K.Ogawa¹, A.Ikegami¹, H.Tsuji¹, T.Kato¹, N.Aoki^{1,2}, K.Adachi³,
S.Iida³, and Y.Ochiai^{1,2}

¹ Graduate School of Science and Technology, Chiba University, 1-33 Yayoi-cho,
Inage-ku, Chiba 263-8522, Japan

² Department of Electronics and Mechanical Engineering, Chiba University

³ Ichikawa Research Laboratory, Sumitomo Metal Mining Co.Ltd., 3-18-5 Nakakokubunn,
Ichikawa, Chiba 272-8588, Japan

A new type of C₆₀ needle, or “nano-whisker”, has been obtained by the liquid-liquid interfacial precipitation (LLIP) method [1]. Typical C₆₀ nano-whiskers that we obtain by LLIP are typically less than 0.3 μm in diameter and more than 50 μm in length (Fig. 1). In this work, we have fabricated C₆₀ nano-whisker based FETs (C₆₀NW-FETs) and have investigated their electrical properties, as well as performing structural characterization by x-ray diffraction, AFM, and transmission electron microscopy (TEM).

For fabricating the C₆₀ NW-FET device structure in our study, we have used a Si wafer as the substrate, with a thermally-grown SiO₂ insulating top layer. Ti/Au source and drain electrodes were fabricated on the surface of SiO₂ layer. Roughly fifty C₆₀ nano-whiskers or a C₆₀ nano-whisker were then used to bridge the electrodes and the fabricated device was annealed at 440 K under 1 × 10⁻⁶ Torr for about 24 hours.

Transistors curves for the C₆₀ NW-FET are shown at various gate voltages in Fig. 2. From this data, we conclude that the C₆₀ NW-FET is of *n*-channel enhancement-type FET, and according to standard FET theory, the carrier mobility of this C₆₀ NW-FET can be roughly estimated to be 2 × 10⁻² cm² V⁻¹ s⁻¹ under vacuum conditions at room temperature. The details of the electrical properties and structural characterization will be shown at the symposium.

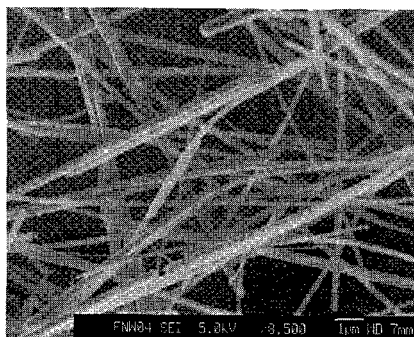


Fig. 1, SEM image showing typical C₆₀ NW

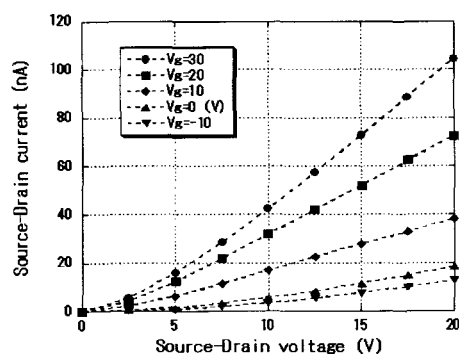


Fig. 2, Transistors curves for the C₆₀ NW-FET

[1] K.Miyazawa, Y.Kuwasaki, A.Obayashi, and M.Kuwabara: J. Mater. Res. 17, 83 (2002)

Corresponding author: Yuichi Ochiai

Tel.043-290-3428, Fax.043-290-3427, e-mail:ochiai@faculty.chiba-u.ac.jp

Deposition of platinum nano-particles on carbon nanohorn particles by electrochemistry and their magnetism

○¹Motohiro Sugaya, ¹Takayuki Inagaki, ²Masako Yudasaka, ¹Shunji Bandow, ^{1,2}Sumio Iijima

¹*Department of Materials Science and Engineering,
21st century COE Program "Nano Factory",*

Meijo University, 1-501 Shiogamaguchi, Nagoya, 468-8502, Japan

²*SORST-JST, NEC Corporation, 34 Miyukigaoka, Tukuba, 305-8501, Japan*

Deposition of Pt-nanoparticles on the nanohorn-aggregates was carried out by the electrochemistry. Samples were prepared by the following way: First, we dropped acetone liquid onto the nanohorn-aggregates and made nanohorn-paste. Then we patched this nanohorn-paste onto the Pt mesh as an electrode and dried the acetone. This nanohorn patched Pt mesh was soaked in the aqueous solution of $\text{H}_2\text{PtCl}_6 \cdot 6\text{H}_2\text{O}$ (0.0023 atomic %) and the voltage of -1.4 V was applied to the electrode. Figure 1a is the electron micrograph taken for the sample with the electrochemistry duration of 5 hours. Figure 1b is the size distribution of the Pt-nanoparticles attached on the nanohorns. From this figure, we can find the mean size of the particle is ~ 6.2 nm with FWHM of ~ 5.0 nm. According to the experiment of the reaction time dependence on the particle size, it was found that the mean size of the particles is increased with increasing the reaction time, but the number of particles on each nanohorn did not change remarkably.

Magnetism of Pt deposited nanohorn particles was also measured by SQUID susceptometer. Figure 2 shows the results of the temperature dependent magnetism. In this figure, we can see the magnetism associated with the Curie spin for the sample of pristine nanohorn particles and the magnitude of this Curie tail was decreased as the reaction time increased. This experimental fact clearly indicates that the spin concentration of nanohorns is decreased by the reaction, which may indicate that the Pt-nanoparticles can be attached on the site where the radical spin exists. Detail of the analyses will be presented in the poster.

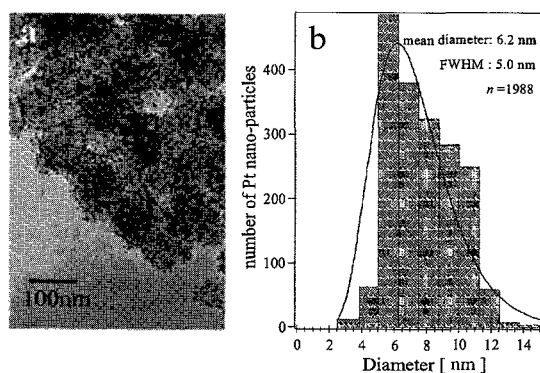


Fig.1. Electron micrograph and size distribution of Pt-nanoparticles. TEM image from the sample with the electrochemistry duration of 5 hours is shown in (a). Black small particles attached on the nanohorns are Pt nanoparticles and their size distribution is in (b).

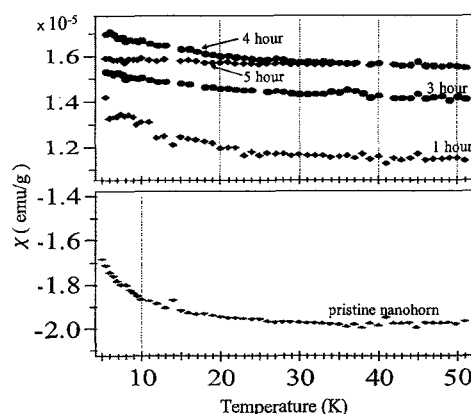


Fig. 2. Temperature dependences of magnetic susceptibility for pristine (lower panel) and Pt-deposited (upper panel) nanohorns.

Corresponding Author: Motohiro Sugaya
E-mail: m0434021@cmailg.meijo-u.ac.jp
Tel&Fax: +81-52-834-4001

**Simulation of high-energy ion/atom impact on nano-carbons:
Electronic shake up and structural change**

○Yoshiyuki Miyamoto, Arkady Krasheninnikov*, David Tománek**

*Fundamental and Environmental Res. Labs., NEC, 34 Miyukigaoka, Tsukuba
305-8501, Japan*

** Accelerator Laboratory, University of Helsinki, P.O.Box 43, FIN 00014, Finland*

*** Physics and Astronomy Department, Michigan State University, East Lansing, MI
48824-2320, USA*

We are exploring feasibility of structural modification of nano-carbons by irradiations of ions. For achieving well-designed structures, precise understanding of the atomic scale dynamics and tuning of irradiation-condition are highly demanded.

In most cases of experiment, irradiation is performed with kinetic energy in the order of KeV or 100 eV. In such energy region, an irradiated ion is expected not only to hit atoms but also to shake up electronic system. In cases where a high-energy H atom passes through or runs parallel to a graphene sheet, we have found significant stopping effect on the H atom due to 'shake-up' effect in electronic systems. This 'shake-up' can be monitored by the time-dependent density functional theory (TDDFT) approach [1] coupled with molecular dynamics (MD) simulation with use of computer code FPSEID (First-Principles Simulation tool for Electron Ion Dynamics) [2]. Meanwhile, conventional ab-initio MD method based on the static electronic-structure calculation cannot reproduce such 'shake-up' effect, and thus is not suitable for simulating the high-energy collisions.

Furthermore, we will discuss whether such 'shake-up' effect in electronic system is also the case in lower energy H-collision on graphene sheets and thin-nanotubes.

This work is supported by NAREGI Nanoscience Project, Ministry of Education, Culture, Sports, Science and Technology, Japan.

References

[1] E. Runge and E. K. U Gross, Phys. Rev. Lett. **52**, 997 (1984).

[2] O. Sugino and Y. Miyamoto, Phys. Rev. **B59**, 2579 (1999); Phys. Rev. **B66**, 89901(E) (2002).

Corresponding Author: Yoshiyuki Miyamoto

E-mail: y-miyamoto@ce.jp.nec.com

Tel&Fax: +81-29-850-1586

Tailored Synthesis of Double Walled Carbon Nanotubes by Super-Growth

○Takeo Yamada¹, Tatsunori Namai¹, Kenji Hata¹, Jing Fan², Masako Yudasaka^{2,3}
Don N. Futaba¹, Kohei Mizuno¹, Motoo Yumura¹, Sumio Iijima¹

¹*Research Center for Advanced Carbon Materials, National Institute of Advanced Industrial Science and Technology (AIST), 1-1-1 Higashi, Tsukuba, Ibaraki 305-8565, Japan*

²*Japan Science and Technology Agency, 34 Miyukigaoka, Tsukuba, Ibaraki 305-8501, Japan*

³*NEC Corporation, 34 Miyukigaoka, Tsukuba, Ibaraki 305-8501, Japan*

Double-walled carbon nanotubes (DWNT) can be considered as a blend structure of single-walled (SWNT) and multi-walled carbon nanotube (MWNT) in that they possess the electrical and thermal stability of MWNTs but also the flexibility of SWNTs. The superior physical characteristics and field emission properties of DWNTs are expected to open exciting opportunities for applications such as field emission displays and super-tough fibers.

The use and availability of DWNTs have been significantly limited because of the lack of techniques and knowledge that could realize selective growth. In addition, the low efficiency of DWNT synthesis has limited not only the availability of DWNTs but also the purity of the as-grown material, necessitating chemical purification to remove impurities.

In this presentation, we will show how one can tailor the catalysts to achieve high and maximized selective growth of DWNTs. First, a phase diagram of the relative population of SWNT, DWNT, and MWNT vs. the tube diameter grown from Fe thin films as a catalyst was constructed from hundreds of TEM images. Second, we found that the average tube diameter is roughly proportional to the thickness of the Fe thin film catalyst. Combined with the phase diagram, we arrive at a direct way to engineer the relative proportion of SWNTs, DWNTs, and MWNTs by tailoring the catalyst thickness. More importantly, we can find exactly the optimum catalyst thickness to maximize the proportion of DWNTs. Our best result is 85% DWNTs in the as-grown material, representing one of the highest, if not the highest, reported selectivity towards DWNT synthesis. Furthermore, our ability to tailor the catalyst for selective growth of DWNTs when combined with water-assisted synthesis (super-growth [1]) we can synthesize DWNTs materials that possess fascinating characteristics, such as impurity-free vertically-aligned forests on the millimeter scale that can be patterned into macroscopic organized structures. We believe our results represent a significant step forward in the DWNT field concurrently addressing critical issues, such as engineered selectivity, highly efficient growth, impurity-free material, and the realization of organized macroscopic structures. Furthermore, we anticipate that our current work will stimulate further efforts to deepen our understanding regarding this unique material.

[1] K. Hata, D. N. Futaba, K. Mizuno, T. Namai, M. Yumura, S. Iijima, *Science*, **306**, 1362 (2004).

Corresponding Author: Kenji Hata

E-mail: kenji-hata@aist.go.jp

Tel: +81-29-861-5080 ext 46763, Fax: +81-29-861-4851

Influence of Co/Mo Ratio on Synthesis of Single-Walled Carbon Nanotubes from Carbon Monoxide

○ Toshiaki Nishii^{1,2}, Suguru Noda², Hiroshi Sugime², Naoto Masuyama¹,
Yoichi Murakami² and Shigeo Maruyama²

¹*J-Power, 1-9-88 Chigasaki, Chigasaki, Kanagawa 253-0041*

²*The University of Tokyo, 7-3-1 Hongo, Bunkyo-ku, Tokyo 113-8656*

Co and Mo are often used as catalysts for the catalytic chemical vapor deposition (CCVD) synthesis of single-walled carbon nanotubes (SWNTs) on a substrate. We succeeded in synthesizing random, vertical and parallel aligned SWNTs on Co and Mo dip-coated quartz substrates from carbon monoxide (COCCVD) in 2004. But we need more detailed knowledge concerning the influence of the Co/Mo ratio on the SWNT synthesis for mass production and application to optical or electronic devices. In this study, it was evaluated by the combinatorial method [1], using a library (silicon substrate with oxide layer) of sputter-deposited Co and Mo patterns.

COCCVD was done at 800°C at 1atm using hydrogen / carbon monoxide (500 / 500 sccm) with the library and restricted SWNT formation region was confirmed by HRSEM observation and micro Raman spectroscopic analysis (Fig.1). For the comparison CCVD from ethanol (ACCVD) was done at 800°C at 12 torr. It resulted that the Co/Mo ratio for SWNT formation was large in the order of COCCVD, ACCVD and CoMoCAT [2] (Fig.2).

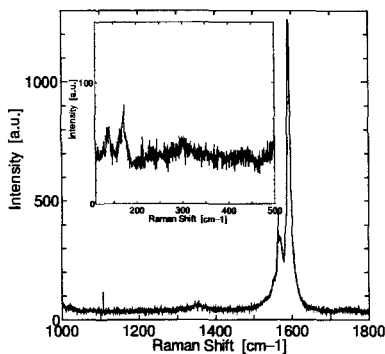


Fig.1 Raman Spectrum from COCCVD

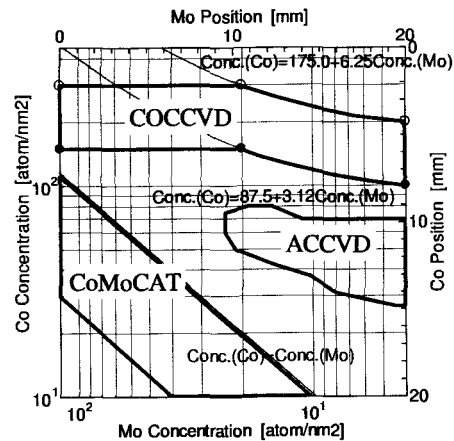


Fig.2 SWNT formation Region

[1] S. Noda, et al., Appl. Phys. Lett., 86 (2005)173106.

[2] J.E.Herrera et al., J. Catalysis 204 (2001), 129.

Corresponding Author: Shigeo Maruyama

E-mail: maruyama@photon.t.u-tokyo.ac.jp **Tel & Fax:** +81-3-5800-6983

Purification of Double Wall Carbon Nanotubes by Dispersion

OHiro-michi Yoshida¹, Satoshi Kikuchi¹, Toshiki Sugai¹, Hisanori Shinohara^{1,2,3}

¹ Department of Chemistry, Nagoya Univ. Nagoya 464-8602, Japan

² CREST, Japan Science Technology Corporation, c/o Department of Chemistry, Nagoya Univ. Nagoya 464-8602, Japan

³ Department of Chemistry & Institutes for Advanced Research, Nagoya Univ. Nagoya 464-8602, Japan

The purification of double wall carbon nanotubes (DWNTs) has revealed the importance of layer interaction and potential of DWNTs for various applications [1]. The purification with high temperature air oxidation, however, has difficulties on yields and selectivity. Recently, we have improved the method with a dispersion technique to achieve higher selectivity and yield [2]. Here, we have clarified the dispersion effect and achieved higher yield with H₂O₂ for low temperature mild oxidation.

DWNTs synthesized by the pulsed arc discharge method [1] were dispersed into sodium dodecyl sulfate (SDS) solution by sonication. The solution was mixed with excess of fumed silica and was dried to powder. This powder was refluxed at 120 °C in H₂O₂ for a day to remove SWNTs. The purified DWNTs were obtained from the powder after elimination of metal particles with HCl and of silica with saturated NaOH solution. The same procedure without dispersion was carried out with as grown crude samples.

Figure 1 shows the Raman spectra of the samples purified with dispersion (bold) and without dispersion (dash). The relative intensity between the peak around 150-170 cm⁻¹ of SWNTs and that at 214 cm⁻¹ of DWNTs is clearly enhanced by dispersion. These results are confirmed with TEM observation. Thin bundles are dominant in the dispersed sample while thick ones are in the non-dispersed sample. Figure 2 shows a TEM image of purified DWNTs with dispersion and reflux with H₂O₂ at 120 °C for 3 days. The purity is about 95 % and yields are enhanced by several times compared to that of air oxidation. These results clearly show that the dispersion is the key process to purify DWNTs and that reflux in H₂O₂ is effective to purify DWNTs as well as SWNTs, which has been commonly used.

[1] T. Sugai et al., *Nano Lett. (Comm.)*, **3**, 769 (2003)

[2] T. Sugai et al., *29th F&NT symposium*, 3-5 (2005)

Corresponding Author : Hisanori Shinohara

E-mail : noris@cc.nagoya-u.ac.jp

Tel : 052-789-2482 Fax : 052-789-1169

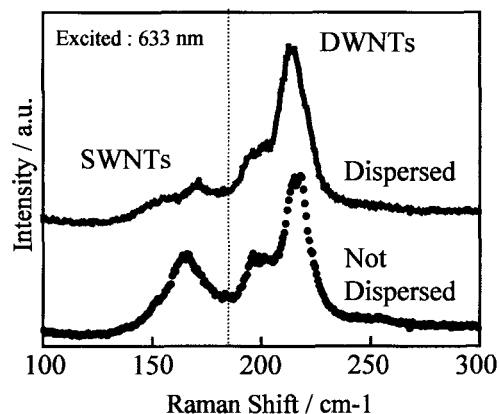


Fig.1 RBM of purified soot

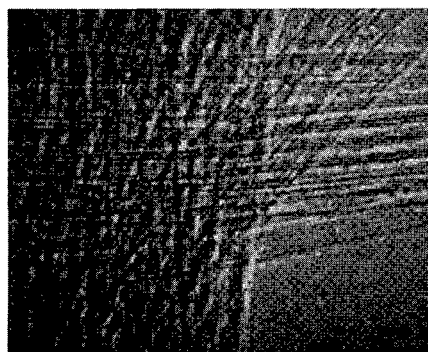


Fig.2 TEM image of DWNTs purified by dispersion method

Synthesis of single-wall carbon nanotubes by alcohol CCVD methods using mesoporous silica with different pore size

○Yuya Izumi and Hironori Ogata

Department of Materials Chemistry, Hosei University, Kajinocho, Koganei, Tokyo 184-8584, Japan

The alcohol catalyst chemical vapor deposition (ACCVD) method has been reported as one of the simplest synthesis methods of single-walled carbon nanotubes (SWNTs) [1]. Many of the support materials to synthesize SWNTs reported are zeolite. It is well known that MCM-41 has a regular mesopore system, in which the pore diameter is controlled systematically between 2-10 nm. We report here the synthesis of SWNTs by ACCVD methods with metal catalysts supported with high temperature stable mesoporous silica by surfactant-directed sol-gel method [2] to clarify the relation between pore size and the diameter of the resultant SWNTs obtained. The obtained samples were analyzed by using transmission electron microscopy (TEM).

Figure 1 shows the TEM image of the sample with Fe/Co catalysts with mesoporous silica (surfactant: C₁₆TMABr, pore size: 3 nm) with the reaction temperature at 800°C. Bundles of SWNTs are observed. Average diameter of SWNTs is evaluated to be about 1 nm. However, SWNTs of a diameter of 2.8 nm are also observed.

Detailed results using another mesoporous silica with different pore size will be presented.

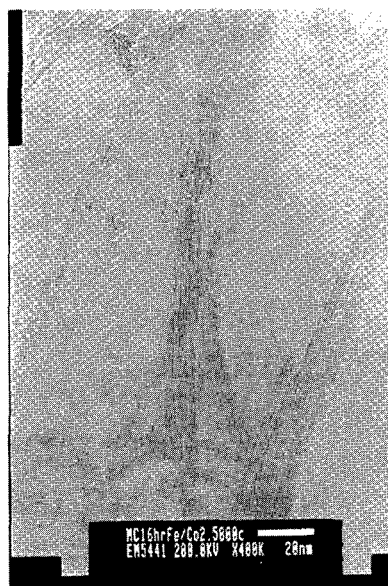


Fig.1 TEM image of SWNTs(C₁₆TMABr)

[1] S.Maruyama, R. Kojima, Y.miyauchi, S.Chiashi,M.Kohno,Chem.Phys.Lett..360,229(2002)

[2] M.Grün, Klaus.K.Unger, A.Matsumoto, K.Tsutsumi, Micro.Meso.Mater..27,207(1999)

Corresponding Author Hironori Ogata Email hogata@k.hosei.ac.jp Tel: 042-387-6172

Dispersion and Separation of Small Diameter Single-Walled Carbon Nanotubes

○Makoto Kanda,¹ Yutaka Maeda,² Shin-ichi Kimura,¹ Tadashi Hasegawa,² Yongfu Lian,¹ Takatsugu Wakahara,¹ Takeshi Akasaka,¹ Said Kazaoui,³ Nobutsugu Minami,³ Toshiya Okazaki,³ Tetsuo Shimizu,³ Hiroshi Tokumoto,⁴ Jing Lu,⁵ Shigeru Nagase,⁶

¹Center for Tsukuba Advanced Research Alliance, University of Tsukuba, Tsukuba 305-8577, Japan, ²Department of Chemistry, Tokyo Gakugei University, Koganei 184-8501, Japan, ³National Laboratory of Advanced Industrial Science and Technology, Tsukuba 305-8565, Japan, ⁴Research Institute for Electronic Science, Hokkaido University, Sapporo 060-0812, Japan, ⁵Department of Physics, Peking University, Beijing 100871, People Republic of China, ⁶Department of Theoretical Molecular Science, Institute for Molecular Science, Okazaki 444-8585, Japan

Single-walled carbon nanotubes (SWNTs) have excellent mechanical and electrical properties that have led to the proposal of many potential applications. However, SWNTs are typically grown as the bundles of metallic and semiconducting tubes and this hinders their widespread applications. Since there is no method for selective preparation of metallic and semiconducting SWNTs, it is technologically critical to separate SWNTs based on electrical properties.

Recently, an effective exfoliation method of SWNTs in organic solvents with amine as a dispersion reagents [1] and a convenient amine-assisted separation method for SWNTs that makes metallic SWNTs remarkably enriched in a simple way [2] have been developed. We herein report the dispersion and separation of small diameter SWNTs by amine-assisted method.

A typical dispersion procedure is as follows: 1mg of AP-SWNTs (CoMoCAT) were added to 10 mL of a 1.0 M tetrahydrofuran (THF) solution of amine and then sonicated followed by centrifugation to remove non-dispersible SWNTs. This dispersion and centrifugation process is useful for separation of small diameter SWNTs by means of Vis-NIR, photoluminescence, and Raman spectroscopy.

[1] Maeda, Y. *et al.*, *J. Phys. Chem. B* **2004**, *108*, 18395.

[2] Maeda, Y. *et al.*, *J. Am. Chem. Soc.* **2005**, *127*, 10287.

Corresponding Author: Takeshi Akasaka

TEL: +81-29-853-6409, FAX: +81-29-853-6409, E-mail: akasaka@tara.tsukuba.ac.jp

Synthesis and characterization of single-walled carbon nanotubes by catalytic decomposition of alcohol

Yanli Zhao^{1,2}, Kazuyuki Seko¹, Kensuke Okumura¹ and Yahachi Saito¹

¹Department of Quantum Engineering, Nagoya University, Furo-cho, Nagoya 464-8603

²Venture Business Laboratory, Nagoya University, Furo-cho, Nagoya 464-8603

To produce high quality single-walled carbon nanotubes (SWNTs) with chemical vapor deposition (CVD) synthesis approach, choice of alcohol over other hydrocarbons is important due to its low cost, high purity and high efficiency, even at low temperatures [1]. In our alcohol CVD experiments, Co and Mo bimetallic catalysts with and without Al underlayer are prepared by vacuum deposition. Three kinds of catalysts/substrates i.e., (1) Si/SiO₂ (100 nm)/Co (1 nm)/Mo (1 nm), (2) Si/Al (10 nm)/SiO₂ (100 nm)/Co (1 nm)/Mo (1 nm), and (3) Si/SiO₂ (100 nm)/Co (2 nm)/Mo (1 nm) were examined. Figures 1 (a)-(c) show SEM images after CVD process (alcohol pressure 10 Torr, temperature 750 °C, and duration 60 min) for above substrates, respectively. Comparison between Fig. 1a and Fig. 1b reveals that the introduction of Al increases SWNTs' yield. In Fig. 1c, where Co thickness is twice as that of substrate (1), the yield of SWNTs is reduced. This reduction maybe is due to the large size of catalysts. Atomic force microscope (AFM) images of the substrates (1) and (2) heated at 750 °C in vacuum before CVD are shown respectively in Figs. 2a and 2b, in which different particle sizes are observed. We think the observed large particle size in Fig. 2b is from Al particle aggregation. When the substrate are heated to high temperature, the Al layer melts and forms droplets which absorb from the SiO₂ layer and oxidize quickly to form thermally stable Al₂O₃ clusters. These in turn provide the support for the formation of catalysts nano-particles and promote SWNTs growth [2]. Raman spectra are also measured and SWNTs are identified from their RBM peaks, with diameters changing from 1.20-1.30 nm, which is consistent with TEM characterizations.

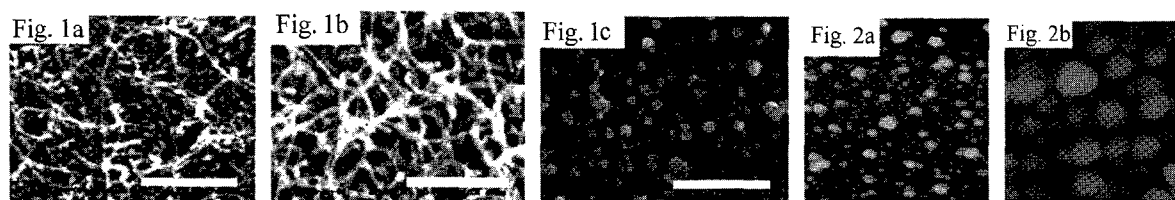


Fig. 1 a-c

Scan bar is 500 nm

Fig. 2 a—b

Images size: 1 μm × 1 μm

[1] Shigeo Maruyama et al., Chem. Phys. Lett. 360 (2002) 229. [2] Ruth Y. Zhang et al., Nano Lett. 3 (2003) 731

Corresponding Author: Yanli Zhao, Yahachi Saito

E-mail: zhao@surf.nuqe.nagoya-u.ac.jp, ysaito@surf.nuqe.nagoya-u.ac.jp

Tel&Fax: +81-52-789- 4459, +81-52-789- 3703

2P-26

Supported Ni catalysts of nominal submonolayers grew single-walled carbon nanotubes.

○Kazunori Kakehi¹, Suguru Noda¹, Shohei Chiashi² and Shigeo Maruyama²

¹*Department of Chemical System Engineering, The University of Tokyo,
7-3-1 Hongo, Bunkyo-ku, Tokyo 113-8656, Japan*

²*Department of Mechanical Engineering, The University of Tokyo,
7-3-1 Hongo, Bunkyo-ku, Tokyo 113-8656, Japan*

Fe, Co, and Ni is known catalytically effective to grow carbon nanotubes (CNTs). However, when Ni is supported on substrates, it comes to yield just multi-walled CNTs (MWNTs) but not single-walled CNTs (SWNTs). This characteristic may be understood when we consider the possible surface diffusion of metals at the elevated temperatures of chemical vapor deposition (CVD). Over oxide surfaces such as SiO₂, which are often used as supports for these metals, oxidative interaction dominates the metal/support interaction, which affects island structures and surface diffusion of metals [1]. Because Ni has the smallest heat of oxidation among these metals, it can easily diffuse over oxide surfaces at the CVD temperatures, and possibly results into particles too large to grow SWNTs.

If the amount of Ni is limited to 1 nm³ per the area of surface diffusion, it should spontaneously form 1-nm-sized particles. By using our combinatorial method [2], we prepared a thickness profile of Ni on a SiO₂/Si or SiO₂ wafer and carried out alcohol catalytic CVD (ACCVD, [3]) at 800 °C. Micro-Raman spectra as well as field-emission scanning electron microscope (FE-SEM) images showed the formation of SWNTs and nominal submonolayers was optimal to grow SWNTs.

[1] M. Hu, S. Noda, and H. Komiyama, *Surf. Sci.* **513**, 530 (2002).

[2] S. Noda, Y. Tsuji, Y. Murakami, and S. Maruyama, *Appl. Phys. Lett.* **86**, 173106 (2005).

[3] S. Maruyama, R. Kojima, Y. Miyauchi, S. Chiashi, and M. Kohno, *Chem. Phys. Lett.* **360**, 229 (2002).

Corresponding Author: Suguru Noda

E-mail: noda@chemsys.t.u-tokyo.ac.jp

Tel: +81-3-5841-7330 Fax: +81-3-5841-7332

Preparation of Single-Wall Carbon Nanotubes with Rh/Pd -Carbon Composite Rods in Nitrogen Atmosphere

○Nobuyuki Asai¹, Shinzo Suzuki¹, Hiromichi Kataura², and Yohji Achiba¹

¹*Department of Chemistry, Tokyo Metropolitan University, Tokyo 192-0397, Japan*

²*Nanotechnology Research Institute, National Institute of Advanced Industrial Science and Technology (AIST), Central 4, Higashi 1-1-1, Tsukuba, Ibaraki 305-8562, Japan*

The diameter distribution of single-wall carbon nanotubes (SWNTs) prepared by laser vaporization technique strongly depends on the kind of metal catalyst and the ambient temperature. A characteristic example is, those prepared with Rh/Pd-carbon composite rods in Ar gas atmosphere at lower ambient temperature (1200°C or less) [1]. They show the smaller diameter distribution (less than 1 nm), almost comparable to that of C₆₀ or other higher fullerenes. On the other hand, the yield of SWNTs prepared by laser vaporization in nitrogen gas atmosphere becomes higher than those prepared in Ar gas atmosphere [2]. It is interesting to see whether the diameter distribution of SWNTs and/or the yields of co-prepared empty higher fullerenes become different from those obtained in Ar gas atmosphere.

In this presentation, Rh/Pd(1.2/1.2atom%)-carbon composite rods were used for the preparation of SWNTs by applying laser furnace technique in nitrogen gas atmosphere. Fig. 1 shows a Raman spectrum of the raw soot prepared at 1150°C in 750 torr nitrogen gas atmosphere. The figure indicates that there exist SWNTs having several different diameters, including larger ones (more than 1nm). The analysis of empty higher fullerenes co-prepared with SWNTs is also presented and used for further discussion.

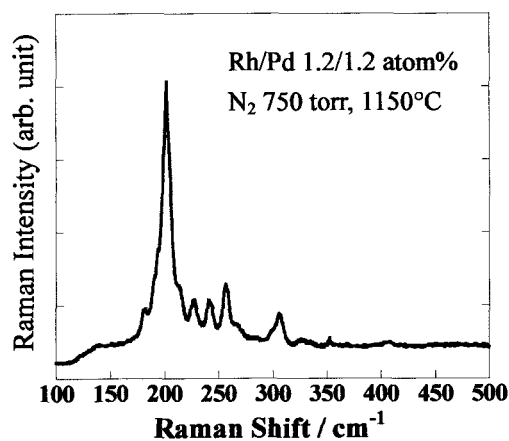


Figure 1.

This study was partly supported by Industrial Technology Research Grant Program from New Energy and Industrial Technology Development Organization (NEDO) of JAPAN, and the Grants-in-Aid for Scientific Research (B) (No.16351104) from MEXT.

References:

[1] H. Kataura et al., *Carbon.*, **38**, 1691-1697(2000). [2] D Nishide et al., *Chem. Phys. Lett.*, **309**, 392(2004).

Corresponding Author: Shinzo Suzuki

E-mail: suzuki-shinzo@c.metro-u.ac.jp **Tel:** +82-426-77-2533 **Fax:** +81-426-77-2525

Role of Bimetallic Catalysts for Growth of Single-Walled Carbon Nanotubes

○ Toshiya Murakami¹, Kazuya Mitikami¹, Satoru Ishigaki¹, Kazuyo Matsumoto¹, Kenji Kisoda², Koji Nishio¹, Toshiyuki Isshiki¹, and Hiroshi Harima¹

¹*Dept. Electronics and Information Science, Kyoto Institute of Technology, Kyoto 606-8585, Japan*

²*Wakayama University, Wakayama 640-8510, Japan*

To obtain single-walled carbon nanotubes (SWNTs) with controlled chirality is of much importance to realize electronic devices based on them. In the case of chemical vapor deposition (CVD), the size of catalytic particle is an important factor in controlling the diameter of SWNTs [1]. Earlier reports claimed that bimetallic catalysts like Co-Fe [2] and Co-Mo [3] tended to form small particles similar to the diameter of SWNTs in comparison with single element catalysts.

We focused on the role of bimetallic catalytic particles after reduction in CVD process. Transmission electron microscopy observations were performed to compare the particles sizes formed by bimetallic catalysts Co-Fe with these by single elemental catalysts Co or Fe on Si/SiO₂ substrates and SiO₂ powders. The figure shows the size distributions of catalytic particles. We confirmed that bimetallic Co-Fe catalysts system tended to form smaller particles than single elements (Co) catalysts. In addition, after CVD process, the quantity of SWNTs was larger using the bimetallic system. In the case of the growth of SWNTs on Si/SiO₂ substrates using Co-Fe catalysts, thin layer formed by Fe between small Co particles and SiO₂ after reduction. We propose a model as follows: Fe particles diffuse into SiO₂ layer and form the layer contained Fe. The layer prevented Co from aggregating into large particles and from alloying Co silicide which is inactive as a catalysts.

[1] T. Saito, *et al.*, J. Phys. Chem. B, **109**, 10647 (2005)

[2] P. Coquay, *et al.*, J. Phys. Chem. B, **109**, 17813 (2005)

[3] Y. Murakami, *et al.*, Jpn. J. Appl. Phys. **43**, 1221 (2004)

Corresponding Author: Toshiya Murakami

E-mail: dj990101@djedu.kit.ac.jp

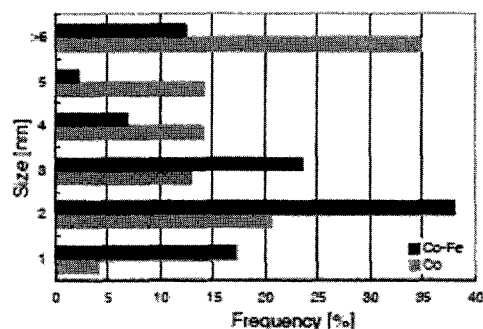


Figure: Size distributions of bimetallic Co-Fe and single element (Co) catalysts on SiO₂ powder after reduction.

Formation process of carbon nanocap from SiC(0001) surface through thermal decomposition

○T. Maruyama^{1,2}, Y. Kawamura¹, H. Bang², N. Fujita¹, T. Shiraiwa¹, K. Tanioku¹,
Y. Hozumi¹, S. Naritsuka^{1,2} and M. Kusunoki³

¹*Dept. of Materials Science & Engineering, Meijo Univ. Nagoya 468-8502, Japan*
²*Meijo Univ. 21st CENTURY COE program "Nano Factory", Nagoya 468-8502, Japan*
³*Japan Fine Ceramics Center, Nagoya 456-8587, Japan*

Aligned zigzag-type carbon nanotubes (CNTs) with fairly uniform tube diameters can be selectively produced only by heating SiC(0001) at sufficient high temperature in a vacuum. Although nanosized cap structures are observed at the initial stage of CNT growth, a detailed process of the carbon nanocap formation has not yet been clarified. In this study, we investigated the decomposition of 6H-SiC(0001) surface and the formation process of carbon nanocap during heating using ultrahigh vacuum scanning tunneling microscopy (UHV-STM) and X-ray photoelectron spectroscopy (XPS).

After being etched with hydrofluoric acid (10%), 6H-SiC(0001) samples were annealed in UHV. The annealing temperature was increased from 400 to 1250°C in increments of 50°C. During heating, the chamber pressure was kept below 1×10^{-6} Pa. After STM observation, XPS measurements were performed to investigate the surface composition.

Si 2p and C 1s XPS spectra for SiC(0001) after heating at 1000°C showed that both evaporation of residual oxides and decomposition of the SiC surface occur below 1000°C, in contrast to the case of heating in a vacuum electric furnace [1]. Figure 1 shows topographical STM images of SiC(0001) after heating at 1100, 1150 and 1200°C SiC(0001). These results show that carbon nanocaps were formed by coalescence of the amorphous carbon nanoparticles in the clusters, followed by crystallization.

[1] T. Maruyama et al. The 29th Fullerene & Nanotube General Symposium, 2P-21 (2005).

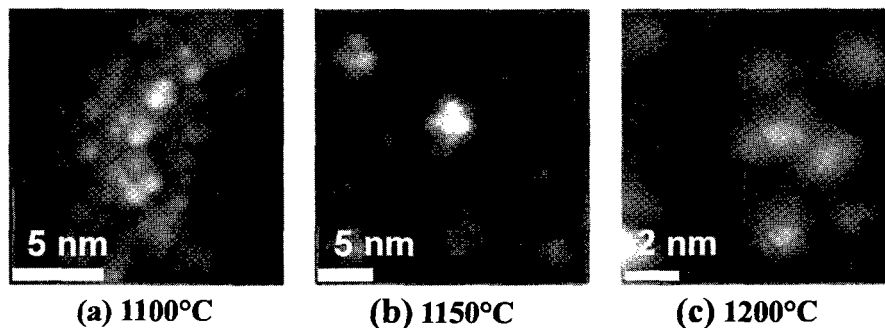


Fig. 1

Encapsulating p-nitroaniline into Single-Walled Carbon Nanotube

○ Takashi Murakami^{1,2}, Yuika Saito², Hiromichi Kataura³, Kazuhito Tsukagoshi²,
Kazuhiro Yanagi³, Yasumitsu Miyata^{3,4}, and Satoshi Kawata^{2,5}

¹*Department of Physics, Gakushuin University, Mejiro, Toshima-ku, Tokyo 171-8588, Japan*

²*RIKEN (The Institute of Physical and Chemical research), Wako, Saitama 351-0198, Japan*

³*National Institute of Advanced Science and Technology (AIST), Nanotechnology Research Institute, Tsukuba, 305-8562, Japan*

⁴*Graduate School of Science, Tokyo Metropolitan University, Hachioji 192-0397, Japan*

⁵*Department of Applied Physics, Osaka University, Suita, Osaka 565-0871, Japan*

Single-walled carbon nanotube (SWNT) can encapsulate various organic molecules. However, these small molecules are not stable inside of SWNTs, because small molecules are easy to go out from SWNTs by heat treatment in vacuum followed by solvent treatment. So small molecules encapsulated in SWNTs have difficulties for practical applications as it is.

Since C₆₀ takes relatively stable state in the SWNT, we propose to use C₆₀ as a “cap” for nanotubes in which small unstable molecules are encapsulated. The C₆₀ behaves as sealing cap of small molecules in SWNTs. In the cleaning process such as heating in vacuum and solvent treatment, encapsulated small molecules won't go out from SWNTs.

We used p-nitroaniline (PNA), which is small in size and have strong Raman signal, as the target molecules. Fig.1 shows Raman spectra of PNA encapsulated SWNTs using C₆₀ (PNA-C₆₀@SWNTs) and without using C₆₀ (PNA@SWNTs). After encapsulation, these samples are washed to remove outer molecules of SWNTs. Only spectrum of PNA-C₆₀@SWNTs, PNA peak is observed.

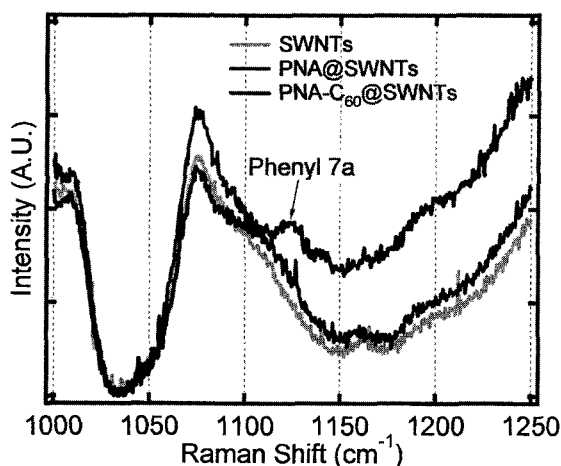


Fig.1 Comparison of Raman spectra of PNA encapsulated SWNTs.

Excitation: 488nm, exposure time: 1000sec.

Corresponding Author: Yuika Saito

E-mail: yuika@riken.jp

Tel: 048-467-9339, Fax: 048-462-4653

Formation of *n*-type double-walled carbon nanotubes by a Cs-plasma irradiation method

○Y. F. Li, T. Izumida, R. Hatakeyama, T. Kaneko, T. Okada, and T. Kato

Department of Electronic Engineering, Tohoku University, Sendai 980-8579, Japan

In recent years, carbon nanotubes field-effect transistors (FETs) are intensively investigated in both experiments and theory. However, the current research on carbon nanotubes FETs is mainly focused on the single-walled carbon nanotubes (SWNTs) and multi-walled carbon nanotubes (MWNTs). In contrast, electronic transport properties of double-walled carbon nanotubes (DWNTs) have rarely been studied due to difficulties in yielding them with high purity [1]. As an intermediate between MWNTs and SWNTs, DWNTs have attracted much attention of numerous scientists during the past several years because it is believed that DWNTs have novel structural, mechanical and electronic properties when compared to those of SWNTs and MWNTs. In this sense, DWNTs may provide an ideal carbon nanotubes system for fabricating novel molecular devices. Nevertheless, it remains an open question as to what the characteristics of DWNTs-based FETs may be in detail and how to improve their electronic properties until now. In this regard, much more work is still needed to systematically investigate the transport properties of DWNTs.

In this work, functional DWNTs with *n*-type semiconducting behavior are created by Cs encapsulation via a plasma irradiation method [2]. The structure and morphologies of Cs-encapsulated DWNTs are confirmed by several technologies which include HRTEM, EDX, and Raman Spectrum analyses. Figure 1 gives a TEM image of the Cs-encapsulated DWNT. Electronic properties of DWNT-FET indicate pristine DWNTs are found to exhibit both *p*- and *n*-type semiconducting behavior, and typically show a lower conductance in *n*-channel than in the *p*-channel. For comparison, an interesting conversion from ambipolar to high performance *n*-type semiconducting behavior is found for Cs-encapsulated DWNTs-based FET devices. Figure 2 depicts a current versus voltage (I_{DS} - V_G) characteristic of the *n*-type Cs-encapsulated DWNT-FET.

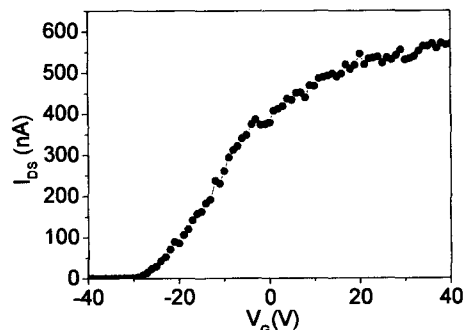
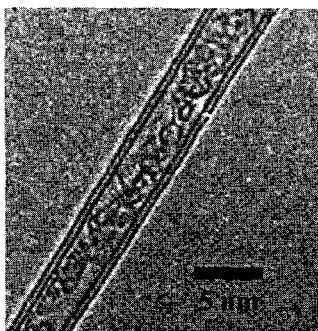


Fig. 1. A TEM image of Cs-encapsulated DWNT Fig. 2. A I_{DS} - V_G curve for *n*-type Cs-encapsulated DWNTs

[1] T. Shimada et al., *Appl. Phys. Lett.* **84**, 2412 (2004).

[2] Y. F. Li et al., Abstract of 29th Fullerene General Symposium, 2P-27 (2005).

Corresponding Author: Yongfeng Li, **E-mail:** yfli@plasma.ecei.tohoku.ac.jp

Tel & Fax: 81-22-795-7046/263-9225

Magnetic Analysis of Nano-peapods by Soft X-ray Magnetic Circular Dichroism (MCD) Spectroscopy

○Ryo Kitaura¹, Haruya Okimoto¹, Tetsuya Nakamura², Yutaka Kitamura, Daisuke Ogawa and Hisanori Shinohara^{1,4,5}

¹*Department of Chemistry, Nagoya University, Nagoya 464-8602, Japan*

²*JASRI-the Spring-8, Hyogo 679-5198, Japan*

³*Institute of Industrial Science, Tokyo University, Tokyo 106-8558, Japan*

⁴*Institute for Advanced Research, Nagoya University, Nagoya 464-8602, Japan*

⁵*CREST, Japan Science and Technology Corporation, c/o Department of Chemistry, Nagoya University, Nagoya 464-8602, Japan*

Nano-peapods have attracted wide scientific attention owing to their unusual structural and electric properties, as well as commercial interests due to their potential applications in field effect transistors.^[1] One of the most interesting aspects of nano-peapods is that they possess one-dimensional crystalline arrays of endohedral metallofullerenes in carbon nanotubes. Intermolecular distances of encapsulated endohedral metallofullerenes are much shorter than that of bulk crystals, and this affects magnetic properties greatly. However, the investigation of magnetic properties of encapsulated metallofullerenes is very difficult due to ferromagnetic impurities such as Co and Ni particles, which are used as carbon nanotube synthesis catalyst. Here we report element specific magnetization of encapsulated endohedral metallofullerenes by using soft x-ray magnetic circular dichroism at SPring-8 BL25SU. A high brilliance synchrotron soft x-ray radiation source enables us to obtain MCD signals from very small amounts of samples (several micrograms).

Figure 1 shows synchrotron powder X-ray diffraction patterns of empty single-walled carbon nanotubes and Gd@C₈₂ nano-peapods. Observed reduction of (10) peak intensity represents that Gd@C₈₂ molecules are encapsulated in SWNT in high-yield. New diffraction peak, which is marked by an arrow in Fig 1, represents intermolecular distances of Gd@C₈₂ in SWNT. The obtained intermolecular distance is 10.5 Å, which is much shorter than that of bulk Gd@C₈₂ crystal. MCD spectrum measured in a magnetic field 2.0 T in the high-temperature range (50 > T > 13 K) revealed that magnetization of Gd ions follows the Curie law and suggesting the presence of ferromagnetic interactions between the Gd atoms.

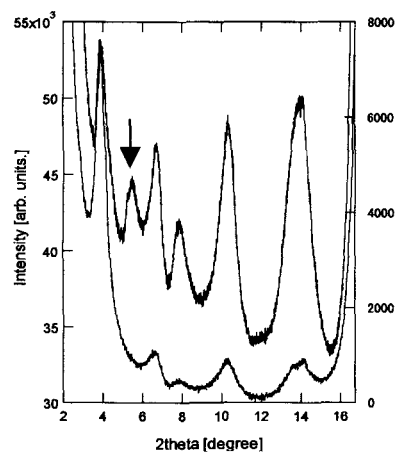


Figure 1. Powder x-ray diffraction patterns of Gd@C₈₂ peapod (upper pattern) and empty SWNT.

[1] T. Shimada, T. Okazaki, R. Taniguchi, T. Sugai, H. Shinohara, et al, App. Phys. Lett., **81**, 4067 (2002).

Corresponding Author: Hisanori Shinohara

TEL: +81-52-789-2482, FAX: +81-52-789-1169, E-mail: noris@cc.nagoya-u.a.jp

High Yield Purification of Carbon Nanohorn

○Goshu TAMURA, Shunji BANDOW, and Sumio IJIMA

21st Century COE Program "Nano Factory"
Department of Materials Science and Engineering
Meijo University

1-501 Shiogamaguchi, Tenpaku, Nagoya 468-8502, Japan

Abstract: When we measure TGA of as-grown nanohorn (made by laser ablation), there are 2 major components that have peaks of differential curve at about 900 K and 1,100K. The lower temperature component indicates nanohorns, and higher one indicates GG (Giant-Graphitic) balls. GG balls are impurities and are made in the process of production of nanohorn. In products, 10-20 % of GG balls are contained.

After following procedure: ultrasonic dispersion in ethanol, centrifugal separation, and drying treatment by rotary evaporator, we did TGA measurement both the supernatant and the precipitation.

If we directly measured TGA after dipped into ethanol, both of the peaks were shifted lower (than as-grown) by 50-150 K. The shift would be caused by the effect of ethanol. If we cure the effect of ethanol, we should conduct a treatment in H₂ at 1473 K for 1 hour. Then only the component of nanohorns was remained in the supernatant. Although both components of nanohorns and GG balls appeared in the precipitation, the relative ratio of nanohorns and GG balls was changed to 2: 8. Therefore, it was found that the separation of nanohorns and GG balls can be achieved by the combination processes of ultrasonic dispersion and centrifugal separation.

When we want to separate nanohorns and GG balls more easily, centrifugal separation is not necessary. After ultrasonic dispersion, solution must be left at rest more than 12 hours. GG balls are settled down by gravitational sedimentation, then supernatant, which consists of almost nanohorn only, can be sucked up carefully using pipette. Purity of nanohorn in the suspension is in excess of 99 weight percent. This way of separation is very easy to yield high purity nanohorns.

Corresponding Author Goshu TAMURA

E-mail : m0441505@ccmailg.meijo-u.ac.jp

Tel&Fax: 052-834-4001

Fractionation of Arc-Soot and Dispersion of Pu-Ru Catalysts. (Reactivity with Methanol)

○ K. Higashi¹, A. Niwa¹, K. Shinohara¹, H Takikawa¹, T. Sakakibara¹,
G. Xu², S. Itoh³, T. Yamaura³, K. Miura⁴, K. Yoshikawa⁴

¹*Department of Electrical and Electronic Engineering,
Toyohashi University of Technology*

²*Shonan Plastic Mfg. Co., Ltd.*

³*Product Development Center, Futaba Corporation*

⁴*Fuji Research Laboratory, Tokai Carbon Co., Ltd.*

Carbon nanohorn (CNH) is considered to be a candidate of conductive support of metal catalyst particle for the electrode of direct methanol fuel cell (DMFC)^[1]. CNH can be synthesized by not only laser ablation method^[2] but also anodic arc discharge method^[3]. In the case of anodic arc discharge method, CNH can be found in the arc-soot evaporated from anode and deposited on the apparatus wall or caught in ambient media like water, when the arc is operated at around atmospheric pressure with nitrogen dominant ambient. However, there is usually coexistence of non-CN H particle in the arc-soot. Moreover, non-dahlia-like CNH may not be more suitable for the support than dahlia-like CNH.

In the present study, in order to investigate the influence of co-product in the arc-soot on dispersion of catalyst particle, the arc-soot was separated into larger graphitic macro-particle and smaller nano-particles. Pt-Ru particle was dispersed on three types of arc-soot: as-prepared arc-soot, graphitic macro-particle, and nano-particle. From TEM observation and simple test of reaction activity with methanol, it was found that the as-prepared arc-soot was most preferable. Figure 1 shows the as-prepared arc-soot with Pt-Ru dispersion.

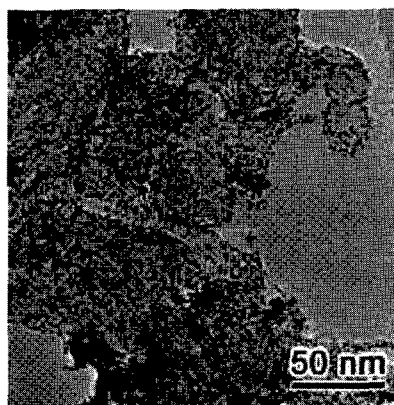


Fig.1 TEM micrograph of as-prepared arc-soot with Pt-Ru dispersion.

[1] T. Yoshitake, *et al.*: *Physica B.*, **323**, 1627 (2002)

[2] S. Iijima, *et al.*: *Chem. Phys. Lett.*, **309**, 165 (1999)

[3] G. C. Xu, *et al.*: *New Diamond Front. Carbon Technol.*, **15**, pp.73-81 (2005)

Corresponding Author: Keisuke Higashi, Hirofumi Takikawa

TEL: +81-532-44-6644, FAX: +81-532-44-6644, E-mail: higashi@arc.eee.tut.ac.jp

TEL: +81-532-44-6727, FAX: +81-532-44-6727, E-mail: takikawa@eee.tut.ac.jp

Stability of Field Emission Current from a Carbon Nanotube

○Y. Konishi¹, H. Tanaka¹, L. Pan^{1*}, S. Akita¹ and Y. Nakayama^{1,2}

¹Department of Physics and Electronics, Osaka Prefecture University, 1-1 Gakuen-cho, Sakai, Osaka 599-8531, Japan

²Handai Frontier Research Center, Graduate School of Engineering, Osaka University, 2-1 Yamadaoka, Suita, Osaka 565-0871, Japan

The stability of field emission from carbon nanotubes (CNTs) is very important for application of CNTs to electron emitters of field emission display (FED). In order to clarify the main reasons resulting in the instability of electron emission, the field-emission properties of a single CNT have been investigated by using a field emission microscope (FEM)[1]. We report the current fluctuation for individual double-wall carbon nanotubes (DWNTs), which exhibits excellent properties as field emitters.

Figure 1 shows the temporal current fluctuations for a DWNT at several fixed voltages in a vacuum of 10^{-7} Pa. The average current fluctuations (standard deviation) for an hour under the emission levels of 10^{-6} , 10^{-7} , 10^{-8} , 10^{-9} and 10^{-10} A are approximately 7.2%, 26.3%, 0.7%, 1.5% and 1.7%, respectively. It is observed that the emission current becomes unstable when the emission level is increased from 10^{-8} to 10^{-7} A. Although the reasons for this phenomenon, including the thermal noises, thermoelectric effect, are complicated and are needed to be further investigated, the result itself indicates that the average emission current for an individual CNT in emitter arrays for an FED should be designed to be less than 10^{-7} A.

Besides the emission level, the pressure and the kinds of residual gases are considered to be the main factors affecting the stability of field emission. Fig.2 (a) and (b) show the current fluctuation at the level of 10^{-8} A measured at the pressures from 10^{-7} to 10^{-4} Pa, respectively, by introducing N_2 with or without an amount of H_2O . It is found that the current fluctuation increases largely when the pressure increases from 10^{-5} to 10^{-4} Pa because of the obvious effect of adsorption and desorption of the gas molecules. Compared with that without introducing H_2O , the field emission in the case of introducing H_2O is relatively unstable, suggesting that H_2O has a larger effect than N_2 [2] and should be removed in the process of FED fabrication.

Acknowledgement: This work was supported by CNT-FED project of NEDO.

References: [1] H.Tanaka *et al.*, Jpn. J. Appl. Phys. **43**, L1651(2004). [2] K. A. Dean and B. R. Chalamala, Appl. Phys. Lett. **75**, 19 (1999).

Corresponding Author: Lujun Pan E-mail: pan@pe.osakafu-u.ac.jp TEL&FAX: +81-72-254-9265

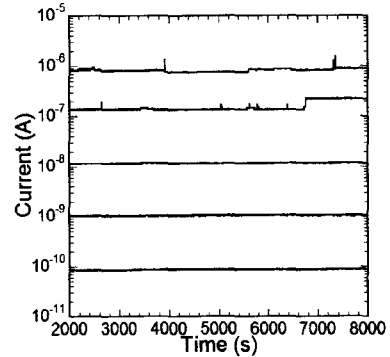


Fig.1 Current fluctuation for a DWNT at several fixed voltages

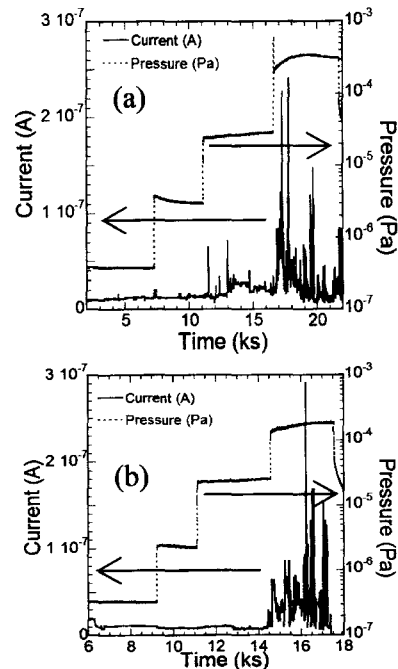


Fig.2 The dependence of current fluctuation on pressure for a DWNT while introducing N_2 (a) with and (b) without H_2O .

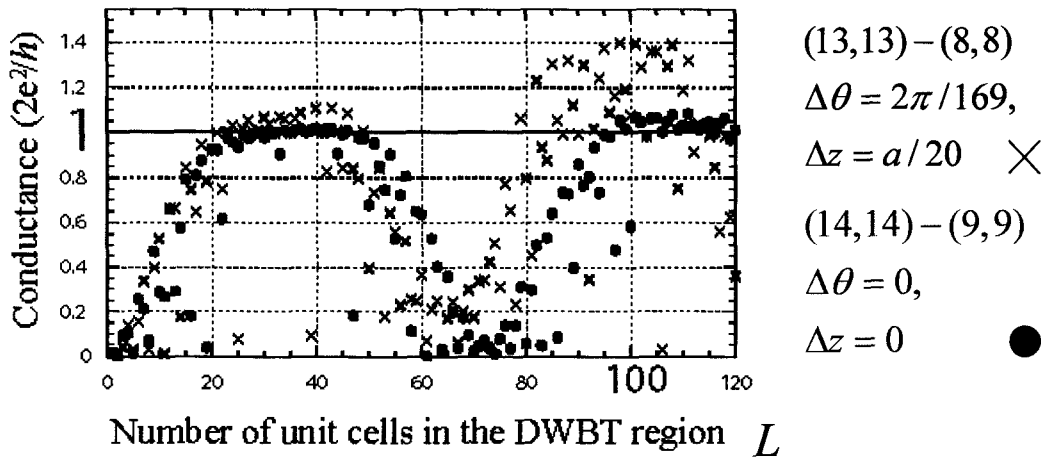
Conductance of telescoped double-wall armchair nanotube

Ryo Tamura

Abstract:

The conductance of telescoped double-wall nanotubes (TDWNTs) composed of two armchair nanotubes $((n_o, n_o)$ and $(n_o - 5, n_o - 5)$ with $n_o \geq 10$) is calculated using the Landauer formula and a tight binding model. The results are in good agreement with the conductance calculated analytically by replacing each single-wall nanotube with a ladder, as expressed by $(2e^2/h)(T_+ + T_-)$, where T_+ (T_-) is the transmission rate of the pseudo symmetry (pseudo anti-symmetry) channel. Interlayer hopping of the $-$ channel in the ladder model explains two key results: the low value of T_- for TDWNTs except when $n_o = 10$, and the particularly low value of T_- when either n_o or $n_o - 5$ is a multiple of three. In the latter case, T_- becomes zero when the saturation of the number of interlayer bonds per atom is neglected.

(Figure caption) $\Delta\theta$ represents the relative rotation angle with respect to common tube axis, while $(L-0.5)a + \Delta z$ is the overlap length between the two armchair NTs with lattice constant $a \sim 0.25$ nm..



References: R. Tamura, Y. Sawai and J. Haruyama, Phys. Rev. B 72, 045413 (2005), Erratum, Phys. Rev. B 72, 119903(E) (2005)

Corresponding Author: Ryo Tamura

E-mail: trtamur@ipc.shizuoka.ac.jp

Tel&Fax: 053-478-1294

Direct Observation of Inter-layer Interaction of Double-Walled Carbon Nanotubes by using UHV-STM

ON. Fukui¹, H. Yoshida¹, T. Sugai¹, S. Heike², M. Fujimori², Y. Suwa², Y. Terada³,
T. Hashizume² and H. Shinohara^{1,4,5}

¹*Department of Chemistry, Nagoya University, Nagoya 464-8602, Japan*

²*Advanced Research Laboratory, Hitachi, Ltd., Hatoyama, Saitama 350-0395, Japan*

³*Institute of Applied Physics, University of Tsukuba, Tsukuba, Ibaraki 305-8573, Japan*

⁴*Institute for Advanced Research, Nagoya University, Nagoya 464-8602, Japan*

⁵*CREST, Japan Science and Technology Corporation, c/o Department of Chemistry,
Nagoya University, Nagoya 464-8602, Japan*

Carbon nanotubes have attracted much attention by virtue of their one-dimensional structure and of unique electronic properties. STM (Scanning Tunneling Microscopy) is a powerful tool of analyzing surface electronic states of atoms, molecules and nano materials. Direct observation of MWNTs (multi-walled carbon nanotube) [1] and SWNTs (single-walled carbon nanotube) [2,3] by STM reveals presence of the super-structure induced by inter-layer interaction and the lattice images correspond to honeycombs structures, respectively. However, DWNTs (double-walled carbon nanotubes) have not been reported as high resolution surface images by STM. Recently, the development of CNTs synthesis enables us to prepare high-quality DWNTs[4]. Here, we report the first observation of super-structures and lattice images of DWNT by STM.

The DWNTs were prepared by the pulsed-arc discharging method and the remaining SWNT was removed by thermal oxidation [4]. Clean surface of the Cu(111) was prepared by repeated Ar- sputtering and annealing in a preparation chamber (PC) under UHV condition, and was confirmed by STM observation. The Cu surface was then introduced into a load-lock chamber kept at a 10^{-5} -Pa range vacuum. The DWNTs in a chloroform solution were immediately pulse-injected onto the surface [5] in vacuum. The sample was transferred to PC and was annealed at 700K to remove the residue solvents.

Figure 1 shows an STM image of a DWNT on the Cu surface after image processing to enhance the contrast. Both a high resolution of lattice image (a white line for an example) and a long periodic structure (white dots) are successfully observed. We have found that the super-structure is caused by the interference between the inner and outer tubes of the DWNT.

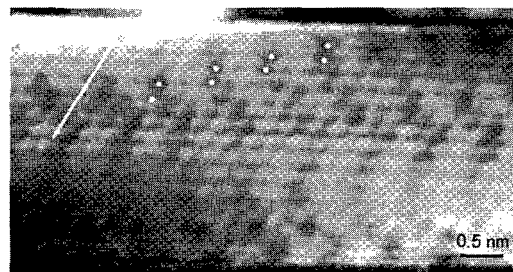


Fig.1. STM image of DWNT
after contrast enhancement.

Reference

- [1] Maohui Ge and Klaus Sattler, *Science*, **260**, 515 (1993)
- [2] J. W. G. Wildöer *et. al.*, *Nature*, **391**, 59 (1998)
- [3] T. W. Odom *et. al.*, *Nature*, **391**, 62 (1998).
- [4] T. Sugai *et. al.*, *Nano. Lett.*, **3**, 769 (2003).
- [5] Y. Terada *et. al.*, *Nano. Lett.*, **3**, 527 (2003).

E-mail : noris@cc.nagoya-u.ac.jp

Corresponding Author: Hisanori Shinohara

Tel: +81-52-789-2482, FAX: +81-52-789-1169

Observation of Photoluminescence from Small-Diameter DWNTs Synthesized by the Zeolite-CCVD Method

ONaoki Kishi¹, Satoshi Kikuchi¹, Toshiki Sugai¹ and Hisanori Shinohara^{1,2,3}

¹Department of Chemistry, Nagoya University, Nagoya 464-8602, Japan

²CREST, Japan Science and Technology Agency, c/o Department of Chemistry, Nagoya University, Nagoya 464-8602, Japan

³Institute for Advanced Research, Nagoya University, Nagoya 464-8602, Japan

Photoluminescence (PL) measurements are a powerful tool to characterize CNTs. It is not easy, however, to measure PL from DWNTs because of the difficulty to observe PL peaks from SWNTs and DWNTs separately. We have reported PL from inner tubes of DWNTs [1] by comparing the PL mappings of the samples obtained before and after concentrating DWNTs by the oxidation method [2]. Here, we report the detailed changes of PL mappings during the concentration process of DWNTs by oxidation.

We have concentrated DWNTs from as-grown SWNTs samples containing small amounts of DWNTs by oxidation and measured PL of the samples in the process of concentrating DWNTs. In this work, we used sodium cholate solution for suspending both SWNTs and DWNTs. The PL measurements were done on a Shimadzu NIR-PL system (CNT-RF). PL signals from SWNTs were observed in the mapping of as-grown sample. The PL peak distribution shifted to a thicker diameter region with increasing oxidation temperature, since SWNTs with smaller diameters are more active against oxidation than thicker tubes. After high-temperature oxidation, new peaks appeared in the thinner diameter region. These peaks stem from inner tubes of DWNTs, since the mean diameter of the inner tubes of the present DWNTs was much smaller than those of as-grown SWNTs [1,3]. PL from SWNTs and inner of DWNTs are observed separately as shown in Figure 1. Further concentration procedure provides PL peaks almost only from inner tubes of DWNTs, whereas the ones from SWNTs disappeared in the PL mapping.

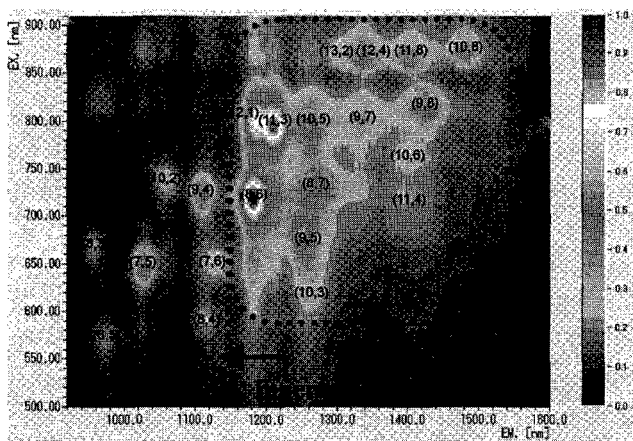


Figure 1. A contour plot of PL spectrum of the sample during the concentration process of DWNTs

References:

- [1] N.Kishi, *et al.* The 29th Fullerene Nanotubes General Symposium 2P-55 (2005)
- [2] T.Sugai, *et al.* *Nano.Lett.* 3 769 (2003)
- [3] N.Kishi, *et al.* The 28th Fullerene Nanotubes General Symposium 3P-3 (2005)

Corresponding Author: Hisanori Shinohara

TEL: +81-52-789-2482, FAX: +81-52-789-1169, E-mail: noris@cc.nagoya-u.a.jp

Morphology effect of optical properties in single walled carbon nanotubes detected by THz to Vis-polarized spectroscopy

○N. Akima¹, J.L. Musfeldt², H. Matsui⁴, N. Toyota⁴, H. Shimoda⁵, O. Zhou⁵,
M. Shiraishi⁶ and Y. Iwasa^{1,3}

¹IMR, Tohoku University, ²University of Tennessee, ³CREST, ⁴Tohoku University,
⁵University of North Carolina, ⁶Graduate School Engineering Science, Osaka University

Recently, several techniques, which produce aligned SWNTs materials, provide the opportunity to carry out polarized dependent spectroscopic studies and clarified the intrinsic properties of one-dimensional tubular structures. However, these studies were only limited to the region between NIR to UV. This is the first report to investigate the polarization dependencies of the absorption spectra from THz- to mid-IR region and carrier doped aligned SWNTs. Then we discuss the morphology effect of optical properties in SWNTs by comparing the aligned films and unoriented films. To obtain pristine (hole doped) samples, SWNTs were sonicated in toluene (F₄TCNQ/Toluene) for

3 hours at room temperature, then the suspension was mixed with the PE/Toluene suspension at 160°C and stirred until solvent has reduced completely. The obtained SWNT/PE composite films were mechanically stretched at elevated temperatures. The degree of SWNTs alignment was determined by polarized Raman spectroscopy and Maximum Entropy analysis implies that 90% of SWNTs in the film are aligned along the stretch direction, with a mosaic angle of $\pm 25^\circ$. Fig1. shows the highly anisotropic and insulator like behavior in the FIR region. In poster, we discuss the FIR peaks and MIR structure, which appears only in unoriented films, with the object of SWNT's morphology.

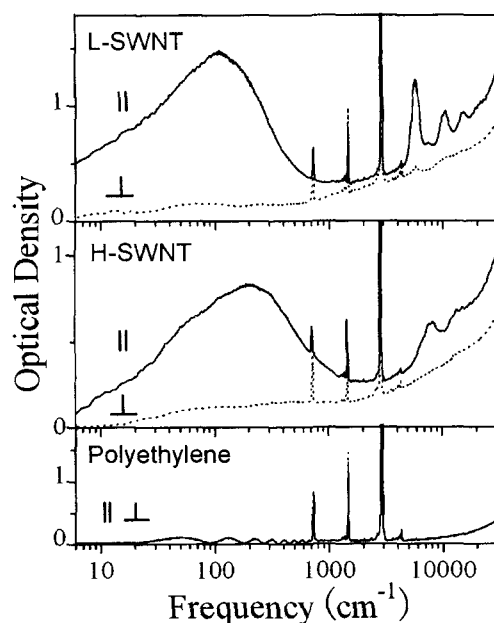


Fig1. Polarized absorption spectra of aligned SWNTs in PE matrix.

Corresponding Author: Nima Akima

Institute for Materials Research, Tohoku University,

Tel: +81-22-215-2032

e-mail : akima@imr.tohoku.ac.jp,

Exciton-photon matrix elements in single-wall carbon nanotubes

○J. Jiang, R. Saito, Y. Oyama, K. Sato, J. S. Park

Department of Physics, Tohoku University and CREST, Sendai, 980-8578, Japan

Due to the rotational symmetry around a horizontal C_2 axis, which intersects the center of two hexagons located at opposite sides of a carbon nanotube, and the translational symmetry around the axis of the nanotube, the excitonic states [1-2] in a nanotube can be classified into four kinds: A^\pm , E and E^* states. Among them, A^+ state is a bright state, where the optical transitions with light polarization along the tube axis are allowed. The other states A^- , E and E^* are dark states, where the optical transitions are forbidden.

A^+ states can be further classified into several serial states (energy subbands), which correspond to E_{11} , E_{22} , E_{33} ...transitions in the single-particle picture, and into s, p, d,...states for each energy subband. Within a subband, the optical matrix element is largest for the first state with the lowest energy. The diameter and chiral angle dependences of the matrix elements for the lowest energy states, corresponding to E_{11} , E_{22} , and E_{33} transitions are studied and compared to those in the single-particle picture. The similarity between the results by the two pictures is explained by the Fourier transform of the wave functions for these excitonic states.

[1] Catalin D. Spataru, Sohrab Ismail-Beigi, Lorin X. Benedict, and Steven G. Louie, *Phys. Rev. Lett.*, **92**, 077402 (2004).

[2] Vasili Perebeinos, J. Tersoff, and Phaedon Avouris, *Phys. Rev. Lett.*, **94**, 027402 (2005).

Corresponding Author: Jie Jiang

TEL: +81-22-795-6475, FAX: +81-22-795-6475, E-mail: jiang@flex.phys.tohoku.ac.jp

Electronic and Magnetic Properties of Finite-Length Carbon Nanotubes with Hydrogen Atoms Encapsulated

○Masahiro Nigawara ¹⁾, Shigekazu Ohmori ²⁾, Akihiro Ito ^{1,3)}, and Kazuyoshi Tanaka ^{1,3)}

¹⁾ *Department of Molecular Engineering, Graduate School of Engineering, Kyoto University, Kyoto, 615-8510, Japan*

²⁾ *Venture Business Laboratory, Kyoto University, Kyoto, 606-8501, Japan*

³⁾ *CREST, Japan Science and Technology Agency (JST), Japan*

Carbon nanotubes (CNTs) have attracted a great deal of interest and have been widely studied in the both experimental and theoretical fields. Recently, the spin-valve effect due to the misalignment of the magnetic moments of the two electrodes connecting the nanotubes was reported.¹⁾ This research may extend to a new conduction mechanism to evaluate the potential of CNTs as nano-spintronics devices. The purpose of our study here is to investigate the possibility of spin-polarized conducting CNT.

In this work, we considered several hydrogen atoms encapsulated into a finite-length CNT (6,6)^{2,3)} with an injected electron. This CNT is terminated by hydrogen atoms in each end. It is expected that double-exchange mechanism⁴⁾ appears followed by high-spin correlation among the electrons of encapsulated hydrogen atoms and those of CNT, resulting in spin-polarized current on CNT. In particular, we focus on whether high-spin correlation of the encapsulated hydrogen atoms is stable or not. In order to obtain the geometries and electronic structures of these hydrogen atoms, the geometrical optimization was carried out based on the *ab initio* self-consistent-field molecular orbital (SCF-MO) calculation (6-21G basis set) using the Gaussian 03 program package.

References:

1. K. Tsukagoshi et al., *Superlatt. Microstruct.*, **27**, 565 (2000).
2. T. Yumura et al., *J. Phys. Chem. B*, **108**, 11426 (2004).
3. Y. Matsuo et al., *Org. Lett.*, **5**, 3138 (2003).
4. A. Ito et al., *Polyhedron*, **22**, 1829 (2003).

Corresponding Author: Masahiro Nigawara

E-mail: nigawara@mec.mbox.media.kyoto-u.ac.jp

Tel: +81-75-383-2551 & **FAX:** +81-75-383-2556

Resonance Raman and Photoluminescence Spectra of Suspended Single-Walled Carbon Nanotubes in Ceramics

○Taro Ueno^{1,2}, Shingo Okubo³, Tsuneaki Miyahara¹, Shinzo Suzuki⁴, Yohji Achiba⁴,
Kazuhiro Tsukagoshi⁵, Toshiya Okazaki³, Hiromichi Kataura^{2,1}

1. Department of Physics, Tokyo Metropolitan University, 192-0397, Tokyo

2. Nanotechnology Research Institute, Advanced Industrial Science and Technology (AIST), 305-8562, Tsukuba

3. Research Center for Advanced Carbon Materials, AIST, 305-8562, Tsukuba

4. Department of Chemistry, Tokyo Metropolitan University, 192-0397, Tokyo

5. RIKEN, 351-0106, Wako

Abstract:

Isolated single-walled carbon nanotubes (SWCNTs) should have different physical properties from bundled ones due to charge transfer and interlayer interactions. Actually, many researchers have measured photoluminescence (PL) and resonance Raman spectra (RRS) of individual single-walled carbon nanotubes (SWCNTs) to reveal the intrinsic electronic structure of SWCNTs. Most of them have used HiPco dispersed in water with surfactant [1,2]. However, the micelle-SWCNTs are not ideally isolated but are expected interaction between SWCNTs and surfactant. For that purpose, really isolated SWCNTs are required.

We synthesize isolated SWCNTs suspended between nanoparticles in air by alcohol catalytic chemical vapor deposition (ACCVD) technique [3] using porous magnesium oxide (MgO) block. The sample showed very narrow RBM Raman lines and PL without any treatment. In this presentation, we will discuss RRS and PL spectra of suspended SWCNTs compared with the result of SDS-HiPco dispersed in water.

Reference:

[1] S. M. Bachilo *et al.* Science, 298 (2002) 2361

[2] C. Fantini *et al.* Phys. Rev. Lett. 93 (2004) 147406

[3] S. Maruyama *et al.* Chem. Phys. Lett., 360 (2002) 229

Corresponding Author: Hiromichi Kataura

E-mail: h-kataura@aist.go.jp Tel: 029-861-2551, Fax: 029-861-2786

Air-Stable N-type Single-Walled Carbon Nanotube Field Effect Transistors Functionalized by Amine Molecules

○ Tetsunori Matsumoto^{1,3}, Satoru Suzuki^{2,3}, Goo-Hwan Jeong²,
Yoshihiro Kobayashi^{2,3}, and Yoshikazu Homma^{1,3}

¹ Department of Physics, Tokyo University of Science, Shinjuku, Tokyo 162-8601, Japan

² NTT Basic Research Laboratories, NTT Corporation, Atsugi, Kanagawa 243-0198, Japan

³CREST/JST, Japan Science and Technology Corporation

Single-walled carbon nanotubes (SWNTs) have attracted great attention as promising candidates for nanoscale electronic devices. A pristine SWNT-field effect transistor (FET) with ordinary metal electrodes normally exhibits only p-type transport behavior in air. However, fabricating nanotube-based integrated circuits requires n-type SWNT-FETs as well as p-type ones.

Amines are known to act as electron donors when they are coupled to other molecules. In this study, we demonstrated the conversion of a SWNT-FET from p-type to n-type by 3-(aminopropyl)triethoxysilane (APTES, $\text{NH}_2(\text{CH}_2)_3\text{Si}(\text{OEt})_3$) treatment following appropriate acid treatments. The acid treatments are crucial for covalent chemical bond formation between the APTES and SWNTs.

The SWNT-FET with Au/Ti electrodes was fabricated by the conventional lithography technique. Figure 1 shows the drain current (I_{ds}) versus gate voltage (V_{gs}) characteristics for the SWNT-FET in air before and after APTES treatment. The SWNT-FET before APTES treatment exhibited p-type characteristics, as usual. On the other hand, after APTES treatment, it exhibited n-type characteristics with normally-on.

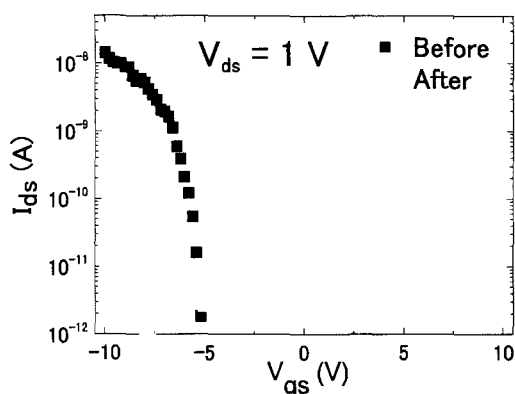


Fig. 1. $I_{\text{ds}}-V_{\text{gs}}$ curves of SWNT-FET before and after amine treatment

The change of transport type is explained by the donation of electrons from amine molecules to the SWNT. Although changing the transport properties of SWNT-FET by physical adsorption of APTES has been reported by Kong et al. [1], they didn't achieve n-type FET properties. These results indicated that the covalent chemical bond formation between APTES and SWNTs is effective for making n-type SWNT-FETs.

[1] Jing Kong et al., J. Phys. Chem. B **105**, 2890 (2001)

Corresponding Author: Tetsunori Matsumoto

E-mail: t.matsu@will.brl.ntt.co.jp, **Tel:** +81-46-240-3485, **FAX:** +81-46-240-4718

Development of Micro-focused X-ray Source by Using Carbon Nanotube Field Emitter

○Kunihiko Kawakita, Koichi Hata, Hideki Sato and Yahachi Saito[†]

*Department of Electrical and Electronic Engineering, Mie University,
Kurima-Machiya 1577, Tsu 514-8507, Japan*

[†]*School of Engineering, Nagoya University, Furo-cho, Nagoya 464-8603, Japan*

X-ray source with cold cathode is attracting much attention, and X-ray sources using carbon-related materials as a field emitter have been reported by several authors [1]. We have reported on a preliminary micro-focused X-ray source with a carbon nanotube (CNT) bundle cathode and a simple einzel lens consisting of three parallel plates, and its imaging capability was demonstrated [2]. To improve its performance, i.e., intensity, penetrating power, resolution of X-ray images, we developed a new micro-focused X-ray source equipped with an optimized electron optical system.

The X-ray source composed of a field emission cathode, a Butler lens [3], and a Cu anode, as illustrated in Fig. 1. The cathode used in this study was a bundle of multi-walled carbon nanotubes (MWNTs) produced by arc discharge in helium gas. The CNT cathode assembly was mounted on an XYZ stage for alignment with the optical axis. Owing to this alignment function, an anode current increased by twice as much as the case without the function. The Butler lens consisted of an extraction electrode and a focusing electrode, whose configuration was designed by computer simulations of electron beam trajectories. Since the maximum voltage applied to the cathode and the anode were -30 kV and +30 kV, respectively, the X-ray source can generate X-ray with high penetrating power enough to image non-biological specimens such as LSI. X-ray radiated from the anode was extracted in the atmosphere passing through a Be window, and X-rays transmitted through a specimen were recorded on an electron microscope (EM) film. Experiments were done under an ordinary vacuum pressure of 2×10^{-7} Torr for practical use.

Figure 2 shows an X-ray image of wiring of LSI taken at an acceleration voltage of 23 kV for which -9.0 kV and +14.0 kV were applied to the cathode and anode, respectively. The EM film was placed close behind the LSI specimen, and therefore the magnification was unity. Each of wires, whose width was $30 \mu\text{m}$, is perfectly resolved. Use of the Butler lens led to significant improvement of resolution of the X-ray images.

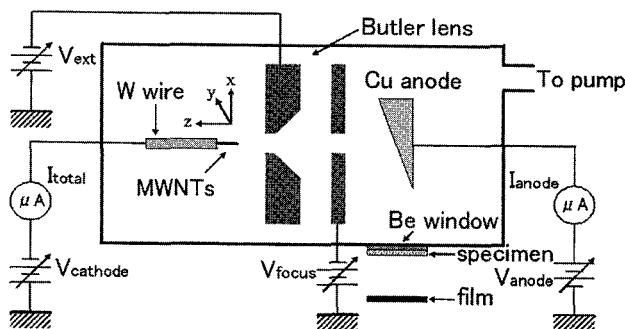


Fig. 1 Schematic diagram of the newly developed X-ray source.

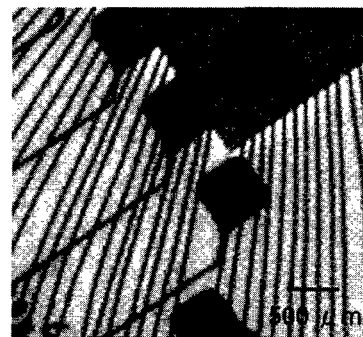


Fig. 2 X-ray transmission image of a LSI at the acceleration voltage of 23 kV.

References

- [1] A. Haga, S. Senda, Y. Sakai, Y. Mizuta, S. Kita and F. Okuyama : *Appl. Phys. Lett.*, **84** (2004) 2208
- [2] K. Kawakita, K. Hata, H. Sato and Y. Saito : Submitted to *J. Vac. Sci. & Technol.*
- [3] E. Munro : *Proc. Fifth European Congress on Electron Microscopy*, p. 22 (1972)

*Corresponding author

E-mail: kawakita.k@elec.mie-u.ac.jp Tel & Fax: +81-59-231-9404

Spectral Properties of Single-Walled Carbon Nanotubes Dissolved in Aqueous Solutions of Biosurfactants

Ayumi Ishibashi and Naotoshi Nakashima*

*Department of Chemistry and Biochemistry
Graduate School of Engineering, Kyushu University
744 Motoooka, Fukuoka 819-0395, Japan*

We report the solubilization of SWNTs in aqueous solutions of biosurfactants. In this study, ten different anionic-, zwitter ionic- and nonionic steroid moiety-carrying biosurfactants, and three different sugar biosurfactants are used (Figure 1). All these compounds have been known as membrane protein solubilizers. Especially, bile salts such as sodium cholate and its analogues are composed of a rigid hydrophobic steroid backbone carrying two or three hydroxy groups stereochemically and form specific structures and biological functions in water. The critical micellar concentrations (cmc) of these micelles are rather high, which is the advantage to remove them from the solutions. We describe a strong chemical structure dependence and the effect of cmc on the solubilization of CNTs using the biosurfactants.

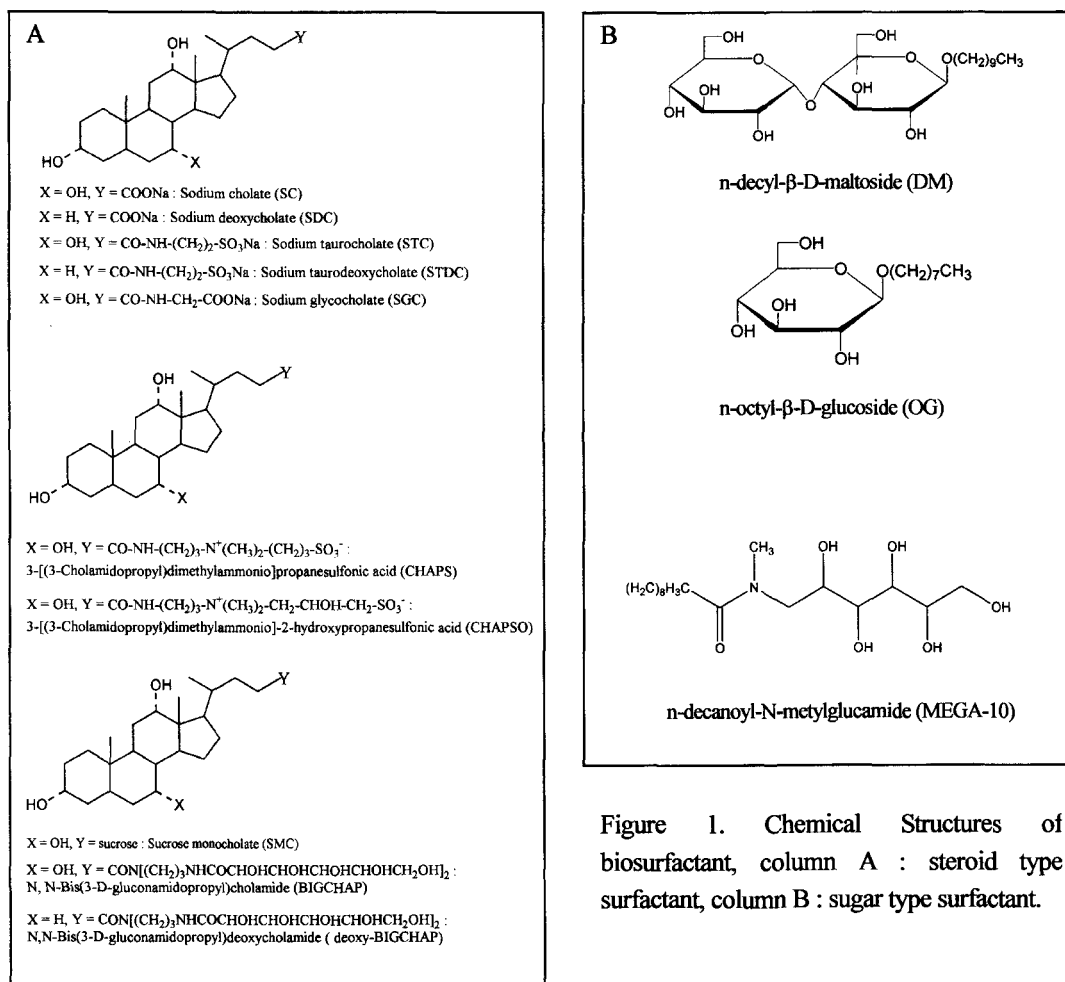


Figure 1. Chemical Structures of biosurfactant, column A : steroid type surfactant, column B : sugar type surfactant.

Corresponding Author E-mail: nakashima-tcm@mbox.nc.kyushu-u.ac.jp

Tel&Fax: +81-92-802-2840

NIR Laser Irradiation toward SWNTs in Solution

○Kaori Narimatsu, Hiromi Shinohara, Yasuro Niidome and Naotoshi Nakashima*

*Department of Applied Chemistry, Graduate School of Engineering,
Kyushu University, Motoooka 744, Nishi-ku, Fukuoka 819-0395, Japan*

We have already reported that anthracene-carrying copolymer **1** (Figure 1) can dissolve single walled carbon nanotubes (SWNTs) in solution¹⁾. In this study, we examine the effect of laser irradiation onto this SWNT solution.

A DMF solution of **1**/SWNTs was prepared by sonication, and subsequent centrifugation¹⁾. Upon irradiation by Nd:YAG pulse laser (wavelength : 1064 nm) to this solution, we recognized a formation of a black-colored precipitate, and the decrease in the absorbance of the vis-NIR absorption of SWNTs (Figure 2). The absorption of anthracene moiety on **1** did not change by this procedure. The Raman spectrum of the precipitate separated from the solution was almost the same as that of SWNTs before laser irradiation, suggesting that the laser irradiation induces desorption of solubilizer **1** from SWNTs and produces bundled insoluble SWNTs in solution.

References : 1) K. Narimatsu, J. Nishioka, H. Murakami, N. Nakashima, *Polymer Preprints, Japan*, **54**, 1G31 (2005).

Corresponding Author : Naotoshi Nakashima

E-mail : nakashima-tcm@mbox.nc.kyushu-u.ac.jp

Tel&Fax : 092-802-2840

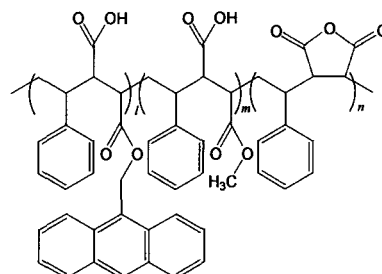


Figure 1. Chemical structure of **1**.

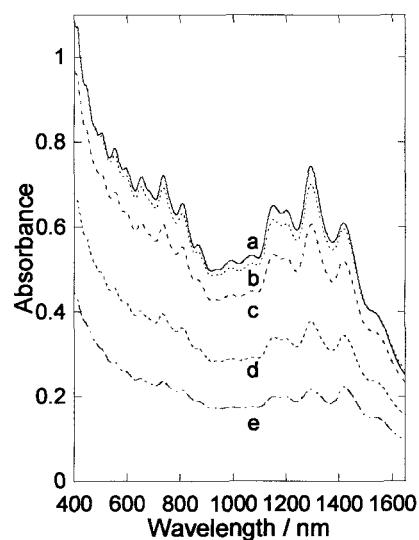


Figure 2. Vis-NIR spectra of **1**/SWNTs in DMF. Nd:YAG pulse laser (at 1064 nm) irradiation time were: (a) 0, (b) 5, (c) 10, (d) 30, and (e) 60 min. Optical cell length ; 1 cm.

Dielectrophoresis of SWNTs in a Microchip

○Masashi Shinagawa,¹ Hiroki Ago,^{*,1,2} Naoki Isigami,¹ Masaharu Tsuji,^{1,2}
Tastuya Ikuta,³ and Koji Takahashi³

¹ Graduate School of Engineering Sciences, Kyushu University, Kasuga, Fukuoka 816-8580

² Institute for Materials Chemistry and Engineering, Kyushu University and CREST-JST

³ Graduate School of Engineering, Kyushu University, Motoooka, Fukuoka 819-0395

Recently, dielectrophoresis (DEP) has been proposed to separate metallic SWNTs (M-SWNTs) from semiconducting SWNTs (S-SWNTs) [1]. The DEP force is strongly dependent on the permittivity of a SWNT, which is inversely proportional to a square root of the band gap of a nanotube. Thus, M-SWNTs having infinite permittivity are suggested to be attracted more strongly to the electrode as compared with S-SWNTs. One major issue of the metal-semiconductor separation by DEP is the reliability of the Raman spectra of SWNTs deposited on the electrode, because the spectrum is very sensitive to an aggregated state of SWNTs [2]. Therefore, direct evidences, such as an absorption spectrum, are necessary to discuss effectiveness of the separation.

Here, we report on the DEP of SWNTs in a microchip having interdigitated electrodes with 10 μm gap. The DEP force is supposed to influence on SWNTs effectively in a confined space. Furthermore, this method allows us to obtain the dispersion after the DEP for the absorption measurement. HiPco-SWNTs dispersed in D₂O/SDS solution was introduced into the microchip and suffered from the non-uniform electric field generated by a function generator, 20 V_{pp} (peak-to-peak) and 15 MHz, as shown in Fig. 1(a). Fig.1(b) shows the absorption spectra of the original dispersion and that collected after the DEP. There is no obvious change in their absorption spectra, suggesting the co-existence of M-SWNTs and S-SWNTs even after the DEP. Effects of an electric double layer and electrolysis of the solution will also be discussed.

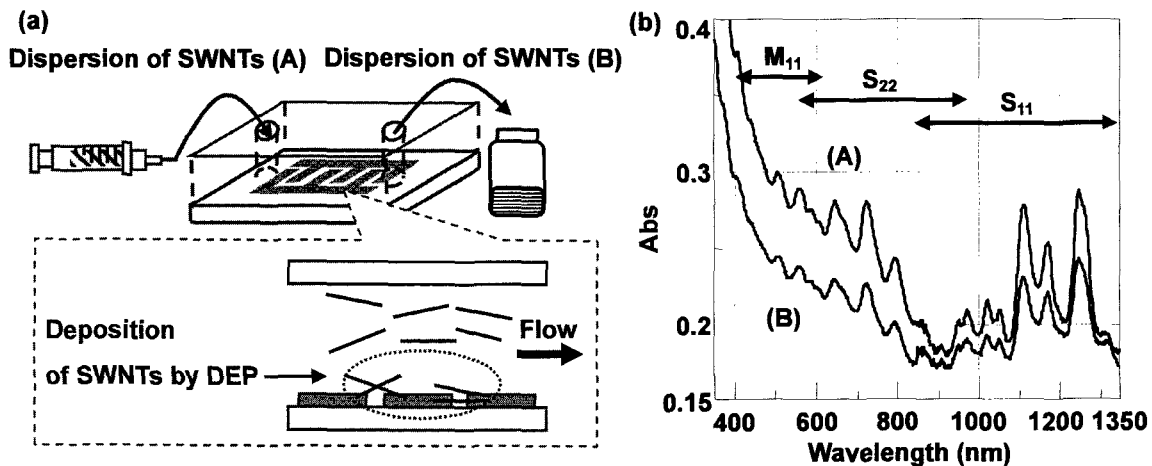


Figure 1. (a) Schematic illustration of the DEP of SWNTs in the microchip. The channel size is 20 μm height, 6 mm width, and 13 mm length. (b) Comparison of absorption spectra of the SWNTs dispersions.

Acknowledgements: The authors acknowledge support from CREST-JST, Grant-in-aid for Scientific Research from MEXT (#16710087), and Iketani Science Foundation.

References: [1] R. Krupke *et al. Science*, **301**, 344 (2003). [2] S. Baik *et al. J. Phys. Chem.*, **108**, 15560 (2004).

Corresponding Author: Hiroki Ago (E-mail: ago@cm.kyushu-u.ac.jp, Tel&Fax: +81-92-583-7817)

Metal-free Formation of Spiral Carbon Structures

○Akira Koshio, Teruyuki Tanaka, Toshiki Sunouchi and Fumio Kokai

*Department of Chemistry for Materials, Mie University, 1577 Kurimamachiya-cho, Tsu,
Mie 514-8507, Japan*

Carbon coils with helical/spiral structures, such as carbon nanocoils and microcoils, are expected for use as electromagnetic absorber, nano-springs and emitters for field emission. The carbon coils can be grown by catalytic thermal decomposition of hydrocarbon gases such as acetylene. It is well known that metal catalysts, such as iron and indium tin oxide and nickel, are essential for effective growth of carbon coils. Recently, we found that carbon coils were formed without metal by arc vaporization using graphite electrodes in a hydrogen atmosphere. In this study, we examined the formation of spiral carbon structures without a metal catalyst.

Preparation of samples was carried out by vaporization of graphite as an anode using a conventional arc discharge method. Hydrogen gas was put into the arc chamber at more than 0.1 MPa. The arc discharge was performed intermittently for 5 min.

Figure 1(a) shows moss-like aggregates on the surface of a cathode after arc discharge. Electron microscopic observation revealed that the moss-like aggregates consisted of highly dense multi-wall carbon nanotubes. This result is similar to that of an RF plasma method [1]. In addition, various types of spiral carbon structures, such as thin single coils with diameters of about 200-300 nm (Fig. 1(b)) and thick double-helix coils with diameters of 2-3 μm (carbon microcoils) (Fig. 1(c)), were formed on the surface of an anode. We will discuss details of the metal-free formation of carbon coils.

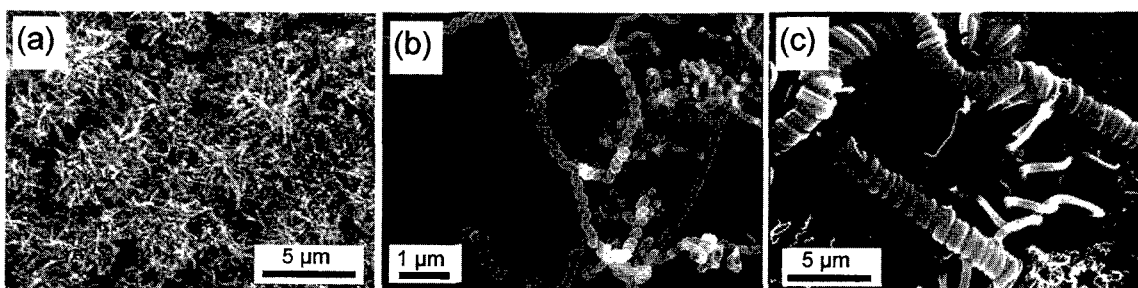


Fig. 1 SEM images of (a) moss-like aggregates of MWNTs formed on a surface of the cathode deposit, (b) thin single carbon coils and (c) thick double-helix carbon coils formed on the surface of an anode.

References

[1] A. Koshio *et al.*, *Chem. Phys. Lett.* **356**, 595 (2002).

Corresponding Author: Akira Koshio

E-mail: koshio@chem.mie-u.ac.jp **Tel&Fax:** +81-59-231-5370

On Critical Sizes of Multiply-Charged Fullerene Clusters

Masato Nakamura and Paul-Antoine Hervieux

*Physics laboratory, College of Science and Technology Nihon University
7-24-1, Narashinodai, Funabashi, 274-8501 Japan
Institute de Physique et Chimie des Matériaux, Université Strasbourg I,
Strasbourg, 67034 France*

Recently, the critical sizes of fullerene clusters $(C_{60})_n^{z+}$ have been experimentally measured for multiply charged of $z = 2 - 5$ [1]. To explain experimental measurements, we calculate the energy barrier for various fission channels and estimate the critical sizes of multiply-charged fullerene clusters for $z = 2 - 6$. We calculate energy barriers for various fission channels by assuming that the fragment cluster are in contact at the transition state[2]. The energy of charged clusters is estimated either by using the results of accurate calculations for $(C_{60})_n$ clusters[3] or the use of the liquid drop model. The results are shown in Table 1. The experimental measurements are reproduced within a considerable accuracy in both methods. Although the liquid drop model essentially explains the appearance sizes for $z = 2 - 5$, shell effects are expected to be important for $z = 6$. Furthermore, multiply-charged clusters larger than the critical size are not always stable due to shell effects even for $z < 6$. Details will be presented in article [4].

Table 1: Critical sizes for multiply charged fullerene clusters with charge z . Numbers in parenthesis are those calculated from the liquid drop model

z	Theory	Exp[1]
2	6 (6)	5
3	12 (12)	11
4	22 (20)	22
5	31 (31)	33
6	38 (45)	--

References

- [1] B. Manil, et al., Phys. Rev. Let. 91, 215504 (2003).
 [2] O. Echt, et al, Phys. Rev. A 38, 3236 (1988).
 [3] P. J. K. Doe, D. J. Wales, W. Bran, and F. Calvo, Phys. Rev. B64, 235409 (2001)
 [4] M. Nakamura and H. Hervieux, Phys. Rev. A (submitted)

Corresponding author: Masato Nakamura

e-mail mooming@phys.ge.cst.nihon-u.ac.jp

Tel. & Fax. +81-47-469-5578

3P-1

Photochemical reaction of C₆₀ with cyclic organosilicon compounds

○Junko Nagatsuka¹, Tsukasa Nakahodo¹, Sachie Sugitani¹, Masahiro Kako²,
Takatsugu Wakahara¹, Yutaka Maeda³, Takahiro Tsuchiya¹, Takeshi Akasaka¹,
Yoshiko Sasaki⁴, Osamu Ito⁴, Kaoru Kobayashi⁵, Shigeru Nagase⁵

¹*Center for Tsukuba Advanced Research Alliance,*

Department of Chemistry, University of Tsukuba, Tsukuba, Ibaraki 305-8577

²*Department of Applied Physics and Chemistry,*

The University of Electro-Communications, Chofu, Tokyo 182-8585

³*Department of Chemistry, Tokyo Gakugei University, Koganei, Tokyo 184-8501*

⁴*Institute of Multidisciplinary Research for Advanced Materials,*

Tohoku University, Katahira, Sendai, 980-8577

⁵*Department of Theoretical Studies, Institute for Molecular Science, Okazaki, 444-8585*

It is well known that the ground state of C₆₀ is a good electron acceptor. The excited triplet state of C₆₀ becomes a much stronger electron acceptor and has a far longer life time compared to its excited singlet state. Furthermore, the quantum yield to the excited triplet state of C₆₀ from its excited singlet state is very high, and it has a potential for causing chemical reaction with other materials. Thus, it is expected that C₆₀ will smoothly react with electron donor compounds under the photo-irradiation condition. Under this concept, chemical functionalization of C₆₀ with organosilicon compounds has been performed to give the fascinating results.^{1,2}

Here we report the photochemical reaction of fullerene with cyclic organosilicon compounds. It was observed that the cyclo-addition of the silacyclopropanes to C₆₀ forms the 5-membered ring on the carbon cage. Silacyclopropanes with diphenyl and phenyl substituents on one side of the carbon atoms in the ring also affords the open type of C₆₀ mono-adduct as well as the cyclo-addition adduct. The reaction mechanism and the structure analyses of these C₆₀-mono adducts will be reported in this presentation.

1) Akasaka, T. et al. *J. Am. Chem. Soc.*, **1993**, 115, 10366.

2) Wakahara, T. et al. *Current Organic Chemistry*, **2003**, 7, 927.

Corresponding author: Takeshi Akasaka

Tel & Fax: +81-29-853-6409, E-mail: akasaka@tara.tsukuba.ac.jp

A New Effective Search Algorithm for $C_{60}R_n$ Structure: Cones Product Strategy

○Tatsuo Toida, Katsumi Uchida, Tadahiro Ishii and Hirofumi Yajima

*Department of Applied Chemistry, Faculty of Science, Tokyo University of Science,
Kagurazaka, Shinjuku-ku, Tokyo 162-8601, Japan*

This work describes the computer aided search program for multi-adduct fullerene $C_{60}R_n$ structures by tracing the family tree of precursors and derivatives of every physical possible multi-adductions (Geometrical Evolution Graph)[1]. We developed a new searching algorithm, named Cones Product Strategy (Figure), based on the multi-dimensional network pathways. When applied to the highly symmetrical hexa-adduct C_{60} we obtained 3 possible pathways to hexa-adduct descendents. T_h symmetrical hexa-adduct is the only hexa-adduct that is able to derive from *e* and *trans-1* bis-adduct isomers. D_3 symmetrical hexa-adduct is the only hexa-adduct that is able to derive from the tris-adduct 0x0200 0081 (expressed as structure ID [2]) that is the only tris-adduct able to derive from *e*, *trans-3* and *trans-2* bis-adduct. D_{3d} symmetrical hexa-adduct is the only hexa-adduct that is able to derive from the tris-adduct 0x0001 2001 which structure has very simple biconical zone. This algorithm could facilitate the development of new complex chemical structures.

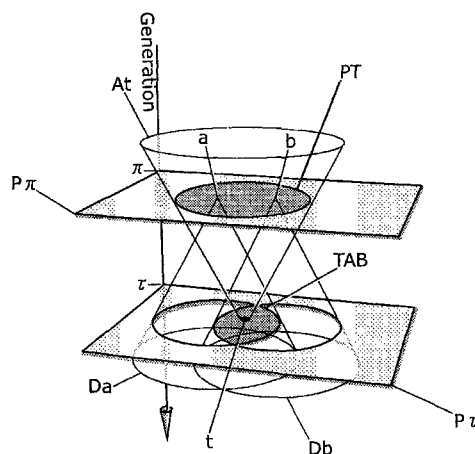


Figure. Graphic representation of the *Cones Product Strategy* that selects the best precursor pair (a,b) for its derivatives including target structures mainly.

References and Notes:

- [1] T. Toida, Y. Hori, K. Nemoto, K. Uchida, T. Ishii, and H. Yajima, *J. Computer Aided Chem.*, **6**, 11 (2005)
 [2] The structure ID that is 8 digits hexadecimal index (30 bits width) corresponding to any adduct patterns on 30 kinds of hex-hex double bond of C_{60} fullerene is classified to the minor structure ID which is impossible to distinguish and the Major structure ID which is representative for the minor structure IDs. The Major structure ID is the index without duplications of structure isomers and it is able to compare any two adduct patterns directly. In this study the software tools to visualize the structure ID for the Schlegel diagram are also developed. The tools are able to output the Major structure ID and its enantiomeric Major structure ID.

Corresponding Author: Tatsuo Toida **E-mail:** tatsuo@toida.jp

Tel: +81-3-5228-8381

Fax: +81-3-5261-4631

3P-3

Syntheses of water-soluble fullerene-chitosan conjugates and their radical scavenging activities

○ Katsumasa Nemoto¹, Hitoshi Sashiwa², Katsumi Uchida¹, and Hirofumi Yajima¹

¹Department of Applied Chemistry, Tokyo University of Science, Tokyo 162-8602, Japan

²National Institute of Advanced Industrial Science and Technology, Osaka 563-8577, Japan

Recently, a large number of studies have been extensively made with respect to the syntheses of water-soluble antioxidant fullerene derivatives and their scavenging activities against reactive oxygen species such as hydroxyl radical and superoxide. However, a few reports on fullerene derivatives with effective biological activities such as biocompatibility and biodegradability have been just presented.

In order to develop a novel biomedical material with multiple and effective functionalities using fullerenes, the conjugates of fullerenes and chitosans were synthesized and their scavenging activities were examined by means of ESR measurements.

The conjugation was carried out according to the method described in a previous work^[1] and confirmed by ¹H-NMR measurements. The degree of substitution of fullerene was determined to be 0.25. Furthermore, the dispersion properties of the conjugates in aqueous solution were analyzed by dynamic light scattering (DLS). As a result, it was suggested that the conjugates assumed self-assembly in analogy with amphiphilic polymers or surfactants (Fig.1).

At present, the studies on the self-assembly mechanism and radical scavenging activities of the conjugates are in progress.

[1] K.Nemoto et al., Abstracts of the 29th Fullerene-Nanotubes General Symposium, 2P-2 (2005)

Corresponding Author: Katsumasa Nemoto
TEL: +81-3-5228-8381
FAX: +81-3-5261-4631
E-mail: nemoto@nov.rikadai.jp

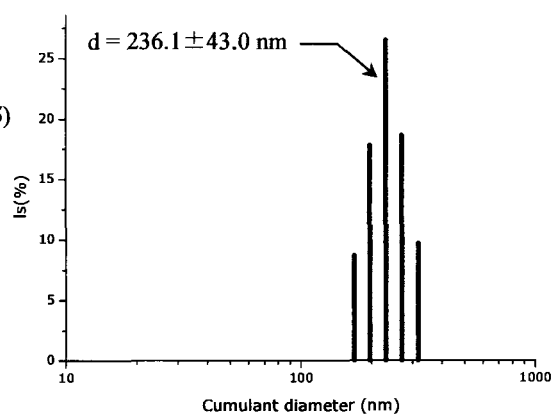


Fig. 1 Size distribution of Chitosan-Fullerene conjugate in aqueous solution analyzed by DLS.

(26.2°C detection angle was 90°, Histogram Marquadt method)

One Pot Synthesis of Highly Water-Soluble Fullerenol

○Hiroshi Tategaki¹, Sayako Kawahama¹, Kenji Matsubayashi², Hiroya Takada²,
Ken Kokubo¹ and Takumi Oshima¹

¹*Division of Applied Chemistry, Graduate School of Engineering, Osaka University,
Suita, Osaka 565-0871, Japan*

²*Vitamin C60 BioResearch Corporation, 1-8-7 Kyobashi, Chuo-ku, Tokyo 104-0031, Japan*

Water-soluble fullerene is a promising material in the field of life science, as medicine or cosmetic, in view of its high ability of capturing active oxygens [1]. Thus, facile synthesis of the water-soluble fullerenes has been eagerly desired from the beginning of fullerene chemistry. Since the polyhydroxyl fullerene, fullerenol, can be one of the candidates for the water-soluble fullerenes, several synthetic methods have been already reported [2,3]. The fullerenols with less than 12 hydroxyl groups on a fullerene cage still showed a very poor water solubility, whereas the fullerenols with more greater number of hydroxyl groups exhibited a good solubility. However, its applicability is restricted by the unfavorable contamination of Na ion which is inevitably introduced under the treatment with NaOH.

Recently, we have succeeded in synthesizing the milky white-colored fullerenols with 36–40 hydroxyl groups (estimated average) as a Na free compound [4]. This compound, we called “StarFullereneTM”, showed the higher solubility of 58.9 g/L to neutral water. However, two step procedures were essential for the synthesis of desired StarFullerene from C₆₀.

In this study, we improved the previous synthetic method by addition of some promoter to the above preparation solution, achieving the one pot reaction. This newly prepared fullerenol contains additional N-containing groups and showed the more higher water solubility as over 200 g/L (Table 1).

Table 1. Water solubility of some fullerenols

Compounds	Average Structure	Elemental Analysis	Water cont. ^a / %	Solubility g/L
		%		
StarFullerene 1	C ₆₀ (OH) ₃₆ · 7H ₂ O	C:48.1, H:3.6, O:48.3	8.9	17.5
StarFullerene 2	C ₆₀ (OH) ₄₀ · 9H ₂ O	C:46.3, H:3.7, O:50.1	9.6	58.9
Present fullerenol	C ₆₀ (OH) _{<i>l</i>} X _{<i>m</i>} · <i>n</i> H ₂ O ^b	C:35.9, H:4.2, O:48.9, N:11.0	17.6 ^c	>200

a) Water contents determined by TGA analysis. b) X = NH₂, NHOH, NO, NO₂ etc; N-containing group. c) Determined by Karl Fischer Moisture Titrator.

[1] Xiao, L.; Takada, H.; Maeda, K.; Haramoto, M.; Miwa, N. *Biomed. Pharmacother.* **2005**, *59*, 351.

[2] Chiang, L. Y.; Wang, L.-Y.; Swirczewski, J. W.; Soled, S.; Cameron, S. *J. Org. Chem.* **1994**, *59*, 3960.

[3] Li, J.; Takeuchi, A.; Ozawa, M.; Li, X.; Saigo, K.; Kitazawa, K. *J. Chem. Soc., Chem. Commun.* **1993**, 1785.

[4] T. Oshima *et al.*, Abstracts of The 28th Fullerene-Nanotubes General Symposium, p.105, 2005.

Corresponding Author: Ken Kokubo

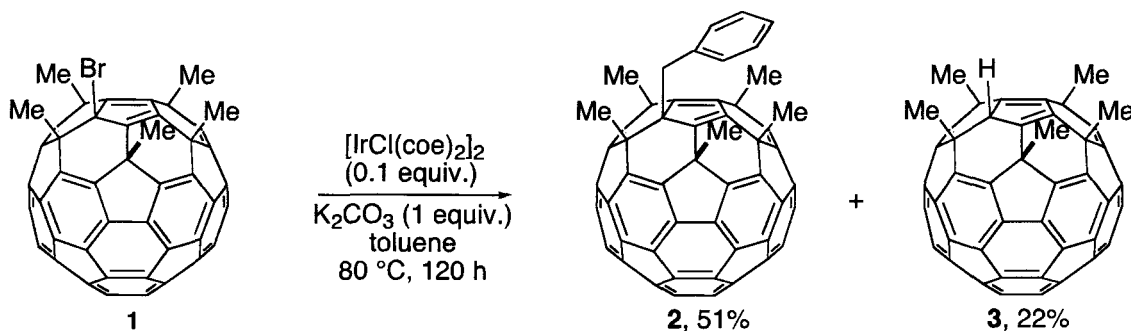
TEL: +81-6-6879-4592, FAX: +81-6-6879-4593, E-mail: kokubo@chem.eng.osaka-u.ac.jp

Synthesis of Alkylated Pentamethyl[60]fullerene by Iridium Catalyzed C-H Bond Activation of Toluene

○Akihiko Iwashita¹, Yutaka Matsuo², Eiichi Nakamura^{1,2}

¹Department of Chemistry, The University of Tokyo and ²Nakamura Functional Carbon Cluster Project, ERATO, JST, Hongo, Bunkyo-ku, Tokyo 113-0033, Japan

Penta(organo)fullerene ($C_{60}R_5H$; R = various alkyl and aryl groups) is one of the most promising fullerene derivatives because of their availability with large scale and their unique chemical and physical properties such as liquid crystals, vesicles, ligands of transition metal complexes. Chemical modification of penta(organo)[60]fullerene can make it possible not only to build up a value-added compound but also to substitute a reactive hydrogen atom in the cyclopentadiene moiety of $C_{60}R_5H$ with organic groups to obtain stable hexa(organo)[60]fullerenes, $C_{60}R_6$. We present here the novel synthetic method to obtain alkylated penta(organo)fullerene by iridium catalyzed C-H bond activation reaction.



The reaction of bromo(pentamethyl)[60]fullerene, $C_{60}Me_5Br$ (**1**) with catalytic amount of $[\text{IrCl}(\text{coe})_2]_2$ (coe = cyclooctene) in toluene at 25 °C for 120 h gave benzyl(pentamethyl)[60]fullerene, $C_{60}Me_5(\text{CH}_2\text{Ph})$ (**2**) in 51% yield through C-H bond activation of toluene. The conversion of **1** was 100%, and $C_{60}Me_5H$ (**3**, 22%) and several oxidized products such as $C_{60}Me_5O_3H$ were given as byproducts. The characterization of **2** was performed by ^1H and ^{13}C NMR and HR-MS measurements as well as an X-ray crystallographic analysis. The present procedure is a quite rare example of catalytic functionalization of fullerenes. We believe that the new methodology expands a molecular library of stable functionalized fullerenes.

Corresponding Author: Eiichi Nakamura

E-mail: nakamura@chem.s.u-tokyo.ac.jp

TEL/FAX: +81-(0)3-5800-6889

Promoting effect of water-soluble fullerene derivatives on growth of neurites of PC-12 cells that were differentiated by nerve growth factor

○Syo Kawahara¹, Yuki Fujisawa¹, Hiroki Tsumoto^{1,2}, Kohfuku Kohda², Takayoshi Suzuki¹, Hidehiko Nakagawa¹ and Naoki Miyata¹

¹*Graduate School of Pharmaceutical Sciences, Nagoya City University, Tanabe-dori, Mizuho-ku, Nagoya, 467-8603, Japan*

²*Faculty of Pharmaceutical Sciences, Musashino University, Shin-machi, Nishitokyo, Tokyo, 202-8585, Japan*

Fullerenes show very unique photo-, electro-chemical and physical properties, which can be exploited in various biological fields. However, the solubility of fullerenes in polar solvents is known to be quite poor. Because of this property, biological application of fullerenes has been very limited. Recently, the preparation methods for water-soluble fullerene derivatives were being developed, and we also synthesize several water-soluble fullerene derivatives. We herein report the finding of the promoting effect of a water-soluble fullerene on growth of neurites of rat pheochromocytoma PC-12 cells that were differentiated by nerve growth factor (NGF).

PC-12 cells were plated and grown in a growth medium containing 10 % horse serum and 10 % fetal bovine serum. For induction of neuronal phenotype, the medium was replaced with the differentiation medium without serum, and the cells were treated with 50 ng/mL NGF in the presence or absence of the fullerene derivatives. After 72 h incubation at 37 °C under a humidified CO₂ incubator, PC-12 cells in neuronal phenotype were observed. In the presence of 560 μM of C₆₀/γ-cyclodextrin (γ-CyD) with 50 ng/mL of NGF, the length of neurites was increased as compared with that of NGF alone (Figure). As a result, C₆₀/γ-CyD enhanced the growth of neurites of PC-12 cells that were differentiated by NGF. The effects of fullerol and other water-soluble fullerene derivatives are under investigation.

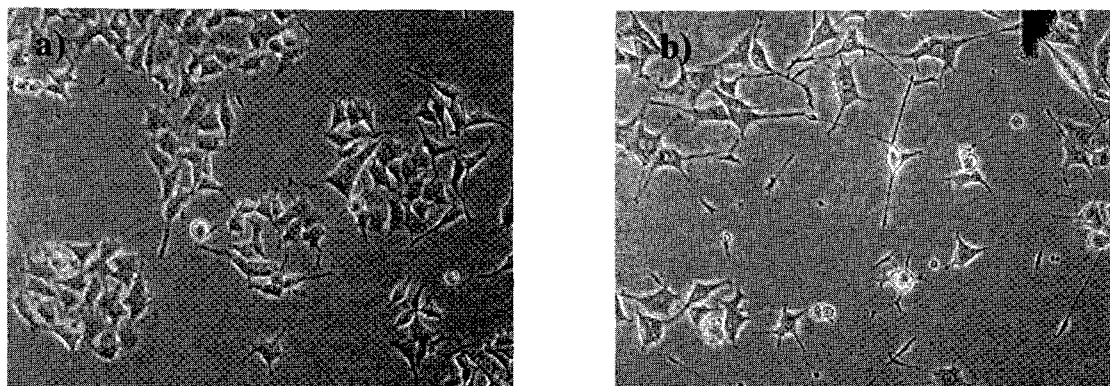


Figure The promoting effect of C₆₀/γ-CyD on growth of neurites of PC-12 cells that were differentiated by NGF a) NGF 50 ng/mL, b) NGF 50 ng/mL + C₆₀/γ-CyD 560 μM

Corresponding Author: Naoki Miyata
E-mail: miyata-n@phar.nagoya-cu.ac.jp
Tel&Fax: +81-52-836-3407

Mechanisms of mechanochemical oxidation of fullerene under oxygen atmosphere

○Hiroto Watanabe, Eitaro Matsui, Takahiro Kubo, and Mamoru Senna*

*Faculty of Science and Technology, Keio University
3-14-1 Hiyoshi Kohoku-ku, Yokohama-shi
Kanagawa-ken 223-8522, Japan*

Abstract: Solid-state organic syntheses were recently gathering interests not only on the standpoint of green-chemistry, but also from the viewpoint of unusual reactions under mechanical stressing via a mechanochemical route. Applications of mechanochemical reactions to organic chemistry and the analysis of their reaction mechanism are recently becoming an essential subject for mechanochemists. Solid-state mechanochemical reactions are widely applied to the chemical modification of C₆₀ to overcome a notorious drawback of too low-solubility of C₆₀ in any conventional solvents [1].

From well-documented mechanochemistry of inorganic materials we learn that various types of lattice imperfections serve as an active center for the subsequent mechanochemical reaction. Unlike inorganic crystals, organic ones are mostly molecular crystals with much weaker cohesive forces of van der Waals in nature. Although similar effects are expected on the organic substances, direct evidences of mechanochemical effects on the organic molecules at the lattice points are yet to be explored. We therefore try in this study to discuss mechanochemical effect on C₆₀ in crystalline state by exerting mechanical stressing by simple milling devices under various atmospheres.

As we ball-milled crystallite C₆₀ in O₂ atmosphere, we observed formation of oxidized fullerene, C₆₀O_n, containing C-O and C=O bonds as determined by infrared spectroscopy.

It is known that the oxidation reaction of C₆₀ under UV irradiation in O₂ atmosphere takes place by the participation of ¹O₂, generated by energy transfer from ³C₆₀*, as a key active species [2]. During the mechanochemical oxidation reaction, we also observed generation of ¹O₂ by ESR spin trapping method. Furthermore, oxidation reaction was inhibited with trapping ¹O₂ by addition of 2,2,6,6-tetramethyl-4-piperidone serving as a ¹O₂ scavenging agent [3].

From those observations, we conclude that ¹O₂ is a key activate species in the present mechanochemical oxidation of C₆₀. We also discuss about correlation between mechanisms of generation of ¹O₂ and inverse Jahn-Teller effects [4] during mechanical stressing of C₆₀.

References:

- [1] (a) K. Komatsu, *Top Curr. Chem.*, **2005**, *254*, 185. (b) Pu Zhang, Hualong Pan, Dougfang Liu, Zhi-Xin Guo, Fushi Zhang, Daoben Zhu, *Synthetic commun.*, **2003**, *33*, 2469. (c) Yasujiro Murata, Aihong Han, Koichi Komatsu, *Tetrahedron Lett.*, **2003**, *44*, 8199.
- [2] (a) David I. Schuster, Phil S. Baran, Russell K. Hatch, Ahsan U. Khan, Stephen R. Wilson, *Chem. Commun.*, **1998**, 2493. (b) O.B.Danilov, I.M.Belousova, A.A.Mak, V.P.Belousov, A.S.Grenishin, V.M.Kiselev, A.V.Kris'ko, A.N.Ponomarev, E.N.Sosnov, *Opt. Spectrosc.*, **2003**, *95*, 833.
- [3] Yoko Yamakoshi, Naoki Umezawa, Akemi Ryu, Kumi Arakane, Naoki Miyata, Yukihiko Goda, Toshiki Masumizu, Tetsuo Nagano, *J. Am. Chem. Soc.*, **2003**, *125*, 12803.
- [4] John J. Gilman, *Science*, **1996**, *274*, 65.

Corresponding Author Tel.: +81-045-566-1569; fax: +81-045-564-0950; e-mail: senna@applc.keio.ac.jp.

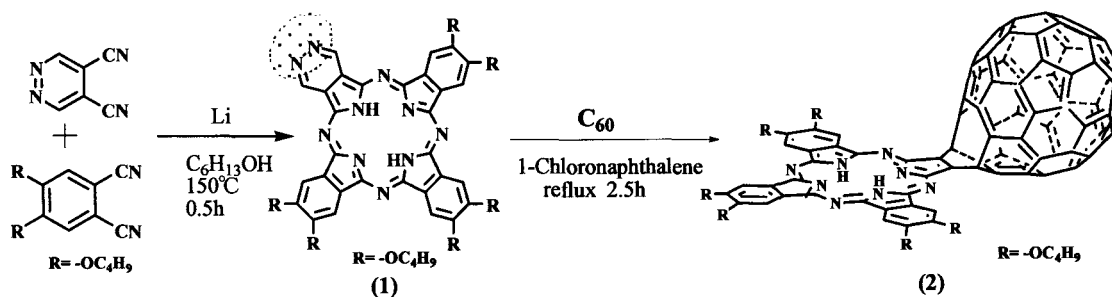
Novel C₆₀-Phthalocyanine Conjugates Having Open-Cage C₆₀ Skeleton

○Naoaki Hashimoto, Takamitsu Fukuda, and Nagao Kobayashi

*Department of Chemistry, Graduate School of Science, Tohoku University,
Sendai 980-8578, Japan*

A variety of functionalized fullerene (C₆₀) derivatives have become available recently. No dye-C₆₀ heteroconjugates, however, have been reported to date, despite the fact that these types of derivative are potential candidates for future optical and electronic applications due to the extensive molecular orbital (MO) interaction between the constituent moieties. Phthalocyanines (Pcs) are important classes of dye materials, and have found widespread industrial applications. Recently, our group has succeeded in synthesizing novel C₆₀-Pc conjugates by using 1,2-dicyanofullerene as one of the starting materials [1]. In this conjugate, the C₆₀ and Pc units are linked directly and, therefore, the distance between them is minimized. Interestingly, spectroscopic properties of the conjugates are clearly different from those of Pc as a consequence of extensive MO mixing between the C₆₀ and Pc moieties. Quantum chemical calculations indicate that the excited states of C₆₀-Pc conjugates are sensitive to the relative arrangement of C₆₀ and Pc.

In this study, we have attempted another synthetic approach to introduce C₆₀ moiety to the Pc skeleton. We first prepared a Pc containing the pyridazine unit (**1**), which was further reacted with C₆₀ in refluxing 1-chloronaphthalene for 2.5 h to give a novel C₆₀-Pc conjugate (**2**). Due to the open-cage C₆₀ skeleton in **2**, the component moieties are fixed in close proximity. Synthetic methods and spectroscopic properties of **2** and its metal complexes will be presented in more detailed.



[1] Masuda, S.; Fukuda, T.; Kobayashi, N. *Abst. The 28th Fullerene-Nanotube General Symposium, 2005*, Nagoya, Japan, p. 116.

Corresponding Author: Nagao Kobayashi

Tel & Fax: +81-22-795-7719, **E-mail:** nagaok@mail.tains.tohoku.ac.jp

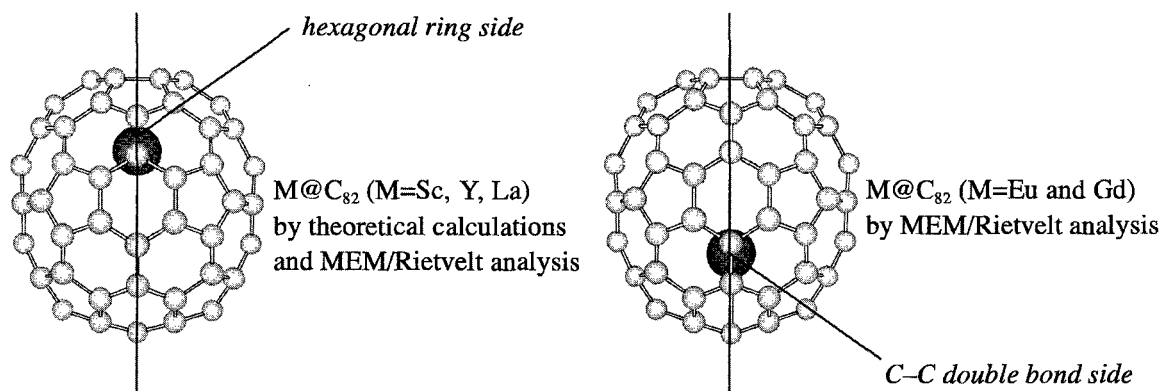
Endohedral Structures of Eu@C_{82} and Gd@C_{82}

○Naomi Mizorogi¹ and Shigeru Nagase^{1,2}

¹*Department of Structural Molecular Science, The Graduate University for Advanced Studies, Okazaki 444-8585, Japan*

²*Department of Theoretical Studies, Institute for Molecular Science, Okazaki 444-8585, Japan*

Endohedral metallofullerenes are known to have several unique properties. To apply these to new materials, it is important to clarify the endohedral structures and electronic properties. M@C_{82} (M=Sc, Y, and La) has been extensively investigated both theoretically and experimentally. It has been determined that the metal atom is located at an off-centered position on the C_2 axis adjacent to a hexagonal ring of C_{2v} - C_{82} cage by theoretical calculations and MEM/Rietvelt analysis of X-ray powder diffraction data. Recently, the endohedral structures of Eu@C_{82} [1] and Gd@C_{82} [2] have been determined by MEM/Rietvelt analysis. It has been shown that the metal atom is located on the C_2 axis and adjacent to the C–C double bond on the opposite side of the C_{2v} - C_{82} cage, unlike the M@C_{82} (M=Sc, Y, and La) case. We report density functional calculations of the endohedral structures and electronic properties of Eu@C_{82} and Gd@C_{82} .



References

- [1] B.-Y. Sun, T. Sugai, E. Nishibori, K. Iwata, M. Sakata, M. Takata, H. Shinohara, *Angew. Chem.* 44 (2005) 4568.
 [2] E. Nishibori, K. Iwata, M. Sakata, M. Takata, H. Tanaka, H. Kato, H. Shinohara, *Phys. Rev. Lett.* 69 (2004) 113412.

Corresponding Author: Naomi Mizorogi

E-mail: mizorogi@ims.ac.jp Tel: +81-564-55-7260 Fax: +81-564-53-4660

3P-10

A New Metallofullerene Growth Mechanism II -A Mechanism of Two or Three Metal Atoms Encapsulation-

Yohji Achiba

Department of Chemistry, Tokyo Metropolitan University,
Hachioji, Tokyo, Japan

We have proposed a new fullerene network growth model by which several unknown factors related with the formation of stable endohedral metallofullerenes ($M_x@C_{2n}$) are safely described. In this model, we proposed a specific carbon skeleton consisting of three fused hexagons coupled with isolated three pentagons, might be called "phenalenyl skeleton", as a key carbon network (see Fig.1). In this model, we assume that at the first stage, carbon ring and/or chain clusters start to form carbon aggregates like a "carbon nest", as those demonstrated in the previous study of fullerene molecular dynamics simulations. In the carbon aggregates, we further assume that P(phenalenyl)- skeleton plays an essential role as a "center" of the 5- and 6-membered network carbon cage formation of a metal encapsulated metallofullerene.

In this work, we here try to apply the p-center model to understand the process how the second or third metal atoms are entrapped in the cage. In Table 1, we summarized the numbers of the p-active centers for the metallofullerene cages with different sizes and symmetries. It is quite interesting to

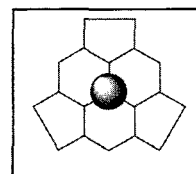


Fig. 1

note that all the cages in which two or three metal atoms are safely entrapped possess at least four p-center active sites. Furthermore, it should also be noted that the spatially relative position of each active site is very important to explain the specific cages for $M_2@C_{2n}$ or $M_3@C_{2n}$.

All the cage network having two or three metal atoms inside seem to satisfy the condition in which two or three p-center active sites are located with each other with a certain long distance.

Numbers of a P-center Active site and Metallofullerenes			
Size	Sym.	Active site	Metallofullerenes
66	C2v(NonIPR)	2	Sc2@C66
68	D3 (NonIPR)	8	Sc3N@C68
72	C2v(NonIPR)	8	La2@C72
74	D3h	2	Ca@C74, La@C74
76	Td	4	Lu2@C76,
	C2v(NonIPR)	4	Ca@C76
78	D3h(5)	6	La2@C78, Ca@C78
80	Ih(7)	20	La2@C80, Sc3N@C80
82	C2v(9)	8	Ca@C82, La@C82
	Cs(6)	6	Er2@C82
	C3v(8)	10	Y2@C82
	C2(5)	4	Ca@C82
	C3v(7)	2	
84	Cs(4)	2	
	D2d(23)	0	Sc2C2@C84

Table 1

E-mail: achiba-yohji@c.metro-u.ac.jp, Tel:+81-426-77-2534 Fax:+81-426-77-2525

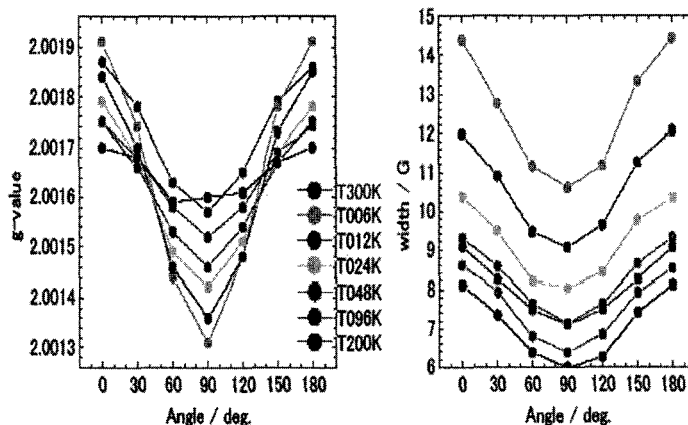
ESR Spectrum of La@C₈₂(Ad) Single Crystal

○Ryuhei Nara^{J)}, Yutaka Maeda^{G)}, Takatsugu Wakahara^{T)}, Takahiro Tsuchiya^{T)},
Kazuhiro Takeuchi^{J)}, Makoto Fukushima^{J)}, Takeshi Akasaka^{T)}, Tatsuhisa Kato^{J)*}

^{J)}Department of Chemistry, Josai University, Sakado 350-0295, Japan, ^{T)} Center for
Tsukuba Advanced Research Alliance, University of Tsukuba, Ibaraki 305-8577, Japan,

^{G)}Department of Chemistry, Tokyo Gakugei University, Tokyo 184-8501, Japan, ^{J)}
Institute for Molecular Science, Okazaki 444-8585, Japan,

The g-tensor of the magnetization of La@C₈₂(Ad) (Ad=adamantylidene) single crystal was determined by the high-field (W-band) ESR spectroscopy at various temperatures, from 6K to 300K. The single crystal of La@C₈₂(Ad) was recently synthesized by the Gakugei and Tsukuba group of the authors, and the X-ray analysis gave it's unambiguous crystal structure⁽¹⁾. It's ESR spectrum exhibits a very sharp single line at the g-value depending on the orientation of the crystal to the static magnetic field, see the left hand side figure. The high-field (W-band) ESR spectrometer gives the precise g-tensor of the crystal from the orientation-depending analysis. The g-tensors at various temperatures are determined, and the anisotropy of the g-tensor decreases with increasing temperature. And the line width of the spectrum depends on the orientation of the crystal and becomes sharp with increasing temperature, see the right hand side figure. The feature of the anisotropy and the line width reflects the magnetic interaction among molecules in the crystal structure.



References: 1)Y. Maeda et al., J. A. C. S. 126(2004) 6858-6859.

Corresponding Author: Tatsuhisa Kato

E-mail: rik@josai.ac.jp

Tel: 049-271-7295 Fax: 049-271-7985

Synthesis and Characterization of Carbene Derivatives of $\text{La}_2@C_{80}$

○ Chika Someya,¹ Michio Yamada,¹ Takatsugu Wakahara,¹ Takahiro Tsuchiya,¹ Yutaka Maeda,² Takeshi Akasaka,¹ Naomi Mizorogi,³ and Shigeru Nagase³

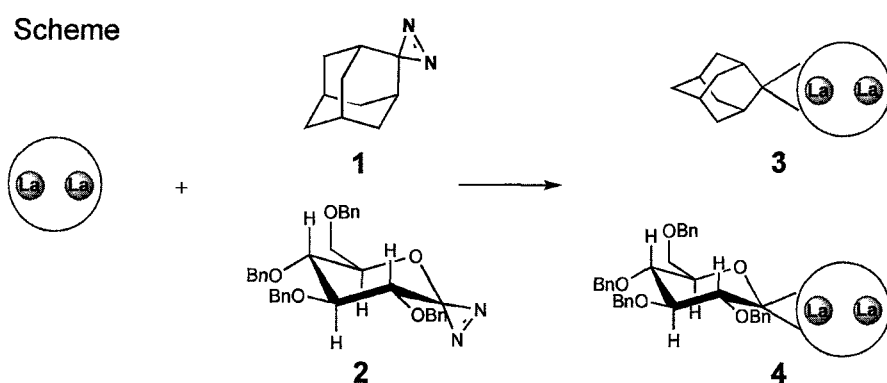
¹ Center for Tsukuba Advanced Research Alliance, University of Tsukuba, Tsukuba, Ibaraki 305-8577, Japan

² Department of Chemistry, Tokyo Gakugei University, Koganei, Tokyo 184-8501, Japan

³ Institute for Molecular Science, Okazaki, Aichi 444-8585, Japan

Encapsulation of one or more metal atoms inside hollow fullerene cages is of interest since it leads to new spherical molecules with novel properties unexpected for empty fullerenes. [1] Chemical functionalizations of endohedral metallofullerenes provide an entry into investigations of the biochemical and pharmacological potential of this fascinating class of compounds. Recently, we have isolated and characterized carbene derivative $\text{La}@C_{82}\text{Ad}$ (Ad = adamantylidene) prepared by the reaction of $\text{La}@C_{82}$ with adamantanediazirine. [2]

In this study, we report for the first time the synthesis and isolation of carbene derivatives of $\text{La}_2@C_{80}$ **3** and **4** which were prepared by the reaction of $\text{La}_2@C_{80}$ with adamantanediazirine **1** and sugar diazirine **2**, respectively. Their structures were determined by mass, absorption, NMR spectroscopic analyses. The electrochemical properties of **3** and **4** were also investigated by means of cyclic voltammetry.



[1] *Endofullerenes: A New Family of Carbon Clusters*; Akasaka, T.; Nagase, S., Eds., Kluwer: Dordrecht, 2002.

[2] Maeda, Y.; Matsunaga, Y.; Wakahara, T.; Takahashi, S.; Tsuchiya, T.; Ishitsuka, M. O.; Hasegawa, T.; Akasaka, T.; Liu, M. T. H.; Kokura, K.; Horn, E.; Yoza, K.; Kato, T.; Okubo, S.; Kobayashi, K.; Nagase, S.; Yamamoto, K. *J. Am. Chem. Soc.* **2004**, *126*, 6858.

Corresponding Author: Takeshi Akasaka

TEL & FAX: +81-29-853-6409, E-mail: akasaka@tara.tsukuba.ac.jp

Ion Mobility Studies on Sc metallofullerenes

○T. Sugai¹, M.F.Jarrold², H. Shinohara^{1,3,4}

¹*Department of Chemistry, Nagoya University*

²*Department of Chemistry, Indiana State University*

³*Institute for Advanced Research, Nagoya University*

⁴*CREST, Japan Science and Technology Agency*

Structural studies have been a main issue on metallofullerenes. NMR and X-ray diffraction have clarified their unique structures and properties. These methods, however, require isolated large amount of samples, which prevents us from systematic studies on cage size. For this purpose, we have developed an ion mobility method and have clarified universality of the carbide structures [1] and their cage size dependence.

The Sc metallofullerene samples are prepared by an arc discharge using Sc graphite composite rods. They were extracted and were desorbed and ionized with a XeCl laser. Thus produced ions were introduced into a drift cell filled with He of 500 Torr. After passing through the cell, the ions were mass selected and were detected to measure a drift time which is defined as the time difference between the laser shot and the ion detection.

Figure 1 shows the mobility profiles of various Sc di-metallofullerenes, where two species are identified. The drift time or the mobility difference between the two peaks corresponds to that between C_n and C_{n-2} fullerene cage meaning carbide and normal structures [1]. These series measurements show that $Sc_2C_{82}^+$ tends to have the normal $Sc_2@C_{82}$ structures. The intensity ratio between the normal and the carbide shows maximum at C_{82} , suggesting Sc di-metallofullerenes have special stability with C_{82} cage. For the higher or lower cage size, the ratio decreases indicating the carbide structure is dominant for these fullerenes.

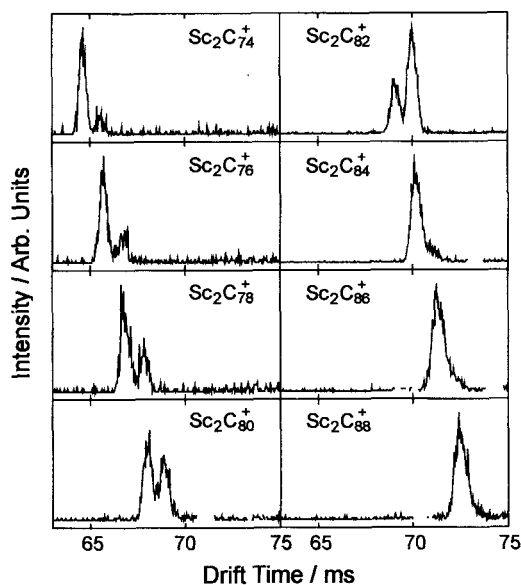


Fig. 1 Mobility profiles of Sc di-metallofullerene

References:

[1] T. Sugai et al., *J. Am. Chem. Soc.* **123**, 6427 (2001).

e-mail: sugai@nano.chem.nagoya-u.ac.jp tel: +81-52-789-2477 fax: +81-52-789-1169

Fabrication and characterization of solution-processed Pd-C₆₀ polymer-based thin film transistors

○ Yukitaka Matsuoka^{1,2}, Kagan Kerman¹, Eiichi Tamiya¹, Akihiko Fujiwara^{1,2}

¹ School of Materials Science, Japan Advanced Institute of Science and Technology,

1-1 Asahidai, Nomi, Ishikawa 923-1292, Japan

² CREST, Japan Science and Technology Corporation,

4-1-8 Honchou, Kawaguchi, Saitama 332-0012, Japan

Over last few years, ubiquitous computing society, which provides information and services anytime and anywhere, has been intense attention. In order to realize it, the development of low-cost and flexible, large-area devices like an *e*-paper is important. It is demonstrated that Organic Thin Film Transistors (OTFTs) are considerably valuable for application to such devices because solution processes are available for the fabrication of OTFTs [1]. However, the contact resistance at interface between electrodes and organic semiconductor is comparable to or exceeds the channel resistance in OTFTs [2]. The contact resistance causes the degradation of the performance of OTFTs. In the OTFTs, therefore, the decrease of the contact resistance is one of the most important issue to be solved.

Recently, the immobilization of cytochrome *c* on C₆₀-palladium (Pd) polymer (Figure. 1) which was modified on Pt electrodes was reported, and the direct electron transfer between the Pt electrode and the immobilized cytochrome *c* was observed [3]. This suggests that the Pt and C₆₀-Pd polymer are tightly connected.

We synthesized the C₆₀-Pd polymer and fabricated the TFTs with the C₆₀-Pd polymer active layer by the solution processes. The output characteristic of a C₆₀-Pd polymer TFT is shown in Figure. 2. This TFT shows n-channel behavior. The I_D first increased linearly with V_{DS} . This linear increase of the I_D suggests low contact resistance. The field effect mobility and current on-off ratio were 3×10^{-4} cm²/Vs and $\approx 10^2$, respectively.

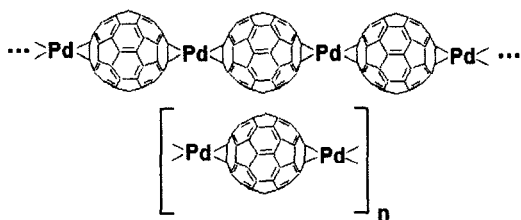


Figure 1. Chemical Structure of a C₆₀-Pd polymer.

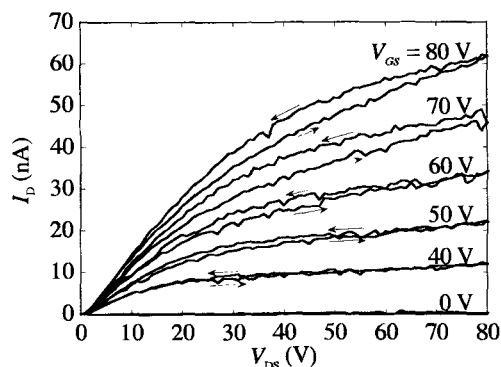


Figure 2. Output characteristic of a C₆₀-Pd polymer TFT.

[1] C. D. Dimitrakopoulos *et al.*, *Adv. Mater.* **14**, 99 (2002).

[2] P. V. Necliudov *et al.*, *Solid State Electron.* **47**, 259 (2003).

[3] F. D'Souza *et al.*, *Bioelectrochemistry* **66**, 35 (2005).

Corresponding Author: Yukitaka Matsuoka

E-mail: yukim@jaist.ac.jp **Tel&Fax:** +81-761-51-1699 ext. 1555 & +81-761-51-1535

Fabrication of high performance fullerene field-effect transistor devices and their performance control

○ Takayuki Nagano^{1,2}, Kenji Ochi¹, Haruka Kusai¹, Toshio Ohta¹, Kumiko Imai^{1,2}, Akihiko Fujiwara^{2,3}, and Yoshihiro Kubozono^{1,2}

¹Department of Chemistry, Okayama University, Okayama 700-8530, Japan

²CREST, Japan Science and Technology Corporation, Kawaguchi, 322-0012, Japan

³Japan Advanced Institute for Science and Technology, Ishikawa 923-1292, Japan

Field-effect transistors (FETs) with organic thin films have many advantages such as large-area coverage, structural flexibility, portability, and shock-resistance. The conventional SiO₂ gate insulators should be replaced by polymer gate insulators in order to bring out these advantages.

We have first fabricated flexible fullerene FET devices with polymer gate insulators on the poly(ethylene terephthalate) (PET) substrates. The *n*-channel normally-off FET properties were observed in the C₆₀ FET device with polyimide gate insulator [1]. The field-effect mobility, μ , was estimated to be $\sim 10^{-2}$ cm² V⁻¹ s⁻¹ at 300 K. On the other hand, the *n*-channel normally-on FET properties were observed in the fullerodendron FET with polyvinyl alcohol (PVA) insulator. The $I_D - V_{DS}$ plots of the fullerodendron/PVA FET is shown in Fig. 1.

The high-carrier injection into the active layer is expected to achieve the low-voltage operation in the FET device. We have fabricated C₆₀ FET device with high-dielectric gate insulator, Ba_{0.4}Ti_{0.6}Sr_{0.96}O₃ (BST). The $I_D - V_{DS}$ plots of the C₆₀/BST FET is shown in Fig. 2. Low-voltage operation was observed in the FET device. Application of fullerene FET devices in practical devices will be reported in this symposium.

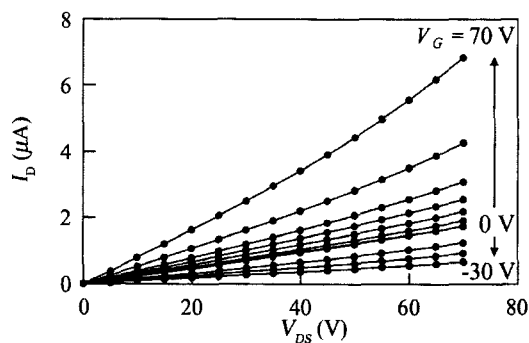


Fig. 1. $I_D - V_{DS}$ plots of fullerodendron/PVA FET.

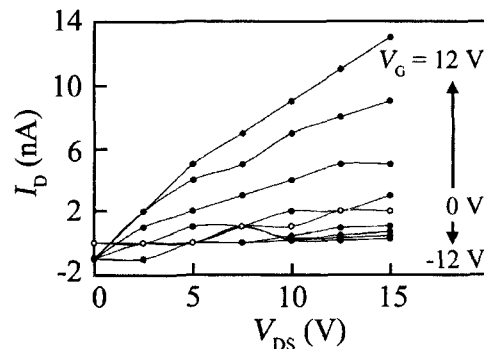


Fig. 2. $I_D - V_{DS}$ plots of C₆₀/BST FET.

[1] Y. Kubozono *et al.*, *Appl. Phys. Lett.* **87**, 143506 (2005).

Corresponding Author: Takayuki Nagano

E-mail: t-nagano@cc.okayama-u.ac.jp

Tel: +81-86-251-7850, Fax: +81-86-251-7853

Surface Modification using Self-assembled Monolayers on the Electrodes in Organic FETs

Nobuya Hiroshiba¹, Hisao Ishii², Ryotaro Kumashiro¹ and ○Katsumi Tanigaki^{1,3}

¹*Graduate School of Science, Tohoku University, Sendai, 980-8578, Japan*

²*Research Institute of Electrical Communication, Tohoku University, Sendai, 980-8577, Japan*

³*CREST, Japan Science and Technology Agency, Kawaguchi, Japan*

Organic field effect transistors (FETs) are important considering future applications to electronic devices, and have intensively been investigated. In order to improve the properties of organic-FETs like C₆₀ FET, the methodologies have not still been established. Especially, one of the most important key issues will be the interfacial problem between organic thin films and gate-insulators and/or electrodes and this is now drawing intense attentions. The surface control using self-assembled-monolayers (SAMs) is a well known method as such a surface modification for providing microscopically good interface regulations. Such efficient surface modifications have been reported to be achieved on SiO₂ gate insulators using silane molecules and on gold electrodes using thiol ones in the case of gold electrodes.

In the present study, interfacial modifications of source and drain gold electrodes using thiol molecules have been studied in detail for pentacene-FETs, using three thiol molecules as SAMs with different functional groups, 4-methyl (4MeBzT), 4-nitro (4-NBzT) and 4-amino (4-ABzT) benzene thiols and the organic FET properties have been investigated. The hole carrier mobility in organic-FETs can be increased by the SAMs modifications when the optimized preparation conditions are employed. Threshold-voltage (V_{th}) has been successfully controlled depending on the end functional-substituents of benzene thiol molecules. The changes in V_{th} observed in the present experiments are considered to be explained in terms of the charge transfer occurring from SAMs to pentacene or vice versa in the interfaces, which is also the very important in addition to the work functions to be modified with the SAMs treatment.

Corresponding Author: Katsumi Tanigaki

E-mail: tanigaki@sspns.phys.tohoku.ac.jp

Tel&Fax: +81-22-795-6469/+81-22-795-6470

Fabrication of field-effect transistor devices with three types of fullerodendrons by solution process, and their electronic properties

○ Haruka Kusai,¹ Takayuki Nagano,^{1,2} Kumiko Imai,^{1,2} Yoshihiro Kubozono,^{1,2}
Yuuki Sako,³ Yutaka Takaguchi,³ Akihiko Fujiwara^{2,4}

¹*Department of Chemistry, Okayama University, Okayama 700-8530, Japan*

²*Crest, Japan Science and Technology Agency, Kawaguchi, 322-0012, Japan*

³*Graduate School of Environmental Science, Okayama University, Okayama 700-8530, Japan*

⁴*Japan Advanced Institute of Science and Technology, Ishikawa 923-1292, Japan*

Solution-processed field-effect transistor (FET) devices have attracted special interests in their applications owing to low-temperature / low-cost fabrication processes. In this study, we have fabricated the FET devices with three types of fullerodendrons by using solution process. Their FET properties are also of interests from the viewpoints of supramolecular chemistry. The molecular structures of fullerodendrons are shown in Figure 1.

The fullerodendron films were formed on SiO₂/Si wafers by spin-coating of chlorobenzene solution of fullerodendron. The source and drain electrodes were formed on the fullerodendron films by thermal deposition of gold. The FET properties were measured under vacuum of 10⁻⁶ Torr. The value of field-effect mobility, μ , of the fullerodendron (II) FET reaches 1.7 x 10⁻³ cm² V⁻¹ s⁻¹ at 300K. The mobility gap and optical gap of fullerodendron (II) have been determined to be 0.30 and 1.4 eV, respectively, from the optical absorption spectrum and temperature dependence of resistivity. The electron transport is expected to occur through overlap of π -orbitals between the C₆₀ moieties in fullerodendron (II). It has been found from the temperature dependence of the μ value that the channel conduction in the fullerodendron (II) FET device follows thermally activated hopping-transport mechanism with activation energy of 0.21 eV. In this study, we have found from the properties of three FET devices that the suitable molecule for FET device is the fullerodendron molecule (II).

References:

Takaguchi, Y et al., *Tetrahedron Lett.* 2003, 44, 5777

Corresponding Author: Haruka Kusai

E-mail: h-kusai@cc.okayama-u.ac.jp

Tel: +81-86-251-7850, **Fax:** +81-86-251-7853

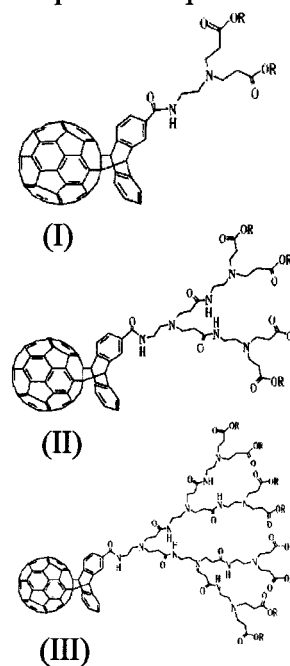


Figure 1

Resonance Raman Spectra of Polyene Molecules

T. Doi, and ○T. Wakabayashi

Department of Chemistry, School of Science and Engineering, Kinki University,
Kowakae 3-4-1, Higashi-Osaka 577-8502, Japan

Abstract: Recently, the hydrogen-capped linear carbon molecules, namely polyynes $\text{H}(-\text{C}\equiv\text{C}-)_n\text{H}$ ($n = 4-8$), were produced by a relatively simple method of laser ablation of carbonaceous particles in solution and characterized by their UV absorption spectra during the analysis using high-performance liquid chromatography (HPLC) [1]. For further analysis, surface enhanced Raman spectroscopy (SERS) was performed for the polyene mixture to observe $\sim 2000\text{ cm}^{-1}$ bands, which are characteristic of stretching modes of the carbon chains [2]. Furthermore, in order to obtain purified samples in macroscopic quantities, preparative HPLC and NMR characterization is in progress in our group [3]. In this poster, we focus on our recent results of Raman spectroscopy for the polyene molecules $\text{H}(-\text{C}\equiv\text{C}-)_n\text{H}$ of $n = 5$ and 6 using the chromatographically separated samples in *n*-hexane.

Figure 1 shows the Raman spectrum with an excitation at 234 nm, which is in resonance to a wavelength within the dipole-allowed electronic absorption band below 252 nm. The line with a Raman shift of 2120 cm^{-1} (designated as “1st” in Fig. 1) is followed by the series of lines (2nd, 3rd, and 4th) exhibiting the characteristic intervals. According to the molecular orbital calculation (B3LYP/cc-pVDZ), the progression is attributed to one of the stretching modes of the C_{10}H_2 molecule. The decay upon UV exposure is also observed.

References:

- [1] M. Tsuji *et al.*, Chem. Phys. Lett. **355**, 101 (2002).
 [2] H. Tabata, M. Fujii, and S. Hayashi, private communications.
 [3] T. Doi *et al.* 29th Fullerene-Nanotube General Symposium, 2P-70 (2005).

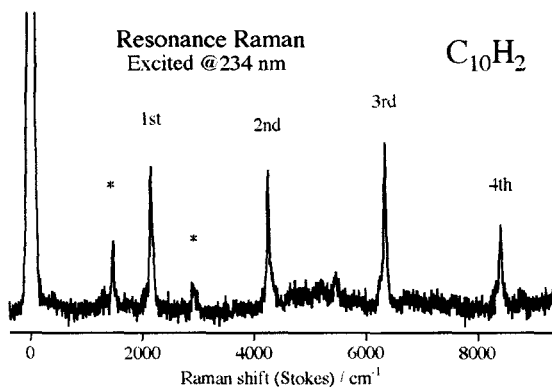


Fig. 1. Resonance Raman spectrum of polyene molecules C_{10}H_2 in *n*-hexane. The UV laser pulses at 234 nm (0.5 mJ/pulse) are irradiated through the solution and the scattered light is dispersed and detected using a 0.3 m monochromator. The Stokes lines of $\Delta\nu=1-4$ are observed with increments of 2120, 2105, 2090, and 2070 cm^{-1} for the 0th-1st, 1st-2nd, 2nd-3rd, 3rd-4th gaps, respectively. The bands with asterisks are due to the Raman signals of the solvent molecules.

Correspondence to Dr. Tomonari Wakabayashi, wakaba@chem.kindai.ac.jp, Tel 06-6730-5880 (ex. 4101)

The ultrasonication power density effects on carbon nanotube dispersion in aqueous solutions

Catalin Romeo Luculescu, Toru Ishii, Teruo Takahashi, Katsumi Uchida, Tadahiro Ishii, and Hirofumi Yajima

Department of Applied Chemistry, Tokyo University of Science, Tokyo 162-8602, Japan

Recently, sonochemistry was successfully applied for nanotube colloidal dispersion in aqueous or organic solvents. The process of debundling is based on powerful cavitation effect and subsequent substitution of powerful nanotube-nanotube Van der Waals forces by surfactant micelles or polymer wrapping. The ultrasonication is a quite complex process and the recent reports have been ambiguous with regard to the mechanism of nanotube dispersion in water [1-2].

In this work we are investigating the effect of ultrasonication parameters on single-walled nanotubes (SWNTs) dispersion in aqueous solutions in order to understand the side reactions and their effect on nanotubes' properties. The ultrasonication is dependent on horn type, cup geometry, power density, reagent's purity, and dispersion agent type. The temperature reached during the ultrasonication in air could be a good indicator of power density of the ultrasound.

We found that ultrasonication power density is a key parameter for SWNTs dispersion. The pH of dispersion is decreasing during mild ultrasonication and is affecting the optical spectra of dispersion as shown in Fig. 1. The chiral distribution is changing only for very high power energy ultrasonication.

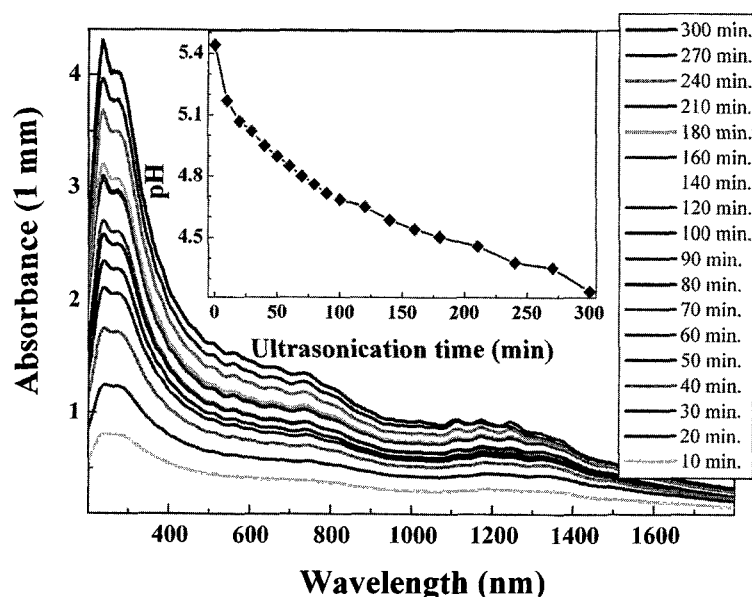


Fig. 1. The absorption spectra of ultrasonicated HiPco nanotubes in sodium dodecyl sulfate aqueous solution in air at 0.2 W/cm^3 power density ($65 \text{ }^\circ\text{C}$ temperature reached) for different durations. The insight is showing the decrease of pH.

[1]. D.A. Heller et al., *Carbon*, **43**, 651 (2005).

[2]. B. Benedict et al., *J. Phys. Chem. B*, **109** 7778-7780 (2005).

Corresponding author. Catalin Romeo Luculescu

Tel.: +81-3-3260-4272 (ext. 5831); Fax: +81-3-3235-2214; E-mail: clucules@rs.kagu.tus.ac.jp

Gas Analysis of CVD Processes for High-Yield Synthesis of Single-Walled Carbon Nanotubes

○Naoyasu Uehara,¹ Hiroki Ago,^{*1,2} Shingo Imamura,¹ Masaharu Tsuji^{1,2}

¹Graduate School of Engineering Sciences, Kyushu University, Fukuoka 816-8580, Japan

²Institute for Materials Chemistry and Engineering, Kyushu University and CREST-JST

Single-walled carbon nanotubes (SWNTs) are attractive material for their unique electronic and mechanical properties. However, an industrial scale synthesis of SWNTs has not been achieved yet. Understanding the kinetics of nanotube growth in chemical vapor decomposition (CVD) reaction is important for the high yield synthesis. Here, we investigated the kinetics through the gas analysis during CVD reaction in terms of catalytic activity and lifetime. SWNTs were synthesized by the thermal pyrolysis of CH₄ over Fe-Mo/MgO catalyst [1], and the exhaust gas was analyzed by a double-column gas chromatography (GC, Agilent 6890N). The methane conversion was determined by the amount of released H₂ and unreacted CH₄. We mainly studied (i) roles of Mo as co-catalyst and (ii) effects of water vapor to the nanotube growth. Fig. 1 shows the methane conversion as a function of reaction time. It was found that Mo co-catalyst significantly improves the catalytic activity as well as the lifetime. This suggests that Mo stimulates the surface decomposition of CH₄ and also prevents from the catalyst poisoning. Addition of the appropriate amount of water into the CVD system (0.8 μm/l) was found to elongate the catalyst lifetime, as shown in Fig. 2. The water vapor is supposed to clean the surface of the catalyst [2]. We also found that the water addition reduces the relative ratio of small-diameter nanotubes, resulting in the enrichment of large-diameter nanotubes. The present study suggests that the gas analysis is an effective tool to clarify the kinetics of SWNTs growth and to realize a high nanotube yield.

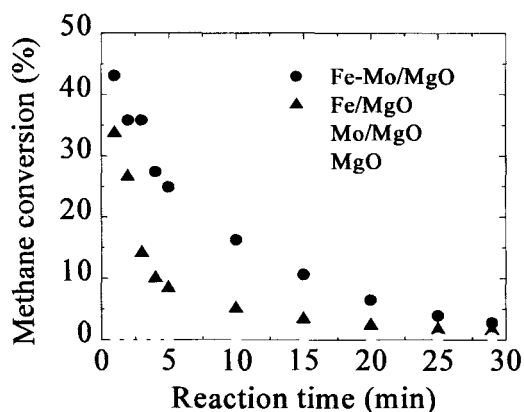


Figure 1 Time dependence of the methane conversion measured for different catalysts.

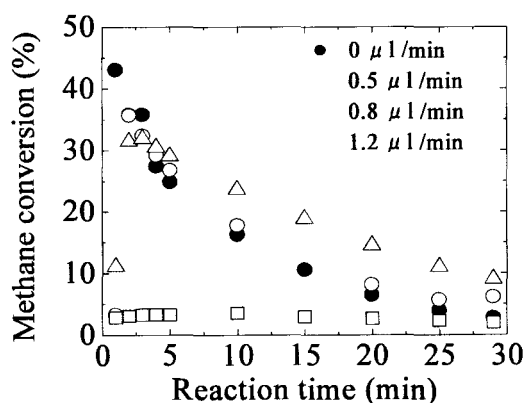


Figure 2 Change of the methane conversion of the Fe-Mo/MgO catalyst in the presence of water.

Acknowledgements The authors acknowledge Dr. T. Setoguchi, Mr. N. Tomonaga, and Dr. A. Tanaka of Mitsubishi Heavy Industries for helpful discussions. This work was supported by Nano-Carbon Technology Project of NEDO.

References [1] H. Ago et al., *J. Phys. Chem. B*, **109**, 10035 (2005). [2] K. Hata, et al., *Science*, **306**, 1362 (2004).

Corresponding Author Hiroki Ago (Tel&Fax: +81-92-583-7817, E-mail: ago@cm.kyushu-u.ac.jp)

Purification of single wall carbon nanotube made by arc plasma jet method

○Tomoko Suzuki, Kenji Suhama, Xinluo Zhao, Sakae Inoue, Yoshinori Ando

*21st COE Program "Nano Factory" Department of Materials Science & Engineering,
Meijo University, Nagoya 468-8502, Japan*

In the arc plasma jet (APJ) method¹⁾, a large amount of soot including single wall carbon nanotube (SWNT) can be made in a short time. However, a lot of impurities, such as amorphous carbon and catalyst metals, are included in the made soot besides SWNT. It is indispensable to remove these impurities to obtain pure SWNT. Here, we reported that it was able to purify easily in large quantities by reflux in the hydrogen peroxide solution using the iron particle.

The most important problem to purify APJ-SWNT is how to remove an amorphous carbon attached to catalyst metals. In the heating method, SWNT burns simultaneously with an amorphous carbon because combustion temperatures of amorphous carbon and SWNT are close, the temperature management is difficult. Then, the purification by the reflux in the hydrogen peroxide solution is tried. However, an amorphous carbon cannot be removed only by usually reflux. Then, it refluxes mixing a small amount of iron particle to activate the oxidation reaction of the hydrogen peroxide solution.

Figures 1 and 2 show TEM images of as-grown and purified APJ-SWNT, respectively. It is clear that there is no catalyst metal and it is purified, though something like a husk remain. Moreover, other experimental results show that the size of the iron particle greatly influences the effect. Those results show that it is possible to reflux more effectively by using smaller iron particles.

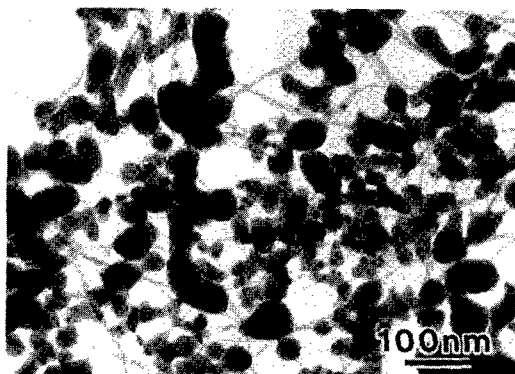


Fig. 1 TEM image of as-grown APJ-SWNT

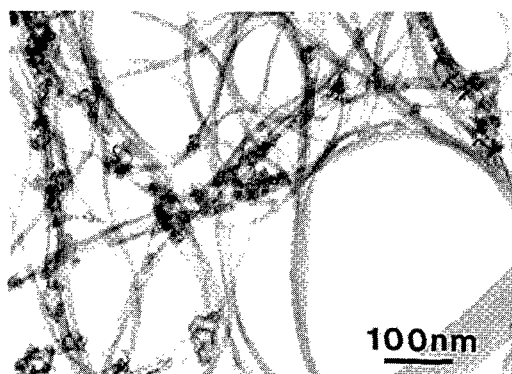


Fig. 2 TEM image of purified APJ-SWNT

References: (1) Y. Ando *et al.*, *Chem. Phys. Lett.* 323 (2000) 580-585

Corresponding Author: Tomoko Suzuki (m0441504@ccmailg.meijo-u.ac.jp)

Growth of carbon nanotubes on Si substrates with nanoprotusions

○Mai Matsubayashi¹, Hideki Sato¹, Koichi Hata¹, Hideto Miyake¹,
Kazumasa Hiramatsu¹, Akinori Ohshita¹ and Yahachi Saito²

¹*Department of Electrical and Electronic Engineering, Mie University
1577 Kurima-machiya-cho, Tsu 514-8507, Japan*

²*Graduate school of engineering, Nagoya University
Furo-cho, Chikusa-ku, Nagoya 464-8603, Japan*

In a growth of carbon nanotubes (CNTs) by chemical vapor deposition (CVD) method, existence of catalyst particles is significantly important. We have found that existence of nanosized protrusions (nanoprotusions) on substrate surface strongly influences to granulation of catalyst thin film that is deposited onto the substrate. Here we show effect of nanoprotusions on formation of catalyst nanoparticles and its influences to growth of CNTs.

Nano-protrusions were formed on Si (100) by reactive ion etching (RIE). A detailed process for formation of the nanoprotusions is described elsewhere [1]. The density of nanoprotusions was 10^{10} cm^{-2} and averaged height of the protrusions was 107nm. After the formations of nanoprotusions, titanium (Ti) buffer film and iron (Fe) catalyst film were deposited by vacuum evaporation. Deposition of titanium with a thickness of 0.5 nm was followed by the deposition of iron with a thickness of 0.5nm. After the deposition of buffer and catalyst film, CNTs were grown by a thermal CVD. C_2H_2 , H_2 and Ar were used as a process gases. The flow rates of C_2H_2 , H_2 and Ar were 5, 30 and 120 sccm, respectively. The growth temperature was 700 °C. The growth time was 5 min.

Fig.1 (a) and (b) are TEM images of the CNTs grown on substrate without and with the nanoprotusions, respectively. Multi-walled structure was seen for both cases. Averaged diameter of CNTs grown on the substrate with the nanoprotusions was about 6 nm, which is about a half of the diameter of the CNTs grown without the nanoprotusions (10nm). Diameter distribution of CNTs was also decreased drastically by using the substrate with nanoprotusion. Detailed examinations showed that the reduction of the diameter stems from difference of granulation behavior between the substrates with and without the nanoprotusions.

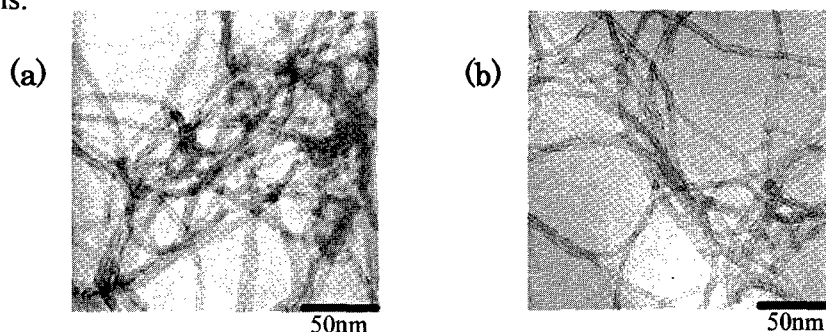


Fig.1 TEM images of the CNTs grown on substrate (a) without nanoprotusions, (b) with nanoprotusions

[1] H Sato, T. Sakai, M. Matsubayashi, K. Hata, H. Miyake, K. Hiramatsu, A. Oshita, and Y. Saito, Vacuum (accepted for publication)

Corresponding Author: Hideki Sato

E-mail: sato@elec.mie-u.ac.jp, Tel/Fax: +81-59-231-9404

Dispersion behavior and spectroscopic properties of SWNTs in various biopolymer solutions

○Teruo Takahashi, Catalin Romeo Luculescu, Katsumi Uchida, Tadahiro Ishii and Hirofumi Yajima

Department of Applied Chemistry, Faculty of Science, Tokyo University of Science (RIKADAI),
12-1 Funagawara-machi, Shinjuku-ku, Tokyo 162-0826, Japan

We have developed the novel dispersion and purification procedures of single wall carbon nanotubes(SWNTs) using biopolymers¹⁾. Recently, we found the cationic polysaccharide chitosan is an efficient dispersion agent for SWNTs²⁾. The spectroscopic properties of chitosan-SWNTs dispersion are different from sodium dodecyl sulfate(SDS)-SWNTs dispersion in acidic conditions. In this paper, we discuss the difference of spectroscopic characteristics of the SWNTs dispersed in chitosan and SDS solutions. SWNTs sample used in this study were HiPco SWNTs. HiPco SWNTs was mixed with SDS/D₂O and chitosan/2% acetic acid/D₂O solution and then treated using an ultrasonic disruptor for 60min. The obtained dispersions were ultracentrifuged to remove large bundles. The SDS-SWNTs (pH 6) and chitosan-SWNTs (pH3.7) dispersion liquids were labeled S and C-SWNTs, respectively. In order to confirm pH effect for the absorption spectra of S-SWNTs, the pH of the S-SWNTs dispersions was changed with 0.1M HCl solution after centrifugation. This sample was labeled AS-SWNTs (pH 3). Figure shows the UV-vis-IR absorption and NIR emission spectra of S, AS, and C-SWNTs, respectively. The spectroscopic features were very different. The S-SWNTs showed well resolved peaks, but, for AS-SWNTs, peaks in semiconductor range disappeared in both absorption and emission spectra. On the other hand, C-SWNTs showed a similar well resolved peaks under the acidic condition. This means chitosan is efficiently protective against the protonation of SWNTs. In addition, Emission and Raman spectra suggest that chitosan could be a chiral separation agent for SWNTs. The detail experimental conditions will be discussed in the presentation.

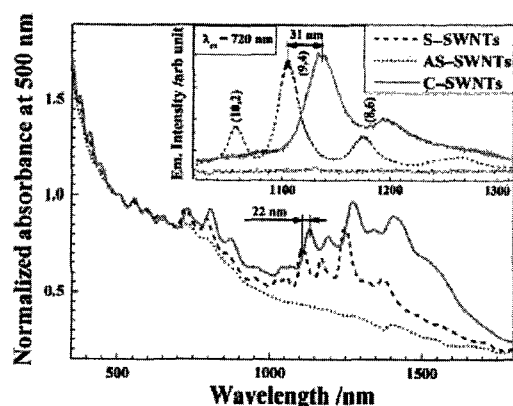


Figure UV-vis-NIR absorption spectra of S-SWNTs(dash line), AS-SWNTs(dotted line), and C-SWNTs(full line). The inset shows emission spectra of the same samples under 720nm excitation. The emission intensity of S-SWNTs was decreased 10times.

References

- 1) T. Takahashi et al *Jpn.J.Appl.Phys* **43** (2004) 3636.
 - 2) T. Takahashi et al *Chem.Lett.* **11** (2005) 1516.
- Corresponding Author; Hirofumi Yajima
E-mail yajima@rs.katu.tus.ac.jp TEL&FAX 03-3260-4272(5760) 03-3235-2214

Selective Chemical Vapor Growth of Vertically Aligned Carbon Nanotubes on Patterned Metal Layers

○Hiroki Okuyama, Nobuyuki Iwata and Hiroshi Yamamoto

College of Science and Technology, Nihon University, Funabashi, Chiba 274-8501, Japan

It is necessary to prepare nano-scaled probes and to control accurate approaching toward specimen for measuring electronic properties of nano-structured specimen. CNTs have many unique characteristics, for example, high mechanical strength, flexibility and high electric conductivity. Furthermore CNTs grow from only fine particles of catalyst, and the growth direction is controllable by applying electric fields during CVD. Those characteristics are applied to prepare novel vertically aligned CNT (VACNT) probes that are easy to prepare and to handle. In this work, we demonstrate the process for selective growth of VACNTs on patterned metal layers.

A Ni catalyst and a Mo metal layer were deposited on a quartz substrate through a metal mask. The boundary of the metal pattern was prepared to become thin gradually. The CNTs were grown by Thermal-CVD and dc Plasma-Enhanced-CVD method. The reactor tube of the CVD equipment was heated up to 600 °C. The flow of C₂H₄ : H₂ : Ar (5 : 50 : 50 ccm) was introduced into the reactor tube. The working pressure was fixed at 2 kPa. A dc voltage and current was -250 V and 0.3 A respectively. The growth time was 5 min.

Figure 1 (a) and (b) shows SEM images of the CNTs grown by the T-CVD and the PECVD methods respectively. By the T-CVD method, CNTs with 15 nm diameters grew with random directions. The CNTs grew at near the boundary of the metal pattern where the surface of the Mo films was rough and porous. The width of the CNT grown region was about 30 μm. In contrast, no CNTs grew on the smooth Mo surfaces. In the case of PECVD method, VACNTs with 30 nm diameters grew up all over the pattern.

The reason why CNTs grew at near the boundary by T-CVD is that the Ni catalysts formed fine particles at the region. The Ni catalysts didn't become fine particles on the smooth surface of Mo due to the high wettability. Rough morphology of the Mo underlayer promoted the Ni catalyst to become fine particles. But in the case of PECVD, in contrast, CNTs grew on the smooth surface of Mo. This result suggests the plasma promoted the Ni catalyst to become fine particles.

Conclusively it was demonstrated that a selective growth of CNTs was realized by controlling the thickness of the underlayer, and using different kind of CVD methods.

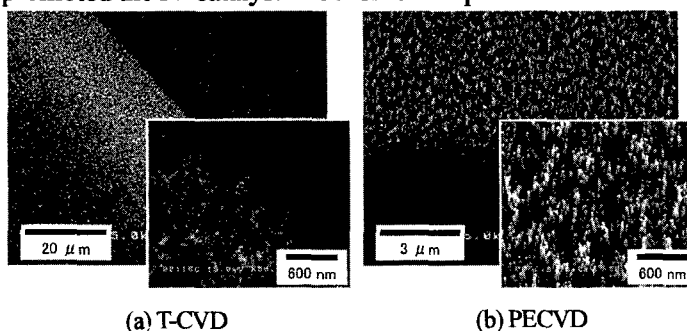


Fig. 1. SEM image of the boundary between metal pattern and substrate.

Corresponding Author: Hiroki Okuyama

Tel & Fax: +81-47-469-5457, E-mail: okuyama@yamanoya.ecs.cst.nihon-u.ac.jp

Preparation of Carbon Nanowires by Using Carbon Electrode Containing Fe Catalyst

○M. Endo, A. Mizutani, X. Zhao, and Y. Ando

21st COE Program “Nano Factory”, Department of Materials Science & Engineering,
Meijo University, Tenpaku-ku, Nagoya 468-8502, Japan

Carbon nanowires (CNWs), which is a one-dimensional (1D) carbon chain inserted inside a multiwalled carbon nanotube (MWNT), have been prepared by dc arc discharge evaporation of pure carbon electrode in H₂ gas¹⁾. Here, we show that the evaporation of carbon electrode containing Fe catalyst by using an arc plasma gun²⁾ or hydrogen arc discharge also results in the formation of CNWs.

Figure 1 shows a typical SEM image taken from the surface of the cathode deposit, prepared by dc arc discharge evaporation of carbon electrode containing 1 at% Fe catalyst in H₂ gas under a pressure of 40 Torr. Many long MWNTs bundles can be seen in this figure. Although 1 at% Fe catalyst has been added into carbon electrode, energy dispersion X-ray analyses indicate that no Fe element coexist with these MWNTs. The Raman spectra obtained by using two kinds of laser sources, 514 and 633 nm, are shown in Fig. 2. The high-graphitization of MWNTs can be confirmed from their G/D ratio. The peaks at approximately 1850 cm⁻¹ originate from the long 1D carbon chains inserted inside MWNTs, and the strong RBM peaks at 328 and 389 cm⁻¹ (see the inset) come from the innermost tubes with diameters of 0.7 and 0.6 nm of MWNTs, respectively. It can be concluded that the preparation of MWNTs with very thin central holes (~ 0.7 nm in diameter) is the essential condition for CNW growth.

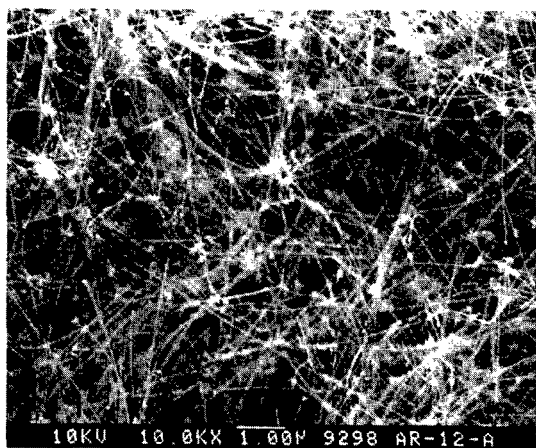


Fig. 1. SEM image of MWNTs.

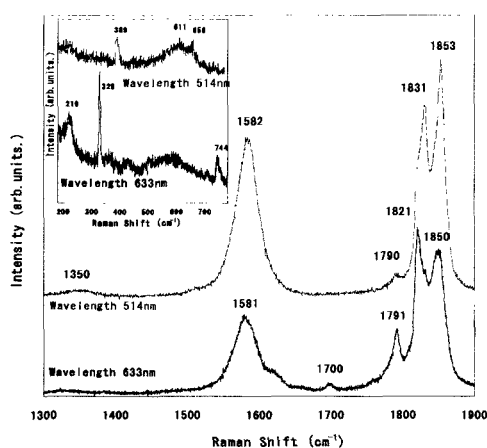


Fig. 2. Raman spectra of MWNTs.

Reference

- 1) X. Zhao *et al.*, *Phys. Rev. Lett.* **90** (2003) 187401.
- 2) M. Endo *et al.*, Abstracts of 29th Fullerene-Nanotubes General Symposium, 1P-17, Kyoto, (2005).

Corresponding Author: Masaaki Endo (E-mail:endo-flip@tf7.so-net.ne.jp)

Coalescence of C₆₀ in a peapod under electron irradiation

○Masanori Koshino¹, Kazutomo Suenaga^{1,2}, Eiichi Nakamura^{1,3}

¹*Nakamura Functional Carbon Cluster Project, ERATO, Japan Science and Technology Agency, 4-1-8 Honcho Kawaguchi, Saitama, Japan,* ²*National Institute of Advanced Industrial Science and Technology, 1-1-1 Higashi, Tsukuba, Ibaraki, Japan and* ³*Department of Chemistry, The University of Tokyo, Hongo Bunkyo-ku, Tokyo, Japan*

Coalescence of C₆₀ peapod is analyzed from high-resolution transmission electron microscopy at 120 kV. At room temperature, isolated C₆₀ molecules dimerize at a smaller electron dosage (Fig.1 bottom), while closely-packed C₆₀ molecules preserve their structure to much higher electron dosage (top). It is expected with a smaller electron dosage that an injected charge or heat be localized within a molecule, resulting in a coalescence of C₆₀ molecules in a peapod with a small dosage. With a shorter distance among closely-packed C₆₀ molecules, on the other hand, charge or heat would be delocalized to adjacent molecules, which stabilizes the C₆₀ structure against electron irradiation. At higher electron dosage, knock-on damage in addition to the ionization becomes substantial, resulting in higher coalescences of C₆₀ molecules in a peapod. A detailed analysis of radiation damage in C₆₀ peapod is applied to interpret the stability of C₆₀ crystal, which shows much higher stability against radiation damage.

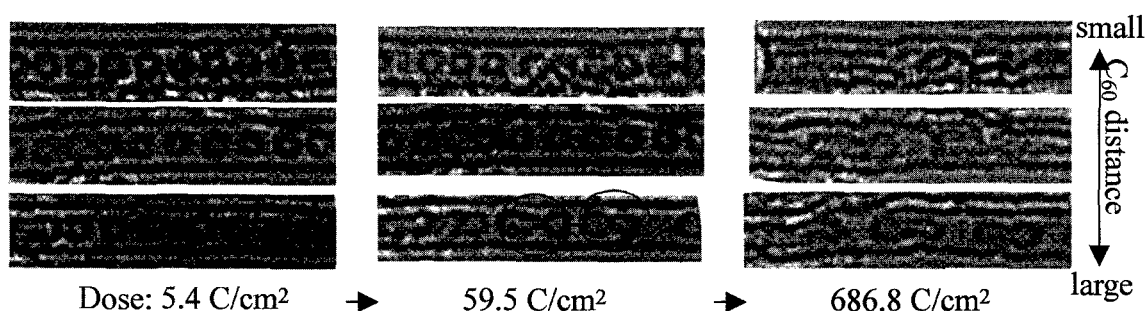


Fig.1 A different sensitivity to the radiation dose in C₆₀ peapods. The larger the C₆₀ distance becomes (top to bottom), the faster C₆₀ molecules coalesce.

References: Urita, K. *et al.* Nano Lett. 2004, 2451-2454.

Corresponding Author: Masanori Koshino

E-mail: m-koshino@aist.go.jp

Tel&Fax: 029-861-4424/029-861-4415

Large Scale Production of Carbon Nanohorns with High Purity

○ Takeshi Azami^{a,*}, Daisuke Kasuya^a, Tsutomu Yoshitake^a, Yoshimi Kubo^a,
Masako Yudasaka^a, and Sumio Iijima^{a,b}

^a *Fundamental and Environmental Research Laboratories, NEC Corporation
34 Miyukigaoka, Tsukuba, 305-8501, Japan*

^b *Department of Material Science and Engineering, Faculty of Science and Technology
Meijo University, 1-501 Shiogamaguchi, Tenpaku-ku, Nagoya, 468-8502, Japan*

Single-wall carbon nanohorns (SWNHs) are a type of single-wall carbon nanotube having diameters of 2–4 nm and horn-shaped tips [1], and they form dahlia-like aggregates. Their unique structures make SWNHs well suited for various applications such as catalyst support for fuel cells [2]. SWNH aggregates are produced by CO₂-laser ablation of pure graphite in an Ar-gas atmosphere [1]. The highest SWNH purity previously achieved is about 90% [1,3]. In this report we describe how we achieved a purity of about 95% by improving the fabrication equipment.

We modified the CO₂-laser ablation apparatus so that a large graphite rod (diameter 100 mm; length 500 mm) can be inserted and so that the used rod is semi-automatically replaced with a new one. This enables continuous laser irradiation. We also optimized the laser ablation conditions. The target rod is rotated at 2 rpm, meaning that the laser spot velocity on the target surface is about 10 mm/s. The laser power is about 3.5 kW and the spot diameter is 3.5 mm, corresponding to a laser power density on the target surface of about 30 kW/cm². As a result, about 50 g of SWNHs can be obtained from one rod.

Figure 1 shows the results of thermo gravimetric analysis (TGA) of SWNHs obtained with the improved equipment. The SWNHs exhibited a main peak at about 600°C and a small peak at about 750°C. The 750°C peak is ascribed to an impurity component (about 5%) in the form of a giant graphite ball (GG ball) [3]. Little amorphous carbon was found. The purity of the SWNHs was thus about 95%. Transmission electron microscopy observations confirmed the high purity and the “dahlia-like” forms of the SWNH aggregates (diameters 80–120 nm).

The improved equipment can thus be used for large-scale production of SWNHs with high purity.

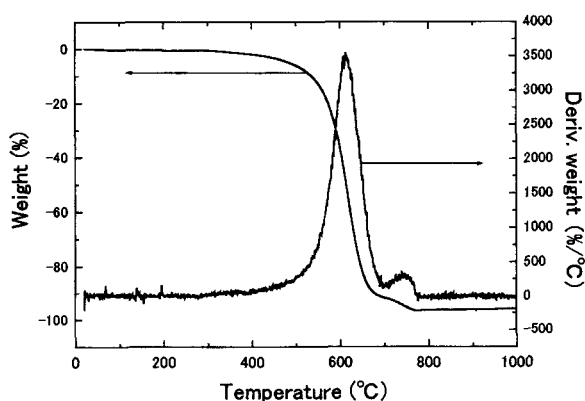


Figure 1. TG analysis of the SWNHs, heating rate of 10 °C/min in 100% O₂.

This work was performed under NEDO's research grant "Manufactured Goods Applying Nanocarbon Project".

[1] S. Iijima, et al., Chem. Phys. Lett. **309** (1999) 165.

[2] T. Yoshitake, et al., Physica B **323** (2002) 124.

[3] J. Fan, et al., J. Phys. Chem. B **109** (2005) 10756.

* Corresponding author: Takeshi Azami

E-mail: t-azami@cd.jp.nec.com, Tel: +81-29-850-2616, Fax: +81-29-856-6137

Mechanism of Plastic deformation of Carbon Nanotubes

○Hideki Mori¹, Shigenobu Ogata^{2,3,4}, Seiji Akita¹, Yoshikazu Nakayama^{1,4}

¹Department of Physics and Electronics, Osaka Prefecture University,
1-1 Gakuen-cho, Sakai, Osaka 599-8531, Japan.

²Center for Atomic and Molecular Technologies., Osaka University, Osaka 565-0871,
Japan

³Department of Mechanical Engineering, Osaka University, Osaka 565-0871, Japan

⁴Handai Frontier Research Center, Graduate School of Engineering, Osaka University,
2-1 Yamadaoka, Suita, Osaka 565-0871, Japan

Getting control over plastic deformation of carbon nanotubes (CNTs) is vital to prepare functional elements for miniaturized electronic and mechanical devices. Recently, Nakayama *et al.* have succeeded in induction of a plastic bend deformation to double-walled CNTs by applying a current flow.[1] Although many theoretical studies have been reported in the last decade, a mechanism from a standpoint of thermodynamics remains obscure. In this work energetics of the plastic deformation of single-walled CNT is studied.

Stone-Wales (SW) defect is known as a topological defect of CNTs. The formation of this defect is an initiation. Then the SW defect splits into two pentagon-heptagon (p-h) pairs by a rotation of a neighboring bond. This is the first split step. The two p-h pairs move away each other by further bond rotations and the chirality in the domain between the two p-h pairs changes consequently. These steps are the 2nd, 3rd, --- split step. The separating of the two p-h pairs causes the plastic bend deformation to carbon nanotubes.

We found that the local strain due to mechanical loading deformation effectively decreases the activation energy and the formation energy of the SW defect nucleation and splitting of the defects as shown in Fig. 1. These theoretical results are consistent with the previous experimental result.

References: [1] Y. Nakayama *et al.*, Jpn J. Appl. Phys. 44 L720.(2005)

Corresponding Author: Hideki Mori, Tel&Fax: +81-72-254-9265,

E-mail: mori@dd.pe.osakafu-u.ac.jp

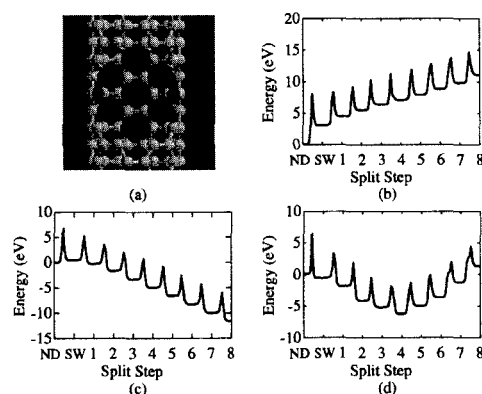


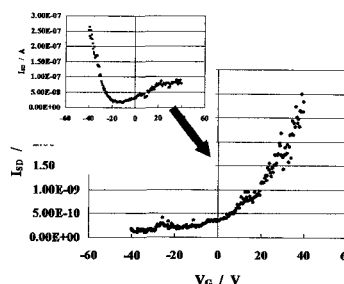
Fig.1 (a) snapshot of a SW defect. The potential energy plotted along the path of defect migration with (b) no-load condition, (c) tensile condition and (d) bending condition

FET Properties of Surface Silylated Carbon Nanotubes

○Ryotaro Kumashiro¹, Hiroataka Ohashi¹, Takeshi Akasaka², Yutaka Maeda³,
Takeshi Izumida⁴, Rikizo Hatakeyama⁴ and Katsumi Tanigaki^{1,5}

¹ Graduate School of Science, Tohoku University, Sendai, Japan: ² Center for Tsukuba, Advanced Research Alliance, University of Tsukuba, Tsukuba, Japan: ³ Department of Chemistry, Tokyo Gakugei University, Tokyo, Japan: ⁴ Graduate School of Engineering, Tohoku University, Sendai, Japan: ⁵ CREST, Japan Science and Technology Agency, Kawaguchi, Japan:

Carbon nanotubes (CNTs) have a bright prospect as the electronic material for nano-scale devices in the future, and a large number of studies have been made in recent years. In particular, it is well known that the field effect transistors (FETs) fabricated by CNTs having semiconducting properties show high ability in terms of the mobility. However, carriers in pristine CNTs are mostly hole, therefore, CNTs-FETs usually show the p-type properties. For applying CNTs to electronic devices, it is necessary to control the both carriers of electrons as well as holes, that is, the electron carrier doping should be established. As electron carrier doping techniques for CNTs, two major techniques are generally possible. One is endohedral and the other the exohedral modifications. It has been known that the doping with alkali metals or organic molecules can change the properties of CNTs-FET [1,2]. We reported the FET properties of exohedrally modified CNTs using Si-containing organic molecules in the last meeting [3], and demonstrated that p-type nanotubes can be converted to n-type ones as shown in Fig.1. In this meeting, we will present comparison of the FET properties between separated individual and bulk samples of exohedrally silylated CNTs, and will discuss the effect of surface silylation on the electronic states of these CNTs in more detail.



[1] C. Zhou et al., *Science*, 290, 1552 (2000). [2] T. Takenobu et al., *Nature Materials*, 2, 683 (2003). [3] R. Kumashiro et al., The 29th Fullerene-Nanotubes General Symposium, 3-2 (2005).

Corresponding Author: Ryotaro Kumashiro, **E-mail:** rkuma@sspns.phys.tohoku.ac.jp
Tel&Fax: +81-22-795-6468/+81-22-795-6470

High Field Magneto-optical Study of Unbundled Single-walled Carbon Nanotubes to 120 T

○Hiroyuki Yokoi¹, Noritaka Kuroda¹, Yeji Kim², Kanae Miyashita², Said Kazaoui², Nobutsugu Minami², Eiji Kojima³, Kazuhito Uchida³, Shojiro Takeyama³

¹*Dept. of Mechanical Eng. and Materials Sci., Kumamoto Univ., 2-39-1 Kurokami, Kumamoto-shi, Kumamoto 860-8555*

²*Nanotechnol. Research Inst., Nat'l Inst. of Advanced Industrial Sci. and Technol., Higashi, Tsukuba, Ibaraki 305-8565*

³*Inst. for Solid State Phys., Univ. of Tokyo, Kashiwanoha, Kashiwa, Chiba 277-8581*

Single-walled carbon nanotubes (SWNTs) have cylindrical structure made of a graphene sheet, which leads to theoretical predictions of their novel properties, including the emergence of the Aharonov-Bohm (AB) effect when threaded with a magnetic flux. [1] Apart from the AB effect observed in nanometer-sized structures of semiconductors, the AB effect modifies the band structure of an SWNT itself. The modification of the first-subband gaps in semiconducting SWNTs has been demonstrated through magneto-optical studies in magnetic fields to 45 T by Zaric et al. [2] However, no variations were observed for the second-subband gaps of semiconducting tubes and metallic tubes, which would be attributed to the innate broadness of the corresponding absorption peaks. We have conducted interband magneto-absorption study in the visible light region for highly unbundled SWNTs embedded in gelatine or carboxymethylcellulose films under high magnetic fields up to 120 T. Absorption peaks originated from the second-subband gaps in semiconducting tubes and metallic tubes were observed to split by the application of magnetic fields in parallel to the linear polarization of the incident light while not in perpendicular to it, which confirms a manifestation of the AB effect in the band structure of metallic tubes as well as semiconducting tubes. These observations suggest the magnetic field induced metal-semiconductor transition in the metallic tubes strongly.

[1] H. Ajiki and T. Ando, J. Phys. Soc. Jpn. **62**, 1255-1266 (1993).

[2] S. Zaric et al., Science, **304**, 1129-1131 (2004).

Corresponding Author: Hiroyuki Yokoi

E-mail: yokoihr@kumamoto-u.ac.jp

Tel&Fax: +81-96-342-3727(T)/3710(F)

Environmental effects of PL/Raman spectra from suspended SWNTs

○Y. Kobayashi¹, D. Takagi² and Y. Homma²

¹*NTT Basic Research Laboratories, NTT Corporation, Atsugi-shi 243-0198, Japan*

²*Tokyo University of Science, and CREST/JST, Shinjuku-ku, Tokyo 162-0825, Japan*

Suspended single-walled carbon nanotubes (SWNTs) do not make contact with foreign materials such as a substrate, and environmental interaction, which affects SWNT optical properties, is expected to be reduced significantly. We have investigated optical properties of suspended SWNTs and observed extremely intense signals of photoluminescence (PL) and Raman spectra [1,2]. In this work, we examined the environmental effects due to SDS wrapping, Si oxide substrates and bundle formation, based on PL and Raman spectra obtained from an identical suspended SWNT [2].

The chirality of a specific SWNT grown by CVD between a pair of SiO₂ pillar can be determined by the combination of Raman and PL signals from the identical suspended SWNT. The analysis results are summarized in Fig.1 as the relation between the chiralities of each SWNT and RBM frequencies. The RBM frequencies can be better fitted using the equation $\text{RBM freq. } \omega[\text{cm}^{-1}] = 223.5/\text{diameter } d[\text{nm}] + 12.5$, which is based on the results for SDS-wrapped SWNTs [3], rather than the equation $\omega = 248/d$, which is derived from the results on Si oxide substrates [4]. In other words, environmental effects in Raman spectra are very strong for oxide substrates and cause higher frequency shifts of the RBM signals but are negligible for the SDS wrapping. The latter result for SDS wrapping makes sharp contrast with the PL spectra, in which all of the PL peaks from SDS-wrapped SWNTs [1-3] are clearly shifted from that of suspended SWNTs. This indicates that SDS wrapping has a significant environmental effect on PL spectra compared with Raman spectra. The observed systematic shift to lower RBM frequencies due to bundle formation by about 5 cm⁻¹ is quite contrary to the theoretical prediction [5] and also intuitive expectation. These results indicate very complicated features of environmental effects.

References: [1] J. Lefebvre et al.: Appl. Phys. A78 (2004)1107. [2] Y. Kobayashi et al.: 29th Fullerene Nanotubes General Symp. 1P-55 (Kyoto, July 2005). [3] B. Weisman et al.: Nanolett. 3(03)1235. [4] A. Jorio et al.: PRL86(2001)1118. [5] L. Henrard et al.: PRB 64(2001)205403

Corresponding Author: Yoshihiro Kobayashi
E-mail: kobayashi.yoshihiro@will.brl.ntt.co.jp
Tel&Fax: +81-46-240-3424/4718

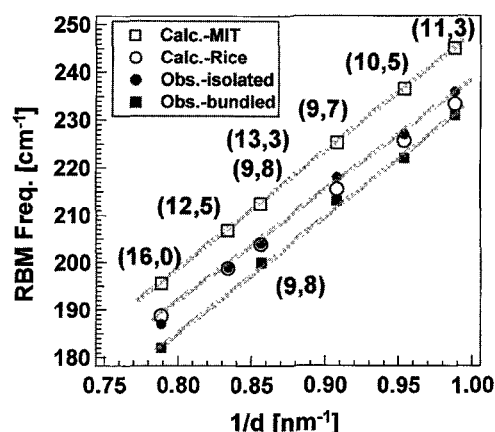


Fig.1: Relation between analyzed chiralities of individual (solid circles) and bundled (solid squares) suspended SWNTs and RBM frequencies observed from them. Calculated frequencies based on refs.[3,4] are also plotted for comparison.

Raman study of laser-induced defects in single-wall carbon nanotube bundles

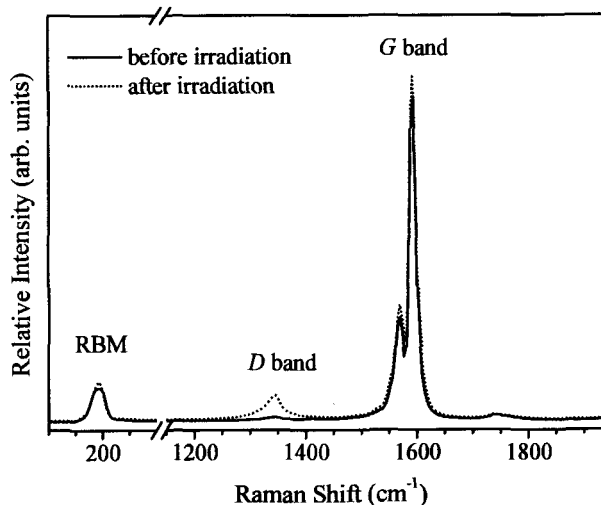
○Takashi Uchida, Masaru Tachibana and Kenichi Kojima

*Graduate School of Integrated Science, Yokohama City University
22-2 Seto, Kanazawa-ku, Yokohama 236-0027, Japan*

Defects in single-wall carbon nanotubes (SWNTs) significantly affect the physical properties of SWNTs. Evaluating and controlling of the defects in the SWNTs are very important for characterization and nanotechnological application of the SWNTs. Resonant Raman spectroscopy has been shown to be a powerful tool for characterizing the structure of SWNTs. In the Raman spectrum of the SWNTs, defect-induced Raman band (so-called *D* band) is observed at $\sim 1350\text{ cm}^{-1}$. It is known that defect-induced *D* band originates from the double resonance process. However, the structure of the defect related to the *D* band formation is not understood yet. In this study, we investigate the defects in SWNT bundles due to the laser irradiation using the resonant Raman spectroscopy.

The SWNT bundles using in this study were produced by electric arc discharge method. A catalyst with a 1:1 Ni:Y atomic ratio was used in the synthesis. Laser irradiation was carried out with pulsed KrF excimer laser (LAMBDA.physic, COMPEX 205). The Raman spectra were acquired on a micro-Raman system (NRS-1000, JASCO) composed of an optical microscope ($\times 100$ objective), a holographic notch filter, a single-grating spectrometer (1800 gr/mm grating) and an air-cooled charge-coupled device (CCD) detector. The spectra excitation was provided with a Nd:YVO₄ laser of a wavelength of 532 nm. The excitation laser power in the focal spot of about $1\ \mu\text{m}$ in diameter was kept below 0.02 mW, which corresponds to an average laser power density of 2 kW/cm^2 . The measurements were performed using a back-scattering geometry.

Raman spectra of SWNT bundles including RBM, *D* band and *G* band were obtained before and after irradiation (Fig.1). The intensity of the *D* band relative to the *G* band (I_D/I_G) being roughly proportional to the amount of the disordered sp^2 carbon is about 0.01 before irradiation. The I_D/I_G increased five-fold after irradiation. This indicates that the defects were introduced to the SWNTs by laser irradiation. In the meeting, the characteristic of the defects will be discussed by comparing TEM images.



Corresponding Author: Masaru Tachibana

E-mail: tachiban@yokohama-cu.ac.jp

Tel&Fax: +81-45-787-2307

Fig.1 Raman spectra of the SWNT bundles before and after irradiation. The laser irradiation was provided with pulsed KrF excimer laser (150 mJ/pulse at 248 nm).

Optical Properties of Double-Walled Carbon Nanotubes

○Taro Ueno^{1,2}, Shingo Okubo³, Tsuneaki Miyahara¹, Shinzo Suzuki⁴, Yohji Achiba⁴,
Toshiya Okazaki³, Kazuhito Tsukagoshi⁵, Hiromichi Kataura^{2,1}

1. Department of Physics, Tokyo Metropolitan University, 192-0397, Tokyo

2. Nanotechnology Research Institute, Advanced Industrial Science and Technology (AIST),
305-8562, Tsukuba

3. Research Center for Advanced Carbon Materials, AIST, 305-8562, Tsukuba

4. Department of Chemistry, Tokyo Metropolitan University, 192-0397, Tokyo

5. RIKEN, 351-0106, Wako

Abstract:

Double walled carbon nanotube (DWCNT) is a multi-walled carbon nanotube (MWCNT) that has the lowest number of layers. While most of MWCNTs have incomplete carbon layers, DWCNTs have closed cylinder structure like single-walled carbon nanotubes (SWCNTs). Thus DWCNTs can be regarded as an ideal material to see interlayer interactions in carbon nanotubes. To date, many groups have synthesized double-walled carbon nanotubes (DWCNTs) by catalytic chemical vapor deposition (CCVD) technique. In most cases, however, as-grown sample contains SWCNTs as impurities. Since SWCNTs show much more intense optical response than multi-layered nanotubes, it is very important to remove SWCNTs to see intrinsic physical properties of DWCNTs.

In this work, high-purity DWCNTs sample was realized by a simple production and purification procedures. DWCNTs containing SWCNTs sample was produced by CCVD method using Fe catalyst and was purified by a simple treatment. Finally we obtained high-quality bucky paper of DWCNTs just like the bucky paper of DWCNT by Endo's group [1]. Raman spectra and optical absorption spectra of the DWCNT will be discussed.

References:

[1] M. Endo *et al. Nature* 433 (2005) 476.

Corresponding Author: Hiromichi Kataura

E-mail: h-kataura@aist.go.jp

Tel: 029-861-2551, Fax: 029-861-2786

Lithium Ion Storage Property of Peapod

○S. Kawasaki^a, Y. Iwai^a, I. Watanabe^a, H. Kataura^b

^a*Nagoya Institute of Technology,*

Gokiso, Showa, Nagoya 466-8555, Japan

^b*National Institute of Advanced Industrial Science and Technology,*

Central 4, Higashi 1-1-1, Tsukuba, Ibaraki 305-8562,

Single-walled carbon nanotube (SWNT) bundle having ordered porous structure is one of the good candidates as new anode materials for lithium ion secondary battery. However, according to a recent paper[1], tube interior does not act as an efficient site for the lithium ion storage. If lithium insertion inside the tube will be possible, the storage capacity of SWNT bundle will be much improved. C₆₀-peapod, a SWNT including C₆₀ molecules inside the tube, has a different tube interior environment from empty SWNT. In this study, we report on the storage capacity of the peapod sample.

SWNT samples used in the present study were prepared by laser-ablation method. The tube diameter was estimated to be 1.35-1.45 nm by Raman scattering (JASCO, NRF-2200) measurement of radial breathing modes (RBM), by TEM (JEOL, JEM-2010) and XRD (Rigaku, RINT-2200) measurements. For the preparation of C₆₀-peapod sample, after decapping the SWNTs, C₆₀ molecules were introduced into tubes by heating C₆₀ powders with SWNTs in a sealed quartz tube. The C₆₀-occupancy of the pods was estimated to be more than 80% by the decrease of (10) XRD diffraction. The discharge-charge (DC) experiments were performed using three electrode configuration. The peapods and SWNTs were used as the working electrode and Li metal is used as the reference and counter electrodes. 1 M LiClO₄ solution in 1:1 ethylene carbonate and diethyl carbonate mixture was used as the electrolyte.

The potential profile of the peapod sample from the galvanostatic DC experiment is shown in Fig. 1. The reversible capacity is about 210 mAh/g and is about 1.3 times greater than that of the empty SWNT sample. In the symposium, we will also discuss the lithium ion storage site.

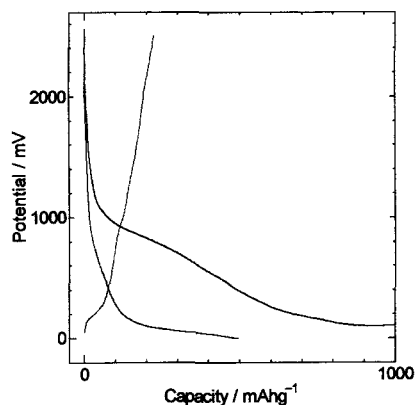


Fig. 1 DC curves of the peapod sample.

[1] S. Komiyama et al., *Tanso*, 25 (2005).

Energetics of Graphene Intrinsic Defects

Kazuaki Yamashita and ○Mineo Saito

Division of Mathematical and Physical Science, Graduate School of Natural Science & Technology, Kanazawa University, Kakuma-machi, Kanazawa 920-119

Graphenes as well as carbon nanotubes recently attract much attention since they are candidates for nano device materials. To achieve nano devices, control of defects is very important as in the case of silicon technology. Compared with conventional silicon device, the effect of defects is expected to be very serious because of the low dimensional conductivity. Therefore, the study of defects in carbon materials is invoked.

In this paper, we perform first principles calculations on fundamental intrinsic defects, mono- and di-vacancies and mono- and di-interstitial (adatom) defects. It is found that the divacancy forms pentagon-octagon-pentagon structure and is very stable. The reaction, $2V \rightarrow V_2$ is found to be exothermic and the reaction energy is very large (7.71 eV). Since the divacancy is very stable, its migration energy is expected to be higher than that of monovacancy. So, we speculate that the divacancy is experimentally detectable in some temperature range.

In the most stable di-interstitial structure, two adatoms make bonds to graphene sheet and form two pentagons. Because of this pentagon formation, the di-interstitial defect is found to be stable, i.e., the reaction, $I+I \rightarrow I_2$ is exothermic and the reaction energy is very large (6.0 eV). We thus expect that the di-interstitial defect is detectable in some temperature range. Since the migration energy of mono-interstitial defect is expected to be lower than that of mono-vacancy, the temperature at which the diinterstitial defect is detected is lower than that at which the divacancy is detected.

Corresponding Author: Mineo Saito**E-mail: m-saito@cphys.s.kanazawa-u.ac.jp****Tel&Fax: +81-76-264-6132**

Suspended SWNTs Functionalization with DNA and Metal Nanoparticles

○ G. -H. Jeong¹, T. Matsumoto², S. Suzuki¹, Y. Kobayashi¹, and Y. Homma²

¹ NTT Basic Research Laboratories, NTT Corporation, Atsugi, Kanagawa 243-0198, Japan

² Dept. of Physics, Tokyo University of Science, Tokyo 162-8601, Japan

We have performed nanotube functionalization to create nanotube-based novel hybrid structures that can be applied to biosensors and electronic devices. DNA and Au nanoparticles (NP) were selected for nanotube functionalization due to their specific assembling property.

Suspended single-walled carbon nanotubes (SWNTs) were synthesized using ferritin molecules by CVD [1], and functionalized by amide coupling process [2]. Thiolated single-strand DNA (ss-DNA, 15 mer) was used for coupling with Au NP (5-nm diameter). Finally, SWNTs were modified with Au NP [Figs. 1(a), (b)] or Au/ss-DNA [Fig. 1(c)]. The density of Au NP along the SWNTs was controlled by the time of the amide coupling. In contrast to the Raman result of pristine tubes, additional peaks, which should not be resonant with a probe laser (633 nm), appeared in the frequency region of radial breathing modes (RBM) after Au NP attachment [Fig.2]. Surface-enhanced Raman scattering effects induced by the Au NP may play a significant role in the appearance of these non-resonant RBM signals. A peak-intensity change of RBM and D-bands in Raman spectra and change of electronic transport properties from the SWNTs/Au/ss-DNA suggest the possibility of functionalization by Au NP and DNA, and further applications for electronic devices and sensors.

We would like to thank Prof. H. Yoshimura at Meiji University for the ferritin supply.

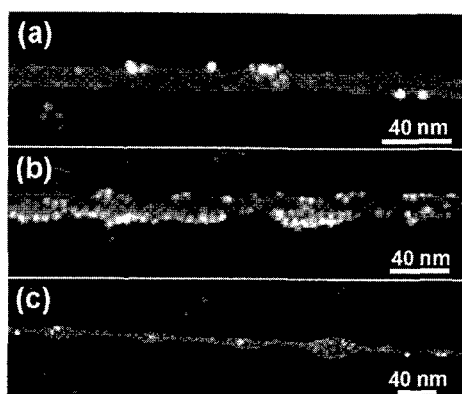


Fig. 1. (a), (b) Different Au NP density on SWNTs surface. (c) SWNTs/Au/ss-DNA hybrids.

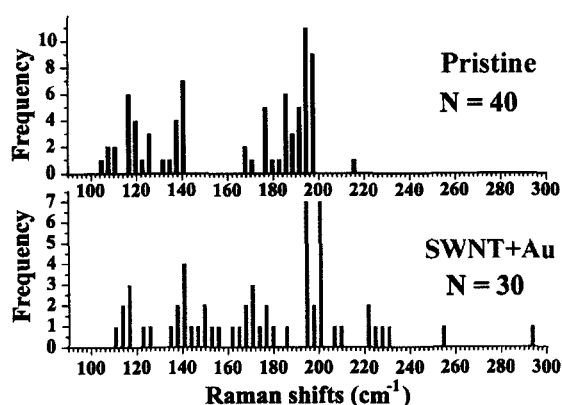


Fig. 2. Statistical distribution of observed RBM signals measured before/after Au functionalization.

[1] G. -H. Jeong *et al.*, *J. Am. Chem. Soc.*, **127**, 8238 (2005).; *J. Appl. Phys.*, in press.

[2] G. -H. Jeong *et al.*, Abstracts of the 28th Fullerene-Nanotubes Symposium, 3P55, 2005.

Corresponding author: jeong@will.brl.ntt.co.jp, Tel: +81-46-240-3564, Fax: +81-46-240-4718.

AFM imaging of wrapped multi wall carbon nanotube in DNA

○Hirotohi Takahashi, Shigenori Numao, Shunji Bandow, Sumio Iijima

*Department of Materials Science and Engineering, Meijo University,
1-501 Shiogamaguchi, Tenpaku, Nagoya 468-8502, Japan*

Wrapping of multi wall carbon nanotubes (MWNTs) in deoxyribonucleic acid (DNA) was carried out. MWNTs used in this study was prepared by using RF plasma method¹⁾ in a mixture flow of Ar (20 l/min) and H₂ (3.1 l/min) at 460 Torr. Method for wrapping is follows: first we prepared aqueous solutions of DNA and MWNTs separately with nearly equal concentration of ~10 μg/ml. Then, a few drops of DNA solution were put into the MWNT solution and the mixture was shaken several times. After leaving for 2 days, several droplets of suspension were spin-coated onto a highly oriented pyrolytic graphite (HOPG) substrate. For control experiments, we also prepared samples of pristine MWNTs and DNA by the spin-coat. Fig. 1 is AFM images. Here, in (a), we can only identify the agglomerated form of DNA molecules deposited on HOPG substrate like as the dot structures. Most of the isolated dots have nearly the same size with ~25 nm in width and ~1.3 nm in height. Therefore, we consider that DNA molecules agglomerate together in the water and form spongy spherical structure. From Fig. 1b, it can be found that the surface of pristine MWNT is fairly smooth. In Fig. 1c, we cannot see any dot structured DNA assemblies on the surface of MWNT unlike as shown in Fig. 1a. Instead, we can see arch-like structured material adhering to MWNT as indicated by the arrow in Fig. 1c, which implies a disentangled structure of DNA molecules²⁾. From these facts, we suggest that the DNA molecules agglomerate and form spongy spherical structures in the water, and these agglomerated DNA molecules are disentangled and immobilized on the MWNT surface when we only soak MWNTs in the DNA solution.

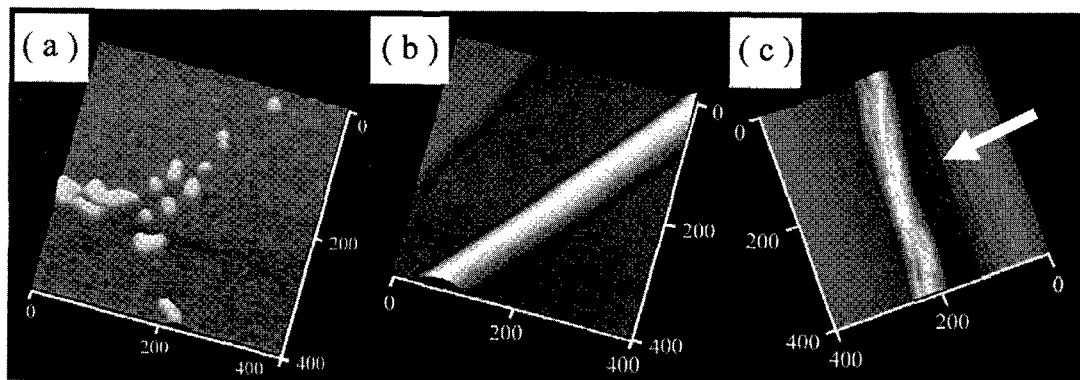


Fig. 1. AFM images ($400 \times 400 \text{ nm}^2$) taken for (a) DNA, (b) pristine MWNT, and (c) DNA-wrapped MWNT on HOPG.

- References** 1) A. Koshio, M. Yudasaka, S. Iijima, *Chem. Phys. Lett.* **356**, 595 (2002).
2) H. Takahashi, S. Numao, S. Bandow, S. Iijima, *Chem. Phys. Lett.* *in press.*

Corresponding Author : Hirotohi Takahashi
E-mail : m0434024@ccmailg.meijo-u.ac.jp
Tel&Fax : +81-52-834-4001

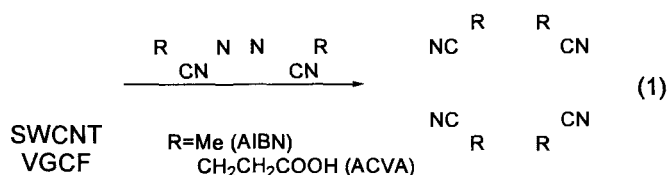
DERIVATIZATION OF SWCNT AND VGCF BY A RADICAL ADDITION REACTION

Takahiro Gunji, Minako Akazawa, Koji Arimitsu, and Yoshimoto Abe

*Department of Pure and Applied Chemistry, Faculty of Science and Technology,
Tokyo University of Science
2641 Yamazaki, Noda, Chiba 278-8510 Japan*

Single wall carbon nanotubes (SWCNTs) and vapor growth carbon fibers (VGCFs) exhibit many unique mechanical and electrical properties. The application of SWCNTs and VGCFs have been limited up to now because of their low ability of dispersion in matrices. The demerit in dispersion would be improved by the functionalization of SWCNTs and VGCFs. Up to now, several derivatization approaches on the sidewalls of SWCNTs have been successful, such as hydrogenation, fluorination, addition of azomethine ylides, ozonization, electrochemical reduction of aryl diazonium salts, and addition of peroxides. In this work, the reaction of azo-type radical initiators with SWCNTs or VGCFs was examined to derivatize SWCNTs and VGCFs with good solubility in solvents by the simple and clean process, according to the equation (1).

VGCFs (40 mg) were placed in a flask and *o*-dichlorobenzene (120 mL) was added. 2,2'-Azobis(isobutyronitrile) (1.2 g) or 4,4'-azobis(4-cyanovaleric acid)



(ACVA) (2.0 g) was added. Then, the mixture was heated for 4 h at 80 °C (for AIBN) or 130 °C (for ACVA) then another 4 h at 130 °C (for AIBN) or 150 °C (for ACVA). After filtration by using membrane filter, the residue was washed three times by tetrahydrofuran. The residue was dried to provide derivatized VGCFs.

When standing several hours a mixture of VGCFs, *o*-dichlorobenzene, and AIBN, VGCFs were precipitated and the upper layer was clear and transparent because VGCFs are insoluble in *o*-dichlorobenzene. The upper layer of the solution was colored in black after heating, which suggests the reaction of AIBN with VGCFs. After filtration of the reaction mixture, black fibers were recovered. The amount of addition of isobutyronitrile radical to VGCFs was calculated based on the weight of crude products and thermogravimetric analysis. This product was mixed with organic solvent such as methanol, tetrahydrofuran, and chloroform and then subjected to the sonication to provide a dispersion of derivatized VGCFs in organic solvents.

The reaction of ACVA with VGCFs was carried out by heating a mixture of VGCFs, *o*-dichlorobenzene, and ACVA. A paste-like product was precipitated at the bottom and wall of the flask with the increase in the heating time. After filtration of the reaction mixture, black fibers were recovered. The ability of dispersion of the derivatized VGCFs was monitored by the color of the upper layer of the mixture after standing for 48 h. The derivatized VGCFs were well dispersed in water. Ultra violet and visible spectrum of the filtrate of the dispersion in water suggests the dispersion of derivatized VGCFs with the length of *ca.* 300 nm

Corresponding author: Takahiro Gunji

e-mail gunji@rs.noda.tus.ac.jp tel +81-4-7122-9499 fax +81-4-7123-9890

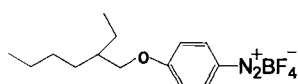
Separation of Semiconducting and Metallic Single-Walled Carbon Nanotubes using a Long-Chain Benzenediazonium Compound

○ Shouhei Toyoda¹, Yasuhiko Tomonari²,
Masataka Hiwatashi², Hiroto Murakami², and Naotoshi Nakashima¹

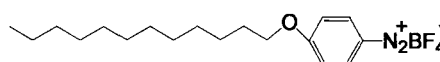
¹*Department of Applied Chemistry, Faculty of Engineering, Kyushu University, 744 Motoooka, Nishi-ku, Fukuoka 819-0395, Japan,* ²*Department of Science and Technology, Graduate School of Material Science, Nagasaki University, Nagasaki, 852-8521, Japan*

Very recently, considerable attention has been focused on the separation of metallic and semiconducting SWNTs. The combination of chemical modification and physical adsorption on SWNTs has been reported to be useful for the separation. Strano et al.¹ reported an interesting method to separate metallic and semiconducting SWNTs, in which the separation is based on the difference in the reaction rates of 4-chlorobenzenediazonium tetrafluoroborate toward metallic and semiconducting SWNTs that are dissolved individually in an aqueous micelle of sodium dodecylsulfate.

We have modified their methods. We synthesized a double-chain benzenediazonium tetrafluoroborates (1) and reported the separation of semiconducting and metallic SWNTs.²⁾ Here, we synthesized long single-chain benzenediazonium tetrafluoroborates (2). Aqueous solutions of the compound was added to individually dissolved SWNTs in an aqueous solution of sodium cholate. By using the kinetically controlled reaction of SWNTs and the compounds, we examined the separation of metallic and semiconducting SWNTs.



(1)



(2)

References

- 1) M. S. Strano, C. A. Dyke, M. L. Usrey, P. W. Barone, M. J. Allen, H. Shan, C. Kittrell, R. H. Hauge, J. M. Tour, and R. E. Smalley, *Science*, **301**, 1519 (2003).
- 2) N. Nakashima, Y. Tomonari, H. Murakami, The 28th Fullerene-Nanotubes General Symposium, Nagoya, p.41, 2005.

Corresponding Author : Naotoshi Nakashima

E-mail: nakashima-tcm@mbox.nc.kyushu-u.ac.jp

Tel&Fax : 092-802-2840

Excellent field emission from camphor-grown carbon nanotubes

○Kyohei Yasuda¹, Mukul Kumar¹, Yoshinori Ando¹, Mineo Hiramatsu²

¹Department of Materials Science and Engineering, Meijo University, Tempaku-ku, Nagoya 468-8502, Japan

²Department of Electrical and Electronic Engineering, Meijo University, Tempaku-ku, Nagoya 468-8502, Japan

During the last few years, camphor has emerged as an efficient carbon nanotube (CNT) precursor. Camphor-grown CNTs (CGCNTs) have low amorphous carbon and extremely low metal impurity, and raw material-to-product yield is very high [1]. The only drawback is that CGCNTs consist of a lot of pentagonal defects. However, this demerit becomes a merit when it comes to extract field emission from CNTs. It has been well established that CNTs are excellent field emitters by virtue of the localized density of states at pentagonal sites.

MWNTs grown from camphor with 1 wt% ferrocene catalyst have shown appreciable field emission properties [2]. With continued efforts on optimization of catalyst concentration at the growth stage, we have been able to reduce the turn-on field down to 0.6 V/ μm (corresponding to an emission current density of 10 $\mu\text{A}/\text{cm}^2$) and threshold field down to 3 V/ μm (corresponding to an emission current density of 10 mA/cm^2). Thus CGCNTs meet technologically demanded field emission characteristics. As far as stability is concerned, we held the emission current density at 1 mA/cm^2 and monitored for 72 hours at a constant applied field; there was no appreciable fall in current. Hence we hope it has a good stability. More study is underway.

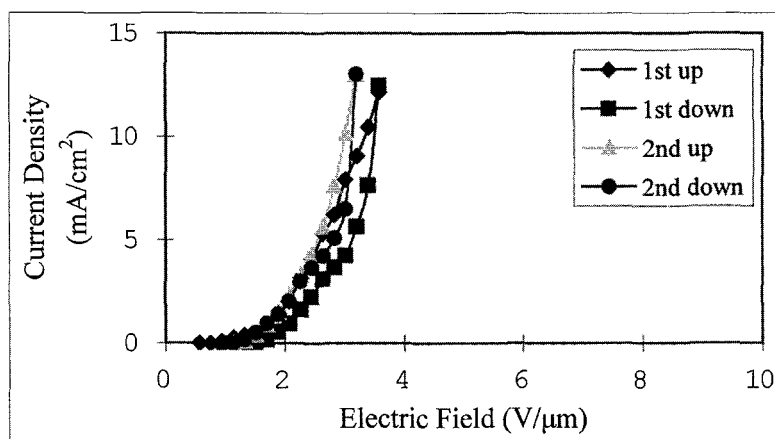


Fig. 1 Field emission plot of as-grown MWNTs

References

- [1] M. Kumar, Y. Ando, *Chem. Phys. Lett.* **374** (2003) 521-526.
 [2] M. Kumar, K. Kakamu, T. Okazaki, Y. Ando, *Chem. Phys. Lett.* **385** (2004) 161-165.

Corresponding author's e-mail: yasuda_k0705@yahoo.co.jp

Novel Photosynthetic Model Nanohybrids Composed of Single-Walled Carbon Nanotube Functionalized with Porphyrinic Peptides

OKenji SAITO,^a Nathalie SOLLADIE,^b and Shunichi FUKUZUMI^a

^aDepartment of Material and Life Science, Division of Advanced Science and Biotechnology, Graduate School of Engineering, Osaka University, SORST, Japan Science and Technology Agency (JST), 2-1, Yamada-oka, Suita, Osaka 565-0871, Japan

^bGroup of Synthesis of Multiporphyrinic Systems, Laboratoire d'Electrochimie et de Chimie Physique du Corps Solide Institut Le Bel, 4 rue Blaise Pascal 67070, Strasbourg, France

In natural photosynthesis, one reaction center is associated with a number of light harvesting units in which the harvested light energy is efficiently transferred to the reaction center. Extensive efforts have so far been devoted to construct artificial photosynthetic reaction centers. Carbon nanotubes and, in particular, single-wall carbon nanotubes (SWNT), have recently attracted much attention as potentially useful materials to construct donor-acceptor nanohybrids. However, artificial photosynthetic model systems containing SWNTs and light harvesting moieties, which can cause energy transfer processes, have yet to be developed because the attachment of such antenna moieties to SWNTs has been very difficult.¹

We report herein that α -herical porphyrin-peptide hexadecamer which contains 16 porphyrins ($P(H_2P)_{16}$) forms supramolecular assembly with full-length SWNTs (Figure 1).

The purification procedure of SWNTs (Carbon Nanotechnologies, Inc.) was adopted from the reported procedure.² The reaction between $P(H_2P)_{16}$ and purified SWNTs was carried out by heating a DMF mixture of the two at 100 °C. After centrifugation at 15000 rpm, the centrifuged solid was resuspended in DMF. Unreacted SWNTs were separated by 20 minutes of centrifugation at 5000 rpm.

The stable dispersion of $P(H_2P)_{16}$ /SWNTs nanohybrids was confirmed by the visible–near-infrared (vis-NIR) absorption spectrum as shown in Figure 2. Importantly, the SWNTs' van Hove singularities, which fall into groups of metallic transition (i.e., E_{11}) in the 500–600 nm range and of semiconductor transitions in the 600–900 nm (i.e., E_{22} semiconductor transitions) and also in the 1000–1500 nm regions (i.e., E_{11} semiconductor transitions) are discernable in $P(H_2P)_{16}$ /SWNTs. We report herein the photophysical properties and structural characterization in $P(H_2P)_{16}$ /SWNTs nanohybrids.

References

- (1) Majima, T. *et. al. J. Phys. Chem. B.* **2005**, *109*, 33.
- (2) Smalley, R. E.; Hauge, R. H. *et. al. J. Phys. Chem. B.* **2001**, *105*, 8297.

Corresponding Author: Shunichi FUKUZUMI

E-mail: fukuzumi@chem.eng.osaka-u.ac.jp

Tel: +81-6-6879-4585, **Fax:** +81-6-6879-7370

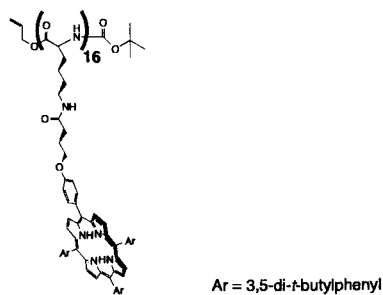


Figure 1. Structure of porphyrin-peptide hexadecamer.

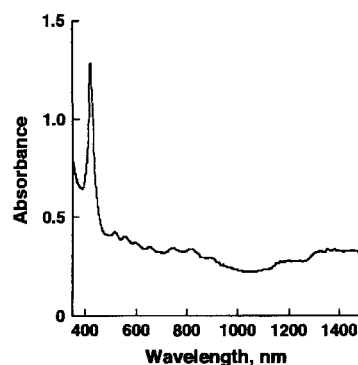


Figure 2. Absorption spectrum of suspension of $P(H_2P)_{16}$ /SWNTs in DMF.

Photoinduced Electron-Transfer Reduction of Cup-Stacked-Type Carbon Nanotube

O Masataka OHTANI, Kenji SAITO and Shunichi FUKUZUMI

Department of Material and Life Science, Division of Advanced Science and Biotechnology, Graduate School of Engineering, Osaka University, SORST, Japan Science and Technology Agency (JST), 2-1, Yamada-oka, Suita, Osaka 565-0871, Japan

Carbon nanotubes (CNTs) is studied in a variety of fields such as chemistry, physics, and material engineering because of the electronic and mechanical properties that derive from the unique structure. These properties depend on the length, diameter and chirality of CNTs. However, CNTs are produced as the mixtures that vary in length, diameter and chirality. In addition, the accurate separation method has yet to be well established. In this study, we focused on cup-stacked-type carbon nanotubes (CSCNTs) as a novel type of CNTs. CSCNTs have large hollow core, and form the unique structure which stacked the cup moieties.¹ The length and diameter of each cup moieties are *ca.* 50 nm. We report herein that the cup-stacked structures of CSCNTs are electrostatically disassembled by the electron-transfer (ET) reduction.

The reduced species of CSCNTs were produced by the photoinduced electron-transfer (PET) reduction with an NADH dimer analog [(BNA)₂] under photoirradiation ($\lambda > 340$ nm) as shown in Scheme 1.

Figure 1 shows the UV-visible spectral change observed in the PET reduction of CSCNTs with (BNA)₂ in deaerated MeCN. The absorption band of (BNA)₂ at 348 nm decreased, accompanied by increase in the new absorption band at 260 nm due to the BNA^{•+}. The PET from (BNA)₂ to CSCNTs gives (BNA)₂^{•+}. This step is followed by a fast cleavage of the C-C bond of the dimer to produce BNA[•] and BNA⁺. The subsequent second ET from BNA[•] to CSCNTs should be much faster than the first, as BNA[•] is a strong reductant. Thus, once PET from (BNA)₂ to CSCNTs occurs, two equivalents of CSCNTs are reduced. The formation of the reduced products was confirmed by ESR spectroscopy. The structural characterization of the disassembled species produced by the PET reduction has been performed by SEM, TEM, AFM and raman spectroscopy.

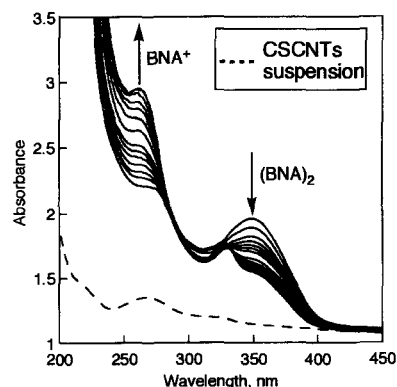
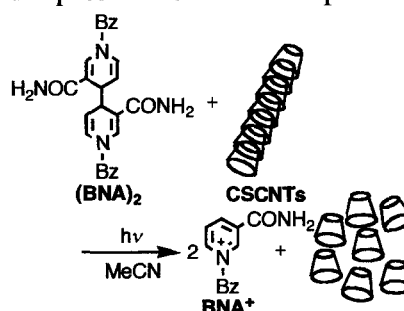


Figure 1. UV-vis spectra observed in the photoreduction of CSCNTs by (BNA)₂ (1.0×10^{-4} M) in deaerated MeCN.

Reference

(1) Endo, M.; Kim, Y. A.; Hayashi, T.; Fukai, Y.; Oshida, K.; Terrones, M.; Yanagisawa, T.; Higaki, S.; Dresselhaus, M. S. *Appl. Phys. Lett.* **2002**, *80*, 1267–1269.

Corresponding Author: Shunichi FUKUZUMI

E-mail: fukuzumi@chem.eng.osaka-u.ac.jp

Tel: +81-6-6879-4585, **Fax:** +81-6-6879-7370

FT-ICR Study of Reaction of Cobalt Clusters with Alcohol, Ether and Hydrocarbon

○ Daisuke Yoshimatsu, Kohei Koizumi, Naoki Suyama and Shigeo Maruyama

*Department of Mechanical Engineering, The University of Tokyo
7-3-1 Hongo, Bunkyo-ku, Tokyo, 113-8656, Japan*

SWNTs are expected for various applications for extraordinary physical and chemical characters based on the unique geometric structure. As for the macroscopic generation, the ACCVD technique appears to be one of best synthesis methods [1]. However its synthetic mechanism has not yet been made clear, hence the fundamental research is necessary for generation of better quality SWNTs. In order to investigate the initial reaction of alcohol or hydrocarbon with a metal nano-particle, we have been studying the chemical reaction of transition metals clusters by FT-ICR (Fourier Transform Ion Cyclotron Resonance) mass spectrometer with laser-ablation supersonic-expansion cluster beam source [2]. Our previous FT-ICR studies have compared the reactivity of Fe, Co, and Ni clusters with ethanol. The dehydrogenation process on Co clusters was studied in detail by using isotopically modified ethanol. The dehydrogenation reaction was observed only in the limited size range of Co clusters i.e. $\text{Co}_{12} \sim \text{Co}_{17}$. On the other hand, all the tested Ni clusters tested always showed immediate dehydrogenation reaction, whereas such reaction was not observed for Fe clusters. Among these transition metals, cobalt clusters are studied to gain better insights on the initial reaction of catalysts with carbon containing molecules.

In this paper, we have explored the basic reaction mechanisms of relatively large catalyst clusters of cobalt with ethanol, methane, ethylene and diethyl ether which are commonly used as carbon source for SWNTs generation. Fig. 1 shows mass spectra of reaction of cobalt clusters with ethylene and diethyl ether (RT, 1×10^{-8} torr). For ethanol, ethylene and diethyl ether, the dehydrogenation reactions were observed. Furthermore, not only one molecule, but a few molecules adsorption to cobalt clusters were observed.

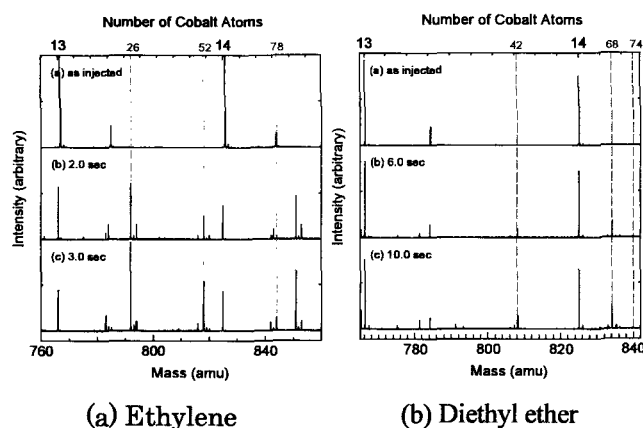


Fig. 1. FT-ICR mass spectra of reaction of Co clusters with (a) ethylene, (b) diethyl ether.

References

- [1] S. Maruyama et al., Chem. Phys. Lett., 360 (2002) 229.
[2] S. Maruyama et al., Rev. Sci. Instrum., 61 (1990) 3686.

Corresponding Author: Shigeo Maruyama

Fax: +81-3-5800-6983 E-mail: maruyama@photon.t.u-tokyo.ac.jp

Preclinical Safety Evaluation of Fullerenes: Acute Oral Administration and Mutagenic Studies

○ Yuki Fujimoto¹, Hiroya Takada¹, Tomohisa Mori², Kenji Matsubayashi¹, Shinobu Ito¹, Nobuhiko Miwa³ and Toshiko Sawaguchi²

¹*Vitamin C60 BioResearch Corporation, c/o Mitsubishi Corporation, Chiyoda-ku, Tokyo 100-8086, Japan*

²*Department of Legal Medicine, Tokyo Women's Medical University, 8-1 Kawada-cho, Shinjuku-ku, Tokyo 162-8666, Japan*

³*Laboratory of Cell-Death Control BioTechnology, Faculty of Life and Environmental Sciences, Prefectural University of Hiroshima, Shobara, Hiroshima 727-0023, Japan*

Fullerenes characterized as an antioxidant are believed to reduce various reactive chemical species, such as free radicals, and their characteristic features have been disclosed to furnish many useful pharmatherapeutic technologies [1,2]. Despite the numerous applications for the biological efficacy of fullerenes, less is known about the toxicity of fullerenes in mammals. Hence, the protocol was designed to determine the acute oral median lethal dose and evaluate the acute toxicity of fullerenes when administrated as a single dose to Sprague-Dawley rats. In an acute toxicity test, fullerenes were administered once orally to a single group of male and female at a dose level of 2000 mg/kg. No deaths were observed and the body weights in both sexes of 2000 mg/kg group increased in a similar pattern to the control group. Genotoxicity of fullerenes was also assessed in a bacterial reverse mutation assay (Ames test) and the chromosomal aberration test in cultured Chinese hamster lung (CHL/IU) cells. Although structural chromosomal aberrations were induced at up to 5000 µg/mL, there was no significant increase in the frequency of chromosomal aberrations at any dose level regardless with or without metabolic activation. Fullerenes did not cause genetic damage in *Salmonella typhimurium* TA100, TA1535, TA98 and TA1537 and *Escherichia coli* WP2uvrA/pKM101.

The excellent preclinical safety profile of fullerenes has been born out in a series of standard preclinical evaluation. These results indicate that fullerenes were not considered to be of toxicological significance. The fact strongly supports the promising medical application of fullerenes.

References

- [1] H. Takada, L. Xiao, R. M. Islam, S. Suzuki, H. Mimura, K. Maeda and N. Miwa, In *Technology of Evidence Based Cosmetics*; CMC Publishing: Tokyo, **2004**, 291–308.
- [2] L. Xiao, H. Takada, K. Maeda, M. Haramoto and N. Miwa, *Biomed. Pharmacother.* **2005**, *59*, 351–358.

Corresponding Author: Hiroya Takada

E-mail: hiroya.takada@vc60.com, **TEL:** +81-3-3538-5917, **FAX:** +81-3-3538-5911

発表索引
Author Index

Author Index

Abdou Hassaien	2S-3	Baopeng Cao	2P-11
Abe Hisao	1P-28	Catalin Romeo Luculescu	3P-19, 3P-23
Abe Yoshimoto	3P-38	Chiashi Shohei	2P-26, 3-1
Achiba Yohji	1P-28, 2-3, 2P-10, 2P-27, 2P-42, 3-2, 3P-10, 3P-33	Chikamatsu Masayuki	1P-16
Adachi Kenji	2P-17	David Tomanek	2P-19
Adam M. Gilmore	1-6	Deguchi Shigeru	1P-14
Ago Hiroki	1-7, 1P-46, 2P-47, 3-3, 3P-20	Doi Tatsuya	2-11, 3P-18
Ajima Kumiko	1P-33	Don N. Futaba	1P-31, 2P-20, 3-6
Akada Misaho	2P-13	Dragan Mihailović	2S-3
AKAI Yoshio	3-12	Enda Jun	1P-7
Akasaka Takeshi	1P-9, 1P-10, 1P-11, 1P-12, 2-1, 2-2, 2P-1, 2P-11, 2P-12, 2P-24, 3P-1, 3P-11, 3P-12, 3P-29	Endo M.	3P-25
Akazawa Minako	3P-38	Endo Morinobu	3-7
Akima N.	2P-39	Erik Einarsson	1P-22, 1P-45
Akimoto Ikuko	2P-16	Ernst Horn	1P-10, 2-1
Akita Seiji	1-11, 2P-35, 3P-28	Fan J.	1P-31
Alan Maigne	1P-33	Fan Jing	2P-20
Aleš Mrzel	2S-3	Fueno Hiroyuki	1P-40
Ando Yoshinori	1P-29, 3P-21, 3P-25, 3P-40	Fujieda Tadashi	1P-5
Aoki Nobuyuki	2P-17	Fujimori M.	2P-37
Aoki Yosuke	1P-28	Fujimoto Yuki	3P-44, 3P-6
Aonuma Shuji	1P-21	Fujita N.	2P-29
Aoyagi Yoshinobu	3-9	Fujita Takeshi	2P-2
Arikai Hideki	3-7	Fujiwara Akihiko	1P-17, 3P-14, 3P-15, 3P-17
Arimitsu Koji	3P-38	Fukuda Takamitsu	3P-8
Arkady Krasheninnikov	2P-19	Fukui N.	2P-37
Asai Nobuyuki	2P-27, 3-2	Fukushima Makoto	3P-11
Asano Koji	1P-42	Fukuzumi Shunichi	2-2, 3P-41, 3P-42
Awano Yuji	1-10, 1P-42	G. M. Aminur Rahman	1P-10, 2P-1
Azami Takeshi	3P-27	G.-H. Jeong	3P-36
Azehara Hiroaki	1P-5	Goo-Hwan Jeong	2P-43
Azumi Reiko	1P-16	Gunji Takahiro	3P-38
Balakrishnan Nalini	1-5	H. Bang	2P-29
Bandow Shunji	2P-18, 2P-33, 3P-37	Hamanaka Yasushi	1-7
		Hara Takumi	1P-6
		Harigaya K.	3-11
		Harima Hiroshi	1P-27, 2P-28
		Hasegawa Tadashi	2P-24
		Hashimoto Hisayosi	2S-4
		Hashimoto Naoaki	3P-8
		Hashizume T.	2P-37

Hata Kenji	1P-31, 2P-20, 3S-5, 3-6	Ikuta Tatsuya	2P-47
Hata Koichi	1P-24, 1P-25, 2P-44, 3P-22	Imai Hideto	1P-32
Hata Yasunori	1P-44	Imai Kumiko	1P-17, 3P-15, 3P-17
Hatakeyama Rikizo	1-13, 1P-26, 2P-31, 3P-29	Imamura Sadanobu	1-7
Hatori Hiroaki	3-6	Imamura Shingo	3P-20
Hayamizu Yuhei	3-6	Inagaki Takayuki	2P-18
Hayashibara Mitsuo	1P-5	Inakuma Masayasu	2-12
Hayazawa Norihiko	1P-37	Inakura Hideki	3-4
Heike S.	2P-37	Inoue Sakae	1P-29, 3P-21
Hiasa Ken	1P-25	Inoue Takashi	1P-13, 1P-30, 2-4, 2P-9
Hidaka Kishio	1P-5	Inouye Yasushi	1-3
Higashi Keisuke	2P-34	Ishi Hisao	3P-16
Higashi Taijiro	2P-3	Ishibashi Ayumi	1P-2, 2P-45
Hino Shojun	2-5	Ishida Kohtaro	3-8
Hiramatsu Kazumasa	3P-22	Ishida Masashi	1P-30
Hiramatsu Mineo	3P-40	Ishida Yasuhiro	2P-8
Hiraoka Tatsuki	3-6	Ishigaki Satoru	2P-28
Hirooka Motoyuki	1P-5	Ishigami Naoki	1P-46, 2P-47
Hiroshiba Nobuya	3P-16	Ishihara Masayuki	2P-9
Hiwatashi Masataka	3P-39	Ishii Tadahiro	3P-2, 3P-19, 3P-23
Homma Yoshikazu	2P-43, 3P-31, 3P-36	Ishii Toru	3P-19
Honda Hiroyuki	1P-43	Isobe Hiroyuki	1-15, 1P-8, 1P-32, 2-7
Honma Takeshi	1P-6	Isshiki Toshiyuki	1P-27, 2P-28
Horikoshi Koki	1P-14	Itakura Atsushi	1P-16
Hoshino Mikio	1P-6	Itatani Taro	3-8
Hozumi Y.	2P-29	Ito Akihiro	2P-41
Igimi Daisuke	1-9	Ito Hiroshi	1P-43
Igusa Masahiro	3-8	Ito Osamu	3P-1
Iida Sadahiro	2P-17	Ito Shinobu	3P-44
Iiduka Yuko	2-1	Ito Yasuhiro	2-5, 2P-9
Iijima Sumio	1-15, 1P-31, 1P-32, 1P-33, 1P-39, 2-6, 2P-18, 2P-20, 2P-33, 3-5, 3-6, 3-7, 3P-27, 3P-37	Itoga Emiko	3-8
Ikeda Ken-ichi	3-3	Itoh Shigeo	2P-34
Ikeda Noriaki	1P-1	Iwai Yuki	3P-34
Ikegami Asato	2P-17	Iwasa Yoshihiro	1P-17, 2P-39, 3-9
Ikenaga Eiji	1-10	Iwasaki Kentaro	2-5
Ikeuchi Takahiro	1P-3	Iwasaki Shinya	1-4
		Iwashita Akihiko	3P-5
		Iwata Nobuyuki	1P-44, 3P-24
		Izumi Yuya	2P-23
		Izumida Takeshi	1-13, 2P-31, 3P-29
		J. Jiang	1-2, 2P-40
		J. S. Park	2P-40

J.L. Musfeldt	2P-39	Kishi Naoki	2P-38
James M. Mattheis	1-6	Kishimoto Shigeru	1-4, 1P-43
Jing Lu	2P-24	Kisoda Kenji	1P-27, 2P-28
Kadota Naoki	2-10	Kitamura Hiroshi	2P-3
Kadowaki Masayuki	1P-22, 1P-45	Kitamura IT.	1P-29
Kagan Kerman	3P-14	Kitamura Yutaka	2-4, 2P-32
Takehi Kazunori	2P-26	Kitaura Ryo	1P-13, 1P-30, 2-4, 2P-32
Kakiuchi Toru	2P-13	Kobata Masaaki	1-10
Kako Masahiro	3P-1	Kobayashi Kaoru	1P-9, 2-1, 2-2, 2P-11, 3P-1
Kakudate Yozo	3-6	Kobayashi Keisuke	1-10
Kan'no Ken-ichi	2P-16	Kobayashi Keita	1P-19
Kanbara Takayoshi	3-9	Kobayashi Nagao	3P-8
Kanda Makoto	2P-24	Kobayashi Yoshihiro	1P-41, 2P-43, 3P-31, 3P-36, 1P-40
Kaneko Toshiro	1-13, 2P-31	Kodama Takeshi	2-3, 2P-10
Kasanuma Yuka	1P-5	Kohda Kohfuku	2P-5, 3P-6
Kasuya Daisuke	3P-27	Koizumi Kohei	3P-43
Kataura Hiromichi	1-14, 1P-23, 1P-28, 1P-37, 2S-3, 2P-27, 2P-30, 2P-42, 3-2, 3-7, 3-8, 3P-33, 3P-34	Kojima Eiji	3P-30
Kato Masayuki	2-5	Kojima Kenichi	1P-38, 1P-47, 3P-32
Kato Tatsuhisa	1P-9, 1P-11, 2-1, 2-2, 2P-12, 3P-11	Kokai Fumio	1-16, 1P-19, 2P-48
Kato Tomohiro	2P-17	Kokubo Ken	2P-3, 3P-4
Kato Toshiaki	1-13, 1P-26, 2P-31	Komaki Tomohito	2-3
Kawabata Akio	1-10, 1P-42	Komatsu Koichi	1P-2, 1P-8, 2-8, 2P-13
Kawahama Sayako	3P-4	Komatsu Masaharu	1P-2, 3-10
Kawahara Syo	3P-6	Komatsu Naoki	1P-21, 2-10
Kawai Takazumi	3S-6	Komiya Satoshi	1-10
Kawakami Kiminori	1P-7	Kondo Daiyu	1-10, 1P-42
Kawakita Kunihiko	2P-44	Konishi Yasumoto	2P-35
Kawamoto Hironori	1P-38	Konno Takashi	1P-4
Kawamura Y.	2P-29	Kono Takayoshi	1P-9, 1P-11
Kawasaki Shinji	3-7, 3P-34	Konstantin Iakoubovskii	1-5
Kawata Satoshi	1-3, 1P-37, 2P-30	Koshino Masanori	3P-26
Kazaoui Said	3P-30	Koshio Akira	1-16, 1P-19, 2P-48
Kikuchi Koichi	1P-16, 2-3, 2P-10	Kubo Takahiro	2P-6, 3P-7
Kikuchi Satoshi	2P-22, 2P-38	kubo Yoshimi	1-15, 3P-27
Kikuchi Takashi	1P-10	Kubozono Yoshihiro	1P-17, 2-14, 3P-15, 3P-17
Kim Jung-Jin	1-10	Kumashiro Ryotaro	3P-16, 3P-29
Kim Yeji	1-5, 3P-30	Kuroda Noritaka	3P-30
Kimura Shin-ichi	2P-24	Kusai Haruka	1P-17, 3P-15, 3P-17
Kimura Takahide	1P-21, 2-10	Kusunoki M.	2P-29

Kusunoki Michiko	1-9	Miura Kouji	2P-34
Kuwahara Shota	1P-36	Miwa Nobuhiko	3P-44
Kyushin Soichiro	2P-1	Miyahara Tsuneaki	2P-42, 3P-33
Lemiègre Loïc	2-7	Miyake Hideto	3P-22
Li Yongfeng	1-13, 2P-31	Miyake Koji	1-9, 3-6
Lian Yongfu	1P-12	Miyake Takashi	1P-35, 3-12
M.F.Jarrold	3P-13	Miyake Yoko	2-3, 2P-10
Maeda Fumihiko	1P-41	Miyamoto Hisakazu	1P-3
Maeda Shuhei	2-8	Miyamoto Yoshiyuki	2P-19
Maeda Yutaka	1P-9, 1P-10, 1P-11, 2-1, 2-2, 2P-1, 2P-12, 2P-24, 3P-1, 3P-11, 3P-12, 3P-29	Miyashita Kanae	1-5, 3P-30
Maja Remškar	2S-3	Miyata Naoki	2P-5, 3P-6
Maniwa Yutaka	1P-23	Miyata Yasumitsu	1-14, 1P-23, 2P-30
Markus Waelchli	1P-12	Miyauchi Yuhei	1-1, 1P-20, 3-1
Maruyama Shigeo	1-1, 1-4, 1P-20, 1P-22, 1P-34, 1P-35, 1P-45, 2P-21, 2P-26, 3-1, 3P-43	Miyawaki Jin	1-15, 1P-32, 1P-33
Maruyama T.	2P-29	Mizorogi Naomi	1P-9, 1P-10, 1P-12, 2-1, 2-2, 2P-1, 2P-12, 3P-9, 3P-12
Masunari Kosuke	2-14	Mizuno Kohei	2P-20, 3-6
Masuyama Naoto	2P-21	Mizuno Kyoza	1P-48
Matsubayashi Kenji	3P-4, 3P-44	Mizutani A.	3P-25
Matsubayashi Mai	3P-22	Mizutani Takashi	1-4, 1P-43
Matsui Eitaro	2P-6, 3P-7	Mori Hideki	3P-28
Matsui H.	2P-39	Mori Tomohisa	3P-44
Matsumoto Hideyuki	2P-1	Moribe Hiroe	2-5, 2P-9
Matsumoto Kazuyo	1P-27, 2P-28	Moriyama Hiroshi	1P-1, 2-13
Matsumoto Shiro	1P-6	Motohashi Satoru	1P-15, 2P-14, 2P-15
Matsumoto Tetsunori	2P-43, 3P-36	Motoyama Yukihiro	1P-46
Matsunaga Yoichiro	1P-9	Mukai Sada-atsu	1P-14
Matsuo Yutaka	1P-8, 2P-2, 2P-4, 3P-5	Mukul Kumar	3P-40
Matsuoka Yukitaka	3P-14	Murakami Hiroto	3P-39
Matsushita Tomohito	2-4	Murakami Takashi	1P-37, 2P-30
Matsuura Koji	1P-39, 3-5	Murakami Toshiya	1P-27, 2P-28
Matsuzaki Shun	3-8	Murakami Yoichi	1-4, 1P-20, 1P-22, 1P-45, 2P-21, 3-1
Meguro Akira	2P-1	Murata Michihisa	1P-2, 1P-8, 2-8
Michael T. H. Liu	2-1, 2P-1	Murata Naomi	2P-10
Minami Nobutsugu	1-5, 2P-24, 3P-30	Murata Yasujiro	1P-2, 1P-8, 2-8, 2P-13
Misaki Yohji	1P-3	Muro Takayuki	2-4
Mitani Yuichi	2P-4	Nagano Takayuki	1P-17, 3P-15, 3P-17
Mitikami Kazuya	2P-28	Nagasawa Hiroshi	1P-28
		Nagase Shigeru	1P-9, 1P-10, 1P-11, 1P-12, 2-1, 2-2, 2P-1, 2P-11, 2P-12, 2P-24,

	3P-1, 3P-9, 3P-12	Ochi Kenji	3P-15
Nagatsuka Junko	3P-1	Ochiai Yuichi	2P-17
Nakagawa Hidehiko	3P-6, 2P-5	Ogata Hironori	1P-15, 2P-14, 2P-15,
Nakagawa Tatsuo	1P-19		2P-23
Nakagita Tsuyoshi	1P-25	Ogata Shigenobu	3P-28
Nakahodo Tsukasa	1P-9, 1P-10, 1P-11, 2-1, 2-2, 2P-1, 2P-11, 2P-12, 3P-1	Ogawa Daisuke	2P-32
		Ogawa Kenichi	2P-17
Nakai Hiroshi	1P-47	Ohashi Hirotaka	3P-29
Nakamura Arao	1-7	Ohdo Ryota	3-3
Nakamura Eiichi	1-15, 1P-8, 1P-32, 2-7, 2P-2, 2P-4, 3P-5, 3P-26	Ohkubo Kei	2-2
		Ohmori Shigekazu	1P-40, 2P-41
Nakamura Kazuhiro	3-3	Ohno Masatomi	1P-48
Nakamura Masato	2P-49	Ohno Yutaka	1-4, 1P-43
Nakamura Tetsuya	2-4, 2P-32	Ohshima Satoshi	1P-39, 3-5
Nakamura Yosuke	1P-4	Ohshita Akinori	3P-22
Nakanishi Waka	2-7	Ohta Toshio	2-14, 3P-15
Nakashima Naotoshi	1P-2, 2P-45, 2P-46, 3-10, 3P-39	Ohtani Masataka	3P-42
		Okada Shinichi	2P-7
Nakayama Yoshikazu	1-11, 2P-35, 3P-28	Okada Susumu	1-12, 1P-35
Namai Tatsunori	2P-20, 3-6	Okada Takeru	1-13, 2P-31
Nanao Susumu	2-4	Okajima Takaharu	1P-5
Naniki Takashi	1P-15	Okamoto Hiroshi	1S-2
Nara Ryuhei	3P-11	Okazaki Toshiya	1P-39, 2-6, 2P-24, 2P-42, 3-5, 3P-33
Narimatsu Kaori	2P-46		
Naritsuka S.	2P-29	Okimoto Haruya	2-4, 2-5, 2P-32
Nemoto Katsumasa	3P-3	Okino Fujio	3-7
Nigawara Masahiro	2P-41	Okochi Mina	1P-43
Nihei Mizuhisa	1-10, 1P-42	Okubo Shingo	1P-9, 2-6, 2P-42, 3P-33
Niidome Yasuro	1P-2, 2P-46	Okumura Kensuke	2P-25
Nikawa Hidefumi	1P-10, 2P-1	Okuyama Hiroki	3P-24
Nishibori Eiji	2P-9	Osawa Eiji	1S-1, 2-10, 2-12, 2-13
Nishide Daisuke	1P-30	Osedo Hiroki	2-9
Nishii Toshiaki	2P-21	Oshima Takumi	2P-3, 3P-4
Nishimura Jun	1P-4	Oyama Y.	1-2, 2P-40
Nishio Koji	2P-28	Ozawa Masaki	2-12
Niwa Hiroaki	2P-34	Ozeki Yuji	1P-20
Noda Suguru	2P-21, 2P-26	P. A. Hervieux	2P-49
Nojima Yoshio	3-7	Pac Chyongjin	1P-1
Nouchi Ryo	2-14	Pan Lujun	2P-35
Numao Shigenori	3P-37	Pedro Molina-Morales	1P-47
O. Zhou	2P-39	Ray K. Kaminsky	1-6
Oba Mototeru	1-1, 1P-35	Said Kazaoui	1-5, 2P-24
		Saigo Kazuhiko	2P-8

Saito Kenji	3P-41, 3P-42		2P-32, 2P-37, 2P-38,
Saito Mineo	3P-35		3P-13
Saito R.	1-2, 2P-40	Shinohara Kenji	2P-34
Saito Susumu	3-12	Shiomi Junichiro	1P-34
Saito Takeshi	1P-39, 3-5, 1-7, 1P-24, 1P-25, 2P-25, 2P-44, 3P-22	Shiraishi M.	2P-39
		Shiraiwa T.	2P-29
		Solladié Nathalie	3P-41
Saito Yuika	1P-37, 2P-30	Someya Chika	3P-12
Sakai Takamichi	1P-24	Sonoda Motohiro	2-11
Sakakibara Youichi	3-8	Suenaga Kazutomo	3P-26
Sakata Makoto	2P-9	Sugai Toshiki	1P-13, 1P-30, 1P-36, 2-4, 2-5, 2P-22, 2P-37, 2P-38, 3P-13
Sako Yuuki	3P-17		
Sakuraba Akihiro	2-1		
Sakurai Toshihiko	2-9	Sugaya Motohiro	2P-18
Sano Masahito	1-8	Sugime Hiroshi	2P-21
Sasaki Shinya	3-6	Sugitani Sachie	3P-1
Sasaki Yoshiko	3P-1	Sugiura Takahito	2-13
Sashiwa Hitoshi	3P-3	Sugiyama Hiroyuki	1P-17
Sato Hideki	1P-24, 1P-25, 2P-44, 3P-22	Suhama Kenji	3P-21
		Sunouchi Toshiki	2P-48
Sato K.	1-2, 2P-40	Suwa Y.	2P-37
Sato Kenichi	1P-20	Suyama Naoki	3P-43
Sato Kumiko	2-2	Suzuki Atsushi	1P-24
Sato Shintaro	1-10	Suzuki Masato	1P-4
Sato Syuichi	1-8	Suzuki Satoru	1P-41, 2P-43, 3P-36
Sawa Hiroshi	2P-13	Suzuki Shinzo	1P-28, 2-3, 2P-10, 2P-27, 2P-42, 3-2, 3P-33
Sawaguchi Toshiko	3P-44		
Sawamura Seiji	2P-7		
Sawaya Sintaro	1-11	Suzuki Takayoshi	2P-5, 3P-6
Seike Nozomu	2P-3	Suzuki Tomoko	3P-21
Sekido Masaru	1P-48	Tachibana Masaru	1P-38, 1P-47, 3P-32
Seko Kazuyuki	2P-25	Tada Tomoyuki	2P-8
Senna Mamoru	2P-6, 3P-7	Tajima Yusuke	1P-6, 2-9
Shigeta Masahiro	3-10	Takada Hiroya	3P-4, 3P-44
Shimada Ryoko	2-9	Takagi Daisuke	3P-31
Shimada Takashi	1P-20	Takaguchi Yutaka	3P-17
Shimawaki Takanori	1P-21	Takahashi Hirotoshi	3P-37
Shimizu Tetsuo	2P-24	Takahashi Katsumasa	2P-5
Shimoda H.	2P-39	Takahashi Koji	1P-46, 2P-47
Shinagawa Masashi	1P-46, 2P-47	Takahashi Makoto	2-12
Shinohara Hiromi	2P-46	Takahashi Teruo	3P-19, 3P-23
Shinohara Hisanori	1P-13, 1P-30, 1P-36, 2-4, 2-5, 2P-9, 2P-22,	Takahashi Tetsuo	3-9
		Takano Yuta	2P-12

Takasaki Mikihiro	1P-46		3P-20
Takata Masaki	2P-9	Tsukagoshi Kazuhito	2P-30, 2P-42, 3-9,
Takei Fumio	1P-42		3P-33
Takematsu Yuji	1P-11	Tsumoto Hiroki	2P-5, 3P-6
Takemura Yuta	1-16	Uchida Katsumi	3P-2, 3P-3, 3P-19,
Takenobu Taishi	1P-17, 3-9		3P-23
Takeuchi Kazuhiro	3P-11	Uchida Kazuhito	3P-30
Takeuchi Kazuo	1P-6	Uchida Takashi	1P-38, 3P-32
Takeyama Shojiro	3P-30	Uehara Naoyasu	3-3, 3P-20
Takikawa Hirofumi	2P-34	Ueno Taro	2P-42, 3P-33
Tamiya Eiichi	3P-14	Umeda Rui	2-11
Tamura Goshu	2P-33	Umemoto Hisashi	1P-13, 2P-9
Tamura Ryo	2P-36	Usami Hatsuhiko	1-9
Tanaike Osamu	3-6	Wakabayashi Tomonari	2-11, 3P-18
Tanaka Hiroyoshi	2P-35	Wakahara Takatsugu	1P-9, 1P-10, 1P-11,
Tanaka Kazuyoshi	1P-40, 2P-41		1P-12, 2-1, 2-2, 2P-1,
Tanaka Ryota	2P-16		2P-11, 2P-12, 2P-24,
Tanaka Takatsugu	1P-8, 2-7		3P-1, 3P-11, 3P-12
Tanaka Teruyuki	2P-48	Watanabe Hiroto	2P-6, 3P-7
Tani Kentaro	1P-43	Watanabe Ikumi	3P-34
Tanigaki Katsumi	2P-13, 3P-16, 3P-29	Watanabe Kenichi	1P-2
Tanioku K.	2P-29	Watanabe Miki	1-7
Tategaki Hiroshi	3P-4	Watanabe Satoru	1P-4
Terada Y.	2P-37	Xu Guochun	2P-34
Terauchi Ikuya	2P-9	Xu Wei-Chun	3-5
Tobe Yoshito	2-11	Y. A. Kim	3-7
Tohji Kazuyuki	1P-26	Yajima Hirofumi	3P-2, 3P-3, 3P-19,
Toida Tatsuo	3P-2		3P-23
Tokumoto Hiroshi	1P-5, 2P-24	Yamada Michio	1P-12, 3P-12
Tokumoto Madoka	3-8	Yamada Takayuki	2-4
Tomikawa Takako	1-7	Yamada Takeo	2P-20, 3-6
Tomiyama Tetsuo	1P-13	Yamamoto Hiroshi	1P-44, 3P-24
Tomonari Yasuhiko	3P-39	Yamamoto Kazunori	1P-18
Touhara Hidekazu	3-7	Yamashiki Tomoya	2-9
Toyoda Shouhei	3P-39	Yamashita Kazuaki	3P-35
Toyota N.	2P-39	Yamaura Tatsuo	2P-34
Tsuchida Satoru	2P-14, 2P-15	Yanagi Kazuhiro	1-14, 2P-30
Tsuchiya Takahiro	1P-9, 1P-10, 1P-11,	Yano Taka-aki	1-3
	1P-12, 2-1, 2-2, 2P-1,	Yase Kiyoshi	1P-16
	2P-11, 2P-12, 3P-1,	Yasuda Kyohei	3P-40
	3P-11, 3P-12	Yasuda Toshio	1P-5
Tsuji Hajime	2P-17	Yokoi Hiroyuki	3P-30
Tsuji Masaharu	1P-46, 2P-47, 3-3,	Yomogita Akinori	2P-12

Yongfu Lian	2P-24
Yorimitsu Hideki	1-15, 1P-32
Yoshida Hiromichi	2P-22, 2P-37
Yoshida Yuji	1P-16
Yoshikawa Kazuo	2P-34
Yoshikawa Masahito	1P-20
Yoshikuni Masato	1P-44
Yoshimatsu Daisuke	3P-43
Yoshimura Akihiko	1P-47
Yoshimura Daisuke	2-5
Yoshimura Hirofumi	1P-47
Yoshitake Tsutomu	3P-27
Yoza Kenji	1P-10, 2-1
Yudasaka Masako	1-15, 1P-31, 1P-32, 1P-33, 2P-18, 2P-20, 3-7, 3P-27
Yuge Ryota	1-15, 1P-31
Yumura Motoo	1P-39, 2P-20, 3-5, 3-6
Zhao Xinluo	1P-29, 3P-21, 3P-25
Zhao Yanli	2P-25
Zhong Yu-Wu	2P-4

複写される方へ

本誌に掲載された著作物を複写したい方は、(社)日本複写権センターと包括複写許諾契約を締結されている企業の方でない限り、著作権者から複写権等の行使の委託を受けている次の団体から許諾を受けてください。著作物の転載・翻訳のような複写以外の許諾は、直接本会へご連絡下さい。

〒107-0052 東京都港区赤坂 9-6-41 乃木坂ビル (法) 学術著作権協会

TEL : 03-3475-5618

FAX : 03-3475-5619 E-Mail : naka-atsu@muj.biglobe.ne.jp

アメリカ合衆国における複写については、次に連絡して下さい。

Copyright Clearance Center, Inc.

222 Rosewood Drive, Danvers, MA 01923 USA

Phone : (978)750-8400 FAX : (978)750-4744

Notice about photocopying

In order to photocopy any work from this publication, you or your organization must obtain permission from the following organization which has been delegated for copyright clearance by the copyright owner of this publication.

Except in the USA

Japan Academic Association for Copyright Clearance, Inc.(JAACC)

6-41 Akasaka 9-chome, Minato-ku, Tokyo 107-0052 Japan

TEL : 81-3-3475-5618

FAX : 81-3-3475-5619 E-Mail : naka-atsu@muj.biglobe.ne.jp

In the USA

Copyright Clearance Center, Inc.

222 Rosewood Drive, Danvers, MA 01923 USA

Phone : (978)750-8400 FAX : (978)750-4744

2006年1月7日発行

第30回記念フラーレン・ナノチューブ総合シンポジウム
講演要旨集

<フラーレン・ナノチューブ学会>

〒464-8602 愛知県名古屋市千種区不老町
名古屋大学大学院理学研究科 物質理学専攻
篠原研究室内

Tel : 052-789-5948

Fax : 052-789-1169

E-mail : fullerene@nano.chem.nagoya-u.ac.jp

URL : <http://fullerene-jp.org>

印刷 / 製本 名古屋大学消費生活協同組合印刷部

NANORUPTOR[®] —— バイオの技術をナノテクへ

密閉式超音波処理装置

実施例：燃料電池用触媒評価、カーボンナノチューブの分散。

特徴

●密閉処理

溶媒の蒸発・揮散がありません。
コンタミがありません。
ナノリスク対策に対応可能。

●多試料同時処理

最大24試料を同時に処理できます。

●再現性良好

回転機構の採用により均一な超音波照射が可能です。

●多彩なラインアップ

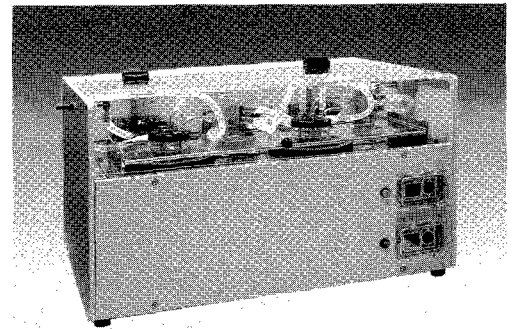
汎用機からハイパワー機および連続処理機をご用意しています。



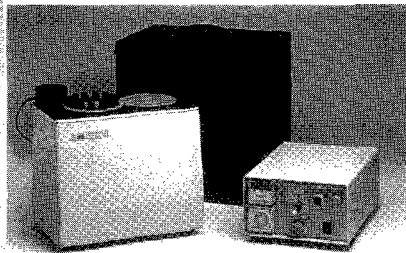
ハイパワー-NANORUPTOR (NR-300)



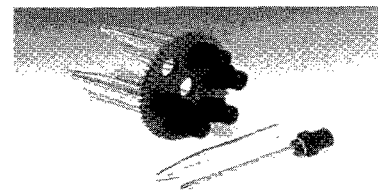
BIORUPTOR (UCD-250)



連続式NANORUPTOR (NR-2028)



BIORUPTOR (UCW-201)



密閉容器

用途

精製・分離・混合・分散・反応促進
・触媒評価・各種スクリーニング

20余年培ってきたバイオのナノテクをご利用ください。

デモ機を
ご用意しております。
どうぞお気軽に
お問い合わせ
ください。

お問い合わせ先

販売



コスモ・バイオ株式会社

〒135-0016 東京都江東区東陽2-2-20 東陽駅前ビル
URL: <http://www.cosmobio.co.jp>
TEL (03) 5632-9610 FAX (03) 5632-9619
営業本部 機器グループ 栗原
e-mail: mkurihar@cosmobio.co.jp

製造



東湘電機株式会社

〒232-0027 神奈川県横浜市南区新川町5-29-2 新井ビル2F
TEL (045) 261-8388 FAX (045) 252-8935
技術部長 伊藤
e-mail: k-ito@bioruptor.jp

ナノテク材料は進化しつづけている。

C13安定同位体置換C60フラーレン (99%)
 C13安定同位体置換C70フラーレン (98%)
 水溶性C60CHCOOH、水溶性C60(OH) $n = 22 \sim 26$
 水溶性C60(H)NH(CH₂)₅COONA
 C60H36フラーレン、C60F36フラーレン、Anti-HIVフラーレン
 Gd@C82金属内包フラーレン、La@C82金属内包フラーレン
 [60]PCBM [Phenyl C61 Butyric Acid Methyl Ester 99.5%]
 [70]PCBM [Phenyl C71 Butyric Acid Methyl Ester 99.0%]
 ハイブリッドC60フェロセン、ハイブリッドC60コバルトセン
 C60・Ptフラーレン、C60・Feフラーレン、C60・Niフラーレン
 Carbon Nano Paper, Aligned Carbon Nanotube Array
 Carbon Nanotube based field emission X-ray tube
 Vertical aligned MWCNT (3~30micron)
 Electron field Emmission Cathode, C60 film
 Triode Cathode ATC Series, C60C (COOE+) 2
 Carbon Nanotube AFM tip, C60 (C (COOE+)) 2
 Carbon Nanofiber, C60Br24, C76, C78, C84, C86

SWNT-COOH, purified (70-80%)
 SWNT-NH₂, purified (70-80%)
 SWNT-CONH-C₁₈H₃₇, purified (70-80%)
 SWNT-COO-R-OH (2-5% rpynn)
 Shorted SWNT-COOH, purity 90%, length 200-500 nm
 Shorted SWNT-NH₂, purity 90%, length 200-500 nm
 Shorted (200-500 nm) SWNT-COO-R-OH (5-10% group)
 Solutions of functionalized SWNT in different solvents
 Substituted pyrrolidinofullerene derivatives
 Lower bulk density SWNT-COOH, purified (70-80%)
 DWNT (double wall CNT), 20-30% purity, 3~5nm
 DWNT (double wall CNT), 90% purity, 140nm

Compounds, Elements
 Single-Metal Oxides
 Multi-Metal Oxides
 Nano-Wire Powders

Particles: MoS₂, CrO₃, HgI₂ (alpha- & Beta-): Diamond Abrasive: <50nm, <100nm, <200nm, <250nm, <500nm, 200-400nm, <1um: Graphite: 15,000 mesh, 10,000 mesh.
 Nanowires (Diameter ~100nm, L=~1-2um): Si, Ga, Bi, InP, GaP, II-VI compounds.
 Composite particles: Dropped, shelled, & cored metals/oxides like Ag/SiO₂ core<100nm.
 Coated particles: Surfactants on oxides, or Metals.
 Shorter length CNTs: 0.5um (SWNTs, MWCNTs), 5um (more easily dispersible).
 SWNTs, MWNTs surface funcationized with -COOH

SWNT	MWNT (regular)	MWNT (short)
Closed SWNT 50-70%	95+%, OD/ID: <8/2-5nm	95+%, OD/ID/L: 8-15/3-5/500nm
Open SWNT 90%	95+%, OD/ID: <10/2-7nm	95+%, OD/ID/L: 10-20/5-10/500nm
MWNT (Aligned)	95+%, OD/ID: 3-20/1-3nm	95+%, OD/ID/L: 20-30/5-10/500nm
95%+OD: 10-20nm	95+%, OD/ID: 8-15/3-5nm	95+%, OD/ID/L: 30-50/5-15/500nm
Carbon Nano Fibers	95+%, OD/ID: 10-20/5-10nm	94+%, OD/WT/L: 20-30/1-2nm
OD: 240-500nm	90+%, OD/ID: 10-30/3-10nm	94+%, OD/WT/L: 20-50/1-2nm
OD: 80-200nm	95+%, OD/ID: 10-30/5-10nm	94+%, OD/ID/L: 40-70/5-40nm
OD: 40-80nm	95+%, OD/ID: 20-30/5-10nm	85%, OD/WT/L: 20-40/5-15nm
OD: 240-500nm (graphitized)	95+%, OD/ID: 20-40/5-10nm	90%, OD/WT/L: 20-40/5-15nm
	95+%, OD/ID: 30-50/5-15nm	95%, OD/WT/L: 20-40/5-15nm
	95+%, OD/ID: 40-60/5-10nm	98%, OD/WT/L: 20-40/5-15nm
	95+%, OD/ID: 50-100/5-10nm	99%, OD/WT/L: 20-40/5-15nm
		85%, OD/WT/L: 40-70/5-30nm
		90%, OD/WT/L: 40-70/5-30nm
		95%, OD/WT/L: 40-70/5-30nm
		98%, OD/WT/L: 40-70/5-30nm
		99%, OD/WT/L: 40-70/5-30nm
		95+%, OD/ID/L: 10-30/5-10/1-2μm
		95+%, OD/ID/L: 20-40/5-10/1-2μm

※詳細資料は下記へご請求願います。

弊社取り扱い製品は <http://www.scilab.co.jp/> でご覧いただけます。



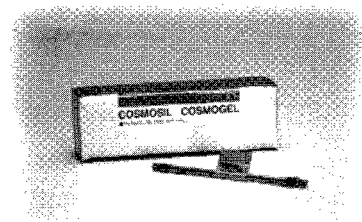
次世代技術知識集団

株式会社サイエンスラボラトリーズ

〒270-0021 千葉県松戸市小金原7丁目10番地25 TEL: 047-309-8311 FAX: 047-309-8310

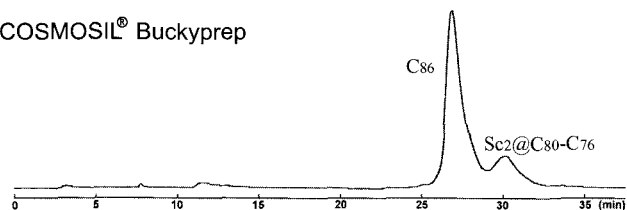
E-mail: sales@scilab.co.jp URL: http://www.scilab.co.jp

今まで分離できなかった
金属内包フラーレンが分離可能！！

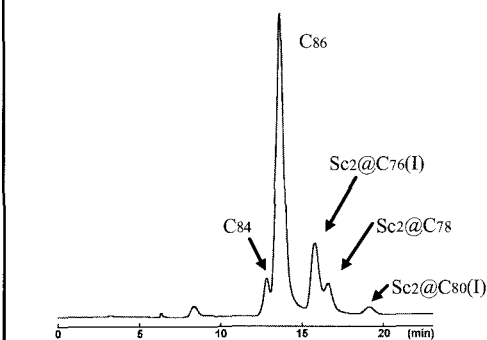


■分析例

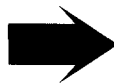
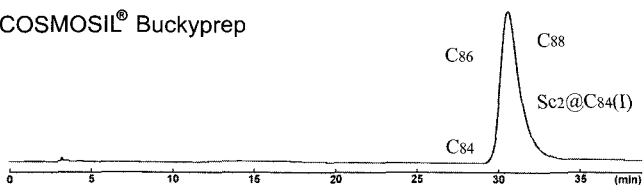
COSMOSIL[®] Buckyprep



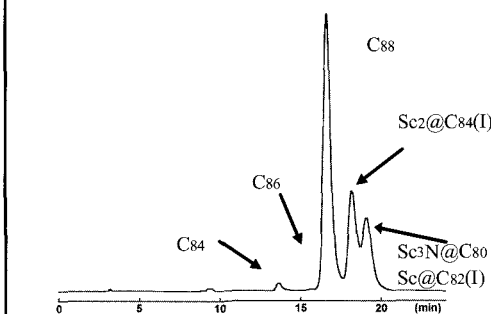
COSMOSIL[®] Buckyprep-M



COSMOSIL[®] Buckyprep



COSMOSIL[®] Buckyprep-M



分析条件

カラムサイズ：4.6mm I.D. × 250mm, 移動相：トルエン, 流速：1.0 ml/min, 温度：30°C, 検出：UV312

資料提供：名古屋大学 大学院理学研究科物質理学専攻 篠原 久典教授

■その他COSMOSIL[®] フラーレン関連カラム

フラーレン分離のスタンダードカラム



COSMOSIL[®] Buckyprep

C₆₀, C₇₀等の大量分取に



COSMOSIL[®] PBB

詳しい情報はWeb siteをご覧ください。

ナカライテスク株式会社

〒604-0855 京都市中京区二条通烏丸西入東玉屋町498

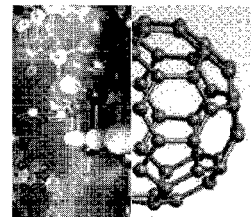
価格・納期のご照会 フリーダイヤル 0120-489-552
製品に関するご照会 TEL: 075-211-2703 FAX: 075-211-2673

Web site : <http://www.nacalai.co.jp>

$$C \times \text{TOYO TANSO} = \infty$$

私たちの炭素の夢は、未来へと無限に広がります。

その優れた特性によって限りない可能性を持つC（カーボン）。私たち東洋炭素は、無限に広がるカーボンの応用分野を求めて、常に人と環境にやさしくをモットーに、未来技術の創造にチャレンジしています。金属内包フラーレンやカーボンナノチューブ合成用原料の開発など、今、私たちに求められているものは何かを常に考え、21世紀に貢献する未来型企業を目指し続けます。



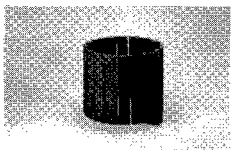
TOYO
 **東洋炭素株式会社**

URL <http://www.toyotanso.co.jp/>

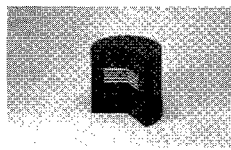
【本社】〒555-0011 大阪市西淀川区竹島5-7-12 TEL 06-6473-7912
 【工場】詫間事業所・大野原技術開発センター・萩原工場・いわき工場
 【営業所】東北・つくば・東京・北陸・静岡・名古屋・大阪・広島・四国・九州
 【国内関係会社】東炭化工株式会社・大和田カーボン工業株式会社

<主な製品>

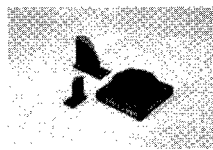
特殊黒鉛製品



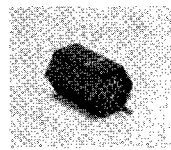
半導体用



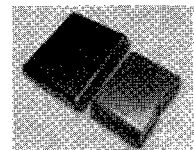
冶金工業用



放電加工用



原子力用



核融合装置用

一般カーボン製品



機械用



電気用

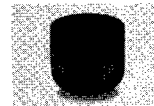
複合材その他製品



SiCコーティング
製品



黒鉛シート



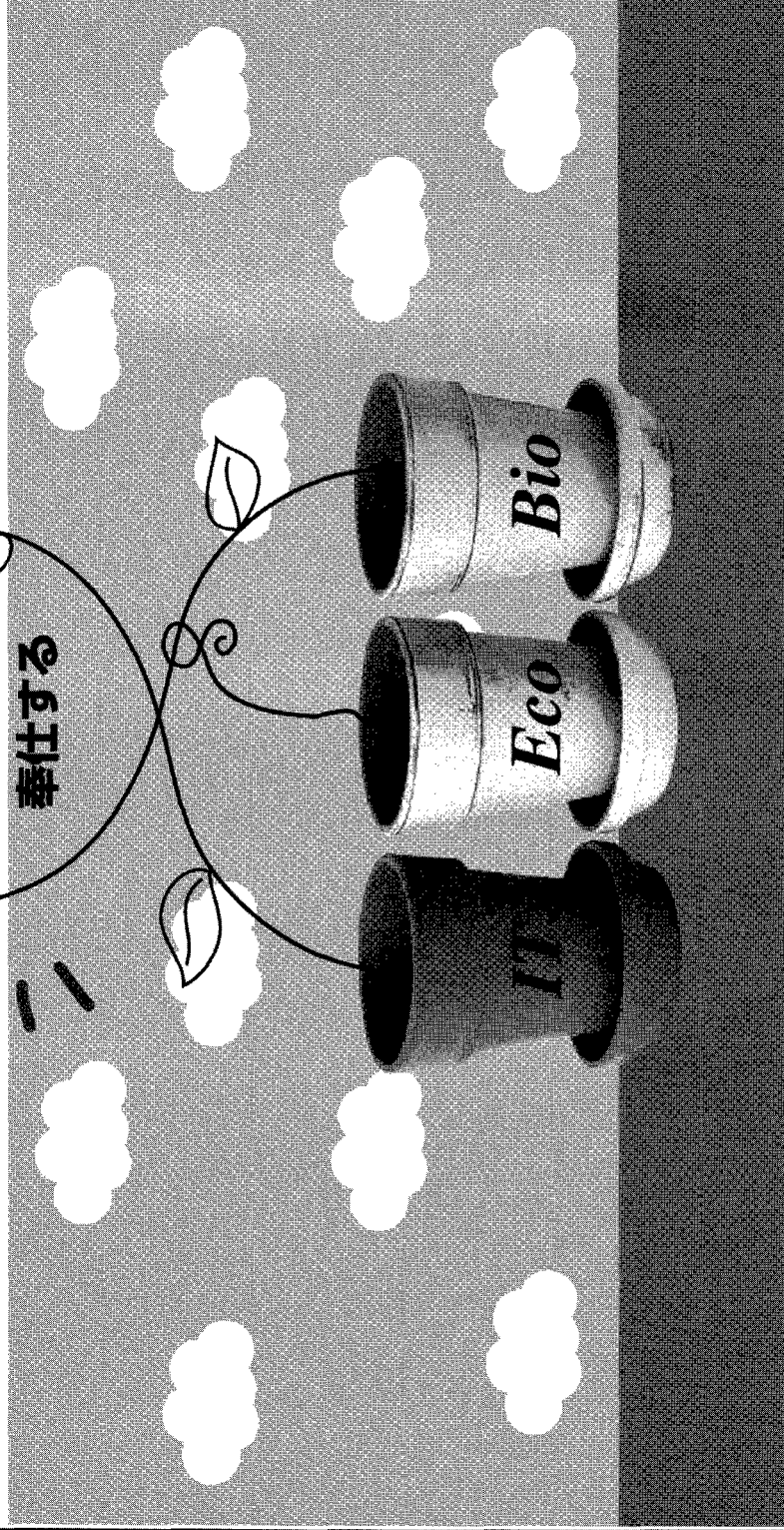
C/Cコンポジット
製品



オンサイト
フッ素発生装置

 OZAWA SCIENCE

未来の科学に
奉仕する



科学機器・計測システムの技術・情報商社

 **オザワ科学株式会社**

本社 / 〒460-0003 名古屋市中区錦三丁目9番22号
TEL (052) 951-5331 (代) FAX (052) 962-7358
本社分室・春日井・刈谷・豊田・豊川・浜松・四日市・亀山・岐阜・商品センター

URL <http://www.ozawasc.co.jp>

E-mail welcome@ozawasc.co.jp



TIIは最先端機器の日本発・世界初に挑戦し
グローバルネットワークを展開中

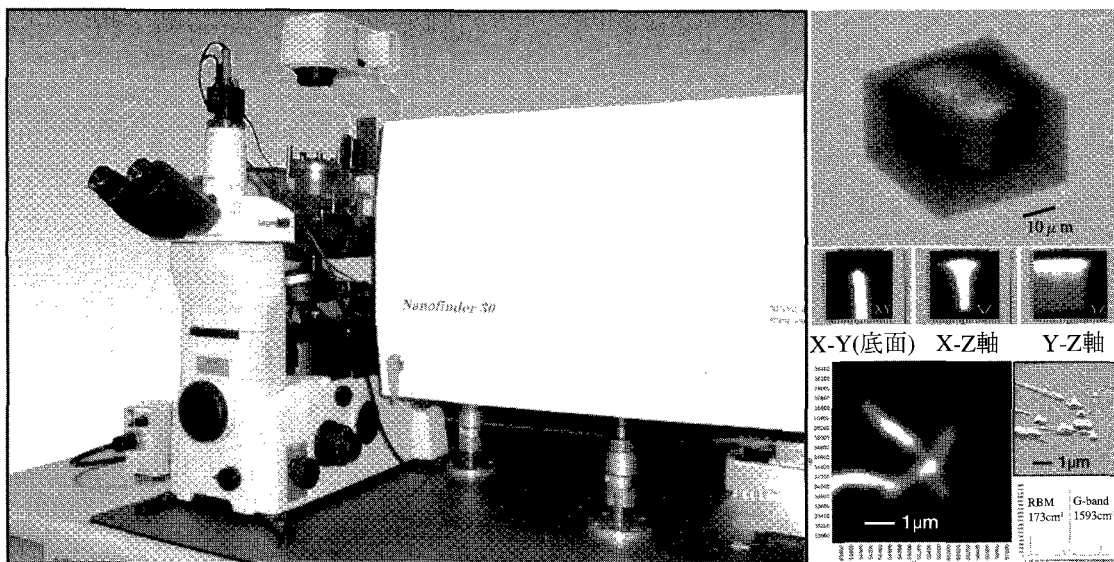
3D顕微ナノラマン装置

Nanofinder[®]30

受賞

- 2004年 ナノテク大賞「評価・計測部門」
- 第16回中小企業優秀新技術・新製品賞

3Dイメージで化学状態を分析すると一目瞭然



高感度10倍以上・機械的歪みが激減・SERS近接場光学顕微鏡・全自動

- 新光學設計により感度が10倍以上(当社比)アップ**
今まで見えないものが見えて来る。
高速測定が可能になり測定環境を気にしない。
更に低パワーレーザー励起(サブmW)で非破壊測定。
- 堅牢な設計で機械的安定度が向上**
レーザー共振器設計技術と分析機器の複合技術を採用
で3D光ナノ計測における機械的ドリフトを解決
- SERS近接場光学顕微鏡対応**
(大阪大学 河田研究室との産学連携品)
目標イメージ 平面空間分解能30nm目標(現80nm)
共焦点レーザー顕微鏡でも150nm(@633nm HeNe レー
ザー使用)達成
- 3Dラマン、形状、AFMの同位置同時計測**
3D光ナノ計測に対応しサンプルを移動することなく
短時間(数分間)でイメージングする画期的測定方法です。
- 偏光測定**
レーザー励起側と検出側に偏光子を装備しました。
- 全自動化**
全ての機能はPCより制御で再調整は不要。
レーザー出力自動調整、共焦点ピンホール
- 多種類のレーザー入射数**
2種類まで標準で、5種類まで同時入力が可能
- モジュールタイプで分光器の選択可**
標準分光器は52cm焦点距離のイメージ分光器で回折
格子は4枚搭載。
ダブル分光器、エッセル分光器、またはお手持の
分光器に接続可能。
- 多機能**
ラマン、蛍光、共焦点顕微鏡、AFMトポグラフィー、
SERS(表面増強ラマン)イメージング

本装置は科学技術振興事業団の独創的研究成果育成事業(平成14年度)による委託により商品化しました。



株式会社 東京インスツルメンツ

〒134-0088 東京都江戸川区西葛西6-18-14 T.I.ビル
http://www.tokyoinst.co.jp/
大阪営業所：〒532-0003 大阪市淀川区宮原4-1-46 新大阪北ビル

TEL 03 (3686) 4711(代) FAX 03 (3686) 0831
e-mail:sales@tokyoinst.co.jp
TEL 06 (6393) 7411(代) FAX 06 (6393) 7055

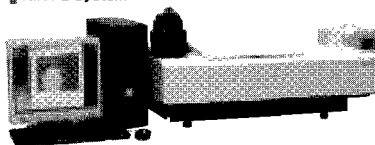
Total Solution focused on Carbon Nanotube

島津は総合分析機器メーカーとして、カーボンナノチューブの計測評価に関する様々なソリューションをご提供致します。

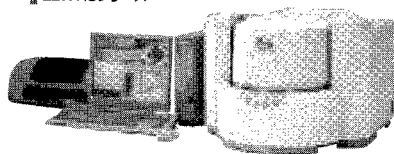
- 微量CNTの純度・熱特性の評価
 - CNTの結晶性と耐熱性の評価
- **マイクロ熱重量測定装置**
TGA-50



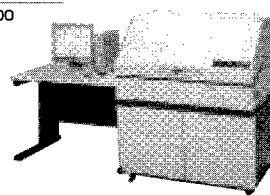
- SWNTの近赤外PL3次元分布測定
- **近赤外フォトルミネッセンス測定システム**
NIR-PL System



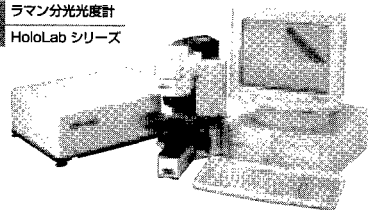
- CNT中の触媒元素の測定
- **卓上型蛍光X線分析装置**
EDX-HSシリーズ



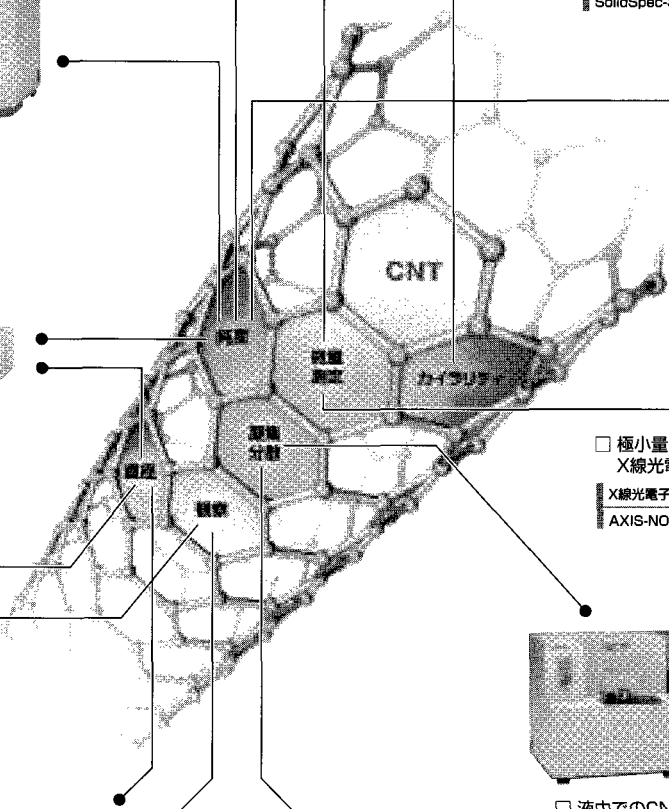
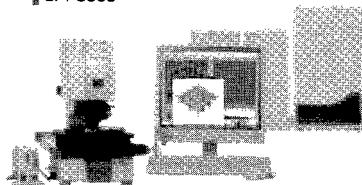
- CNTの紫外可視近赤外吸収スペクトル測定
- **紫外可視近赤外分光光度計**
SolidSpec-3700



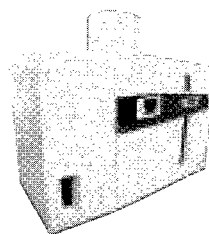
- CNTの直径測定
 - CNTの結晶性と耐熱性の評価
- **ラマン分光光度計**
HoloLab シリーズ



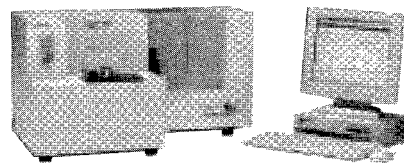
- あらゆるナノテク材料を観察・測定
- **ナノサーチ[®]顕微鏡**
SFT-3500



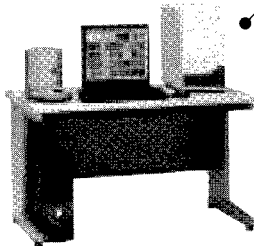
- 極少量CNTのX線光電子分光測定
- **X線光電子分光分析装置**
AXIS-NOVA



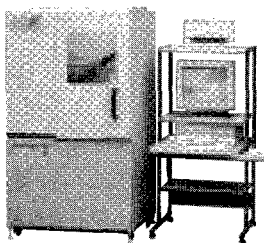
- 液中でのCNTの分散・凝集過程の評価
- **レーザー折式粒度分布測定装置**
SALD-7000



- CNTの直径測定
 - CNTの精製前後の観察
 - CNTとポリマーコンポジット試料の観察
- **定置型フローブ顕微鏡**
SPM-9600 **NEW**



- CNTのバンドル状態の解析
- **X線回折装置**
XRD-6100



株式会社 **島津製作所**

京都市中京区西ノ京桑原町1

<http://www.an.shimadzu.co.jp>

分析計測事業部 (075) 823-1195

お問合せはもよりの営業所へ

- 東京 (03) 3219-5685
- 北関東 (048) 646-0081
- 神戸 (078) 331-9665
- 関西 (06) 6373-6556
- 横浜 (045) 311-4615
- 岡山 (086) 221-2511
- 札幌 (011) 205-5500
- 静岡 (054) 285-0124
- 四国 (087) 823-6623
- 東北 (022) 221-6231
- 名古屋 (052) 565-7531
- 広島 (082) 248-4312
- 郡山 (024) 939-3790
- 京都 (075) 811-8151
- 九州 (092) 283-3334
- つくば (029) 851-8515

株式会社東京プログレスシステム

住所: 107-0052 東京都港区赤坂 2-17-68-502

電話: 03-5570-0457 FAX: 03-5570-0462

URL: <http://www.tokyoprogres.co.jp>

営業品目(詳細は URL をご覧下さい)

◎ダイヤモンド類及びその他超硬材料(販売単位: グラムからキログラムまで)

1. ショックダイヤモンド・パウダー(DD): 爆薬の爆発の温度と圧力で作られるダイヤモンドです。高純度で最高の硬度と研磨性を持っています。
2. 超分散ダイヤモンド(UDD): 爆薬分子中の炭素が爆発によってダイヤモンドに変わったものです。粒径は数ナノの球状ですが、集まってクラスターになっています。エンジンの潤滑剤やエレクトロニクス産業などの高精度研磨・表面処理に用いられています
3. 静圧合成ダイヤモンドーミクロン サイズ : 黒鉛から高圧高温下で合成されるダイヤモンドです。
4. その他 ダイヤモンドペースト ・ BN ・ 合成ダイヤモンド結晶など

◎ フラーレン誘導体 (MTR社製 U.S.A.)

- No. 3 水酸化フラレン: $C_{60}(OH)_n, n=24$
- No. 4 安定同位体置換フラレン: C_{60} : 99% C_{13} , 20~30%置換
- No. 5 安定同位体置換フラレン: C_{70} : 99% C_{13} , 20~30%置換
- No. 6 安定同位体置換フラレン: $C_{60}/70$ 混合物 C_{13} , 10~15%置換
- No. 9 フッ化フラレン: $C_{60}(F)_{36}$, 99%
- No. 10 高次フラレン混合物 : ($C_{76}, C_{78}, C_{80}, C_{82}, C_{84}$)
- No. 16 カルボン酸フラレン: $C_{60}CHCOOH$
(1.2-Methanbofulleren C_{60})-61-carboxylic acid
- No. 17 Bucky Fullerene - molecular hybrid C_{60} with Ferrocene:
 $[\eta^5(C_5H_5)_2Fe]_2 * C_{60}$
- No. 18 Bucky Cobaltocene - ionic hybrid C_{60} with Cobaltocene:
 $(\eta^5-C_5H_5)_2Co * C_{60}$
- No.22 アミノプロロン酸Naフラレン: $C_{60}(H)NH(CH_2)_5COONa$
- No.23 ビスマロン酸エチルフラレン: $C_{60}C(COOEt)_2$
- No.24 ビスマロン酸ジエチルフラレン: $C_{60}[C(COOEt)_2]_2$
- No.26 $C_{60}Br_{24}$
- No.28 $C_{60}F_{36}$ mixture of isomers (T: C_3 : $C_1=25$: 70: 5)
- No.29 Endohedral metallofullerene: $Gd@C_{82}$ 60-80%
- No.30 $La@C_{82}$: purity 70%
- No.31 PCBM (6, 6-Phenyl-C61-Butyl acid - Methylene ester) 99.8%
"For plastic Solar Cells"
- No.32 $C_{60}F_{48}$ (新製品)

その他: 安定同位体・レアメタル・その他の技術調査・翻訳・出版

ナノテクノロジーシリーズの第二弾発刊へ!

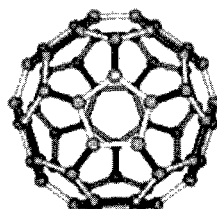
新発売 ナノテクノロジーシリーズⅡ

フラーレンとカーボンナノチューブ (Ⅱ)

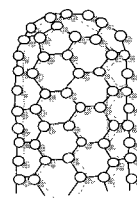
2005年12月刊行 99,750円/冊(総額)

- 好評を頂いた2002年7月発刊「フラーレンとカーボンナノチューブ」*の第二弾
- 内外の関連特許の収録と解析実施
総計：2,253件/2001/8～2004/8
 - ・フラーレン：466件
 - ・カーボンナノチューブ：1,787件
- 最近の新聞情報を整理し纏めた
433件/2001/1～2005/3

フラーレン



カーボンナノチューブ



フラーレンとカーボンナノチューブの最近の研究開発動向について特許情報を整理し調査した。2001年8月～2004年8月までに公開された特許を分類・整理した結果2,253件となったが出来る限り特許請求条件を定量的に記載することを試みた。また、新聞情報もナノカーボンに関する記事433件/2001/8～2005/3についてトピックスとして纏めた。

本書は解説だけでなく技術を集約させてあるので、内外のフラーレンとナノカーボンに関する動向を探求するには最適の書になると確信しております。

カーボンナノチューブとフラーレン 特許情報 CD-R版

2005年より毎月1回刊行 105,000円/年(総額)

尚データは2004年9月より有ります

カーボンナノチューブとフラーレンに関する日本特許及び海外主要国特許情報をカーボンナノチューブとフラーレンそれぞれについて、構造関連、製造関連、応用(用途)に分類したデータベースを1ヶ月に1回、当年1月から当月までをCD-Rに下記仕様で集録し郵送致します。

- ・CSV形式のテキストデータ及び簡易データベース(Microsoft Access2000以上)
- ・内容：書誌事項、要約、クレーム(約5,000文字以内)

<関連刊行物>

「フラーレンとカーボンナノチューブ」*

2002年7月刊 99,750円(総額)



株式会社ダイリサーチマーテック 〒102-0083 東京都千代田区麹町6丁目6番地

企画営業部 TEL 03(5226)0734～0736 FAX 03(5226)0741

E-mail info@drmi.co.jp URL http://www.drmi.co.jp

※ホームページからお申し込み頂けます。

【化学フロンティア⑮】

ナノカーボンの新展開

——世界に挑む日本の先端技術

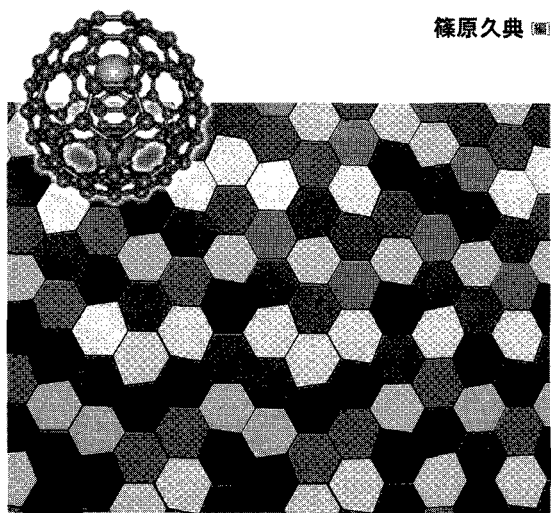
篠原久典 編

化学
フロンティア

ナノカーボンの 新展開

世界に挑む日本の先端技術

篠原久典 編



化学同人

材料、エレクトロニクス、燃料、バイオなど、多様な分野への応用が期待できるフラーレンおよびカーボンナノチューブは、多くの民間企業が重要プロジェクトとして研究開発を推進している。最新のデータに基づいて、これらナノカーボン物質の量産化や応用・実用化研究に向けた戦略などを解説。

B5・224頁・定価4515円

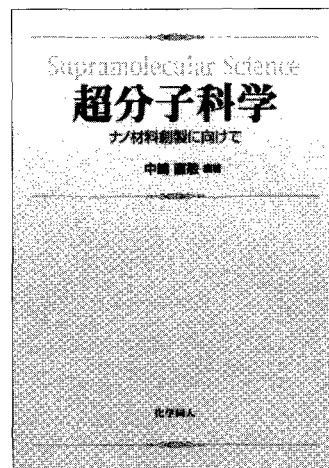
超分子科学

——ナノ材料創製に向けて

中嶋直敏 編著

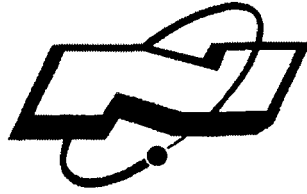
A5・上製・488頁・定価9450円

本書は従来のホスト・ゲスト系超分子、分子組織体だけでなく、ナノ材料創製にもスポットを当てた、第一線研究者による超分子の集大成である。超分子関連の研究者、技術者、院生の必読の書。



化学同人

→ <http://www.kagakudojin.co.jp> (ホームページで書籍注文できます)
〒600-8074 京都市下京区仏光寺通柳馬場西入ル Tel 075-352-3373 Fax 075-351-8301



株式会社 テクノ西村

〒460 - 0012 名古屋市中区千代田 2 - 11 - 11

tel : 052 - 251 - 8771 (総務部) fax : 052 - 264 - 9501

tel : 052 - 251 - 8772 (第一営業部) fax : 052 - 251 - 2138

tel : 052 - 251 - 8773 (第二営業部) fax : 052 - 251 - 2138

URL : <http://www.tekunishi.com>

お客様が望むもの、それが私たちの取扱商品です

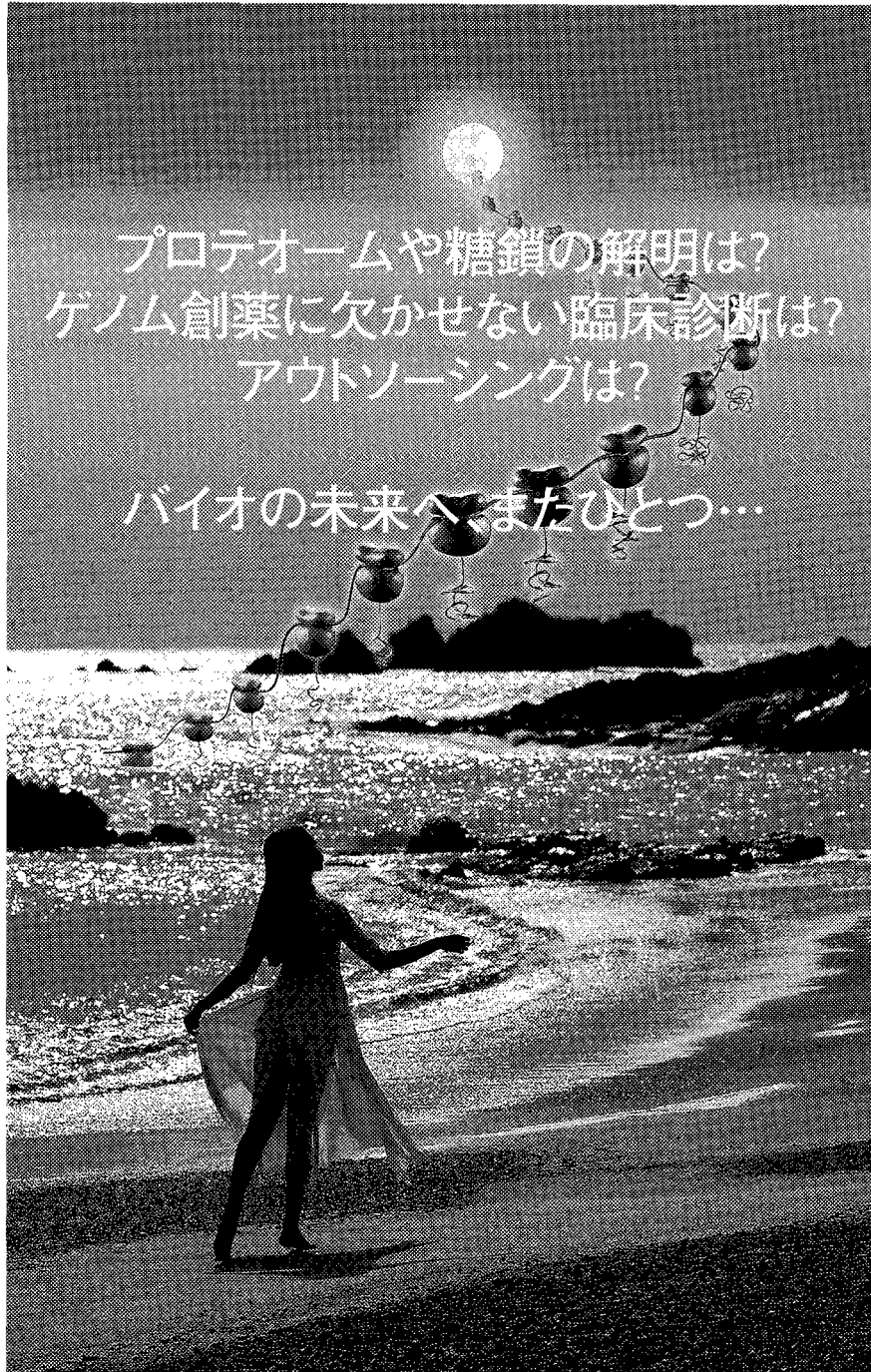
総合力ゆえに情報力、提案力がちがいます。同業他社では望むことのできない総合力が、たとえば設備単体ではなく、システム全体の提案をも可能にします。そうした総合力を活かし、有用性の高い情報を幅広く提供する一方で、課題解決型の営業を展開。お客様が抱える問題点の発見と解決に努めております。

【取扱い分野】

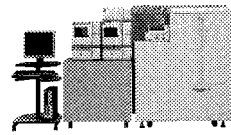
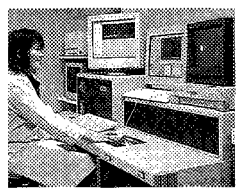
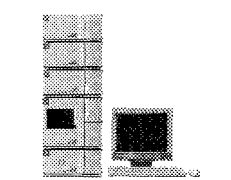
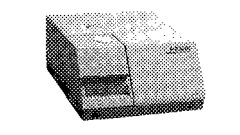
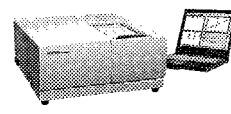
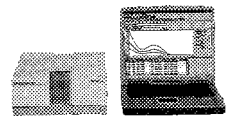
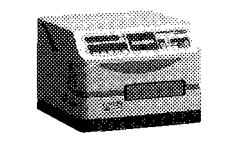
- ★研究開発分野
 - ・汎用科学機器
 - ・分析機器
 - ・実験室設備
- ★品質保証分野
 - ・試験機器
- ★環境保全分野
 - ・環境測定機器

- ★特殊機器分野
 - ・特殊機器製作
- ★教育機器分野
 - ・理化学機器
 - ・視聴覚機器
 - ・教育用教材機器
 - ・家具・遊具

- ★福祉分野
 - ・福祉機器
- ★保健分野
 - ・保健関係機器
- ★情報分野
 - ・情報機器
 - ・事務用機器



プロテオームや糖鎖の解明は?
ゲノム創薬に欠かせない臨床診断は?
アウトソーシングは?
バイオの未来へまたひとつ...

<p>日立タンパク質解析用 液体クロマトグラフ質量分析計</p>  <p>NanoFrontier L</p>	<p>受託解析サービス</p>  <p>ゲノム/プロテオーム/ セローム/薬物動態</p>
<p>日立高速液体クロマトグラフ LaChrom Elite 三次元システム</p> 	<p>日立分光蛍光光度計</p>  <p>F-2500</p>
<p>日立ダブルビーム分光光度計</p>  <p>U-2800A/U-2810</p>	<p>日立ダイオードアレイ型 バイオ光度計</p>  <p>U-0080D</p>
<p>日立小形遠心機</p>  <p>himac RXシリーズ</p>	<p>日立分離用超遠心機</p>  <p>himac CPWXシリーズ</p>
<p>コロナグレーティング マルチマイクロプレートリーダー</p>  <p>SH-8000Lab</p>	<p>コロナ マルチマイクロプレートリーダー</p>  <p>MTP-800Lab</p>

日立ハイテクノロジーズは、バイオ解析・創薬支援システムの提供から受託解析サービスまで、
世界最先端のバイオ・ソリューションをお届けし、お客様と共に生命の新たな未来を切り拓いていきます。
その先は、まだ誰も経験したことのない世界。しかし、私たちはもう歩き始めています。

その先のバイオ分析システムへ

Life Science NAVIGATOR

BIONAVI

<http://www.hitachi-hitec.com/science/>

◎ 株式会社日立ハイテクノロジーズ 〒105-8717 東京都港区西新橋一丁目24番14号 電話 ダイヤルイン (03) 3504-7211
北海道(札幌) (011) 221-7241 東北(仙台) (022) 264-2211 筑波(土浦) (029) 825-4817 中部(名古屋) (052) 219-1683
静岡(054) 262-0561 三島(055) 989-7571 関西(大阪) (06) 4807-2551 京都(京都) (075) 241-1591
四国(高松) (087) 825-9977 中国(広島) (082) 221-4518 九州(福岡) (092) 721-3501 沖縄(那覇) (098) 863-8295

住友商事のカーボンナノチューブ

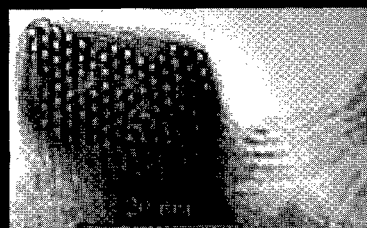
Produced by Carbon Nanotechnologies Inc. (CNI)

◆ 単層カーボンナノチューブ(SWNT)は、グラファイト構造の(グラフェン)シート層で構成されている、直径約1nmの筒状分子です。ナノカーボン材料のなかでも、複数層からなる多層カーボンナノチューブ(MWNT)や、他のカーボン材料に比べて格段に優れた導電性・熱伝導性・構造的特性を有し、幅広い応用が期待されています。住友商事は、CNI社の日本・アジア地域での総代理店として、各種用途に適した製品のご提供に加え、共同開発の推進や事業化支援プロジェクトの実施など、カーボンナノチューブの応用製品開発を総合的に支援しています。

● HiPco® 単層カーボンナノチューブ

直径約1nmの単層カーボンナノチューブです。基礎研究や高機能用途向けに、触媒残留率の異なる下記3製品をご提供しております。

製品名	触媒残留率
HiPco® As Produced (未精製品)	< 35 wt%
HiPco® Purified (精製品)	< 15 wt%
HiPco® Super Pure (超高純度品)	< 5 wt%



* Bucky Plus™(フッ化カーボンナノチューブ)など修飾品も対応可能です。

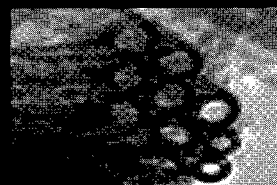
■ 単層カーボンナノチューブ ■

● CNI Xシリーズ

CNI社独自の製法で製造された、用途別産業応用向けカーボンナノチューブです。量産性に優れ、導電性樹脂複合材(EMI, ESD, Anti-Static)、フィールドエミッション用途などに、安定した製品供給が可能です。詳細につきましては、下記連絡先までお問合せください。

● 二層カーボンナノチューブ

CNI社独自の製法で製造された、直径約2nmの二層カーボンナノチューブです。



■ 二層カーボンナノチューブ ■

上記製品群を中心に、研究用から量産対応品、また共同開発によるカスタマイズ対応など、用途に応じたカーボンナノチューブの開発を進めています。弊社までお気軽にお問合せ下さい。

本件に関するお問合せ先

住友商事株式会社 電子材部 (担当:小野/青木)

E-mail : nano@em.sumitomocorp.co.jp

TEL : 03-5166-5857 FAX : 03-5166-6234

住所 : 〒104-8610 東京都中央区晴海1-8-11

URL : www.sumitomocorp.co.jp/section/joho/nanotube.shtml



もっと、向こうへ。
風は、東レグループから。

■ 繊維・ファッション

東レ・デュボン オペロンテックス 大垣扶桑紡績 東レ・テキスタイル
井波テキスタイル マツモト・テキスタイル 東洋整染
東レコーテックス 東和織物(大阪) 東レ・モノフィラメント
東洋タイヤコード 東洋電植 丸一繊維 創和テキスタイル
一村産業 丸佐 東レぎもの販売 東レフィッシング
東レエクセースプラザ 東レ・ディプロモード
サンリッチモード サンエオリジン
日本アパレルシステムサイエンス

■ 商事

東レアイリーブ 東レインターナショナル 関東ゼネラルサービス
東レアルファート 蝶理

■ プラスチック・ケミカル

東レフィルム加工 東洋プラスチック精工 東レベフ加工品
東レ・ダウコーニング 東レ・ファインケミカル 曾田香料

■ 住宅・エンジニアリング

東レ建設 東レACE 東レエンジニアリング 東レ・プレジジョン 東レ水処理メンテナンス
水道機工

■ 医薬・医療

東レ・メディカル

■ 情報・サービス

東レリサーチセンター 東レシステムセンター 東レ・エーシーエス 東レ経営研究所
東レエンタープライズ 知立ホテル 東レ・エージェンシー 東レ・トラベル 東洋実業
東洋運輸 東レ知的財産センター 滋賀ケーブルネットワーク エイトピア 鎌倉テクノサイエンス

関係会社 国内123社、海外109社

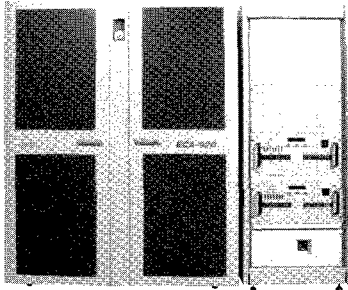


世界最高磁場NMR

JNM-ECA920 高分解能FT NMR装置

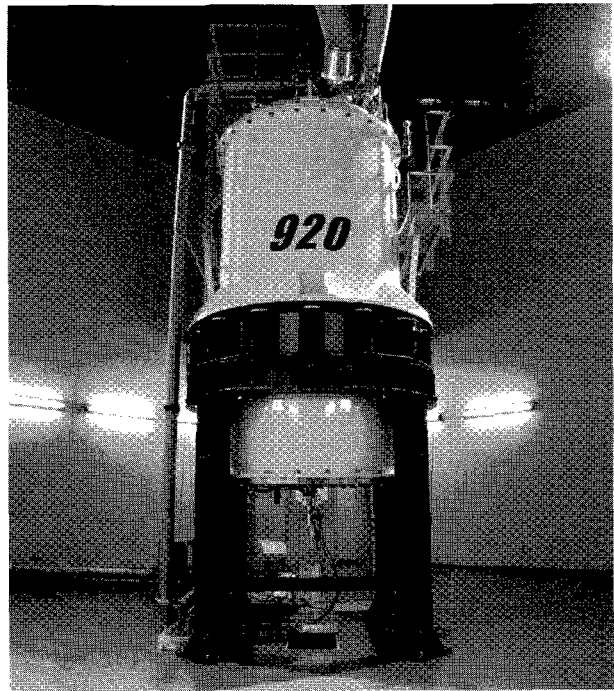
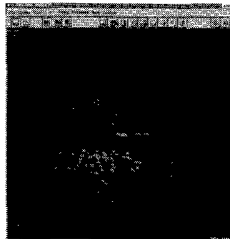
日本電子は、独立行政法人 物質・材料研究機構強磁場構研究センターに世界最高の磁場(21.6T)で動作する920MHz高分解能NMRスペクトロメーターJNM-ECA920を納入致しました。理化学研究所ゲノム科学総合研究センターの協力を得て行われたこれまでの測定では世界最高の磁場に相応した結果が得られております。

※ 弊社ホームページ www.jeol.co.jp/ 技術情報・分析機器からご覧頂けます。



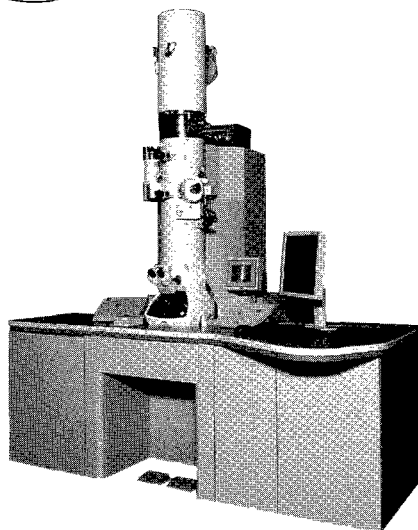
JNM-ECA920で測定した1mM¹³C/¹⁵NラベルユビキチンのHNACB 3Dデータ

《資料ご提供》
独立行政法人 物質・材料研究機構
強磁場研究センター



FT NMR

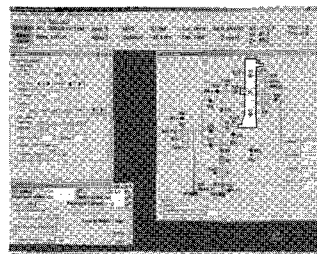
FE TEM



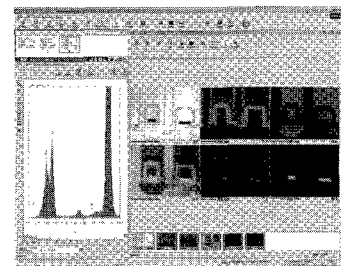
ナノ領域を開くFE電子顕微鏡

JEM-2100F 電界放出形電子顕微鏡

高輝度で干渉性の高い電子線を供給する電界放出形電子銃(FEG)は、高分解能観察やナノ領域分析に欠かせない装備です。JEM-2100Fは、デジタル化を一層進め、装置の機能を十分に発揮できるインテグレーションTEMです。



シンプルな操作性



高分解能EDS分析

お問い合わせは分析営業本部 ☎(042)528-3340

JEOL
Serving Advanced Technology

日本電子株式会社

本社・昭島製作所 〒196-8558 東京都昭島市武蔵野3-1-2 ☎(042)543-1111
営業統括本部 〒190-0012 東京都立川市曙町2-8-3 新鈴春ビル3F ☎(042)528-3353
札幌 (011) 726-9680・仙台 (022) 222-3324・筑波 (029) 856-3220・東京 (042) 528-3211・横浜 (045) 474-2181
名古屋 (052) 581-1406・大阪 (06) 6304-3941・広島 (082) 221-2500・高松 (087) 821-8487・福岡 (092) 411-2381

<http://www.jeol.co.jp/>



週刊 **ナノテク** Nano Tech Weekly

コアテクノロジーからマーケットまで全てをカバー／ナノテクを分かりたい人、ビジネスにしたい人へのベストソリューションを提供／ナノテク国家プロジェクトからナノマテリアル、IT、バイオ、メディスン、エネルギー、MEMSに至るまで徹底取材

雑誌名：週刊ナノテク 予定頁数：16～32頁
発行日：毎週月曜日 体裁：A4変形、中綴じ
発行予定部数：15,000部 年間購読料：5万7,750円(本体5万5,000円)

産業タイムズ社

〒101-0021 東京都千代田区外神田5-5-4 第二日昌ビル
Tel.03-3834-5131 Fax.03-3834-5188
<http://www.semicon-news.co.jp/> <http://www.weeklynano.com>

〒101-0021 東京都千代田区外神田5-5-4
第二日昌ビル
Tel.03-3834-5131(代)/Fax.03-3834-5188

産業タイムズ社の出版案内

詳細カタログ呈

Fax.での注文も承ります。定価は税・送料込み。

好評発売中!

半導体工場ハンドブック2006

ナノプロセスに本格突入した次世代ラインの全貌
A4変形判・150頁・定価3,150円(本体3,000円)

好評発売中!

液晶・PDP・ELメーカー計画総覧2005年度版

薄型テレビ向けで勝者をめざすFPDメーカー各社戦略
B5判・360頁・定価14,700円(本体14,000円)

好評発売中!

アジア半導体/液晶ハンドブック2005

台湾・韓国・中国・東南アジアのメーカー別プロフィール・設備投資を一覧
A4変形判・106頁・定価4,200円(本体4,000円)

好評発売中!

化合物半導体最前線2005

新たな市場に向けて加速するコンパウンドセミコンダクタの最新動向
B5判・397頁・定価12,600円(本体12,000円)

好評発売中!

半導体産業会社録2005年度版

日本で唯一の半導体産業ダイレクトリ“最新・大改訂版”
A4変形判・479頁・定価15,750円(本体15,000円)

好評発売中!

プリント回路メーカー総覧2005年度版

高付加価値商品にシフト! 正念場を迎えた基板メーカーの最新戦略
B5判・310頁・定価16,800円(本体16,000円)

好評発売中!

半導体産業計画総覧2005年度版

先端プロセスで世界をリードする日本半導体
A4変形判・412頁・定価19,950円(本体19,000円)

好評発売中!

半導体産業新聞2004年度版縮刷版

(2004年4月7日号～2005年3月30日号収録)
●半導体、液晶、プリント回路、電子部品・エネルギー、半導体関連の情報を全ファイル!!
A4判・568頁・定価8,400円(本体8,000円)

好評発売中!

燃料電池産業総覧

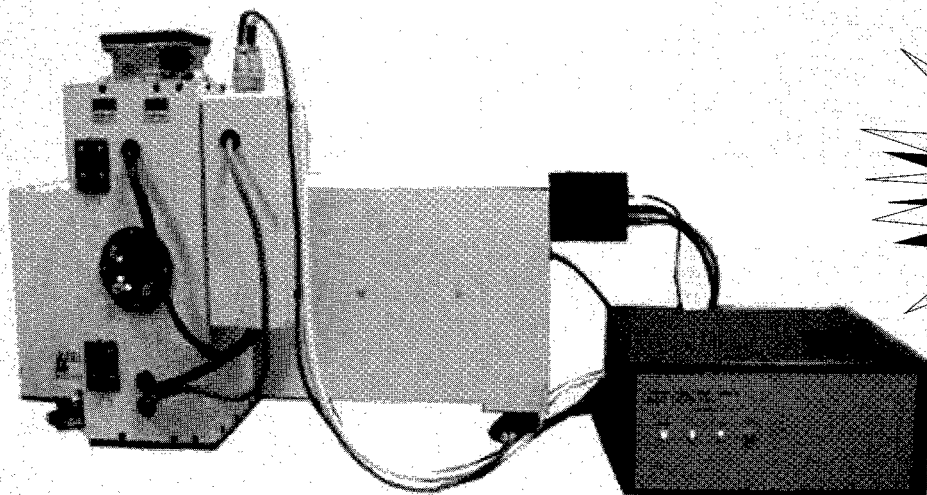
主要100社の最新事業計画・将来戦略を網羅
B5判・280頁・定価18,900円(本体18,000円)

PLE-250S

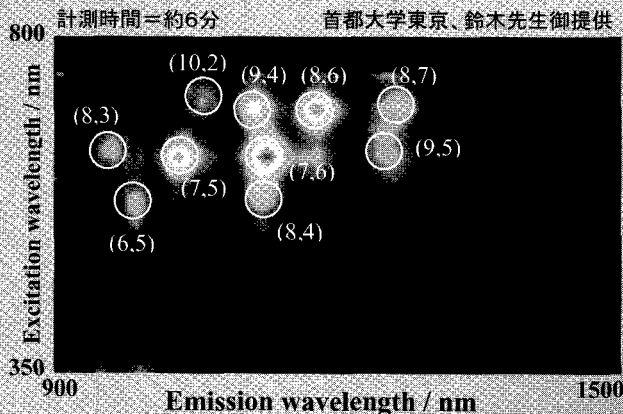
Excitation-Emission spectrum measurement system

励起・蛍光スペクトル計測システム

カーボンナノチューブにおける励起・蛍光スペクトルの2次元マップ計測に最適！



高速簡単計測!!



税込み価格:700万円~
☆装置構成
・PLE-250S 本体
・感度補正用小型分光器
・測定用パソコン

励起光源側仕様

波長範囲	: 380nm~900nm(変更可能)
光源種類	: キセノンランプ500W
回折格子	: 2枚(自動切り替)
スリット	: 固定差し替えスリット式
分解能	: 3nm(1mmスリット幅時)

蛍光受光部仕様

波長範囲	: 900nm~1600nm
検出器	: InGaAs(電子冷却/液体窒素冷却はオプション)
素子数	: 512ch

株式会社ラムダビジョン

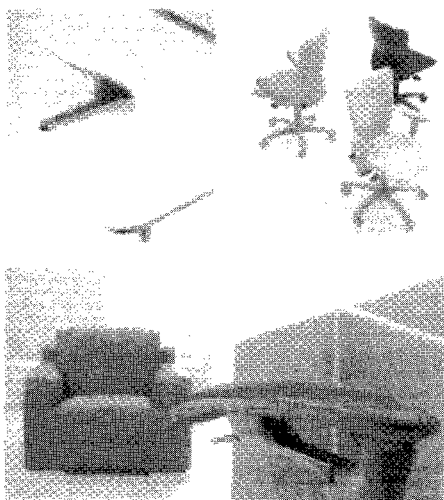
〒242-0001神奈川県大和市下鶴間505-1

TEL 046-272-5666 FAX 046-272-5716

E-mail: user@lambda-vision.co.jp

Web: http://www.lambda-vision.co.jp

**Lambda
Vision**
Revolutionary Spectrograph Technology



オフィス・実験室を
充実化・改修
おまかせ！

(有)菱田 商店

代表取締役 菱田 敦夫

hishi_co@mc.ccnw.ne.jp

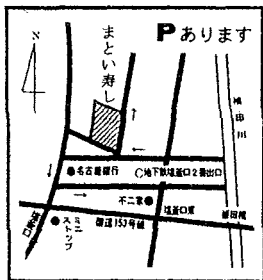
〒458-0847 名古屋市緑区浦里4-207
TEL 052-891-8125
FAX 052-891-3957

スチール製品・カーテン・カーペット・ブラインド・木製家具

Memo

■営業時間 午前 11:30～午後 2:00
午後 5:00～午後 11:00
(ラストオーダーは閉店30分前)
ランチあります

■出前 仕出し致します。
0120-044551



寿し・和食



天白区塩釜口・名古屋銀行北
☎834-1203

きしめん・そば処

新 和

お薦めメニュー

- みそ煮込みうどん
 - きしめん
 - そば
- 麺類以外にも、丼などもあります。

名古屋市天白区塩釜口二丁目 508 番地
(電話) 052-833-5048
名城大学東門と出て、3分。

■営業時間 午前 11時～午後 2時
午後 5時～8時30分

■ランチ 680円 (5種類) ~ (ランチの種類は多数あります)
1月8日 (日) も、特別にランチメニューいたします。
1月9日 (月・祝) は、お休みします。



Coffee & Restaurant CAMPARI

名古屋市天白区塩釜口 1-648
TEL: 052-834-2629

特別に、1月8日 (日)、9日 (月・祝) も営業。
ランチいたします。

- 営業時間 午前 8時～
- モーニング 午前 8時～10時
 - A ドリンク+玉子+トースト+サラダ 420円
 - B ドリンク+ホットケーキ+サラダ 480円
 - C ドリンク+ホットドック+サラダ 530円
- ランチタイム 午前 11時～午後 2時
ランチ 680円 (ドリンクなし)
840円 (ドリンク付き)



‘うるぎ’は健康のことも考えて…



お茶は 鞆そば茶、油は こめ油 を使ってます!!

手打めん処

うるぎ

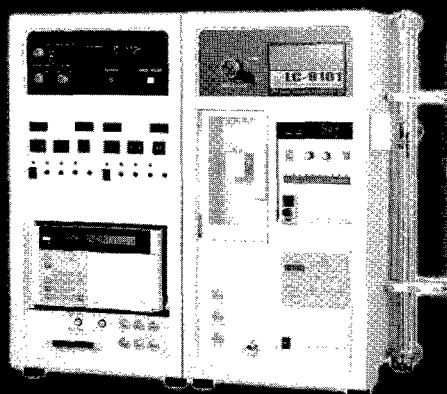
《営業時間》
月～土/AM 11:00～PM 2:15
PM 5:45～AM 0:00
日・祝/PM 4:45～ 11:00



TEL: 052-833-6552

- お薦めメニュー
- ランチ
 - うるぎ定食 (お米もそばもおかずもボリューム満点!!)
 - チーズカレーうどん (とろーり伸びるチーズとほど良いカレー。細めのうどんの絡み具合が絶妙!)

装置販売実績1,000台超！！ 分取HPLCは JAIのLC-9000シリーズ！



LC-9101

リサイクル分取を最重視したLCです。分離困難とされていた試料を容易に分離する事ができます。分離効率の良い合成ポリマー充填剤を使用した高理論段数カラムを多数ラインアップしています。リサイクル分析法では試料の溶解性のより良い溶媒や、単離分取後の溶媒除去が容易な溶媒を使用することで、短時間で効率良く、しかも試料に変化を与えずに分離精製することができます。さらにリサイクル中は、溶媒を全く消費せず、環境にも優しい装置です。



LC-9102

LC-9104

LC-9201/9204

◆LC-9101 標準モデル

専用のGPCカラム(20φ×600mm)を装着すれば、分離能を落とすことなく、常時300mgを注入することができます。NMR測定に充分な量を分取できる上、分子量分布測定など極微量試料の分析にも適しています。

◆LC-9102 グラジエントモデル

グラジエントとリサイクルがワンタッチで切替えられます。低圧4液混合グラジエントが標準装備されています。高圧グラジエント・流量グラジエントのコントローラーが内蔵されているので、応用範囲が広がります。

◆LC-9104 大量分取モデル

専用のGPCカラム(40φ×600mm)を装着すれば、試料処理量は、LC-9101型の約4倍。試料注入から分取まで自動化されています。また、ODS・シリカカラムなど、大量分取用カラムの性能を最大限に引き出す装置設計がなされています。

◆LC-9201/LC-9204 コンパクトモデル

分離分取に定評のあるLC-9101型の高い性能を受け継ぎながら、サイズをコンパクトにし、省スペース化と低価格化を実現しました。LC-9204型は大口径カラムの接続も可能です。

—— 高分子分析の未来と取り組む！ ——



日本分析工業株式会社

URL: <http://www.jai.co.jp/> E-mail: sales-1@jai.co.jp

□本社・工場: 〒190-1213
□大阪営業所: 〒532-0002

東京都西多摩郡瑞穂町武蔵208
大阪市淀川区東三国5-13-8-303

TEL 042-557-2331 FAX 042-557-1892
TEL 06-6393-8511 FAX 06-6393-8525



ハイテクの一步先に、いつも。

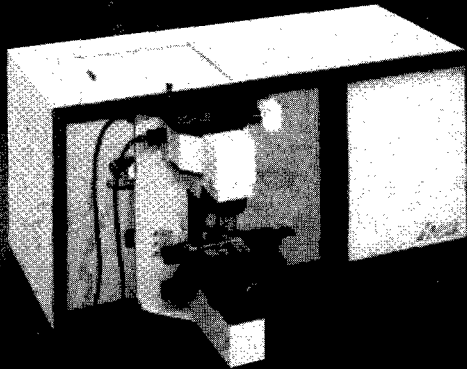
HORIBA

Explore the future

Same Spot™ テクノロジーで RAMAN/PLコンビネーション測定を実現

～ UVからNIRまで2種類の検出器で広い測定レンジ ～

顕微レーザーラマン分光測定装置 LabRamシリーズ



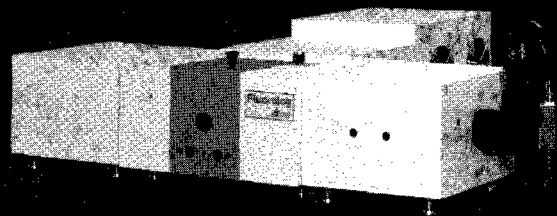
- ・ 焦点距離800mmの高分解能分光器機搭載
- ・ 高分解能用と広範囲スペクトル用に
2種類のグレーティング
- ・ 244～1064nm(紫外～近赤外)のレーザーによる励起可能
- ・ コンフォーカル分光光学系
- ・ 2種類の検出器(CCD、InGaAs)搭載可能
- ・ フォトルミネッセンス計測(オプション)
- ・ 偏光測定(オプション)

SWCNTの近赤外領域の蛍光測定に

近赤外対応蛍光分光測定装置 Fluorolog-NIRシリーズ

- ・ Fluorologシリーズは少量サンプルに対する精密な
結像が可能な全反射光学系採用
- ・ 拡張機能があるのでNIR～IRの蛍光測定にも
対応可能

Fluorolog-NIRはモジュール式装置なので
アプリケーションに応じた各種NIR検出器や
分光器と組合わせた仕様に構築できます。



HORIBA JOBIN YVON

製品に関するお問い合わせは... 科学システム営業部 03-3861-8234 <http://www.jyhoriba.jp>

株式会社堀場製作所

本社 〒601-8510 京都市南区吉祥院宮の東町2 TEL(075)313-8121

●東京(03)3861-8231 ●横浜(045)451-2091 ●名古屋(052)936-5781 ●大阪(06)6390-8011

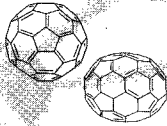
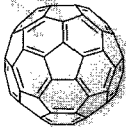
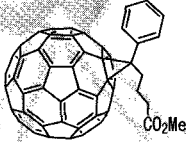
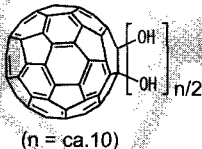
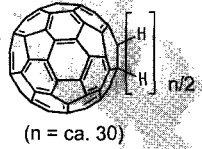
●仙台(022)308-7890 ●つくば(0298)56-0521

●広島(082)288-4433 ●福岡(092)472-5041

<http://www.horiba.co.jp> e-mail: info@horiba.co.jp

nanom

フラーレン関連製品
(フロンティアカーボン株式会社製)

銘柄	分子構造	主な組成・純度 (注1)	取扱数量 (注2)
nanom mix MFシリーズ 混合フラーレン		C60: 約60% (HPLC) C70: 約25% (HPLC) その他: 高次フラーレン	50g~
nanom purple N60シリーズ フラーレンC60		C60: 98.0%以上 (HPLC) C60: 99.5%以上 (HPLC) * 昇華精製品も御座います	10g~ 1g~
nanom orange N70-S フラーレンC70		C70: 95.0%以上 (HPLC)	1g~
nanom spectra 66PCBM-S PCBM		PCBM: 95.0%以上 (HPLC)	1g~
nanom spectra HX10-S 水酸化フラーレン	 (n = ca. 10)	C60(OH) _n n=約10 (MS)	5g~
nanom spectra H30-S 水素化フラーレン	 (n = ca. 30)	C60(H) _n n=約30 (MS)	5g~
nanom spectra 60X 酸化フラーレン	 (n = 1-2 が主成分)	C60(O) ₁ : 約40% (HPLC) C60(O) ₂ : 約30% (HPLC) その他: C60, 三酸化体以降	1g~

(注1) 当該数値は代表値であり、保証値では御座いません

(注2) 大学、公的研究機関様向けに少量対応致します。個別にご相談下さい

【開発・製造元】

● ● ● Frontier Carbon Corporation

フロンティアカーボン株式会社
104-0031 東京都中央区京橋1-8-7
京橋日殖ビル5F
TEL.03-5159-6880 FAX.03-5159-6872

【問い合わせ先】

 第一実業株式会社

新規事業推進室(担当:原)
〒102-0084 東京都千代田区二番町11番19号
興和二番町ビル
TEL.03-5214-8614 FAX.03-5214-8501